CAYLEYPY: LEARNING-GUIDED SEARCH AND EXACT COMPUTATION FOR ALGEBRAIC GRAPH DISCOVERY

Anonymous authors
Paper under double-blind review

ABSTRACT

We present the first public release of CAYLEYPY[1], an open-source Python library for large-scale computation with Cayley and Schreier graphs. Unlike general-purpose computer algebra systems such as GAP and Sage, CAYLEYPY is optimized for massive graph exploration and enables computations on instances far beyond the practical range of existing tools, with orders-of-magnitude speedups in our experiments. The library forms the computational backbone of an AI-assisted conjecture-discovery pipeline that combines fast graph algorithms with reinforcement-learning-guided search over generating sets.

Using CAYLEYPY, we obtain approximately 200 new conjectures A on diameters and growth functions of Cayley and Schreier graphs. Our main empirical discovery is a quasi-polynomiality phenomenon for Cayley graphs of symmetric groups: for many natural families of generators, the diameter appears to be governed by a small collection of linear or quadratic polynomials indexed by congruence classes of $n \bmod s$. We formulate this as a general quasi-polynomiality hypothesis, suggesting that structured diameter problems may admit efficient closed-form solutions despite the general computational hardness of diameter computation.

We further propose a sharpened Babai-type conjecture for undirected Cayley graphs of symmetric groups, predicting that every undirected Cayley graph of S_n has diameter at most

$$n^2/2 + 4n.$$

This improves the expected constant in known $O(n^2)$-type bounds. Our reinforcement-learning-guided searches identify explicit candidate extremal generator families, related to involutions arranged in a "square with whiskers" pattern, and exhaustive search verifies their optimality among tested instances for all $n \leq 15$. We also conjecture an answer to a question posed by V. M. Glushkov in 1968 on directed Cayley graphs generated by a cyclic shift and a transposition. Finally, for nilpotent groups, we formulate conjectural improvements to results of J. S. Ellenberg on upper unitriangular groups over $\mathbb{Z}/p\mathbb{Z}$, predicting linear dependence of the diameter on p.

Together, these results demonstrate how scalable symbolic-combinatorial software and reinforcement learning can support systematic conjecture discovery in group theory.

1 INTRODUCTION

Learning-assisted mathematical discovery requires more than plausible predictions. A useful system must expose the evidence behind a proposed statement, distinguish a successful search from a proof, and make counterexamples easy to test. Cayley graphs provide a concrete setting for this distinction. Given a finite group G and generators S, vertices are group elements and edges apply generators. A path is a word in S: it can be checked by multiplication even when the graph is too large to enumerate. The symmetric group S_n already has $n!$ vertices, so exact transitions remain inexpensive long after global exploration becomes infeasible.

[1] https://anonymous.4open.science/r/cayleypy-1C2E/README.md

Reviewers: please read the Reviewer Guidelines (iclr.cc/Conferences/2027/ReviewerGuidelines) and the AI Policy for Reviewers (iclr.cc/Conferences/2027/AIPolicyForReviewers). If you used AI to expand, edit, or polish your review, please provide the input text to the LLM. Better still, consider skipping the LLM and submitting your original text: we, and the authors, are much more interested in your unedited thoughts than in what an LLM has to say. AI-assisted or not, you are putting your name and reputation behind your review: LLM-generated falsehoods, hallucinations or misrepresentations are subject to disciplinary action, which may include desk-rejecting all papers you have authored.

Growth is the central mathematical object of this study. For a family of groups and generating sets, we investigate the growth sequence—the number of elements at each distance from the identity—and how its statistics and diameter vary with the family parameter. This motivates the name CAYLEYPY GROWTH: the paper introduces a catalogue of explicit growth and diameter conjectures developed through exact computation and RL-guided exploration.

CAYLEYPY represents states as compact tensors and applies generators in batches. Exact enumeration supplies complete growth distributions at tractable sizes; learned search extends exploration to larger instances and tests candidate extremal states. Bellman refinement improves the search heuristic used to find short words, while exact computations supply the small-instance data against which candidate formulas are tested. Appendix A explains how to read a catalogue cell as a mathematical statement, and Appendix G expands the generator definitions, conjectures, and supporting data.

The learning problem has two distinct questions: does a learned ranking improve search over simple heuristics, and does Bellman refinement improve a diffusion-trained ranking? We address the first with a cube experiment that changes the ranking heuristic while holding the search budget fixed, and the second with exact-distance diagnostics and a warm-start ablation on LRX. This separates the usefulness of learning from the additional contribution of RL. A further question—whether either improves the rate of mathematical discovery—remains open.

This paper presents a unified computational study of learning-guided exploration on algebraic graphs. Its contributions are: (i) the CAYLEYPY system, connecting exact graph exploration to learned search through a common transition and certificate interface; (ii) an empirical evaluation of diffusion warm-up and clipped Bellman refinement, including a controlled cube comparison, exact-distance diagnostics, and LRX search ablations; and (iii) a mathematical discovery study combining a catalogue of candidate formulas with explicit counterexamples and a fixed-conjugacy-type quasi-polynomiality conjecture. Appendix A gives the mathematical catalogue and the evidence associated with its entries.

2 RELATED WORK

Learning and mathematical discovery. Machine learning has guided mathematical intuition and the search for combinatorial constructions (Davies et al., 2021; Romera-Paredes et al., 2024). RL in exact symbolic environments also provides examples of search with sparse rewards (Shehper et al., 2024). Our setting emphasizes the interface between a learned proposal mechanism and finite, independently checkable algebraic evidence.

Learning to search. DeepCubeA combines approximate value iteration with search and reports solving all 1,000 tested Rubik's-cube instances, 60.3% optimally (Agostinelli et al., 2019). This demonstrates the combined system's performance, without isolating the RL contribution. Self-supervised inverse-move prediction from random scrambles provides another effective search guide (Takano, 2023); it differs from CayleyPy's regression on walk lengths. Q* search uses action-value heuristics (Agostinelli et al., 2024), whereas the scalar state-distance refinement considered here is fitted value iteration. Our evaluation separates diffusion-only training, Bellman refinement, and their use within combined search systems on algebraic graphs.

Group algorithms and complexity. Schreier–Sims algorithms address membership and structural group computation (Sims, 1970; Knuth, 1991); their decompositions need not minimize word length (Fiat et al., 1989). Minimum-length generator sequences and several puzzle-specific variants are computationally hard (Even & Goldreich, 1981; Jerrum, 1985; Demaine et al., 2017; Bulteau et al., 2015). Specialized search and pattern databases remain strong comparators (Korf, 1997; Rokicki et al., 2014). General diameter bounds (Babai & Seress, 1988; Helfgott & Seress, 2014) and random-walk results (Diaconis & Saloff-Coste, 1993; Helfgott et al., 2015) provide theoretical context, but do not supply exact formulas for every concrete generating family. Hardness results for general inputs do not rule out compact formulas for restricted families.

Table 1: Evidence types that must remain separate in learning-assisted discovery. A long path found by search is not a certificate of a large distance.

Output	What it establishes	What it does not establish
Completed exact BFS	Distances from the root; Cayley diameter	A formula for untested sizes
Replayed word of length ℓ	$d(s, e) \leq \ell$	Optimality or a diameter lower bound
Certified state lower bound b	$d(s, e) \geq b$, hence diameter $\geq b$	An upper bound for every state
Formula fitted to finite data	Agreement on the checked instances	Eventual validity or universality

3 A PIPELINE WITH EXPLICIT EVIDENCE LEVELS

3.1 EXACT TRANSITIONS AND DISTANCE CERTIFICATES

For the right Cayley graph, the neighbor oracle is $\mathcal{N}(g) = \{ga : a \in S\}$. Undirected experiments use $S \cup S^{-1}$; directed experiments must retain their stated action set. Schreier graphs use the corresponding action on cosets or structured states. Each stored path records generator labels, allowing independent replay without the learned model.

Interoperability. The documented interface accepts explicit permutation lists, NumPy arrays, or PyTorch tensors and exposes returned paths as generator IDs. A GAP-format puzzle importer reads named cycle-notation moves and optional identical-piece classes. It supports this restricted file syntax; general GAP/Sage integration requires reconciling the degree, indexing, action convention, and inverse closure. These interfaces support exchanging algebraic inputs and verifiable words without assuming an automatic bridge to every computer algebra system.

For a base vertex v_0, exact BFS computes $L_r = \{v : d(v_0, v) = r\}$ and the growth sequence $\gamma(r) = |L_r|$. If the traversal completes, $\max\{r : L_r \neq \emptyset\}$ is the eccentricity of v_0. In a connected Cayley graph, vertex transitivity makes this the diameter. In a general Schreier graph, a single root traversal supplies an eccentricity; equality with the diameter requires a separate argument or additional traversals. In directed graphs, the direction of the distance must also be specified.

The tensorized implementation batches transitions and deduplicates frontiers; a bitmask backend uses permutation ranks to reduce memory. Appendix D gives the algorithms. The word "exact" requires collision-free state identification or explicit resolution of hash collisions. Exhaustive expansion through the preceding layer certifies distances in each new layer; completing the traversal is additionally required to obtain the full growth sequence and root eccentricity. Hash equality alone is not a mathematical certificate. These conditions matter when growth values are used as ground truth for a conjecture.

3.2 DIFFUSION WARM-UP AND BELLMAN REFINEMENT

Let $d(s) = d(s, e)$. For $s \neq e$, the unit-cost Bellman equation is

$$d(s) = 1 + \min_{t \in \mathcal{N}(s)} d(t), \qquad d(e) = 0. \tag{1}$$

The terminal boundary is imposed separately: applying the nonterminal backup at e would be incorrect. A scalar predictor $f_\theta(s)$ serves as a heuristic for search. Our Bellman-refinement stage learns a state-distance function rather than a conventional action-value network.

Random walks supply cheap supervision without an optimal solver. A walk of length k gives a generally loose upper bound, not an exact distance label. For undirected graphs it can be reversed. To learn distances *to* e on directed graphs, training examples instead need paths ending at e, obtained by walking backward with inverse actions. Forward walks from e cannot automatically bound $d(s, e)$ when inverse actions are unavailable. Repeated-state labels can be replaced by the shortest observed valid path to the target.

Algorithm 1 Search with a learned distance heuristic

Require: Start s_0, target e, actions S, predictor f, beam width W, depth cap M

$B_0 \leftarrow \{s_0\}$; store parent records indexed by depth and state
for $i = 0, \ldots, M$ **do**
  if $e \in B_i$ **then**
    Reconstruct the generator word; replay it from s_0; return it if valid
  end if
  if $i = M$ **then**
    break
  end if
  Expand all $s \in B_i$ with their legal actions, retaining parent/action records
  Deduplicate successor states within the new layer
  $B_{i+1} \leftarrow$ up to W successors with smallest f (fixed tie-breaking)
  if $B_{i+1} = \emptyset$ **then**
    break
  end if
end for
return failure under this search budget

Warm-up minimizes squared error between $f_\theta(s)$ and these path-length labels. A subsequent refinement stage constructs detached targets from a snapshot $f_{\bar{\theta}}$:

$$y(s) = \begin{cases} 0, & s = e, \\ \min\{k(s), \max\{0, 1 + \min_{t \in \mathcal{N}(s)} f_{\bar{\theta}}(t)\}\}, & s \neq e. \end{cases} \tag{2}$$

Here $k(s)$ is the length of a known valid path from s to e, and the known terminal value $f_{\bar{\theta}}(e) = 0$ is imposed in every backup. The target is held fixed during its regression update. This clipping constrains training targets; it does not make the learned prediction an admissible lower bound or guarantee convergence under function approximation. Random-walk sampling also differs from online exploration by a learned policy. The possible benefit is improved ranking of successors after weak path-length supervision, which must be measured separately from the benefit of a larger beam.

Why warm-up, clipping, and bounded-width search? Warm-up supplies a dense signal before useful estimates exist; clipping uses a known feasible path to limit bootstrap targets; a fixed beam permits batched inference with explicit frontier memory. In the exact tabular setting, clipping at any finite valid path bounds preserves the unique nonnegative Bellman fixed point, and synchronous iteration from those bounds reaches exact distances in finitely many sweeps (Appendix I). This elementary guarantee motivates the clip but does not extend to neural regression. The warm-start experiment below therefore tests an empirical design choice rather than a neural convergence theorem.

Algorithm 1 states the minimal search interface; pruning, restarts, and inverse-state ensembles are additional configuration choices that must be reported. Depth-indexed parents prevent cycles in reconstruction when a state reappears. Finite beam width gives neither completeness nor optimality. A failure means that the configured search failed, not that the target is unreachable.

3.3 From search outputs to mathematical questions

For each parameterized generating family, exact BFS produces small-instance growth sequences, diameters, and last-layer states. Finite differences and residue-class fits suggest diameter laws; normalized growth profiles suggest distributional laws. Patterns in the last layers identify candidate antipodes at larger sizes. Diffusion warm-up followed by Bellman refinement supplies a value function for beam search, which seeks short words for these candidates beyond the enumeration range. The outer choice of families and formulas remains a mathematical exploration process.

A candidate formula is tested by further exact enumeration or by search for a shorter decomposition of its proposed extremal states. A word shorter than a proposed *state-distance* value refutes that claim; establishing a diameter still requires bounds covering the graph. Appendix B develops this process and works through LRX: at $n = 28$, the candidate value is 378, while refinement improves

Table 2: Recorded controlled cube experiment. Length statistics include only solved instances; times and candidate totals are per-instance medians. Candidate totals sum states scored after deduplication at each step, not globally distinct states. The original execution report records successful replay of every returned solution against the target. Both non-learned methods stopped for stagnation before the time/depth ceilings. Model training is excluded from the search budget.

Ranking heuristic	Solved / 20	Length mean/med.	Median time (s)	Candidates
Misplaced stickers	0	—	14.06	1.36×10^9
Sticker distance	0	—	23.46	2.13×10^9
Diffusion-trained CayleyPy	18	60.5 / 60	36.89	3.25×10^8

the best recorded word to 382. The expanded family entries link the catalogue's formulas to explicit generators, growth vectors, and numerical examples.

4 Empirical evidence and the role of RL

4.1 Learning versus simple heuristics under fixed search

We compare the diffusion-trained CayleyPy ResMLP with two training-free ranking heuristics on the $4 \times 4 \times 4$ cube on the same 20 test states using one H100 PCIe 80GB. The states are indices 0–19 of the published `rnd` dataset, with search seed 20260802. All conditions use beam width 2^{18}, one attempt, a 1,000-step ceiling, deterministic tie-breaking, a shared stagnation rule, and a 60-second search-time ceiling per instance. Move lengths use the source's UQTM convention. The baselines count misplaced stickers or aggregate sticker distances, using each sticker position's shortest distance to a solved position of the same color. The search algorithm is held fixed; only its ranking heuristic changes. A pilot on the first two states informed the search configuration, so this is not a fully held-out evaluation of configuration selection. Appendix K records the recovered setup and stopping rule.

The learned heuristic solves 90% of these instances, while both simple heuristics fail despite scoring more candidates (Table 2). All 40 baseline failures trigger the shared stagnation rule, so the comparison concerns this fixed stopping policy, not exhaustive use of the time allowance. This supports learned ranking within the stated search protocol; it is neither an optimality result nor a comparison against specialized cube solvers. The checkpoint uses diffusion supervision without Bellman refinement: this experiment isolates learned guidance, while the following LRX experiments assess the additional refinement stage. Training cost is excluded, and the first-20-instance subset limits generalization.

4.2 Comparison with DeepCubeA and EfficientCube

Table 3 compares learned solvers on the 1,000-instance $3 \times 3 \times 3$ benchmark of Agostinelli et al. (2019), using the quarter-turn metric (QTM). DeepCubeA's row uses its reported results; EfficientCube (Takano, 2023) uses the reproduced baseline. A single diffusion-trained CayleyPy model reaches 75.4% optimal solutions versus 69.8% for EfficientCube at the same beam width 2^{18}. Increasing CayleyPy's beam to 2^{24} raises optimality to 97.3%, showing the additional effect of search capacity. These measurements compare complete solvers; the LRX ablation below assesses Bellman refinement separately. Appendix L specifies the model sizes, training data, and provenance of these benchmark records.

4.3 A quantitative Bellman-refinement example

The LRX family uses $L = (1\,2\,\cdots\,n)$, $R = L^{-1}$, and $X = (1\,2)$ as unit-cost generators of S_n. An exact-distance diagnostic measures the quality of the learned ranking before considering search outcomes. Table 4 reports Spearman correlations on LRX graphs. On S_{10}, adding 50 Bellman epochs after 50 diffusion epochs raises correlation from 0.923 to 0.938; a shorter warm-up followed by refinement reaches 0.939. The corresponding S_8 improvement is 0.969 to 0.982. These are three sizes of one generator family. The table supports improved ranking, but does not report a held-out state split or seed uncertainty, and additional training is not compute-matched.

Table 3: Learned-solver comparison on 1,000 common $3 \times 3 \times 3$ cube instances (QTM). All configurations solve all instances. Optimality is the fraction matching the benchmark's exact distances. Each CayleyPy row uses one diffusion-trained model. Equal beam width does not imply equal training or total compute; 2^{24} is 64 times wider than 2^{18}.

Solver	Beam width	Mean length ↓	Optimal ↑
DeepCubeA	—	21.500	60.3%
EfficientCube	2^{18}	21.255	69.8%
CayleyPy, single model	2^{18}	21.137	75.4%
CayleyPy, wider search	2^{24}	20.691	97.3%

Table 4: Spearman correlation with exact LRX distances. DD denotes diffusion supervision and BR Bellman refinement; numbers in headers are training epochs.

LRX graph	DD 5	DD 50	DD 5 + BR 50	DD 50 + BR 50
S_6	0.955	0.990	0.990	0.990
S_8	0.954	0.969	0.980	0.982
S_{10}	0.883	0.923	0.939	0.938

We evaluate four training schedules on a fixed conjecturally longest element in S_{28} (Table 5). Each condition uses ten independent training/search runs. With diffusion warm-up, Bellman refinement gives a median successful length of 402 versus 516 for 100 diffusion-only epochs, a 22.1% reduction, and solves 8/10 rather than 7/10 runs. Cold-start refinement solves only 2/10. These observations motivate warm-started refinement, but do not establish a compute-matched RL advantage: training budgets differ, the successful-run sets differ, and only one starting state is tested. The one-run success difference is not strong statistical evidence.

A recent preprint reports a proof that the shifted reversal $[2, 1, n, n-1, \ldots, 3]$ has LRX distance $n(n-1)/2$ for $n \geq 4$, yielding the same lower bound for the diameter and specializing to distance 378 at $n = 28$ (Antiufeev, 2026, Theorem 1). The best refined word in Table 5 is therefore four moves above this reported state optimum. This reported result concerns the benchmark state's distance; it does not establish the matching upper bound for every state needed to settle the diameter conjecture, and it is separate from the search evidence in Table 5.

4.4 Picture Cube benchmark

The IHES Picture Cube benchmark compares a combined learned-search pipeline with an adapted Kociemba two-phase baseline on the same 1,003 inputs. The baseline, including multi-prefix search and a center lookup, requires 42,718 total moves; the final pipeline requires 23,224, a 45.6% reduction, with all 1,003 solutions passing the recorded validity check (Appendix M). The pipeline retains Kociemba as a fallback and combines learned guidance, wider beams, ensembling, and post-processing. These totals therefore compare complete configurations, without a matched runtime budget.

Within this progression, adding Bellman-refined E6 values *and* inverse-state (NISS) ensembling reduces the total from 24,618 to 24,068 moves, a 550-move or 2.23% improvement. Because refinement and ensembling changed together, this gain cannot be assigned to RL alone. The experiment illustrates how learned values complement classical solving, search engineering, and solution validation.

4.5 Diffusion search versus group decomposition

We also compare diffusion-guided paths with GAP decompositions. On the LRX S_{20} benchmark instance, the returned path lengths are 190 and 217,944, respectively. This establishes a large difference in the returned word lengths for that comparison. It is not an RL ablation: the learned method uses diffusion supervision. GAP's general decomposition routine is also not a specialized shortest-path solver. Aggregated best results over models and restarts should not be interpreted as typical single-run performance. We therefore keep this example separate from Table 5 and do not

Table 5: LRX training-schedule comparison on S_{28}. Medians include successful runs only; failures are excluded. Epoch counts are not matched computational budgets. The reference length is $28 \cdot 27/2 = 378$; its mathematical status is discussed in the text.

Training schedule	Solved / 10	Best length	Median, solved runs
Diffusion, 30 epochs	7	464	650
Diffusion, 100 epochs	7	436	516
Diffusion 30 + Bellman 200	8	382	402
Bellman only, 230 epochs	2	434	471

claim "zero prior knowledge": the state encoding, legal actions, target, sampling process, and search algorithm all supply structure.

4.6 Exact computation and comparison controls

Exact BFS supplies ground-truth distances for the ranking diagnostic and finite diameter data for the mathematical study. In our CPU benchmarks at S_{11}, CayleyPy reduces full-growth runtime relative to GAP by 21.7–57.4× across LRX, Coxeter, all-transposition, pancake, and reversal generators (Appendix E). The Coxeter time is 41 seconds on CPU and 0.601 seconds on P100, a separate 68.2× hardware comparison. These implementation measurements do not measure an RL effect, and small instances can be slower on GPU because of launch overhead.

Search capacity is also a substantial intervention: diffusion-only LRX S_{20} search changes from failure at beam width 2^{10} to a length-190 solution at 2^{20}. The controlled $4 \times 4 \times 4$ comparison holds the search settings and inference-time budget fixed. The LRX training comparison still requires matched training time or transition evaluations, paired test instances, and seed uncertainty to isolate refinement from extra computation. Search failures, conditional path quality, expanded states, memory, and training cost should be reported together. Comparing independently validated discoveries per fixed outer-search budget is a separate experiment that has not been established here.

5 Quasi-polynomial diameter conjecture

A diameter sequence is *eventually quasi-polynomial* if there are a fixed period $q \geq 1$, a threshold N, and rational polynomials $p_0, \ldots, p_{q-1}$ such that

$$D(n) = p_{n \bmod q}(n) \qquad \text{for every } n \geq N. \tag{3}$$

For example, adjacent transpositions give diameter $\binom{n}{2}$, while star transpositions give $\lfloor 3(n-1)/2 \rfloor$. Our catalogue contains further candidate formulas of this form, including the LRX diameter $n(n-1)/2$ for $n \geq 4$. We formulate a precise conjecture for full conjugacy classes of fixed cycle types.

Fix a nonempty finite set Λ of nonempty partitions whose parts are at least two, and put $r = \max_{\lambda \in \Lambda} |\lambda|$. For $n \geq r$, let $C_\lambda(n)$ be the full S_n-conjugacy class of cycle type $\lambda 1^{n-|\lambda|}$, and define

$$X_\Lambda(n) = \bigcup_{\lambda \in \Lambda} C_\lambda(n), \qquad H_\Lambda(n) = \langle X_\Lambda(n) \rangle.$$

These generating sets are inverse-closed. For $n \geq \max(5, r)$, the generated group is A_n if every $|\lambda| - \ell(\lambda)$ is even, and S_n otherwise, where $\ell(\lambda)$ is the number of parts.

Conjecture 1 (Fixed-conjugacy-type quasi-polynomiality)**.** *For every fixed Λ as above, there exist integers $q \geq 1$ and $N \geq \max(5, r)$, positive rational numbers $a_0, \ldots, a_{q-1}$, and rational numbers $b_0, \ldots, b_{q-1}$ such that, for all $n \geq N$,*

$$\operatorname{diam} \operatorname{Cay}(H_\Lambda(n), X_\Lambda(n)) = a_{n \bmod q}\, n + b_{n \bmod q}.$$

The diameter is $\Theta_\Lambda(n)$ (Appendix J), so eventual quasi-polynomiality in this class necessarily has degree one. Known cycle-factorization results give concrete examples (Kishnani et al., 2023; 2024): for all 5-cycles on A_n,

$$\operatorname{diam} \operatorname{Cay}(A_n, C_5(n)) = \left\lceil \frac{n-1}{3} \right\rceil + \mathbf{1}_{n \equiv 4 \pmod{12}}, \qquad n \geq 7.$$

Appendix J derives this period-12 example from the cited theorem.

Full conjugacy closure is a substantive restriction. The conjecture does not cover LRX, adjacent-transposition, or star-transposition generating sets; identifying a wider class covering the catalogue remains open. Bounded support or a uniform generating rule alone is insufficient: transpositions along a broom with path length $\lfloor n^{3/4} \rfloor$ have diameter $\Theta(n^{3/2})$, which cannot be eventually quasi-polynomial. Appendix C gives the obstruction.

6 Conclusion

We presented CayleyPy, a computational framework combining exact algebraic graph exploration with learned search. The cube comparison demonstrates the benefit of learned ranking under fixed search settings, and the LRX experiments evaluate the additional contribution of Bellman refinement. Together with the catalogue of diameter and growth formulas, these experiments support a systematic approach to conjecture discovery. The fixed-conjugacy-type conjecture provides a precise mathematical target for further investigation.

7 Limitations

Learned, finite-width search does not guarantee optimal paths: replaying a returned word certifies feasibility and an upper bound on distance, but not shortestness. Exact distances and diameters require exhaustive computation or a separate mathematical certificate.

Ethics and Societal Impact Statement

This work aims to advance the field of machine learning, particularly AI-assisted mathematical discovery. There are many potential societal consequences of advances in this field; we do not identify any specific to the methods presented here that require separate discussion.

Reproducibility Statement

Sections 3 and 4 describe the state transitions, training objectives, search algorithm, evaluation settings, and reported metrics. Appendices D and B detail exact enumeration and the search-to-conjecture workflow. Experimental configurations and available benchmark records are documented in Appendices K, L, and M. Source code, installation instructions, and documentation are provided in the anonymous repository at `https://anonymous.4open.science/r/cayleypy-1C2E/README.md`.

AI Use Statement

Generative AI tools assisted with literature search and text polishing. Authors are responsible for the conducted experiments.

References

Forest Agostinelli, Stephen McAleer, Alexander Shmakov, and Pierre Baldi. Solving the rubik's cube with deep reinforcement learning and search. *Nature Machine Intelligence*, 1: 356–363, 2019. doi: 10.1038/s42256-019-0070-z. URL `https://doi.org/10.1038/s42256-019-0070-z`.

Forest Agostinelli, Shahaf S. Shperberg, Alexander Shmakov, Stephen McAleer, Roy Fox, and Pierre Baldi. Q* search: Heuristic search with deep q-networks. In *ICAPS Workshop on Bridging the Gap between AI Planning and Reinforcement Learning*, 2024. URL `https://icaps24.icaps-conference.org/program/workshops/prl-papers/9.pdf`.

Grigorii Antiufeev. A lower bound for the diameter of Cayley graph of the symmetric group S_n generated by $(12), (12\dots n), (1n\dots 2)$, 2026. URL `https://arxiv.org/abs/2601.08715v3`. Version 3, June 4, 2026.

S. V. Avgustinovich, E. N. Khomyakova, and E. V. Konstantinova. Multiplicities of eigenvalues of the Star graph. *Siberian Electronic Mathematical Reports*, 13:1258–1270, 2016. doi: 10.17377/semi.2016.13.098. URL https://doi.org/10.17377/semi.2016.13.098.

Laszlo Babai and Akos Seress. On the diameter of cayley graphs of the symmetric group. *Journal of Combinatorial Theory, Series A*, 49(1):175–179, 1988. doi: 10.1016/0097-3165(88)90033-7. URL https://doi.org/10.1016/0097-3165(88)90033-7.

Vineet Bafna and Pavel A. Pevzner. Genome rearrangements and sorting by reversals. *SIAM Journal on Computing*, 25(2):272–289, 1996. doi: 10.1137/S0097539793250627.

Douglas W. Bass and Ivan Hal Sudborough. Pancake problems with restricted prefix reversals and some corresponding cayley networks. *Journal of Parallel and Distributed Computing*, 63(3):327–336, 2003. doi: 10.1016/S0743-7315(03)00033-9.

Laurent Bulteau, Guillaume Fertin, and Irena Rusu. Pancake flipping is hard. *Journal of Computer and System Sciences*, 81(8):1556–1574, 2015. doi: 10.1016/j.jcss.2015.02.003. URL https://doi.org/10.1016/j.jcss.2015.02.003.

Guillaume Chapuy and Valentin Féray. A note on a Cayley graph of S_n, 2012. URL https://arxiv.org/abs/1202.4976v2.

Alex Davies, Petar Velickovic, Lars Buesing, Sam Blackwell, Daniel Zheng, Nenad Tomasev, et al. Advancing mathematics by guiding human intuition with ai. *Nature*, 600:70–74, 2021. doi: 10.1038/s41586-021-04086-x. URL https://doi.org/10.1038/s41586-021-04086-x.

J. W. Davies and A. O. Morris. The schur multiplier of the generalized symmetric group. *Journal of the London Mathematical Society*, 8(4):615–620, 1974. doi: 10.1112/jlms/s2-8.4.615. URL https://doi.org/10.1112/jlms/s2-8.4.615.

Erik D. Demaine, Sarah Eisenstat, and Mikhail Rudoy. Solving the rubik's cube optimally is np-complete, 2017. URL https://arxiv.org/abs/1706.06708.

Persi Diaconis and Laurent Saloff-Coste. Comparison techniques for random walk on finite groups. *The Annals of Probability*, 21(4):2131–2156, 1993. doi: 10.1214/aop/1176989013. URL https://doi.org/10.1214/aop/1176989013.

Shimon Even and Oded Goldreich. The minimum-length generator sequence problem is np-hard. *Journal of Algorithms*, 2(3):311–313, 1981. doi: 10.1016/0196-6774(81)90029-8. URL https://doi.org/10.1016/0196-6774(81)90029-8.

Amos Fiat, Shahar Moses, Adi Shamir, Ilan Shimshoni, and Gabor Tardos. Planning and learning in permutation groups. In *Proceedings of the 30th Annual Symposium on Foundations of Computer Science*, pp. 274–279, 1989. doi: 10.1109/SFCS.1989.63490. URL https://doi.org/10.1109/SFCS.1989.63490.

M.M. Glukhov and A.Yu. Zubov. On the lengths of symmetric and alternating groups with the different systems of generators (in russian). *Mathematical questions of cybernetics*, 8:5–32, 1999.

Harald A. Helfgott and Ákos Seress. On the diameter of permutation groups. *Annals of Mathematics*, 179(2):611–658, 2014. doi: 10.4007/annals.2014.179.2.4. URL https://annals.math.princeton.edu/2014/179-2/p04.

Harald A. Helfgott, Akos Seress, and Andrzej Zuk. Random generators of the symmetric group: Diameter, mixing time and spectral gap. *Journal of Algebra*, 421:349–368, 2015. doi: 10.1016/j.jalgebra.2014.08.033. URL https://doi.org/10.1016/j.jalgebra.2014.08.033.

Marcel Herzog and Kenneth B Reid. Representation of permutations as products of cycles of fixed length. *Journal of the Australian Mathematical Society*, 22(3):321–331, 1976. doi: https://doi.org/10.1017/S1446788700014774. URL https://www.cambridge.org/core/journals/journal-of-the-australian-mathematical-society/article/representation-of-permutations-as-products-of-cycles-of-fixed-length/83E4DCE6CB72942C2EF7D77BFCEB1A1B.

Marie-Claude Heydemann. Cayley graphs and interconnection networks. In Gena Hahn and Gert Sabidussi (eds.), *Graph Symmetry: Algebraic Methods and Applications*, volume 497 of *NATO ASI Series C: Mathematical and Physical Sciences*, pp. 167–224. Kluwer Academic Publishers, Dordrecht, 1997. doi: 10.1007/978-94-015-8937-6_5. URL https://doi.org/10.1007/978-94-015-8937-6_5.

Mark R. Jerrum. The complexity of finding minimum-length generator sequences. *Theoretical Computer Science*, 36:265–289, 1985. doi: 10.1016/0304-3975(85)90047-7. URL https://doi.org/10.1016/0304-3975(85)90047-7.

J. Kececioglu and David Sankoff. Exact and approximation algorithms for sorting by reversals, with application to genome rearrangement. *Algorithmica*, 13:180–210, 1995. doi: 10.1007/BF01188586.

Ekaterina Khomyakova and Elena V. Konstantinova. Catalogue of the Star graph eigenvalue multiplicities. *Arabian Journal of Mathematics*, 10:115–119, 2021. doi: 10.1007/s40065-019-00271-z. URL https://doi.org/10.1007/s40065-019-00271-z.

Harish Kishnani, Rijubrata Kundu, and Sumit Chandra Mishra. Alternating groups as products of cycle classes. *Discrete Mathematics*, 346(7):113470, 2023. doi: 10.1016/j.disc.2023.113470. URL https://arxiv.org/abs/2207.03165.

Harish Kishnani, Rijubrata Kundu, and Sumit Chandra Mishra. Alternating groups as products of cycle classes—II. *Journal of Algebraic Combinatorics*, 59(3):635–660, 2024. doi: 10.1007/s10801-024-01305-2. URL https://arxiv.org/abs/2210.15354.

Donald E. Knuth. Efficient representation of perm groups. *Combinatorica*, 11:33–43, 1991. doi: 10.1007/BF01375471. URL https://doi.org/10.1007/BF01375471.

Donald E. Knuth. *The Art of Computer Programming, Volume 3: Sorting and Searching*. Addison-Wesley, 2 edition, 1998. Exercise 5.1.4–43.

Richard E. Korf. Finding optimal solutions to rubik's cube using pattern databases. In *Proceedings of AAAI/IAAI*, pp. 700–705, 1997. URL https://dl.acm.org/doi/10.5555/1867406.1867515.

Roi Krakovski and Bojan Mohar. Spectrum of Cayley graphs on the symmetric group generated by transpositions. *Linear Algebra and its Applications*, 437(3):1033–1039, 2012. doi: 10.1016/j.laa.2012.03.033. URL https://doi.org/10.1016/j.laa.2012.03.033.

Henri Mühle and Philippe Nadeau. A poset structure on the alternating group generated by 3-cycles. *Algebraic Combinatorics*, 2(6):1285–1310, 2019. doi: https://doi.org/10.5802/alco.83. URL https://alco.centre-mersenne.org/item/ALCO_2019__2_6_1285_0/.

David A Nash and Sara Randall. How do you fix an oval track puzzle? *Mathematics Magazine*, 91 (5):348–358, 2018.

Ya. N. Nuzhin. Generating triples of involutions of alternating groups. *Mathematical Notes*, 51(4): 389–392, 1992. doi: https://doi.org/10.1007/BF01250552. URL https://link.springer.com/article/10.1007/BF01250552.

Tomas Rokicki, Herbert Kociemba, Morley Davidson, and John Dethridge. The diameter of the rubik's cube group is twenty. *SIAM Review*, 56(4):645–670, 2014. doi: 10.1137/140973499. URL https://doi.org/10.1137/140973499.

Bernardino Romera-Paredes, Mohammadamin Barekatain, Alexander Novikov, Matej Balog, M. Pawan Kumar, Emilien Dupont, et al. Mathematical discoveries from program search with large language models. *Nature*, 625:468–475, 2024. doi: 10.1038/s41586-023-06924-6. URL https://doi.org/10.1038/s41586-023-06924-6.

Ali Shehper, Anibal M. Medina-Mardones, Lucas Fagan, Bartlomiej Lewandowski, Angus Gruen, Yang Qiu, Piotr Kucharski, Zhenghan Wang, and Sergei Gukov. What makes math problems hard for reinforcement learning: A case study, 2024. URL https://arxiv.org/abs/2408.15332.

Charles C. Sims. Computational methods in the study of permutation groups. In *Computational Problems in Abstract Algebra*, pp. 169–183. Pergamon, 1970. doi: 10.1016/B978-0-08-012975-4.50020-5. URL https://doi.org/10.1016/B978-0-08-012975-4.50020-5.

Kyo Takano. Self-supervision is all you need for solving Rubik's cube. *Transactions on Machine Learning Research*, 2023. URL https://openreview.net/forum?id=bnBeNFB27b.

Katsuhisa Yamanaka, Erik D. Demaine, Takehiro Ito, Jun Kawahara, Masashi Kiyomi, Yoshio Okamoto, Toshiki Saitoh, Akira Suzuki, Kei Uchizawa, and Takeaki Uno. Swapping labeled tokens on graphs. In *Fun with Algorithms*, volume 8496 of *Lecture Notes in Computer Science*, pp. 364–375. Springer, 2014. doi: 10.1007/978-3-319-07890-8_31. URL https://erikdemaine.org/papers/TokenReconfiguration_FUN2014/paper.pdf.

A CATALOGUE OF GROWTH AND DIAMETER CONJECTURES

The catalogue collects the growth and diameter hypotheses developed through exact computation and RL-guided exploration. It is organized by generating family: Table 6 gives the groups and diameter formulas, Tables 7 and 8 describe growth distributions, and Table 9 records related structural properties. The *Details* column links to expanded appendix discussions wherever available.

What "growth" means. For a group G_n with generators X_n, let $\gamma_n(r) = |\{g \in G_n : d(e, g) = r\}|$ be the number of elements at distance r from the identity. The normalized sequence $\gamma_n(r)/|G_n|$ is the distance distribution of a uniformly sampled element. Its support ends at the diameter $D(n)$; its mean, mode, variance, and shape are the growth statistics listed below. Thus the catalogue studies both growth across distance layers r and how these quantities scale with the family parameter n.

How to turn a cell into a conjecture. Read the row's group and generating set together with the chosen column. A diameter cell $f(n)$ states the candidate law $\operatorname{diam}\operatorname{Cay}(G_n, X_n) = f(n)$, with the orientation, parameter range, and exceptions specified in the detailed entry. For example, the LRX row means:

> For every $n \geq 4$, the undirected Cayley graph of S_n generated by $(1\,2\,\cdots\,n)$, its inverse, and $(1\,2)$ is conjectured to have diameter $n(n-1)/2$.

This is an exact quadratic diameter conjecture, expanded in Appendix G.6. The same row's mean-distance cell instead proposes the empirical scaling $\mathbb{E}[d(e, g)] \approx 0.38n^2 - n$ for uniform $g \in S_n$; its Gumbel entry concerns the shape of the normalized growth distribution. A symbol $\approx$ describes an approximate fit, rather than an exact identity.

Follow the expanded statements. The Details column leads to generator definitions, growth vectors, and full statements. Examples include LX/RX (Conjecture 2), distinguished-letter cycles (Appendix G.12), cubic pancakes (Appendix H.2), and matrix groups (Appendix G.17.7). Appendix B explains how exact layers, formula fitting, and RL-guided search produce and test these conjectures. Each formula uses the orientation, parameter range, and small-size exceptions specified in its detailed entry.

Reading the notation. $^{\mathrm{C}}$ marks a conjecture from this study, $^{\mathrm{P}}$ a proved entry, $^{\mathrm{L}}$ a literature conjecture, and $^{\mathrm{E}}$ a finite enumeration result on the range given in the details. The symbols $+$ and $-$ are availability indicators; ? means that no clear formula is recorded, and a dash denotes an empty entry. A marker without a formula points to a result requiring a fuller description. Parity shorthand $a|b$ gives alternatives in the order specified by the detailed statement; an additive I denotes a periodic correction. An I suffix on a family includes inverse generators.

The distribution labels Gauss and Gumbel describe fitted growth shapes; Fib and Stirling refer to combinatorial growth formulas. Antipodes are elements at maximum distance. The Algorithm and Metric columns record decomposition procedures and explicit word-distance formulas; NP/c denotes NP-hard exact decomposition with a stated factor-c approximation, and a superscript O denotes an optimal algorithm. For spectra, Int means integral, Wig denotes a Wigner-type profile, and Uni denotes an approximately uniform profile.

Table 6: Diameter formulas and conjectures by generator family. The Details column points to expanded family definitions, conjectures, and results in this appendix.

Family	Group	Diameter	Details
Coxeter	S_n	$\frac{n(n-1)}{2}$	§G.1
Cyclic Coxeter	S_n	$\left\lfloor \frac{n^2}{4} \right\rfloor$	§G.2
LRX	S_n	$\frac{n(n-1)}{2}^{\mathrm{L}}$	§G.6
LX-Glushkov	S_n	$\frac{3n^2-8n+9\|12}{4}^{\mathrm{C}}$	§G.6.1
LARX	S_n	$\frac{n^2-2\|5}{2}^{\mathrm{C}}$	§G.9
LARX+I	S_n	$\frac{n(n+6)-12\|19}{4}^{\mathrm{C}}$	§G.9
LSL	S_n	$\frac{n(n-3)}{2} + 3^{\mathrm{C}}$	§G.7
LSL+I	S_n	$\frac{n(n+4)}{4} - 3\|4.25^{\mathrm{C}}$	§G.7
3-cyc	A_n	$\left\lfloor \frac{n}{2} \right\rfloor$	§G.10
$(0ij)$	A_n	$\left\lfloor \frac{3(n-1)}{4} \right\rfloor$	§G.11
$(01i)$	A_n	$\frac{3n-5}{2} + \frac{i^n+(-i)^n}{4}^{\mathrm{C}}$	§G.12
$(01i)I$	A_n	$\left\lfloor \frac{3n-6}{2} \right\rfloor^{\mathrm{P}}$	§G.12
$(i, i+1, i+2)$	A_n	$\left\lfloor \frac{n^2+1}{4} \right\rfloor^{\mathrm{C}}$	§G.13
$(i, i+1, i+2)I$	A_n	$\left\lfloor \frac{n(n-1)}{4} \right\rfloor^{\mathrm{C}}$	§G.13
$(i, \ldots, i+3)$	S_n	$\approx 0.3n^{2\mathrm{C}}$	§G.13
$(i, \ldots, i+3)I$	S_n	$\approx 0.16n^{2\mathrm{C}}$	§G.13
$(i, i+1, i+2)C$	A_n	$\approx \frac{n(n+2)}{8} + I^{\mathrm{C}}$	§G.14
$(i, i+1, i+2)CI$	A_n	$\left\lfloor \frac{n^2}{8} \right\rfloor^{\mathrm{C}}$	§G.14
$(i, \ldots, i+3)C$	S_n	?	§G.14
$(i, \ldots, i+3)CI$	S_n	?	§G.14
Pref.cyc	S_n	$n-1$	§G.15
Pref.cyc+I	S_n	$n-1^{\mathrm{C}}$	§G.15
Down.cyc	S_n	$n-1^{\mathrm{C}}$	§G.16
Down.cyc+I	S_n	$n-1^{\mathrm{C}}$	§G.16
Inc.3cyc	A_n	$n-1\|2^{\mathrm{C}}$	—
Inc.4cyc	S_n	$n-1^{\mathrm{C}}$	—
RapaportM1	S_n	$\left\lfloor \frac{3n}{2} \right\rfloor^{\mathrm{C}}$	§G.17.1
RapaportM2	S_n	$\approx \frac{n^2+n}{2}^{\mathrm{C}}$	§G.17.1
Globes n/1	+	$\left\lceil \frac{5n+12}{4} \right\rceil^{\mathrm{C}}$	§G.17.4
3PancakeS_1	S_n	$\frac{3n(n+2)-48}{8}^{\mathrm{C}}$	§H.2
3PancakeS_2	S_n	$^{\mathrm{C}}$	§H.2
3PancakeS_3	S_n	$^{\mathrm{C}}$	§H.2
3PancakeS_4	S_n	$^{\mathrm{C}}$	§H.2
3PancakeS_5	S_n	$^{\mathrm{C}}$	§H.2
3PancakeS_6	S_n	$\frac{3n(n+2)-48}{8}^{\mathrm{C}}$	§H.2
3PancakeS_7	S_n	$^{\mathrm{C}}$	§H.2
Pancake	S_n	$\approx 1.2n?$	§H.1
Reversals	S_n	$n-1$	§H.4
sReversals	B_n	$n+1$	§H.4
Transposons	S_n	$\left\lceil \frac{n+1}{2} \right\rceil^{\mathrm{E}}$	§H.5
(i, j)	S_n	$n-1$	§G.3
$(1, i)$(Star)	S_n	$\left\lfloor \frac{3(n-1)}{2} \right\rfloor$	§G.4
G-star transp.	S_n	$+$	§G.5
RMK	—	—	§G.8
Nuzhin	A_n	—	§G.17.2
Block	S_n	—	§H.5

Table 7: Growth profiles and typical distances. Distribution, growth-formula, mean, and mode entries are recorded separately from the diameter. Families with no recorded entry in this panel are omitted.

Family	**Distribution**	**Growth formula**	**Mean**	**Mode**
Coxeter	Gauss	+	$n(n-1)/4$	$n(n-1)/4$
Cyclic Coxeter	Gauss$^{\mathrm{C}}$	?	$0.17(n^2-n+1)^{\mathrm{C}}$	≈Mean$^{\mathrm{C}}$
LRX	Gumbel$^{\mathrm{C}}$	?	$\approx 0.38n^2 - n^{\mathrm{C}}$	$\approx 0.39n^2 - n^{\mathrm{C}}$
LX-Glushkov	Gumbel$^{\mathrm{C}}$	Fib /?	$\approx 0.57n^2 - 2n^{\mathrm{C}}$	$\approx 0.57n^2 - 1.6n^{\mathrm{C}}$
LARX	?	?	$0.4n^2 - 0.7n^{\mathrm{C}}$	≈Mean$^{\mathrm{C}}$
LARX+I	?	?	$\approx \frac{n(n+1)}{4}^{\mathrm{C}}$	≈Mean$^{\mathrm{C}}$
LSL	?	?	$\approx 0.4n^2 - 1.5n^{\mathrm{C}}$	≈Mean$^{\mathrm{C}}$
LSL+I	?	?	$\approx 0.2n^2$	$\approx 0.2n^2$
3-cyc	?	$+-$	$\frac{n}{2} - \frac{1}{4}\ln n + O(1)$	?
$(0ij)$	?	?	$\approx 0.55n^{\mathrm{C}}$	≈Mean$^{\mathrm{C}}$
$(01i)$	?	?	$\approx n - 2^{\mathrm{C}}$	$n - 1^{\mathrm{C}}$
$(01i)I$	?	?	$\approx n + 1.25\ln(n) + \cdots^{\mathrm{C}}$	≈Mean$^{\mathrm{C}}$
$(i, i+1, i+2)$	Gauss$^{\mathrm{C}}$	?	$\approx D/2^{\mathrm{C}}$	$\approx D/2^{\mathrm{C}}$
$(i, i+1, i+2)I$	Gauss$^{\mathrm{C}}$	?	$\approx D/2^{\mathrm{C}}$	$\approx D/2^{\mathrm{C}}$
$(i, \ldots, i+3)$	?	?	$\approx 0.16n^{2\mathrm{C}}$	$\approx 0.15n^{2\mathrm{C}}$
$(i, \ldots, i+3)I$	?	?	$\approx 0.036n^{2\mathrm{C}}$	$\approx 0.045n^{2\mathrm{C}}$
$(i, i+1, i+2)C$	?	?	$\approx 0.085n^{2\mathrm{C}}$	$\approx 0.065n^{2\mathrm{C}}$
$(i, i+1, i+2)CI$	?	?	$\approx 0.08n^{2\mathrm{C}}$	$\approx 0.086n^{2\mathrm{C}}$
Down.cyc	?	Stirling	$\approx 0.86n^{\mathrm{C}}$	≈Mean$^{\mathrm{C}}$
Down.cyc+I	?	?	$\approx 0.75n^{\mathrm{C}}$	≈Mean$^{\mathrm{C}}$
Inc.3cyc	?	?	$\approx 0.5n^{\mathrm{C}}$	≈Mean$^{\mathrm{C}}$
Inc.4cyc	?	?	$\approx 0.5n^{\mathrm{C}}$	≈Mean$^{\mathrm{C}}$
RapaportM1	?	?	$\approx 1.4n^{\mathrm{C}}$	≈Mean$^{\mathrm{C}}$
RapaportM2	?	?	$\approx \frac{n^2-3n}{2}^{\mathrm{C}}$	≈Mean$^{\mathrm{C}}$
Globes n/1	?	?	$\approx n + 1^{\mathrm{C}}$	$\approx n + 1^{\mathrm{C}}$
Pancake	?	?	$< \frac{17n}{12}$	$\approx n/2^{\mathrm{L}}$
Reversals	?	?	$\approx n/2$	≈Mean?
Transposons	?	?	$\Theta(n)$	$\Theta(n)$
(i, j)	?	Stirling	$\approx n - \ln n$	$\approx n - \ln n$
$(1, i)$(Star)	?	?	$\approx n - \ln n$	$\approx n - \ln n$

Table 8: Higher moments of the distance distribution. Families with no recorded variance, skewness, or kurtosis entry are omitted.

Family	**Variance**	**Skewness**	**Kurtosis**
Coxeter	$+$	$\to 0$	$\to 0$
Cyclic Coxeter	?	$\to 0^{\mathrm{C}}$	$\to 0^{\mathrm{C}}$
LRX	?	$\to -0.7^{\mathrm{C}}$	$\to 3.3^{\mathrm{C}}$
LX-Glushkov	?	$\to -0.7^{\mathrm{C}}$	$\to 0.5^{\mathrm{C}}$
$(01i)I$	$^{\mathrm{C}}$	$^{\mathrm{C}}$	$^{\mathrm{C}}$
$(i, i+1, i+2)$	$\approx \frac{n^3}{100}$	$\to 0^{\mathrm{C}}$	$\to 0^{\mathrm{C}}$
$(i, i+1, i+2)I$	$\approx \frac{n^3}{100}{}^{\mathrm{C}}$	$\to 0^{\mathrm{C}}$	$\to 0^{\mathrm{C}}$
$(i, \ldots, i+3)$	?	$\approx 0^{\mathrm{C}}$	$\approx 0^{\mathrm{C}}$
RapaportM2	?	$\to -0.6^{\mathrm{C}}$	$\to 0.5^{\mathrm{C}}$
Pancake	$\approx 0.2n$?	?	?
Reversals	$\approx 0.05n$?	?	?
sReversals	$\approx 0.05n$	?	?
(i, j)	$\approx \ln n$	$\approx \frac{1}{\sqrt{\ln n}}$	$\approx \frac{1}{\ln n}$
$(1, i)$(Star)	$\approx \ln n$	—	—

Table 9: Antipodes, algorithms, metric formulas, spectra, and mixing times. Families with no recorded entry in this panel are omitted.

Family	**Antipodes**	**Algorithm**	**Metric**	**Spectrum**	**Mixing time**
Coxeter	1	Bubble	$+$	?	?
Cyclic Coxeter	$1\vert 2^{\mathrm{C}}$	?	+	Wig$^{\mathrm{C}}$	?
LRX	$^{\mathrm{C}}$	$^{\mathrm{C}}$	?	Uni$^{\mathrm{C}}$	$> n^{3\mathrm{C}}$
LX-Glushkov	$^{\mathrm{L}}$	$^{\mathrm{C}}$	?	?	?
LARX	$+^{\mathrm{C}}\vert ?$	?	?	?	?
LARX+I	$+^{\mathrm{C}}$	?	?	?	?
LSL	$+^{\mathrm{C}}$	?	?	?	?
3-cyc	$+$	$+$	$+$	Int	?
$(01i)$	?	$+^{\mathrm{P}}$	?	?	?
$(01i)I$	$^{\mathrm{C}}$	$^{\mathrm{P}}O$	$^{\mathrm{P}}$	Int$^{\mathrm{P}}$	?
$(i, i+1, i+2)I$	$+^{\mathrm{C}}$	?	?	?	?
$(i, i+1, i+2)CI$	$+^{\mathrm{C}}$	?	?	?	?
Down.cyc	$+^{\mathrm{C}}$	?	?	?	?
Down.cyc+I	$+^{\mathrm{C}}$	?	?	?	?
Inc.3cyc	$+-^{\mathrm{C}}$	?	?	?	?
Pancake	$+-$	NP/2?	$-$	?	?
Reversals	$+$	NP/1.5	$-$	?	?
sReversals	$+-$	$+$	$+-$	?	?
Transposons	$-$	NP/1.375	$-$	?	?
(i, j)	$+$	$+$	$+$	Int	$n \ln n$
$(1, i)$(Star)	$+$	$+$	$+$	Int	?

B From exact growth computations and RL-guided search to conjectures

The catalogue is the output of a computational discovery process with two complementary components. Exact breadth-first search measures growth at sizes that can be enumerated. Learned search finds short generator words at larger sizes, where enumeration is no longer practical. The resulting data suggest formulas, explicit candidate antipodes, and constructive decomposition rules. Mathematical interpretation then turns those patterns into the family-specific statements in Appendices G and H.

B.1 Specify a family and compute its exact small instances

Fix a parameterized group and generating rule (G_n, X_n), including whether edges are directed and whether inverse generators are included. These choices are part of the conjecture: changing the move set changes both the diameter and the growth sequence. For a connected Cayley graph, exact BFS from the identity gives the distance layers

$$L_{n,r} = \{g \in G_n : d(e, g) = r\}, \qquad \gamma_n(r) = |L_{n,r}|, \qquad D_n = \max\{r : \gamma_n(r) > 0\}.$$

Completed enumeration therefore gives the diameter and the whole growth distribution in one computation. It also identifies the last layer of antipodes, whose permutation patterns can suggest candidate extremal elements for the next sizes. The same calculation on a Schreier graph gives growth from the chosen root and its eccentricity; any diameter statement additionally uses the relevant symmetry or further root computations.

For example, the catalogue's mean and variance columns summarize

$$\mu_n = \frac{1}{|G_n|} \sum_r r\gamma_n(r), \qquad \sigma_n^2 = \frac{1}{|G_n|} \sum_r (r - \mu_n)^2 \gamma_n(r).$$

The mode is a layer with maximal $\gamma_n(r)$. Rescaling the horizontal axis by $(r - \mu_n)/\sigma_n$ permits comparison of growth shapes across sizes. A diameter formula, a mean-distance fit, and a distributional conjecture thus describe different features of the same exact growth data. This is the sense in which the paper studies *growth* rather than only the performance of a pathfinding solver.

B.2 Learn a heuristic that can explore beyond enumeration

At larger n, the transition rule still supplies training examples and search successors without storing the whole graph. Random walks give states together with lengths of known paths to the target. Diffusion warm-up trains the network on these inexpensive labels. Bellman refinement then compares legal successors using the one-step target in Equation 2. This is the RL component: it trains the value estimate using the shortest-path relation rather than continuing to regress only on random-walk depth.

The refined value is used to rank the states retained by beam search (Algorithm 1). Better ranking can expose short decompositions that a weaker heuristic misses under the same search settings. A returned generator word is replayed algebraically, so its validity does not depend on trusting the network. Directed families use the stated legal moves and training paths in the required direction.

The outer mathematical exploration varies the size, generating family, or candidate extremal state. It need not itself be an RL policy. Patterns in exact last layers supply natural targets for large-instance search; learned scores and the difficulty of finding short words can also prioritize states for further examination. Such prioritization is a way to find candidates, while the mathematical evidence comes from exact computations, valid words, or separate bounds. The catalogue combines these sources; the RL experiments concern the learned search component rather than an assertion that every entry was generated by RL.

B.3 Fit formulas and test the proposed statements

For a fixed family, list the exact diameters across n and compare their finite differences. Constant first or second differences suggest linear or quadratic formulas. If the pattern depends on parity or another congruence condition, examine each residue class separately. A candidate of period q has the form

$$D_n = p_j(n), \qquad n \equiv j \pmod{q}, \qquad n \geq N,$$

where the degree, period, threshold, and small-size exceptions belong to the statement. The same approach applies to exact growth statistics; approximate numerical fits retain the symbol $\approx$ and are not presented as exact identities.

Further computations test the candidate in distinct ways. A completed exact BFS at a new size directly checks a diameter formula and every growth statistic. For a proposed antipode a_n with claimed distance $f(n)$, any valid word shorter than $f(n)$ refutes that state-distance claim. A certified lower bound larger than $f(n)$ refutes a proposed diameter upper bound. Conversely, finding a path of length $f(n)$ for one state supplies only an upper bound on that state's distance; a diameter upper bound must cover every state. These checks explain why searching for shorter words is useful even when the objective is to understand large distances.

For subsequent tests, a reproducible record fixes the conjecture before extending the size range and retains its generating rule, orientation, exactly computed sizes, candidate formula, and search configuration. Freezing the period and degree before evaluating new sizes distinguishes a new test from refitting. When a test fails, inspecting the responsible state or residue class can suggest a corrected threshold, a periodic term, or a more specific generating family.

B.4 Worked example: LRX diameter and a candidate antipode

For LRX, let $G_n = S_n$ and

$$X_n = \{L, L^{-1}, X\}, \qquad L = (1\,2\,\cdots\,n), \qquad X = (1\,2).$$

The catalogue proposes

$$\operatorname{diam}\operatorname{Cay}(S_n, X_n) = \frac{n(n-1)}{2}, \qquad n \geq 4,$$

with the expanded family discussion in Appendix G.6. Exact small-instance growth provides a sequence of diameters and examples of the farthest permutations. A corresponding large-instance test asks how short a word search can find for the designated candidate antipode, rather than attempting to store all $n!$ states.

At $n = 28$, the formula gives $28 \cdot 27/2 = 378$. Table 5 records a best word of length 382 after diffusion warm-up and Bellman refinement, and a median successful length of 402. The diffusion-only comparison has a median successful length of 516. Thus refinement brings the search substantially closer to the mathematical target in this experiment; the best recorded refined word is four moves above it. The unequal training budgets and successful-run sets are specified with the experiment. The paths themselves do not prove the diameter formula. The separate mathematical result about the benchmark state's distance is discussed in the main text, and a matching upper bound for every LRX state is still required to establish the diameter conjecture.

Reading an entry as the end of this process. A catalogue row therefore packages a generating rule, one or more observed patterns, and a precise proposed mathematical statement. Its diameter cell proposes the end of the growth support; its mean, mode, and shape cells describe the distribution inside that support. Follow the row's appendix reference for the generators, formulas, examples, and exceptions, and use the status markers to distinguish conjectures from established formulas. Exact enumeration supplies the finite foundation, while RL-guided search extends the range of states on which the proposed structure can be explored and tested.

C Obstructions to a universal quasi-polynomial law

The following examples show why structural restrictions on generating families are necessary. The fixed-conjugacy-type conjecture in Section 5 imposes such a restriction. Finding a wider class that covers the catalogue remains an open problem.

C.1 Explicit switching between standard families

Let $A_n = \{(i\ i+1) : 1 \le i < n\}$ and $B_n = \{(1\ i) : 2 \le i \le n\}$. Their undirected Cayley diameters are $a_n = \binom{n}{2}$ and $b_n = \lfloor 3(n-1)/2 \rfloor$, respectively. Choose a binary sequence ϵ_n that is not eventually periodic, and set $X_n = A_n$ when $\epsilon_n = 1$ and $X_n = B_n$ otherwise. For an explicit computable example, let $\epsilon_n = 1$ exactly when n is a power of two.

Suppose $D_X(n)$ were eventually quasi-polynomial with period q. Refine the period to $\mathrm{lcm}(q, 2)$, so that on each residue class the diameter and both alternatives agree with polynomials p, a, b. Then $(p-a)(p-b)$ vanishes at infinitely many integers and is identically zero. Hence $p = a$ or $p = b$ on that class. Since $a_n \neq b_n$ for sufficiently large n, the selector must eventually be constant on every residue class. This contradicts the choice of ϵ_n. Simplicity or computability of an individual generating rule is therefore insufficient.

C.2 A broom family with fractional-power growth

For $1 \le m \le n$, take the path $1 - 2 - \cdots - m$ and attach vertices $m+1, \ldots, n$ to vertex 1. Let $X_{n,m}$ consist of the edge transpositions. The underlying tree is connected, so these transpositions generate S_n. We have, uniformly for $n \ge 2$,

$$\operatorname{diam} \mathrm{Cay}(S_n, X_{n,m}) = \Theta(n + m^2).$$

For the lower bound, an n-cycle requires at least $n-1$ transpositions. Independently, reversing the path labels has total token-to-target displacement $\sum_{i=1}^{m} |m+1-2i| = \lfloor m^2/2 \rfloor$. One allowed edge swap changes this potential by at most two, giving an $\Omega(m^2)$ obstruction.

For the upper bound, factor any permutation into star transpositions centered at vertex 1 using its disjoint cycles. Each non-hub vertex occurs at most twice: a cycle not containing the hub uses one of its vertices twice and each of its other vertices once. A hub transposition $(1\ v)$ can be implemented along the tree path in $2d_T(1, v) - 1$ edge swaps. Thus the total cost is at most

$$2\sum_{v \neq 1}(2d_T(1, v) - 1) \le 4\left(n - m + \frac{m(m-1)}{2}\right) = O(n + m^2).$$

Taking $m = \lfloor n^{3/4} \rfloor$ gives diameter $\Theta(n^{3/2})$. This is incompatible with eventual quasi-polynomiality: on each infinite residue class, a nonzero polynomial has integer growth degree. The example is a single explicit parameter rule. These asymptotic arguments are obstructions, not new exact diameter formulas.

D BFS implementations

A key feature of CayleyPy is that BFS is implemented in the style of ML systems. States are encoded as tensors, generator application is batched, deduplication is performed by vectorized hashing, and previously seen states are removed by tensorized membership tests against sorted hash arrays. The recorded benchmarks compare this implementation with the tested general-purpose system. Exactness requires injective state identifiers or explicit collision resolution; unresolved hash collisions invalidate an exactness claim. This makes the implementation close in spirit to a PyTorch data-processing pipeline: the frontier is a batch, the neighbor oracle is a batched transformation, and the next layer is obtained by sorting, masking, and compacting tensors.

The basic tensorized BFS backend is summarized in Algorithm 3. The important point is that the graph is never explicitly constructed. The algorithm stores only the current layer, selected stored layers, and hashes of previously seen states. When the generating set is inverse-closed, only the last

Algorithm 2 BFS-guided conjecture discovery

Require: Generator families $\mathcal{F}$, sizes $\mathcal{I}$, fitting class $\mathcal{Q}$
Ensure: Candidate formulas for diameters, growth functions, and extremal states

for all families $X_\bullet \in \mathcal{F}$ **do**
  Initialize data table $T_X \leftarrow \emptyset$.
  for all sizes $n \in \mathcal{I}$ **do**
    Construct the implicit graph

$$\mathcal{G}_{n,X} = \mathrm{Cay}(S_n, X_n)$$

  or the corresponding Schreier graph.
    Choose a backend: tensorized BFS, distributed BFS, NumPy BFS, or bitmask BFS.
    Run exact BFS from the identity or chosen base vertex.
    Record the growth sequence

$$\gamma_{n,X}(r) = |L_r|.$$

    if BFS completes **then**
      Record the exact Cayley diameter (or root eccentricity for a Schreier graph)

$$D_X(n) = \max\{r : L_r \neq \emptyset\}.$$

      Store representatives of the last layer $L_{D_X(n)}$.
    else
      Store the explored growth prefix and final computed layer.
      Mark the instance for RL-guided or beam-search continuation.
    end if
    Add the computed data to T_X.
  end for
  Fit $D_X(n)$ and growth statistics against candidate laws in $\mathcal{Q}$.
  In particular, search for quasi-polynomial formulas

$$D_X(n) = p_{n \bmod s}(n).$$

  Validate each formula on held-out sizes when exact data are available.
  Store surviving formulas as conjectures.
end for
return the conjecture list with BFS evidence.

Table 10: BFS implementations and variants used in CAYLEYPY.

Implementation	Main use	Main optimization
Tensorized BFS	General exact growth and diameters	Batched generator application and hash-based deduplication
Distributed BFS	Multi-GPU exact BFS	Hash-sharded ownership of states across devices
NumPy BFS	Low-overhead exact growth computation	Compact CPU arrays and simple layer updates
Bitmask BFS	Memory-limited permutation-group BFS	Three bitsets per state-space chunk
Interactive BFS	Early stopping and custom probes	Computes one layer at a time with hooks
Meet-in-the-middle	Shortest-path certification	Intersects two BFS balls grown from opposite sides

two hash layers are needed: a neighbor of a vertex in L_r can lie only in L_{r-1}, L_r, or L_{r+1}. This reduces memory usage in undirected Cayley graphs.

The distributed version keeps the same logic but shards the frontier by hash. Each GPU owns the states whose hashes fall into a fixed residue class modulo the number of GPUs. After local expansion, newly generated candidates are sent to their owner GPU, deduplicated there, and filtered against the owner's seen-state hashes. This is again an ML-systems-style implementation: the expensive operation is not symbolic algebra but tensor movement, sorting, masking, and batched generator application.

For some permutation-group computations, memory is the limiting resource rather than arithmetic throughput. In this regime CAYLEYPY also provides a bitmask BFS backend. The idea is to partition the permutation space into chunks and maintain three bitsets per chunk: already visited states, the

Algorithm 3 Single-device tensorized BFS in CAYLEYPY

Require: Implicit Cayley or Schreier graph $\mathcal{G}$, start states S_0, maximal diameter R, batch size B
Ensure: Growth sequence γ, stored layers, and completion flag

$X_0 \leftarrow \mathrm{Encode}(S_0)$ ▷ tensor of encoded states
$(X_0, H_0) \leftarrow \mathrm{UniqueStates}(X_0)$
$\mathcal{V} \leftarrow [H_0]$ ▷ sorted hashes of seen layers
$\gamma \leftarrow [|X_0|]$
$\mathrm{Layers}[0] \leftarrow \mathrm{Decode}(X_0)$
for $r = 0, \ldots, R-1$ **do**
  $\mathcal{C} \leftarrow [\,], \mathcal{H} \leftarrow [\,]$
  Split X_r into tensor batches $X_r^{(1)}, \ldots, X_r^{(m)}$ of size at most B.
  for $j = 1, \ldots, m$ **do**
    $Y \leftarrow \mathrm{Neighbors}(X_r^{(j)})$ ▷ batched application of all generators
    $(Y, H_Y) \leftarrow \mathrm{UniqueStates}(Y)$ ▷ deduplicate inside the batch
    $M \leftarrow \mathbf{1}$
    for all hash tensor $H_{\mathrm{seen}} \in \mathcal{V}$ **do**
      $M \leftarrow M \wedge \neg\mathrm{IsInSorted}(H_Y, H_{\mathrm{seen}})$
    end for
    for all previous accepted batch hashes $H' \in \mathcal{H}$ **do**
      $M \leftarrow M \wedge \neg\mathrm{IsInSorted}(H_Y, H')$
    end for
    $Y \leftarrow Y[M], H_Y \leftarrow H_Y[M]$
    Append Y to $\mathcal{C}$, append H_Y to $\mathcal{H}$
  end for
  $X_{r+1} \leftarrow \mathrm{VStack}(\mathcal{C})$
  $H_{r+1} \leftarrow \mathrm{Sort}(\mathrm{HStack}(\mathcal{H}))$
  if $|X_{r+1}| = 0$ **then**
    return $(\gamma, \mathrm{Layers}, \mathrm{completed} = \mathrm{true})$
  end if
  Append $|X_{r+1}|$ to γ
  if $|X_{r+1}|$ is below storage threshold **then**
    $\mathrm{Layers}[r+1] \leftarrow \mathrm{Decode}(X_{r+1})$
  end if
  Append H_{r+1} to $\mathcal{V}$
  if the generators are inverse-closed **then**
    Keep only the last two tensors in $\mathcal{V}$.
  end if
end for
return $(\gamma, \mathrm{Layers}, \mathrm{completed} = \mathrm{false})$

last BFS layer, and a temporary buffer for newly generated states. This sacrifices some generality but gives an extremely compact exact BFS representation.

E PERFORMANCE BENCHMARKS

Growth computation is an exact BFS task: starting from the identity, the algorithm computes all layers

$$L_r = \{g : d(e, g) = r\},$$

and hence obtains the full growth sequence

$$\gamma(r) = |L_r|.$$

For connected Cayley graphs, the diameter is then the largest r for which $L_r \neq \emptyset$.

The comparison is focused on exact growth computation, not on membership testing or symbolic manipulation. All timings in Table 11 are wall-clock times in seconds on Kaggle CPU with 32GB

Algorithm 4 Hash-sharded multi-GPU BFS in CAYLEYPY

Require: Current BFS layer X_r, hashes H_r, seen hash shards $\mathcal{V}_0, \ldots, \mathcal{V}_{G-1}$, GPUs $0, \ldots, G-1$
Ensure: Next BFS layer X_{r+1}

Partition the current layer by owner hash:

$$X_r^{(g)} = \{x \in X_r : \mathrm{Hash}(x) \equiv g \pmod{G}\}.$$

Move $X_r^{(g)}$ and its hashes to GPU g.
for all GPUs $g = 0, \ldots, G-1$ in parallel **do**
    Split $X_r^{(g)}$ into tensor batches.
    for all local batches $B \subseteq X_r^{(g)}$ **do**
        $Y^{(g)} \leftarrow \mathrm{Neighbors}(B)$ ▷ batched generator application on GPU g
        $(Y^{(g)}, H^{(g)}) \leftarrow \mathrm{UniqueStates}(Y^{(g)})$
        for $q = 0, \ldots, G-1$ **do**
            Send

$$\{y \in Y^{(g)} : \mathrm{Hash}(y) \equiv q \pmod{G}\}$$

to owner GPU q.
        end for
    end for
end for
for all GPUs $q = 0, \ldots, G-1$ in parallel **do**
    Receive all candidate states owned by q.

$$(Z^{(q)}, H_Z^{(q)}) \leftarrow \mathrm{UniqueStates}(\text{received candidates}).$$

    for all seen hash tensor $H_{\mathrm{seen}} \in \mathcal{V}_q$ **do**
        Remove seen states:

$$Z^{(q)} \leftarrow \{z \in Z^{(q)} : \mathrm{Hash}(z) \notin H_{\mathrm{seen}}\}.$$

    end for
    Store surviving candidates as $X_{r+1}^{(q)}$.
    Update seen shard:

$$\mathcal{V}_q \leftarrow \mathcal{V}_q \cup \{\mathrm{Hash}(z) : z \in X_{r+1}^{(q)}\}.$$

end for
Gather or keep sharded:

$$X_{r+1} = \bigcup_{q=0}^{G-1} X_{r+1}^{(q)}.$$

return X_{r+1}

Table 11: Exact growth-computation time in seconds for GAP and CAYLEYPY on Kaggle CPU with 32GB RAM. The label "bm" denotes the bitmask BFS backend.

	LRX		Coxeter		Transpositions		Pancake		Reversals	
n	GAP	CAYLEYPY	GAP	CAYLEYPY	GAP	CAYLEYPY	GAP	CAYLEYPY	GAP	CAYLEYPY
6	1.97	0.02	0.01	0.038	0.03	0.02	0.01	0.02	0.04	0.02
7	2.04	0.03	0.12	0.052	0.34	0.03	0.08	0.02	0.41	0.05
8	2.66	0.05	1.32	0.079	3.92	0.09	0.80	0.04	4.24	0.10
9	8.75	0.16	13.99	0.293	52.98	1.03	8.90	0.26	54.45	1.089
10	75.72	1.24	172.38	3.54	737.42	14.14	112.37	3.77	762.54	14.8
11	884	22.5	2352	41	10891	296	1559	72	11138	354
12	12024	658	34470	706	–	3331 (bm)	35387	4923	–	26657
13	–	2670 (bm)	–	7308 (bm)	–	$>$ 12h	–	17694 (bm)	–	$>$ 12h

RAM. The benchmark covers five standard generator families: LRX, Coxeter generators, all transpositions, pancake generators, and reversal generators. Missing entries indicate computations that were not completed under the benchmark constraints. The label "bm" denotes the bitmask BFS backend.

Algorithm 5 Bitmask BFS for permutation groups

Require: Permutation Cayley graph $\mathrm{Cay}(G, S)$, maximal diameter R
Ensure: Growth sequence γ

Partition the permutation space into chunks by a fixed suffix.
For each chunk allocate three bitsets:

$$\texttt{visited}, \quad \texttt{last_layer}, \quad \texttt{buffer}.$$

Encode the identity permutation and mark it in the corresponding chunk.
$\gamma \leftarrow [1]$
for $r = 0, \ldots, R-1$ **do**
    Clear all `buffer` bitsets.
    for all chunks C changed on the previous layer **do**
        Materialize the permutations marked in $C.\texttt{last_layer}$.
        for all generators $s \in S$ **do**
            Apply s to the materialized permutations.
            Rank each resulting permutation inside its chunk.
            Mark the corresponding bit in that chunk's `buffer`.
        end for
    end for
    for all chunks C **do**
        Remove already visited vertices:

$$C.\texttt{buffer} \leftarrow C.\texttt{buffer} \;\&\; \neg C.\texttt{visited}.$$

        $C.\texttt{last_layer} \leftarrow C.\texttt{buffer}$

$$C.\texttt{visited} \leftarrow C.\texttt{visited} \mid C.\texttt{last_layer}.$$

    end for
    $m \leftarrow \sum_C \mathrm{PopCount}(C.\texttt{last_layer})$
    if $m = 0$ **then**
        return γ
    end if
    Append m to γ
end for
return γ

The results show two regimes. For small n, both systems are fast and constant overheads dominate. Starting around S_8, CAYLEYPY is typically one to two orders of magnitude faster on CPU. For example, for Coxeter generators on S_{11}, GAP takes 2352 seconds while CAYLEYPY takes 41 seconds on CPU. For the same instance, the GPU benchmark in Table 12 gives 0.601 seconds on a P100 GPU, corresponding to a speedup of more than $3900\times$ relative to the GAP CPU timing.

The main scalability limitation is memory. To address this, CAYLEYPY includes a bitmask BFS backend that stores the search state in a much more compact form. This backend stores only bit-level information about the visited set, the current layer, and a temporary next-layer buffer. It makes computations for S_{13} feasible with only a few GB of RAM and is used for larger exact computations on more powerful machines.

Table 12 illustrates why the implementation is organized around tensor-style batch operations. For small n, GPU overhead can exceed the cost of the computation itself, and CPU execution is competitive. For larger instances, however, batched generator application and tensorized deduplication lead to substantial acceleration. In the Coxeter case, the P100 timing improves from 41 seconds on CPU to 0.601 seconds on S_{11}, and from 705 seconds on CPU to 207 seconds on S_{12}. The improvement is not only in speed: compact bitmask storage also extends the range of exact experiments, which is crucial for fitting and validating diameter formulas.

These benchmarks do not imply that CAYLEYPY is the fastest possible implementation for every specialized puzzle family. Specialized solvers can be faster on particular hand-optimized instances. The advantage of CAYLEYPY is instead its combination of generality and scalability: the same

Table 12: CAYLEYPY growth-computation time in seconds on different hardware for Coxeter generators. Values of the form $a/b(\mathrm{bm})$ report the standard backend and the bitmask BFS backend.

Coxeter generators, CAYLEYPY				
n	CPU	GPU T4	GPU P100	CPU at TPU v3-8
4	0.013	0.013	0.014	0.010
5	0.029	0.026	0.026	0.022
6	0.038	0.043	0.043	0.037
7	0.052	0.068	0.067	0.067
8	0.079	0.151	0.138	0.087
9	0.293	0.110	0.110	0.140
10	3.539	0.199	0.154	0.641
11	41 / 41 (bm)	1.085	0.601	10.8 / 12 (bm)
12	705 / 512 (bm)	214 (bm)	207 (bm)	187 / 151 (bm)
13	7308 (bm)	3004 (bm)	2867 (bm)	2613 / 2180 (bm)

framework supports directed and undirected Cayley graphs, Schreier graphs, different state encodings, CPU/GPU execution, and the exact BFS data used by the conjecture-discovery pipeline.

	LRX		Coxeter		Transpositions		Pancake		Reversals	
n	GAP	CayleyPy	GAP	CayleyPy	GAP	CayleyPy	GAP	CayleyPy	GAP	CayleyPy
6	1.97	0.02	0.01	0.04	0.03	0.02	0.01	0.02	0.04	0.02
7	2.04	0.03	0.12	0.17	0.34	0.03	0.08	0.02	0.41	0.05
8	2.66	0.04	1.32	0.06	3.92	0.07	0.80	0.04	4.24	0.08
9	8.75	0.10	13.99	0.15	52.98	0.42	8.90	0.15	54.45	0.45
10	75.72	0.24	172.38	0.59	737.42	4.25	112.37	1.01	762.54	4.37
11	884	2.46	2352	12	10891	70.39	1559	15	11138	78
12	12024	62	34470	193	-	2737	35387	477	-	4250
13	-	-	-	-	-	-	-	-	-	-

Coxeter CayleyPy				
n	CPU	GPU T4 x2	GPU P100	TPU v3-8
1	-	-	-	-
2	0.126	0.423	0.394	0.005
3	0.010	0.064	0.061	0.005
4	0.013	0.013	0.014	0.010
5	0.029	0.026	0.026	0.022
6	0.038	0.043	0.043	0.037
7	0.052	0.068	0.067	0.067
8	0.079	0.151	0.138	0.087
9	0.293	0.110	0.110	0.140
10	3.539	0.199	0.154	0.641
11	41.008	1.085	0.601	10.822
12	705.746	-	-	187.126
13	-	-	-	2613.550

In this section, we study the maximum diameter for Cayley graphs of the group S_n by the system of generators $S \subseteq S_n$. We would like to start with a review of the situation when the graph is oriented. That is, the system of generators does not have to contain inverse elements. We conducted separate experiments with sets of different numbers of generators, and it always turned out that the maximum diameter is achieved on sets S consisting of two generators. These experiments justify our approach: to study the maximum diameter, we considered all pairs of permutations. Thus, we find the diameters for $\frac{n!\times(n!-1)}{2} \sim n! \times n!$ pairs of permutations, removing those sets that do not generate S_n. This approach allows you to save all the permutations that achieve the maximum. But this method is not effective for large n.

For $n > 6$, we used a different method. Note that the conjugation of all generators does not change the diameter of the Cayley graph. Therefore, one representative can be chosen for all equivalence classes of generators. And for a pair of generators, you can replace one generator with a fixed

representative. Thus, the search will be $n! \times c$, where c is the number of equivalence classes of permutations from S_n (for example, for $n = 7 : c = 15$). This makes it much easier to iterate and is suitable for large n.
For $n > 9$, we considered special pairs of permutations. We analyzed the results for smaller n and put forward hypotheses.

Remark: in fact, for $n = 3, 4$, a complete search was carried out even for sets of $2, 3, 4, 5$ generators (the maximum was achieved on sets of 2 and 3 generators).

Maximal diameter for Cayley graph of the group S_n (oriented graph)		
n	Maximal diameter	Example of a set of generators
3	3	$(01), (02)$
4	7	$(01), (123)$
5	14	$(01)(23), (0314)$
6	18	$(01)(23)(45), (012)(34)$
7	34	$(01)(23)(45), (052)(146)$
8	44	$(01)(23)(45), (1736)(25)$
9	61	$(01)(23)(45), (3647)(12)(58)$
10	83 may be updated	$(01)(23)(45)(67)(89), (185)(237)(469)$
11	93 may be updated	$(01)(23)(45)(67)(89), (1528)(47)(6, 10)$
12	106 may be updated	$(01)(23)(45)(67)(89), (1, 11, 9, 10)(04)(28)(36)$
13	147 may be updated	$(01)(23)(45)(67)(89), (1, 11, 2, 12)(34)(56)(78)(9, 10)$

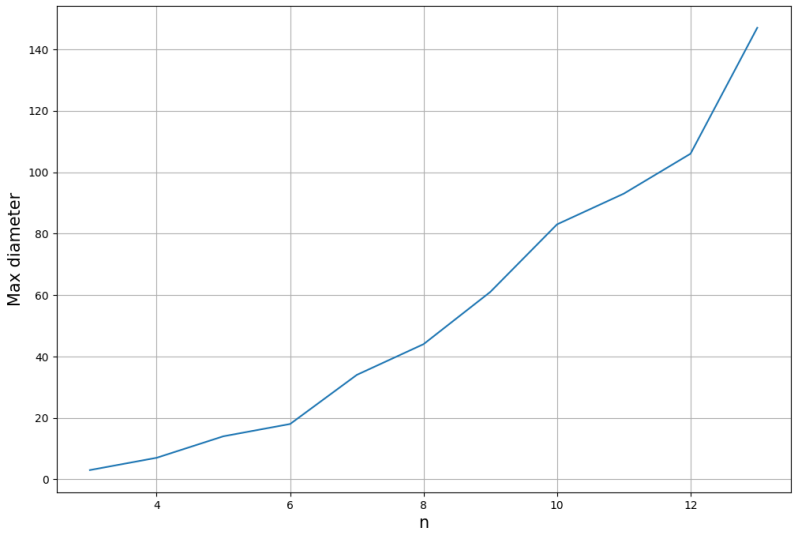


Figure 1: Maximum diameter S_n (oriented graph)

Growth for permutations that give the maximum diameter S_n (oriented graph)		
n	Maximal diameter	Growth
3	3	1, 2, 2, 1
4	7	1, 2, 3, 4, 5, 5, 3, 1
5	14	1, 2, 3, 5, 7, 9, 11, 14, 15, 17, 14, 11, 6, 4, 1
6	18	1, 2, 3, 5, 8, 13, 20, 30, 42, 56, 73, 87, 98, 101, 85, 59, 29, 7, 1
7	34	1, 2, 3, 4, 5, 7, 9, 12, 16, 21, 28, 37, 48, 61, 78, 97, 124, 158, 203, 258, 320, 386, 452, 503, 536, 479, 402, 307, 216, 145, 68, 33, 17, 3, 1
8	44	1, 2, 3, 5, 7, 10, 14, 19, 26, 36, 50, 67, 89, 119, 156, 203, 258, 323, 411, 523, 662, 833, 1027, 1262, 1550, 1883, 2261, 2691, 3118, 3450, 3635, 3514, 3148, 2722, 2195, 1648, 1094, 631, 340, 173, 86, 41, 19, 11, 4
9	61	1, 2, 3, 5, 7, 10, 14, 19, 26, 36, 48, 64, 83, 108, 142, 185, 239, 307, 388, 485, 614, 779, 983, 1228, 1518, 1878, 2323, 2867, 3519, 4281, 5184, 6259, 7563, 9112, 10903, 12952, 15236, 17721, 20367, 22926, 25230, 27077, 27957, 27602, 25637, 22199, 17763, 13133, 9186, 6181, 4149, 2688, 1597, 897, 524, 327, 200, 94, 28, 15, 8, 3
10	83 may be updated	1, 2, 3, 4, 5, 7, 9, 12, 16, 21, 26, 32, 40, 51, 65, 82, 103, 128, 160, 201, 253, 318, 399, 500, 624, 777, 964, 1193, 1476, 1821, 2243, 2773, 3439, 4258, 5258, 6485, 7990, 9815, 12015, 14661, 17871, 21756, 26445, 32115, 38987, 47249, 57108, 68700, 82170, 97707, 115452, 135381, 156909, 179642, 202586, 224842, 244640, 259982, 267676, 263919, 247133, 219255, 181823, 140590, 98943, 62076, 33819, 15938, 6311, 2228, 750, 242, 103, 60, 41, 31, 24, 19, 16, 13, 9, 5, 3, 1
11	93 may be updated	1, 2, 3, 5, 7, 10, 14, 19, 26, 36, 50, 69, 95, 131, 181, 246, 332, 448, 599, 798, 1065, 1414, 1867, 2445, 3199, 4171, 5435, 7074, 9176, 11872, 15295, 19619, 25053, 31766, 40005, 50087, 62485, 77584, 95929, 118121, 144882, 177071, 215735, 262327, 318060, 383812, 461028, 550775, 653969, 771095, 903304, 1051804, 1216067, 1393739, 1581023, 1771655, 1957460, 2129043, 2274957, 2382291, 2437570, 2431027, 2358066, 2218133, 2015103, 1758968, 1466947, 1165490, 884259, 645003, 456070, 314387, 211832, 139610, 89270, 55064, 33391, 20248, 12138, 7062, 4107, 2480, 1559, 982, 572, 297, 138, 74, 49, 31, 20, 12, 7, 3

Growth for permutations that give the maximum diameter S_n (oriented graph)		
n	Maximal diameter	Growth
12	106 may be updated	1, 2, 3, 5, 7, 10, 14, 19, 26, 36, 48, 64, 85, 113, 149, 197, 255, 331, 432, 562, 731, 948, 1218, 1563, 1986, 2513, 3183, 4039, 5110, 6427, 8055, 10106, 12625, 15715, 19512, 24270, 30200, 37435, 46223, 56898, 69760, 85273, 103975, 126512, 153443, 185789, 224171, 269568, 323426, 387228, 462635, 551791, 657245, 781301, 926774, 1097575, 1296891, 1530274, 1802268, 2117595, 2481602, 2900369, 3380811, 3930544, 4562962, 5292340, 6129426, 7082183, 8158652, 9366826, 10715611, 12205544, 13837985, 15601365, 17473303, 19410929, 21357020, 23235842, 24955466, 26395497, 27419742, 27889118, 27673401, 26674169, 24855232, 22270770, 19122232, 15650905, 12149125, 8855632, 6013347, 3781548, 2204185, 1207426, 642547, 337765, 172554, 84245, 40554, 20085, 10167, 4773, 2067, 857, 236, 30, 1
13	147 may be updated	1, 2, 3, 5, 7, 10, 14, 19, 26, 36, 50, 69, 95, 131, 180, 247, 331, 439, 588, 791, 1059, 1409, 1865, 2480, 3292, 4355, 5744, 7568, 9957, 13027, 16936, 21946, 28291, 36321, 46504, 59236, 75049, 94819, 119620, 150248, 187329, 232379, 287576, 355700, 439602, 541562, 664672, 813922, 994489, 1212128, 1473649, 1786937, 2161354, 2608260, 3141608, 3775588, 4525990, 5410239, 6447320, 7653537, 9051054, 10668340, 12536409, 14685405, 17149403, 19953876, 23132836, 26722274, 30756949, 35264400, 40282932, 45853017, 52022966, 58818616, 66247216, 74290985, 82952132, 92226700, 102117465, 112600228, 123605468, 135034466, 146792639, 158760465, 170803871, 182715819, 194300262, 205336190, 215657174, 225070561, 233373924, 240342628, 245685726, 249114325, 250322087, 249011549, 244972983, 238030277, 227990443, 214695080, 198022857, 178104237, 155512681, 131381679, 107225166, 84699078, 65088959, 49026934, 36451377, 26892949, 19746603, 14443684, 10513401, 7602041, 5451218, 3872975, 2719442, 1889394, 1304395, 898396, 616674, 415142, 272979, 176684, 114037, 74791, 49068, 31803, 20035, 12465, 7946, 5220, 3585, 2494, 1693, 1130, 744, 458, 266, 159, 92, 50, 25, 16, 12, 8, 5, 2

Further, we will consider similar undirected graphs. For each generator from the set, it is necessary that the element contained in the set be its inverse. We performed similar calculations, but only in this case we added inverse permutations to the set of generators. Since this set in this way is smaller than the set of all permutation sets, we expect to obtain smaller maximum diameters. Moreover, it can be noted that often the sets of generators on which the maximum is achieved contain

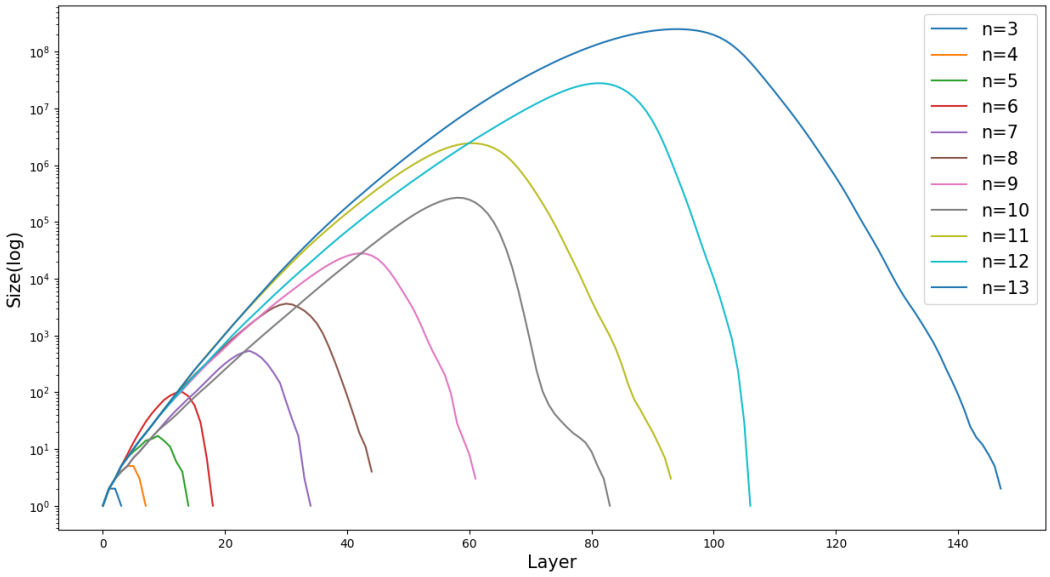


Figure 2: Growth for permutations that give the maximum diameter S_n (oriented graph)

elements that are the opposite of themselves. Thus, the number of elements in the set, on which the maximum is reached, remains small ($k = 2, 3$).

Remark: for $n > 5$, sets of permutations were found separately, which give a larger diameter.

Maximal diameter for Cayley graph of the group S_n (undirected graph)		
n	Maximal diameter	Example of a set of generators
3	3	[0,2,1],[2,1,0]
4	6	$[2,1,0,3],[3,0,2,1],[1,3,2,0]$
5	10	$[4,0,1,2,3],[1,2,3,4,0],[0,1,3,2,4]$
6	15 (16)	$[4,5,3,2,0,1],[2,5,0,3,1,4],[2,4,0,3,5,1]$ $([0,1,2,3,5,4],[0,2,1,4,3,5],[1,0,3,2,5,4])$
7	28 (30)	$[1,0,3,2,5,4,6],[2,6,5,3,1,0,4],[5,4,0,3,6,2,1]$ $([0,1,3,2,4,6,5],[0,4,6,5,1,3,2],[6,1,3,2,5,4,0])$
8	33 (39)	$[3,7,5,6,0,2,4,1],[4,7,5,0,6,2,3,1],[1,0,3,2,5,4,6,7]$ $([0,1,2,3,5,4,7,6],[0,1,3,2,6,7,4,5],[7,3,6,1,4,5,2,0])$
9	(52)	$([8,5,2,7,4,1,6,3,0],[1,2,0,5,3,4,8,6,7],[2,0,1,4,5,3,7,8,6])$
10	(77)	$([0,1,2,3,5,4,7,6,9,8],[1,0,3,2,5,4,8,9,6,7],[0,6,4,8,2,5,1,7,3,9])$
11	(85)	$([1,0,3,2,5,4,7,6,9,8,10],[0,3,4,1,2,6,5,8,7,10,9],[0,4,3,2,1,5,6,7,8,9,10])$
12	(95) may be updated	$([1,0,3,2,5,4,7,6,9,8,11,10],[0,2,1,5,6,3,4,8,7,10,9,11],[0,1,2,6,5,4,3,7,8,9,10,11])$
13	(111) may be updated	$([1,0,2,5,4,3,7,6,9,8,11,10,12],[0,2,3,4,1,6,5,8,7,10,9,12,11],[0,4,1,2,3,6,5,8,7,10,9,12,11])$
14	(132) may be updated	$([1,0,3,2,5,4,7,6,9,8,11,10,13,12],[0,2,1,4,3,6,5,8,7,10,9,12,11,13],[0,1,2,3,5,4,6,7,8,9,10,11,12,13])$
15	(148) may be updated	$([1,0,3,2,5,4,7,6,9,8,11,10,13,12,14],[0,2,1,4,3,6,5,8,7,10,9,12,11,14,13],[0,1,2,3,4,8,7,6,5,9,10,11,12,13,14])$

As we said earlier, all permutations of S_n are divided into equivalence classes. To understand the following notation, let us explain how these equivalence classes are obtained for the group S_n.

Theorem. Two substitutions of S_n are conjugate if and only if they have the same cyclic structure, that is, they have identical sets of cycle lengths.

Using the theorem, we can conclude that each equivalence class corresponds to the decomposition of n into the sum of natural numbers (where each term is the length of a cycle, when a permutation is decomposed into a product of cycles). Therefore, we will write the equivalence class of S_n as $(a_1, ..., a_k)$, where $a_1, ..., a_k \in \mathbb{N}$ and $a_1 + ... + a_k = n$.

The maximum diameter on a set of generators consisting of pairs of permutations is considered. There are many generators that achieve the maximum diameter. However, it can be observed that these are generally $1 - 2$ variants of pairs of permutations, where the equivalence classes are fixed in each pair. That is, $1 - 2$ pairs of equivalence classes are possible, for which there is an example of a

pair of generators on which the maximum is achieved. Next, the results for $n = 3...9$.

Notation: $\leftarrow$ how many second-class representatives there are for any first-class representative
$\rightarrow$ how many first-class representatives there are for any second-class representative

Analysis of generators that give the maximum diameter for S_n(directed graph)					
n	Max diam	Pairs of equivalence classes	Example	$\leftarrow$	$\rightarrow$
3	3	$(2,1)-(2,1)$	$[1,0,2]$, $[0,2,1]$	2	2
4	7	$(2,1,1)-(3,1)$	$[1,0,2,3]$, $[0,2,3,1]$	3	4
5	14	$(2,2,1)-(4,1)$	$[2,1,0,4,3]$, $[1,2,3,0,4]$	8	4
6	18	$(2,1,1,1,1)-(6)$	$[0,1,2,3,5,4]$, $[1,2,3,4,5,0]$	6	48
		$(2,2,2)-(3,2,1)$	$[2,4,0,5,1,3]$, $[1,2,0,4,3,5]$	6	48
7	34	$(2,2,2,1)-(3,3,1)$	$[1,0,3,2,5,4,6]$, $[4,6,2,0,3,1,5]$	96	28
8	44	$(2,2,2,1,1)-(4,2,1,1)$	$[0,5,2,6,7,1,3,4]$, $[1,2,3,0,5,4,6,7]$	16	96
9	61	$(2,2,2,1,1,1)-(4,2,2,1)$	$[1,0,3,2,5,4,6,7,8]$, $[0,2,1,6,7,8,4,3,5]$	32	288

(may be updated)

Analysis of generators that give the maximum diameter for S_n(undirected graph)			
n	Max diam	Pairs of equivalence classes	Example
10	83	$(2,2,2,2,2)-(3,3,3,1)$	$[1,0,3,2,5,4,7,6,9,8]$, $[0,8,3,7,6,1,9,2,5,4]$
11	93	$(2,2,2,2,2,1)-(4,2,2,1,1,1)$	$[1,0,3,2,5,4,7,6,9,8,10]$, $[0,5,8,3,7,2,10,4,1,9,6]$
12	106	$(2,2,2,2,2,1,1)-(4,2,2,2,1,1)$	$[1,0,3,2,5,4,7,6,9,8,10,11]$, $[4,11,8,6,0,5,3,7,2,10,1,9]$
13	147	$(2,2,2,2,2,1,1,1)-(4,2,2,2,2,1)$	$[1,0,3,2,5,4,7,6,9,8,10,11,12]$, $[0,11,12,4,3,6,5,8,7,10,9,2,1]$

It is easy to see that in the cases considered, one of the equivalence classes is always a product of transpositions. Therefore, we hypothesize that one of the equivalence classes is always the product of transpositions. This means that it is now sufficient to consider only the following enumeration of pairs of permutations: the first permutation is the product of transpositions and the second permutation is any one.

We also performed a deeper analysis of the set of permutations that achieve the maximum. It turned out that the last layer always has the same number of permutations. Moreover, the classes of these permutations are fixed and do not depend on the set of permutations that achieve the maximum. The growth is also the same for almost all n. For $n = 7$, there are two growth options.

Permutations on the last layer, for maximum for S_n(directed graph)		
n	Number of permutations	Classes of permutations on the last layer
3	1	$(2,1)$
4	1	$(2,1,1)$
5	1	$(2,1,1,1)$
6	1	$(4,2)$
7	1	$(2,2,1,1,1)$
8	4	$(2,1,1,1,1,1,1)$, $(2,1,1,1,1,1,1,1)$, $(2,1,1,1,1,1,1,1)$, $(2,1,1,1,1,1,1,1)$
9	3	$(2,2,2,1,1,1)$, $(2,1,1,1,1,1,1,1,1)$, $(2,1,1,1,1,1,1,1,1)$
10	1	$2,2,2,1,1,1$
11	3	$(2,2,1,1,1,1,1,1,1)$, $(2,1,1,1,1,1,1,1,1,1)$, $(2,1,1,1,1,1,1,1,1,1)$
12	1	$(3,2,1,1,1,1,1,1,1)$
13	2	$(2,1,1,1,1,1,1,1,1,1,1,1)$, $(2,1,1,1,1,1,1,1,1,1,1,1)$

Some results for enumerating all pairs of permutations: the first is a fixed representative of the equivalence class, and the second is any $n = 9$ Notation: the first and second permutations are defined above, number means the number of options for the second permutation to achieve the maximum

Analysis of generators that give the **maximum diameter** with fixed the first permutation for $\mathbf{S}_9$ (directed)					
	The $1st$ perm	Class of the $1st$ perm	**Max diam**	Number	Class of the $2nd$ perm
1	$[1,0,3,2,5,4,7,6,8]$	$(2,2,2,2,1)$	**47**	384	$(4,2,2,1)$
2	$[1,0,3,2,5,4,6,7,8]$	$(2,2,2,1,1,1)$	**61**	288	$(4,2,2,1)$
3	$[1,0,3,2,4,5,6,7,8]$	$(2,2,1,1,1,1,1)$	**37**	2880	$(8,1)$ $(7,2)$ $(6,3)$
4	$[1,0,2,3,4,5,6,7,8]$	$(2,1,1,1,1,1,1,1)$	**45**	10080	(9)
5	$[1,2,3,4,5,6,7,8,0]$	(9)	**55**	9	$(2,2,2,1,1,1)$
6	$[1,2,3,4,5,6,7,0,8]$	$(8,1)$	**39**	8	$(2,2,2,2,1)$
7	$[1,2,3,4,5,6,0,8,7]$	$(7,2)$	**39**	14	$(2,2,2,1,1,1)$
8	$[1,2,3,4,5,6,0,7,8]$	$(7,1,1)$	**35**	28	$(2,2,2,1,1,1)$
9	$[1,2,3,4,5,0,7,8,6]$	$(6,3)$	**50**	18	$(2,2,2,1,1,1)$
10	$[1,2,3,4,5,0,7,6,8]$	$(6,2,1)$	**38**	12	$(2,2,2,1,1,1)$
11	$[1,2,3,4,5,0,6,7,8]$	$(6,1,1,1)$	**37**	36	$(2,2,2,1,1,1)$
12	$[1,2,3,4,0,6,7,8,5]$	$(5,4)$	**43**	40	$(2,2,2,1,1,1)$ $(3,3,3)$
13	$[1,2,3,4,0,6,7,5,8]$	$(5,3)$	**39**	15	$(2,2,2,1,1,1)$
14	$[1,2,3,4,0,6,5,8,7]$	$(5,2,2)$	**34**	80	$(2,2,2,1,1,1)$
15	$[1,2,3,4,0,6,5,7,8]$	$(5,2,1,1)$	**33**	80	$(2,2,2,1,1,1)$ $(2,2,2,2,1)$
16	$[1,2,3,4,0,5,6,7,8]$	$(5,1,1,1,1)$	**31**	240	$(8,1)$
17	$[1,2,3,0,5,6,7,4,8]$	$(4,4,1)$	**54**	32	$(2,2,2,1,1,1)$
18	$[1,2,3,0,5,6,4,8,7]$	$(4,3,2)$	**35**	24	$(2,2,2,1,1,1)$
19	$[1,2,3,0,5,6,4,7,8]$	$(4,3,1,1)$	**34**	48	$(2,2,2,2,1)$ $(4,2,2,1)$
20	$[1,2,3,0,5,4,7,6,8]$	$(4,2,2,1)$	**61**	32	$(2,2,2,1,1,1)$
21	$[1,2,3,0,5,4,6,7,8]$	$(4,2,1,1,1)$	**42**	48	$(4,2,2,1)$
22	$[1,2,3,0,4,5,6,7,8]$	$(4,1,1,1,1,1)$	**30**	1440	$(3,3,3)$
23	$[1,2,0,4,5,3,7,8,6]$	$(3,3,3)$	**60**	162	$(2,2,2,1,1,1)$
24	$[1,2,0,4,5,3,7,6,8]$	$(3,3,2,1)$	**40**	36	$(2,2,2,1,1,1)$
25	$[1,2,0,4,5,3,6,7,8]$	$(3,3,1,1,1)$	**32**	216	$(3,3,2,1)$ $(8,1)$
26	$[1,2,0,4,3,6,5,8,7]$	$(3,2,2,2)$	**41**	144	$(2,2,2,1,1,1)$
27	$[1,2,0,4,3,6,5,7,8]$	$(3,2,2,1,1)$	**35**	240	$(4,2,2,1)$ $(8,1)$ $(3,2,2,2)$
28	$[1,2,0,4,3,5,6,7,8]$	$(3,2,1,1,1,1)$	**30**	144	$(3,3,3)$
29	$[1,2,0,3,4,5,6,7,8]$	$(3,1,1,1,1,1,1)$	**32**	2160	$(8,1)$

Analysis of generators that give the **minimum diameter** with fixed the first permutation for $\mathbf{S}_9$ (directed)					
	The $1st$ perm	Class of the $1st$ perm	**Min diam**	Number	Class of the $2nd$ perm
1	$[1,0,3,2,5,4,7,6,8]$	$(2,2,2,2,1)$	**30**	16128	$(5,2,1)$ $(7,2)$ $(5,4)$ $(8,1)$
2	$[1,0,3,2,5,4,6,7,8]$	$(2,2,2,1,1,1)$	**30**	14112	$(5,3,1)$ $(7,2)$ $(5,4)$ $(4,3,2)$ $(5,2,2)$ (9)
3	$[1,0,3,2,4,5,6,7,8]$	$(2,2,1,1,1,1,1)$	**30**	1920	$(8,1)$
4	$[1,0,2,3,4,5,6,7,8]$	$(2,1,1,1,1,1,1,1)$	**32**	10080	$(5,4)$
5	$[1,2,3,4,5,6,7,8,0]$	(9)	**21**	738	$(4,3,1,1)$ $(7,2)$ $(5,4)$ $(8,1)$ $(5,2,1,1)$
6	$[1,2,3,4,5,6,7,0,8]$	$(8,1)$	**21**	288	$(7,1,1)$ (9) $(5,3,1)$ $(5,2,2)$
7	$[1,2,3,4,5,6,0,8,7]$	$(7,2)$	**22**	812	$(5,3,1)$ $(4,3,2)$ $(5,2,2)$ (9)
8	$[1,2,3,4,5,6,0,7,8]$	$(7,1,1)$	**21**	112	$(5,2,1,1)$ $(8,1)$
9	$[1,2,3,4,5,0,7,8,6]$	$(6,3)$	**22**	150354	$(5,1,1,1,1)$ $(3,3,2,1)$ $(4,3,1,1)$ $(5,3,1)$ $(6,2,1)$ $(8,1)$ $(6,1,1,1)$ $(5,2,2)$ $(3,2,2,1,1)$ $(5,4)$ $(5,2,1,1)$ $(4,3,2)$ $(6,3)$ (9) $(7,1,1)$
10	$[1,2,3,4,5,0,7,6,8]$	$(6,2,1)$	**22**	108528	$(3,2,1,1,1,1)$ $(3,2,2,2)$ $(4,3,1,1)$ $(7,2)$ $(8,1)$

Analysis of generators that give the **minimum diameter** with fixed the first permutation for $\mathbf{S}_9$ (directed)					
	The $1st$ perm	Class of the $1st$ perm	**Min diam**	Number	Class of the $2nd$ perm
					$(6,1,1,1)$ $(5,4)$ $(5,2,1,1)$ $(6,3)$ $(3,3,2,1)$
11	$[1,2,3,4,5,0,6,7,8]$	$(6,1,1,1)$	**22**	117540	$(4,3,2,2)$ $(3,3,2,1)$ $(4,3,1,1)$ $(5,3,1)$ $(6,2,1)$ $(7,2)$ $(8,1)$ $(6,1,1,1)$ $(5,2,2)$ $(3,2,2,1,1)$ $(5,4)$ $(5,2,1,1)$ $(4,3,2)$ $(6,3)$ (9) $(7,1,1)$
12	$[1,2,3,4,0,6,7,8,5]$	$(5,4)$	**21**	680	$(5,3,1)$ $(4,3,2)$ $(5,2,2)$ (9)
13	$[1,2,3,4,0,6,7,5,8]$	$(5,3)$	**21**	600	$(8,1)$ $(7,2)$ $(5,4)$ $(5,2,1,1)$
14	$[1,2,3,4,0,6,5,8,7]$	$(5,2,2)$	**21**	800	$(4,3,1,1)$ $(8,1)$ $(7,2)$ $(5,4)$
15	$[1,2,3,4,0,6,5,7,8]$	$(5,2,1,1)$	**21**	240	$(7,1,1)$ (9) $(4,3,2)$ $(5,3,1)$
16	$[1,2,3,4,0,5,6,7,8]$	$(5,1,1,1,1)$	**22**	44160	$(4,3,1,1)$ $(8,1)$ $(7,2)$ $(5,4)$ $(5,2,1,1)$ $(6,3)$ $(3,3,2,1)$
17	$[1,2,3,0,5,6,7,4,8]$	$(4,4,1)$	**22**	704	$(5,2,1,1)$ $(8,1)$ $(7,2)$ $(5,4)$

Analysis of generators that give the **minimum diameter** with fixed the first permutation for $\mathbf{S}_9$(directed)					
	The $1st$ perm	Class of the $1st$ perm	**Min diam**	Number	Class of the $2nd$ perm
18	$[1,2,3,0,5,6,4,8,7]$	$(4,3,2)$	**21**	240	$(5,2,1,1)$ $(7,2)$ $(5,4)$
19	$[1,2,3,0,5,6,4,7,8]$	$(4,3,1,1)$	**22**	480	$(5,2,2)$ (9)
20	$[1,2,3,0,5,4,7,6,8]$	$(4,2,2,1)$	**22**	256	$(5,3,1)$ (9)
21	$[1,2,3,0,5,4,6,7,8]$	$(4,2,1,1,1)$	**22**	288	$(8,1)$ $(7,2)$ $(5,4)$
22	$[1,2,3,0,4,5,6,7,8]$	$(4,1,1,1,1,1)$	**23**	56640	$(5,3,2)$ $(7,2)$ $(5,4)$ $(6,1,1,1)$ $(5,2,1,1)$ $(8,1)$
23	$[1,2,0,4,5,3,7,8,6]$	$(3,3,3)$	**24**	32076	$(4,3,1,1)$ $(8,1)$ $(7,2)$ $(5,4)$ $(5,2,1,1)$ $(6,3)$ $(3,3,2,1)$
24	$[1,2,0,4,5,3,7,6,8]$	$(3,3,2,1)$	**24**	89064	$(7,1,1)$ $(4,3,2)$ $(4,3,1,1)$ $(5,3,1)$ $(6,2,1)$ $(8,1)$ $(7,2)$ $(6,1,1,1)$ $(5,2,2)$ $(3,2,2,1,1)$ $(4,3)$ $(5,2,1,1)$ $(5,1,1,1,1)$ $(6,3)$ (9)
25	$[1,2,0,4,5,3,6,7,8]$	$(3,3,1,1,1)$	**24**	23220	$(4,3,1,1)$ $(8,1)$ $(5,4)$ $(7,2)$ $(5,2,1,1)$

Analysis of generators that give the **minimum diameter** with fixed the first permutation for $\mathbf{S}_9$(directed)					
	The $1st$ perm	Class of the $1st$ perm	**Min diam**	Number	Class of the $2nd$ perm
26	$[1,2,0,4,3,6,5,8,7]$	$(3,2,2,2)$	**22**	72864	$(7,1,1)$ $(4,3,1,1)$ $(5,3,1)$ $(6,2,1)$ $(8,1)$ $(7,2)$ $(5,2,2)$ $(5,4)$ $(5,2,1,1)$ $(4,3,2)$ (9)
27	$[1,2,0,4,3,6,5,7,8]$	$(3,2,2,1,1)$	**22**	51120	$(6,1,1,1)$ $(5,3,1)$ $(6,3)$ $(8,1)$ $(7,2)$ $(4,3,1,1)$ $(5,4)$ $(5,2,1,1)$ $(3,3,2,1)$
28	$[1,2,0,4,3,5,6,7,8]$	$(3,2,1,1,1,1)$	**22**	37872	$(7,1,1)$ $(5,3,1)$ $(6,2,1)$ $(8,1)$ (9) $(4,3,2)$ $(5,4)$
29	$[1,2,0,3,4,5,6,7,8]$	$(3,1,1,1,1,1,1)$	**26**	8640	$(7,2)$ $(5,4)$

A similar analysis for A_n (the set of permutations generates A_n, but the equivalence classes for A_n are different, so this enumeration is not complete).

Analysis of generators that give the **maximum diameter** with fixed the first permutation for $\mathbf{A}_9$(directed)					
	The $1st$ perm	Class of the $1st$ perm	**Max diam**	Number	Class of the $2nd$ perm
1	$[1,0,3,2,5,4,7,6,8]$	$(2,2,2,2,1)$	**54**	384	$(4,4,1)$
2	$[1,0,3,2,4,5,6,7,8]$	$(2,2,1,1,1,1,1)$	**39**	960	$(6,2,1)$
3	$[1,2,3,4,5,6,7,8,0]$	(9)	**35**	9	(9)
4	$[1,2,3,4,5,6,0,7,8]$	$(7,1,1)$	**36**	14	$(2,2,1,1,1,1,1)$
5	$[1,2,3,4,5,0,7,6,8]$	$(6,2,1)$	**39**	24	$(2,2,2,2,1)$ $(2,2,1,1,1,1,1,1)$
6	$[1,2,3,4,0,6,7,5,8]$	$(5,3)$	**38**	15	$(4,4,1)$
7	$[1,2,3,4,0,6,5,8,7]$	$(5,2,2)$	**34**	40	$(2,2,1,1,1,1,1)$
8	$[1,2,3,4,0,5,6,7,8]$	$(5,1,1,1,1)$	**36**	120	$(2,2,2,2,1)$
9	$[1,2,3,0,5,6,7,4,8]$	$(4,4,1)$	**54**	32	$(2,2,2,1,1,1)$
10	$[1,2,3,0,5,6,4,8,7]$	$(4,3,2)$	**35**	24	$(2,2,2,1,1,1)$
11	$[1,2,3,0,5,4,6,7,8]$	$(4,2,1,1,1)$	**43**	48	$(2,2,2,2,1)$
12	$[1,2,0,4,5,3,7,8,6]$	$(3,3,3)$	**47**	162	$(2,2,2,2,1)$
13	$[1,2,0,4,5,3,6,7,8]$	$(3,3,1,1,1)$	**35**	108	$(6,2,1)$
14	$[1,2,0,4,3,6,5,7,8]$	$(3,2,2,1,1)$	**36**	96	$(2,2,2,2,1)$
15	$[1,2,0,3,4,5,6,7,8]$	$(3,1,1,1,1,1,1)$	**31**	2160	$(4,4,1)$

Analysis of generators that give the **minimum diameter** with fixed the first permutation for $\mathbf{A}_9$(directed)					
	The $1st$ perm	Class of the $1st$ perm	**Min diam**	Number	Class of the $2nd$ perm
1	$[1,0,3,2,5,4,7,6,8]$	$(2,2,2,2,1)$	**28**	768	$(4,4,1)$
2	$[1,0,3,2,4,5,6,7,8]$	$(2,2,1,1,1,1,1)$	**29**	21120	$(6,2,1)$
3	$[1,2,3,4,5,6,7,8,0]$	(9)	**20**	5220	(9)
4	$[1,2,3,4,5,6,0,7,8]$	$(7,1,1)$	**20**	1876	$(2,2,1,1,1,1,1)$
5	$[1,2,3,4,5,0,7,6,8]$	$(6,2,1)$	**20**	120	$(2,2,2,2,1)$ $(2,2,1,1,1,1,1)$
6	$[1,2,3,4,0,6,7,5,8]$	$(5,3)$	**20**	5430	$(4,4,1)$
7	$[1,2,3,4,0,6,5,8,7]$	$(5,2,2)$	**20**	5680	$(2,2,1,1,1,1,1)$
8	$[1,2,3,4,0,5,6,7,8]$	$(5,1,1,1,1)$	**21**	67320	$(2,2,2,2,1)$
9	$[1,2,3,0,5,6,7,4,8]$	$(4,4,1)$	**21**	9504	$(2,2,2,2,1)$
10	$[1,2,3,0,5,6,4,8,7]$	$(4,3,2)$	**20**	5664	$(2,2,2,2,1)$
11	$[1,2,3,0,5,4,6,7,8]$	$(4,2,1,1,1)$	**21**	9456	$(2,2,2,2,1)$
12	$[1,2,0,4,5,3,7,8,6]$	$(3,3,3)$	**23**	62208	$(2,2,2,2,1)$
13	$[1,2,0,4,5,3,6,7,8]$	$(3,3,1,1,1)$	**23**	45576	$(6,2,1)$
14	$[1,2,0,4,3,6,5,7,8]$	$(3,2,2,1,1)$	**21**	73392	$(2,2,2,2,1)$
15	$[1,2,0,3,4,5,6,7,8]$	$(3,1,1,1,1,1,1)$	**23**	4320	$(4,4,1)$

Current work:

Calculation in `Max_diam_classes_transpositions` for $n = 10$				
Allowed class $g1$	Allowed class $g2$	Max	Time	Number
$(2,2,2,2,2)$	$(3,3,3,1)$	83	$2hGPU$	156
	$(4,2,2,1,1)$	77		213
	$(3,2,2,2,1)$	53	$1h9m$	194
	$(4,3,2,1)$	53	$6h41m$	189
	$(4,4,1,1)$	46	$1h39m$	188
	$(4,4,2)$	48	$2h$	200
	$(6,1,1,1,1)$	43	$1h40tpu$	
	$(3,3,2,1,1)$	42	$2h$	192
	$(4,3,1,1,1)$	39	$2h$	212
	$(4,2,1,1,1,1)$	$0(noS_{10}/A_{10})$	$36min$	191
	$(3,3,1,1,1,1)$	$0(noS_{10}/A_{10})$	$10min$	193
	$(3,2,2,1,1,1)$	$0(noS_{10}/A_{10})$	$45min$	195
	$(6,1,1,1,1)$	$0(noS_{10}/A_{10})$	$32min$	199
$(2,2,2,2,1,1)$	$(4,4,2)$	68	$3h$	269
	$(4,2,2,1,1)$	67	$2.5h$	235
	$(3,2,2,2,1)$	52	$1h$	262
	$(3,3,2,1,1)$	45	$2.2h$	239
	$(4,3,1,1,1)$	35	$1h45m$	234
	$(4,2,2,2)$	A_n48	$45min$	207
	$(3,3,3,1)$	A_n72	$1h22m$	157
	$(4,4,1,1)$	A_n63	$2.5h$	240
	$(4,3,2,1)$	A_n41	$5.5h$	241
	$(4,2,1,1,1,1)$	$0(noS_{10}/A_{10})$	$0.5h$	238
	$(3,3,1,1,1,1)$	$0(noS_{10}/A_{10})$	$14m$	261
	$(3,2,2,1,1,1)$	$0(noS_{10}/A_{10})$	$44min$	268
$(2,2,2,1,1,1,1)$	$(3,3,3,1)$	66	$1.2h$	210
	$(4,4,2)$	66	$2.5h$	208
	$(4,4,1)$	52	$2.5h$	211
	$(4,3,2,1)$	39	$5.2h$	232
	$(4,3,1,1,1)$	$0(noS_{10}/A_{10})$	$1.5h$	233
	$(4,2,2,1,1)$	$0(noS_{10}/A_{10})$	$2h$	236
	$(4,2,1,1,1,1)$	$0(noS_{10}/A_{10})$	$25minCPU$	205
	$(3,3,2,1,1)$	$0(noS_{10}/A_{10})$	$2h9m$	204
	$(3,3,1,1,1,1)$	$0(noS_{10}/A_{10})$	$10minCPU$	201
	$(3,2,2,2,1)$	$0(noS_{10}/A_{10})$	$1hCPU$	202
	$(3,2,2,1,1,1)$	$0(noS_{10}/A_{10})$	$30minCPU$	203
	$(4,2,2,2)$	$0(noS_{10}/A_{10})$	$0.5h$	237

Calculation in `Max_diam_classes_transpositions` for $n = 11$				
Allowed class $g1$	Allowed class $g2$	Max	Time	Number
$(2,2,2,2,2,1)$	$(4,2,2,1,1,1)$	93	$12h$	330
	$(4,4,2,1)$	81	$12h$	338
	$(3,3,3,1,1)$	77	$1.9hTPU$	331
	$(4,2,2,2,1)$	75	$11h43m$	329
	$(5,5,1)$	74	$11h1m$	359
	$(3,2,2,2,1,1)$	65	$12h$	333
	$(4,3,2,2)$	62	$11h32m$	332
	$(4,4,1,1,1)$	60	$12h$	326
	$(3,3,3,2)$	59	$1.9hTPU$	325
	$(3,2,2,2,2)$	59	$1.9hTPU$	324
	$(3,3,2,2,1)$	57	$12h$	335
	$(5,2,1,1,1,1)$	53	$11h$	382
	$(3,3,2,1,1,1)$	52	$12h$	334
	$(4,3,2,1,1)$	51	$12h$	328
	$(5,2,2,2)$	51	$11h$	380
	$(5,2,2,1,1)$	51	$11h$	381
	$(4,3,3,1)$	50	$12h$	327
	$(5,3,3)$	50	$11h$	362
	$(5,4,2)$	48	$11h1m$	360
	$(5,3,1,1,1)$	46	$11h$	379
	$(5,4,1,1)$	44	$11h1m$	361
	$(4,3,1,1,1,1)$	44	$12h$	341
	$(5,3,2,1)$	44	$1.9hTPU$	363
	$(4,3,2,1,1)$	51	$12h$	502
	$(2,2,2,2,2,1)$	$0(noS_{10}/A_{10})$	$1h42m$	358
$(2,2,2,2,1,1,1)$	$(4,4,2,1)$	79	$12h$	314
	$(4,3,2,2)$	52	$12h$	311
	$(3,3,3,2)$	52	$12h$	312
	$(5,4,1,1)$	48	$11h$	383
	$(5,2,2,2)$	46	$11h$	385
	$(4,3,3,1)$	44	$12h$	310
	$(5,3,2,1)$	43	$11h$	384
$(2,2,2,1,1,1,1,1)$	$(4,4,2,1)$	70	$12h$	315
	$(5,5,1)$	64	$11h$	386
	$(4,3,2,2)$	54	$12h$	318
	$(3,3,3,2)$	51	$12h$	319
	$(4,4,3)$	48	$12h$	317
	$(5,2,2,2)$	47	$1.9hGPU$	392
	$(4,3,3,1)$	44	$12h$	316
	$(5,4,2)$	44	$11h$	387
	$(5,3,3)$	43	$1.9hGPU$	389
	$(5,4,1,1)$	42	$11h$	388
	$(5,3,2,1)$	42	$1.9hGPU$	391

Calculation in `Max_diam_classes_transpositions` for $n = 12$				
Allowed class $g1$	Allowed class $g2$	Max	Time	Number
$(2,2,2,2,2,2)$	$(4,4,2,1,1)$	71	$11h$	458
	$(4,4,4)$	70	$1.9hTPU$	402
	$(4,3,2,2,1)$	61	$1.9hTPU$	401
	$(3,3,3,2,1)$	61	$11h$	465
	$(4,3,3,1,1)$	52	$11h$	459
	$(3,3,2,2,2)$	–	–	420
	$(4,3,1,1,1,1,1)$	$0(noS_{10}/A_{10})$	$1.9hTPU$	400
	$(4,2,2,2,2)$	$0(noS_{10}/A_{10})$	$40m$	473
	$(4,2,2,1,1,1,1)$	$0(noS_{10}/A_{10})$	$1.3h$	464
	$(3,3,2,1,1,1,1)$	$0(noS_{10}/A_{10})$	$1h$	466
	$(3,2,2,2,1,1,1)$	$0(noS_{10}/A_{10})$	$6h$	474
$(2,2,2,2,2,1,1)$	$(4,2,2,2,1,1)$	106	$1.9hTPU$	352
	$(4,4,3,1)$	93	$1.9hTPU$	445
	$(3,3,3,1,1,1)$	83	$1.9hTPU$	364
	$(4,4,2,1,1)$	73	$1.9hTPU$	354
	$(3,2,2,2,2,1)$	67	$1.9hTPU$	369
	$(4,4,1,1,1,1)$	65	$1.9hTPU$	344
	$(3,3,2,2,1,1)$	56	$1.9hTPU$	396
	$(4,3,2,1,1,1)$	55	$1.9hTPU$	348
	$(4,3,2,2,1)$	55	$1.9hTPU$	395
	$(4,3,3,1,1)$	51	$1.9hTPU$	347
	$(3,3,3,2,1)$	–	–	–
$(2,2,2,2,1,1,1,1)$	$(4,4,2,1,1)$	63	$11h$	468
	$(3,3,3,2,1)$	56	$11h$	472
	$(4,3,3,1,1)$	55	$1.9hTPU$	469
	$(4,3,2,2,1)$	52	$1.9hTPU$	471
$(2,1,1,1,1,1,1,1,1,1,1)$	(12)	87	$1.9hTPU$	342
	$(11,1)$	71	$1.9hTPU$	343

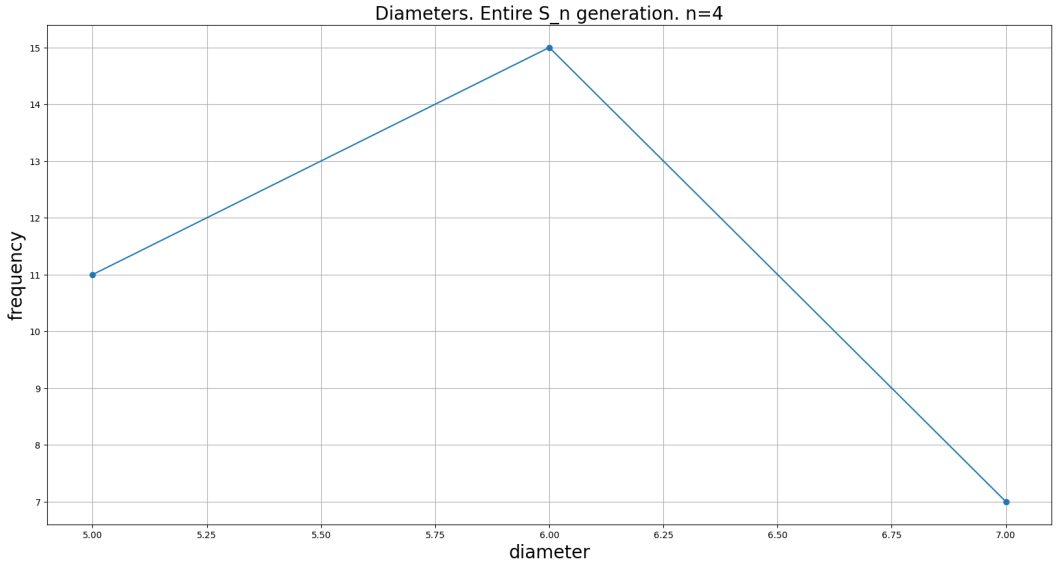


Figure 3: frequency of diameters S_4

Analysis of generators that give give different diameters (not all) for S_5(directed graph)		
Diameter	Pairs of equivalence classes	Example
14	$(2,2,1)-(4,1)$	$[1,2,3,0,4],[2,1,0,4,3]$
12	$(2,2,1)-(3,2)$	$[1,0,3,2,4],[3,4,0,2,1]$
	$(4,1)-(3,1,1)$	$[1,2,0,3,4],[0,3,4,2,1]$
11	$(5)-(4,1)$	$[1,2,3,4,0],[4,1,0,2,3]$
	$(2,1,1,1)-(5)$	$[1,2,3,4,0],[3,1,2,0,4]$
	$(2,1,1,1)-(3,2)$	$[1,2,0,4,3],[3,1,2,0,4]$
10	$(2,1,1,1)-(4,1)$	$[1,0,2,3,4],[4,1,0,2,3]$
	$(3,2)-(3,1,1)$	$[1,2,0,3,4],[2,3,4,1,0]$
	$(3,2)-(3,2)$	$[1,2,0,4,3],[2,4,0,1,3]$
	$(4,1)-(3,2)$	$[1,2,3,0,4],[1,0,4,2,3]$
9	$(3,2)-(5)$	$[1,2,3,4,0],[2,3,4,1,0]$

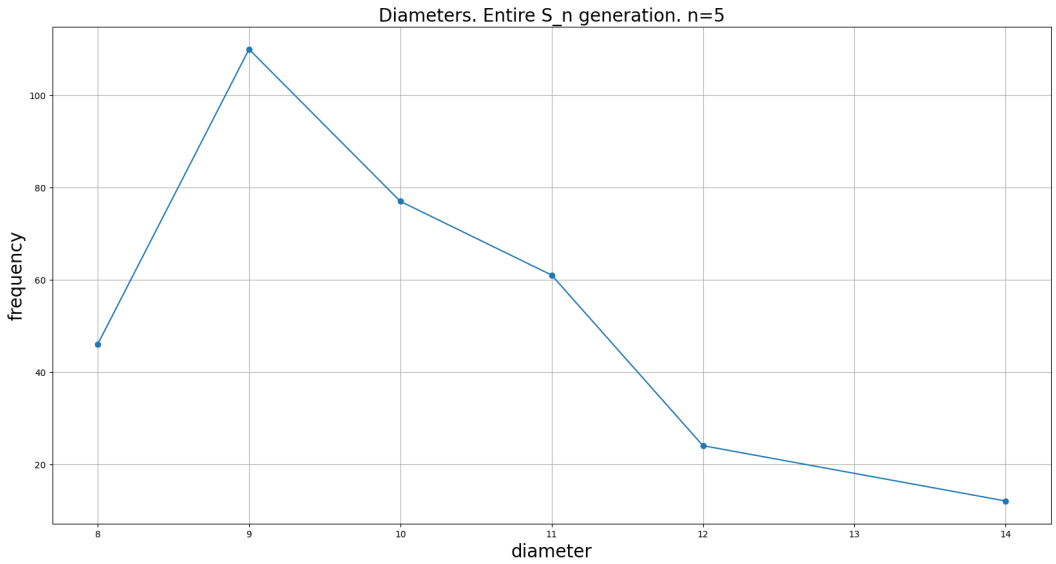


Figure 4: frequency of diameters S_5

Analysis of generators that give give different diameters (not all) for S_6(directed graph)		
Diameter	Pairs of equivalence classes	Example
18	$(2,1,1,1,1)-(6)$	$[1,2,3,4,5,0],[0,1,2,3,5,4]$
	$(2,2,2)-(3,2,1)$	$[1,2,0,4,3,5],[2,4,0,5,1,3]$
17	$(2,1,1,1,1)-(5,1)$	$[1,0,2,3,4,5],[0,2,3,5,1,4]$
	$(2,2,1,1)-(3,2,1)$	$[1,0,3,2,4,5],[0,3,4,1,5,2]$
	$(2,2,1,1)-(6)$	$[1,0,3,2,4,5],[2,0,5,1,3,4]$
	$(2,2,2)-(5,1)$	$[1,0,3,2,5,4],[0,4,5,2,3,1]$
16	$(6)-(5,1)$	$[1,2,3,4,5,0],[4,0,1,2,3,5]$
	$(5,1)-(3,2,1)$	$[1,2,3,4,0,5],[2,1,0,4,5,3]$
15	$(6)-(6)$	$[1,2,3,4,5,0],[1,3,5,4,2,0]$
	$(4,1,1)-(3,1,1,1)$	$[1,2,3,0,4,5],[0,4,2,3,5,1]$
	$(3,3)-(4,1,1)$	$[1,2,0,4,5,3],[3,0,2,4,1,5]$
	$(3,2,1)-(3,2,1)$	$[1,2,0,4,3,5],[0,5,4,1,2,3]$
14	$(6)-(4,2)$	$[1,2,3,4,5,0],[1,5,0,4,3,2]$
	$(6)-(4,1,1)$	$[1,2,3,4,5,0],[0,4,1,2,3,5]$
	$(6)-(3,1,1,1)$	$[1,2,3,4,5,0],[0,3,1,2,4,5]$
	$(4,2)-(3,2,1)$	$[1,2,3,0,5,4],[3,4,1,0,2,5]$
	$(4,1,1)-(3,2,1)$	$[1,2,3,0,4,5],[0,5,4,1,2,3]$
	$(3,3)-(3,2,1)$	$[1,2,0,4,5,3],[1,0,5,3,2,4]$
13	$(6)-(3,2,1)$	$[1,2,0,4,3,5],[4,0,5,2,3,1]$
	$(4,1,1)-(4,1,1)$	$[1,2,3,0,4,5],[4,1,2,5,3,0]$
	$(4,1,1)-(4,2)$	$[1,2,3,0,4,5],[4,0,3,2,5,1]$
12	$(6)-(3,3)$	$[1,2,3,4,5,0],[1,3,5,0,2,4]$
	$(5,1)-(4,1,1)$	$[1,2,3,4,0,5],[0,3,5,2,4,1]$
	$(3,1,1,1)-(3,2,1)$	$[1,2,0,3,4,5],[5,1,3,4,2,0]$

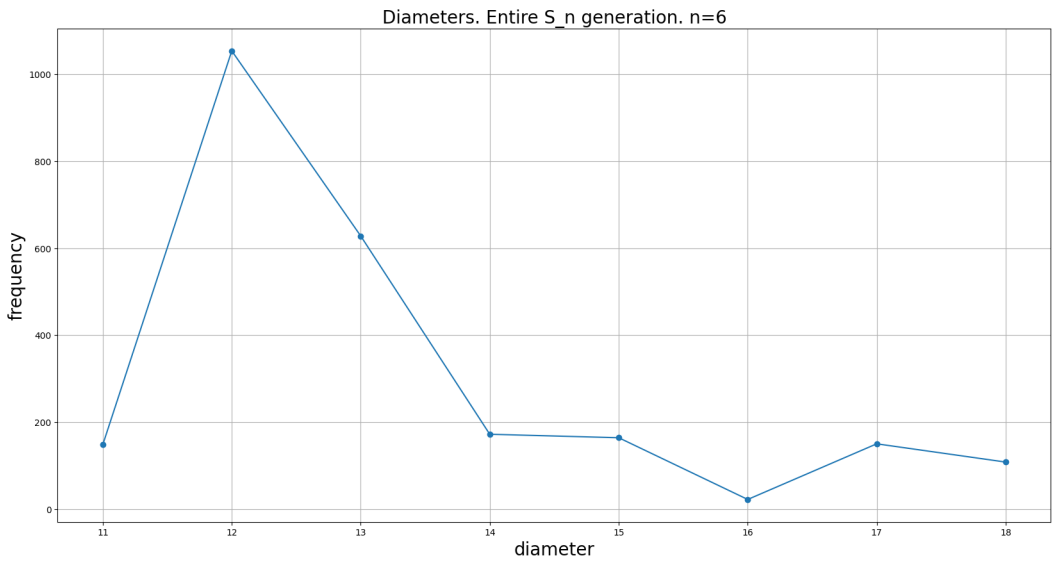


Figure 5: frequency of diameters S_6

Analysis of generators that give give different diameters (not all) for S_7(directed graph)		
Diameter	Pairs of equivalence classes	Example
34	$(2,2,2,1)-(3,3,1)$	$[1,0,3,2,5,4,6],[5,4,0,3,6,2,1]$
28	$(2,2,2,1)-(4,2,1)$	$[1,0,3,2,5,4,6],[0,3,6,4,5,1,2]$
27	$(2,2,2,1)-(3,2,1,1)$	$[1,0,3,2,5,4,6],[6,2,5,3,4,1,0]$
	$(2,2,2,1)-(4,1,1,1)$	$[1,0,3,2,5,4,6],[0,6,2,4,1,5,3]$
	$(2,2,2,1)-(5,2)$	$[1,0,3,2,5,4,6],[4,2,1,6,5,3,0]$
	$(5,2)-(3,3,1)$	$[1,2,3,4,0,6,5],[6,1,0,5,3,4,2]$
26	$(2,2,2,1)-(6,1)$	$[1,0,3,2,5,4,6],[6,4,3,0,2,5,1]$
	$(2,2,2,1)-(3,2,2)$	$[1,0,3,2,5,6,4],[5,1,6,4,3,0,2]$
25	$(2,1,1,1,1,1)-(7)$	$[1,2,3,4,5,6,0],[0,1,2,4,3,5,6]$
	$(2,2,1,1,1)-(6,1)$	$[1,0,3,2,4,5,6],[2,5,1,3,0,6,4]$
	$(3,2,2)-(6,1)$	$[1,0,3,2,5,6,4],[4,5,6,3,2,0,1]$
24	$(6,1)-(4,2,2)$	$[1,2,3,4,5,0,6],[2,1,0,5,3,6,4]$
	$(4,3)-(3,3,1)$	$[1,2,0,4,5,6,3],[6,0,5,2,4,3,1]$
	$(2,2,2,1)-(4,3)$	$[1,2,0,4,5,6,3],[3,4,2,0,1,6,5]$
	$(2,2,2,1)-(7)$	$[1,2,3,4,5,6,0],[2,1,0,4,3,6,5]$
23	$(4,1,1,1)-(7)$	$[1,2,3,4,5,6,0],[5,1,0,3,2,4,6]$
	$(4,3)-(4,3)$	$[1,2,0,4,5,6,3],[5,6,1,0,3,4,2]$
	$(2,2,2,1)-(5,1,1)$	$[1,0,3,2,5,4,6],[5,1,6,3,2,4,0]$
22	$(6,1)-(3,3,1)$	$[1,2,3,4,5,0,6],[6,5,2,1,0,3,4]]$
	$(2,2,1,1,1)-(5,2)$	$[1,0,3,2,4,5,6],[4,3,1,5,0,6,2]$
	$(2,1,1,1,1,1)-(6,1)$	$[1,0,2,3,4,5,6],[0,5,3,6,2,4,1]$
21	$(7)-(4,3)$	$[1,2,3,4,5,6,0],[6,0,5,2,3,4,1]$
	$(7)-(6,1)$	$[1,2,3,4,5,6,0],[5,6,2,1,0,3,4]$
	$(2,1,1,1,1,1)-(4,3)$	$[1,0,2,3,4,5,6],[2,6,5,1,0,4,3]$
	$(2,1,1,1,1,1)-(5,2)$	$[1,0,2,3,4,5,6],[4,3,1,5,0,6,2]$
	$(3,1,1,1,1)-(6,1)$	$[1,2,0,3,4,5,6],[4,1,3,0,5,6,2]$
	$(4,3)-(3,2,2)$	$[1,2,0,4,5,6,3],[4,2,1,5,6,3,0]$
	$(4,3)-(5,2)$	$[1,2,0,4,5,6,3],[5,4,1,6,3,0,2]$

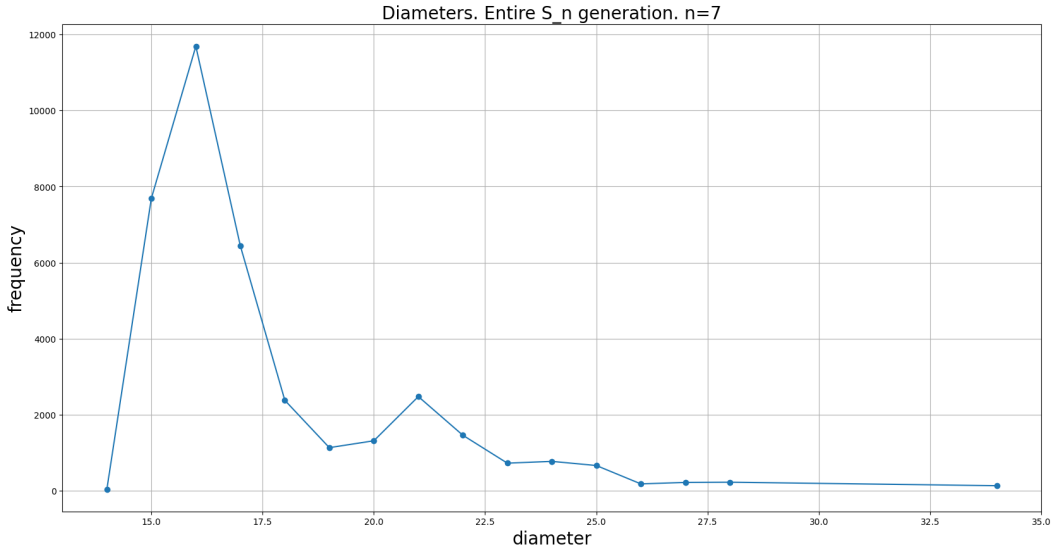


Figure 6: frequency of diameters S_7

E.1 Full search of small graphs ($n \leq 8$)

Here we present the results of the exhaustive search of diameters of the Cayley graphs generated by two permutations $\pi_1, \pi_2 \in S_n$, $4 \leq n \leq 8$ (with or without their inverses, i.e., undirected or directed

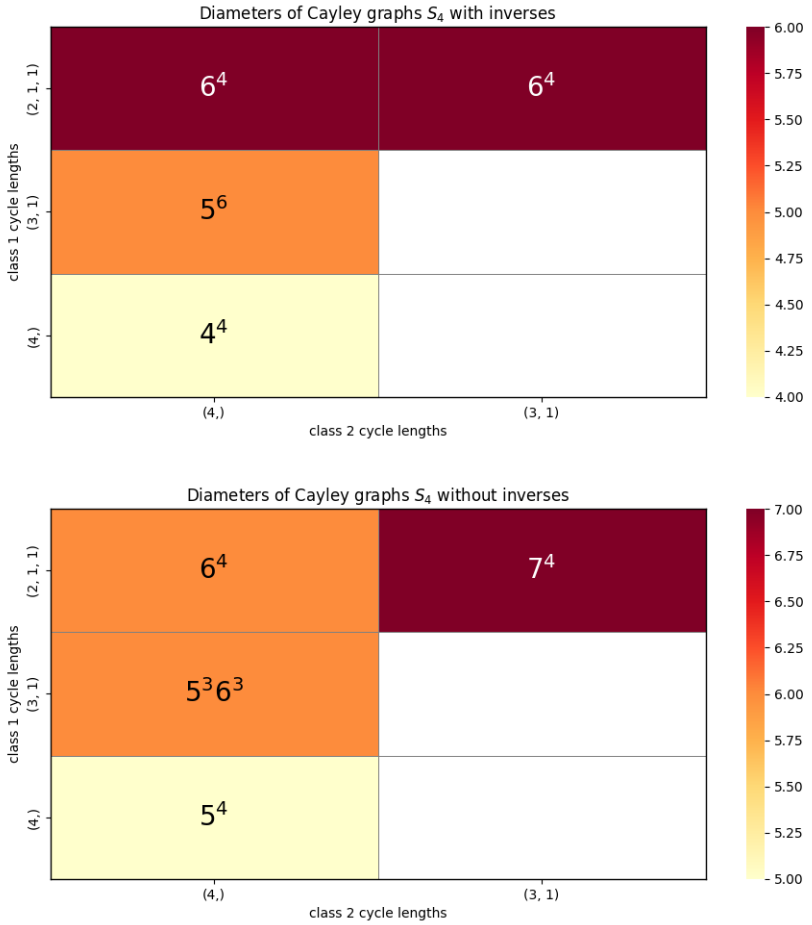


Figure 7: Diameters of all possible Cayley graphs for S_4 generated by two permutations with/without their inverses.

graphs). For a more granular search we fix classes of π_1 and π_2, i.e., ordered cycle lengths of these permutations. Moreover, since conjugating does not change the structure of the Cayley graph, we examine only one permutation π_1 from each class. The total number of classes coincides with $p(n)$ — the number of different partitions of n. Hence, the complexity of the procedure is $O(p(n)n!)$.

For each pair of generator classes all possible diameters are presented in the heatmaps below (7–11).

Consider special pairs of permutations. For convenience, we describe these permutations using a special kind of graphs. The vertices of the graph are numbers from 0 to $n-1$. Two vertices of the graph v_1 and v_2 are connected by an edge if and only if the permutation permutes $v_1 \to v_2$ (or vice versa). Such a graph is oriented, but we will not take this into account yet. For a pair of permutations, this graph will visually demonstrate the connections between the points. The special kind of permutation pair that we want to consider is as follows. One of the permutations contains a 4-cycle: (c_1, c_2, c_3, c_4). In the graph, this cycle will form a quadrilateral. A chain of segments will extend from the two opposite points of this quadrilateral. Note that the colors must alternate.
For n different variants of such pairs of permutations, $n-3$ (so many ways to arrange a square), but due to the symmetry of the different pairs, there are only $(n-2)//2$. Later in this section, k will mean the place where the square is located. The following are examples of such permutations and their graphs.

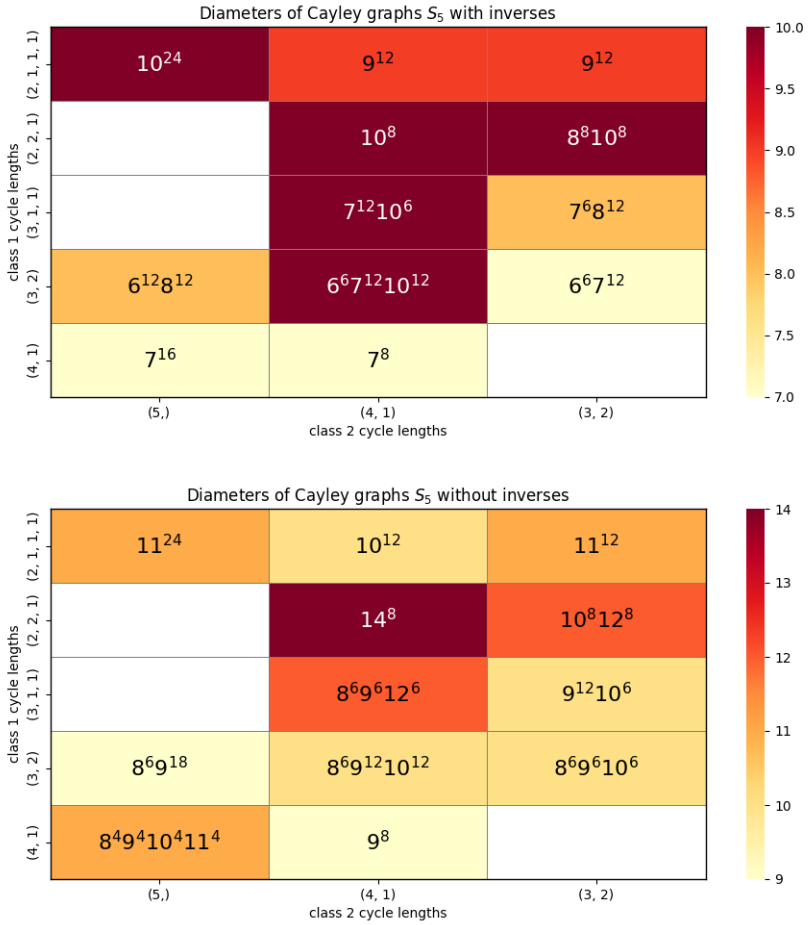


Figure 8: Diameters of all possible Cayley graphs for S_5 generated by two permutations with/without their inverses.

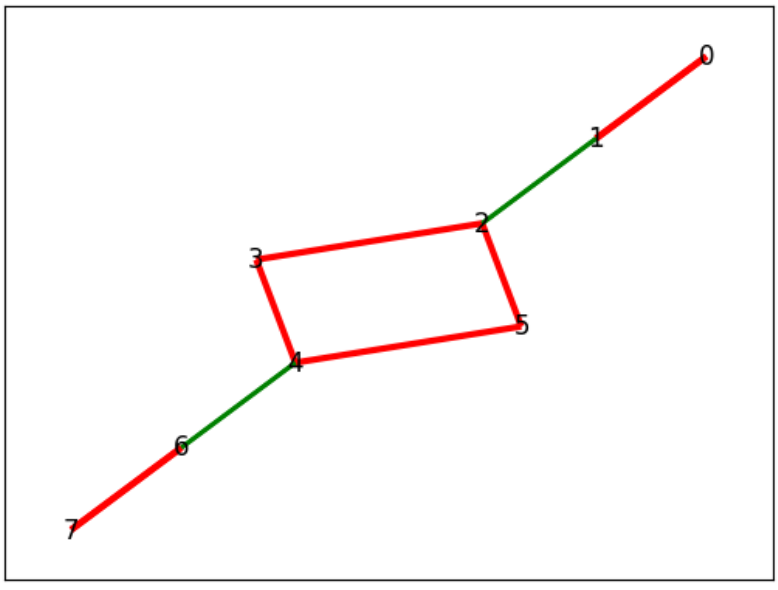


Figure 12: $n = 8, k = 3$

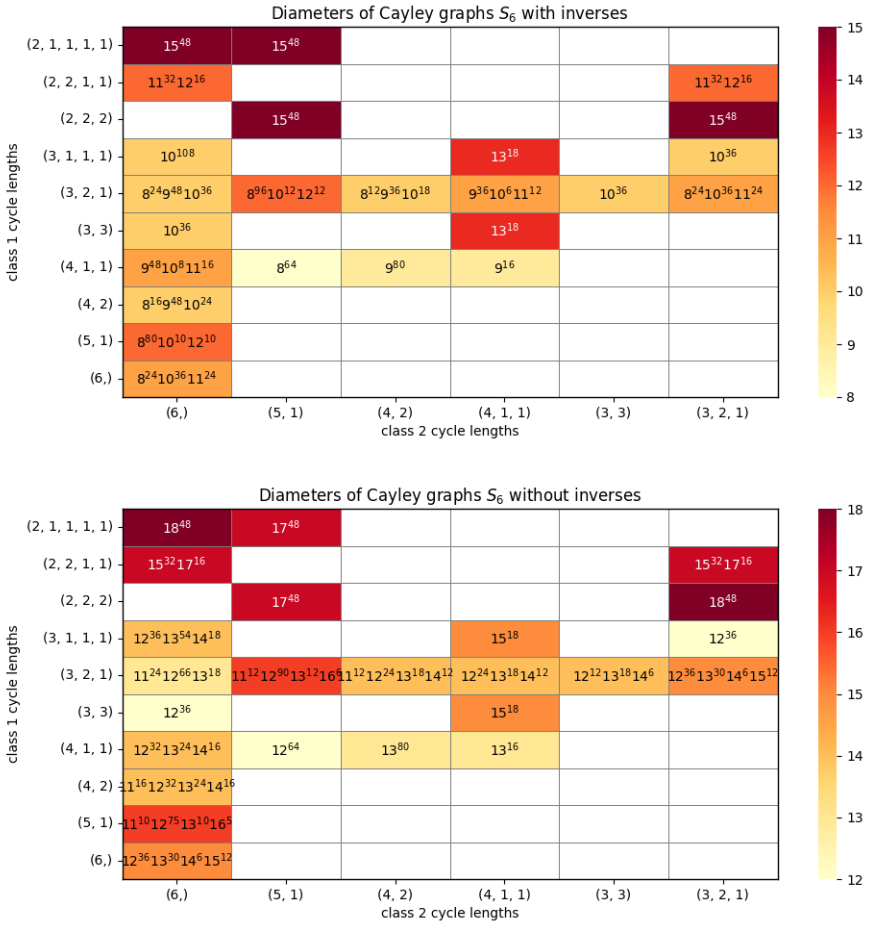


Figure 9: Diameters of all possible Cayley graphs for S_6 generated by two permutations with/without their inverses.

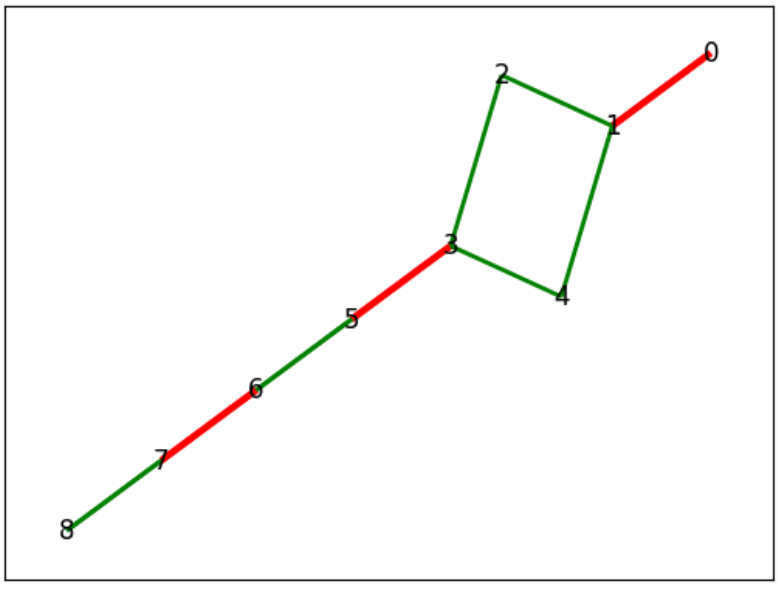


Figure 13: $n = 9, k = 2$

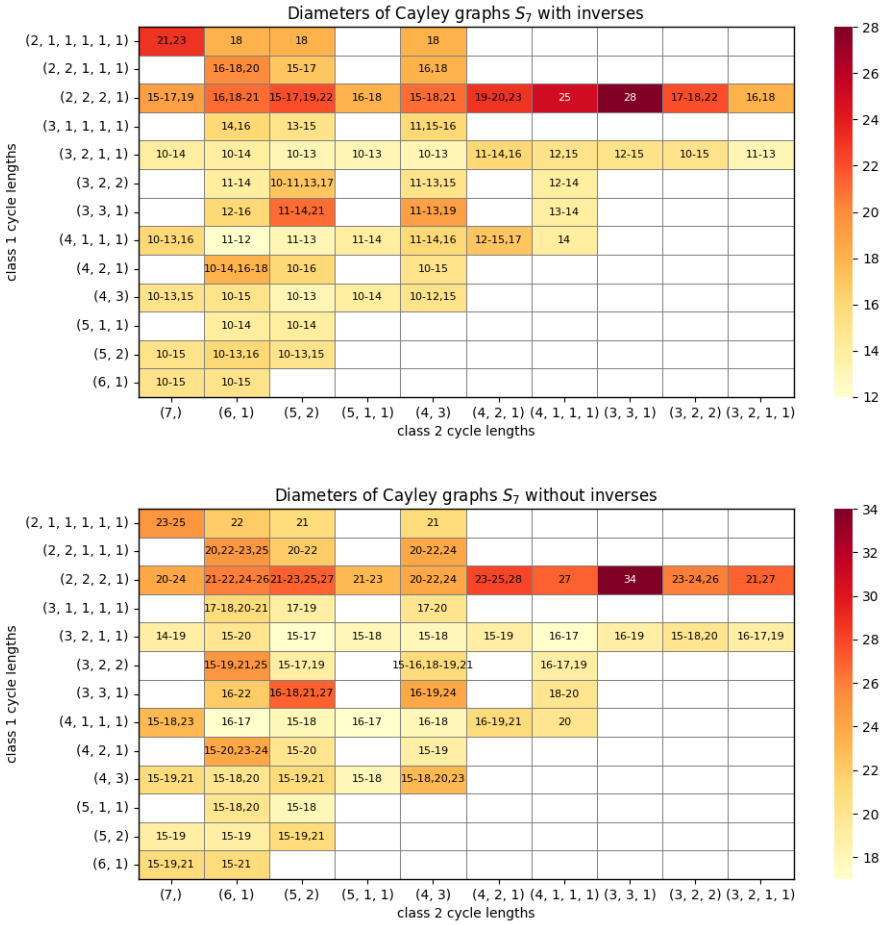


Figure 10: Diameters of all possible Cayley graphs for S_7 generated by two permutations with/without their inverses.

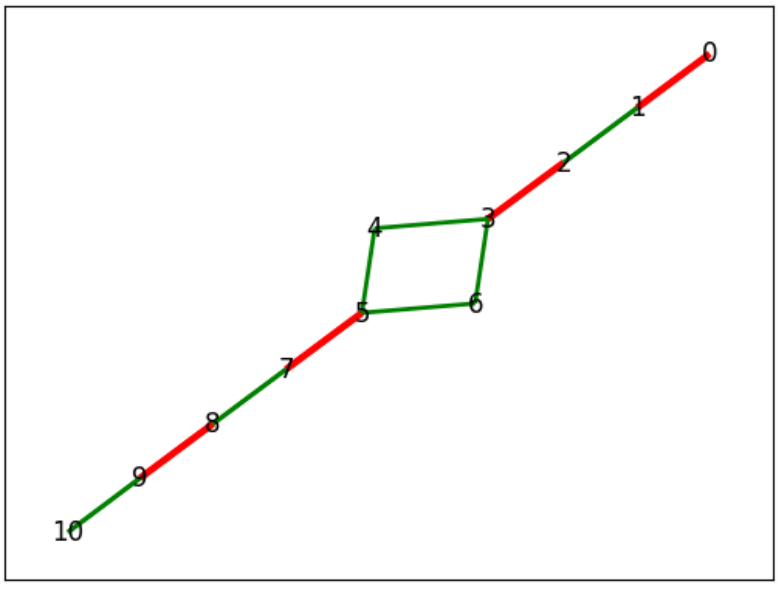


Figure 14: $n = 11, k = 4$

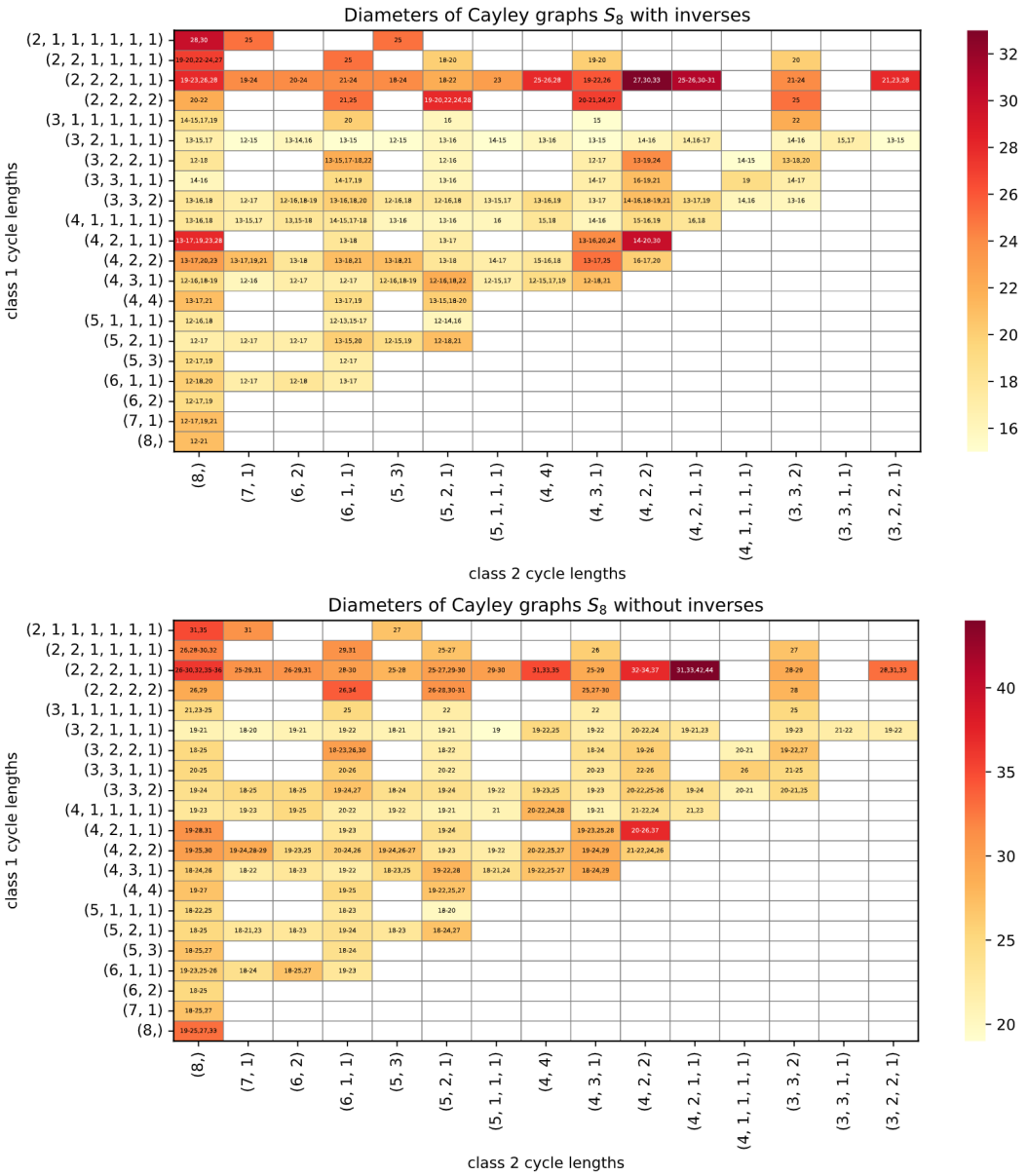


Figure 11: Diameters of all possible Cayley graphs for S_8 generated by two permutations with/without their inverses.

It turned out that in some cases such permutations give a large diameter. Below is a table where the diameters for the different n and k that generate S_n are calculated. Some metrics for growth are also provided. It is worth noting that not all such pairs of permutations generate S_n. We will describe this in more detail below. Comparing this table with the currently known maximum diameters, we can see that it often turns out that such permutations for some k give the maximum diameter. For $n = 14$ and more, we could only find out whether the permutations generate S_n, but not calculate the diameters. However, this information is also important for further analysis.

Analysis of generators from S2 for S_n(directed graph)						
n	Max diam	k	Diam	Std	Skew	Kurtosis
5	14	1	**10**	8.2	0.48	-1.2
6	18	1	$10noS_n$	4.76	0.43	-1.24
		2	$8noS_n$	3.16	0.24	-1.33
7	34	1	$24noS_n$	97.21	0.58	-1.18
		2	$24noS_n$	107.21	0.89	-0.64
8	44	1	$17noS_n$	28.18	0.58	-1.06
		2	**44**	1159.06	1.17	-0.08
		3	$10noS_n$	3.83	0.25	-1.37
9	61	1	**49**	9302.12	0.1	-0.57
		2	$20noS_n$	24.42	0.32	-1.39
		3	**61**	8624.67	1.43	0.64
10	83	1	$34noS_n$	1036.36	0.07	-0.35
		2	**67**	83994.53	1.52	0.89
		3	$39noS_n$	920.66	1.15	-0.12
		4	$16noS_n$	17.02	0.62	-1.11
11	93	1	$71noS_n$	390246.33	1.19	-0.12
		2	$76noS_n$	401641.2	1.46	0.7
		3	$76noS_n$	425342.39	1.62	1.23
		4	$79noS_n$	419880.26	1.68	1.44
12	106	1	$49noS_n$	14922.25	1.28	0.14
		2	$41noS_n$	2684.64	1.22	-0.0
		3	$31noS_n$	169.35	0.69	-1.09
		4	**106**	8038973.82	1.81	1.91
		5	$18noS_n$	16.41	0.45	-1.31
13	147	1	**113**	85492416.58	1.36	0.3
		2	**147**	75144975.47	1.73	1.51
		3	**145**	78279887.14	1.82	1.87
		4	**137**	85800682.0	1.92	2.32
		5	**131**	93792155.01	2.1	3.13
14	–	1	noS_n	–	–	–
		2	**-**	–	–	–
		3	noS_n	–	–	–
		4	**-**	–	–	–
		5	noS_n	–	–	–
		6	noS_n	–	–	–
15	–	1	noS_n	–	–	–
		2	noS_n	–	–	–
		3	noS_n	–	–	–
		4	noS_n	–	–	–
		5	noS_n	–	–	–
		6	noS_n	–	–	–
16	–	1	noS_n	–	–	–
		2	**-**	–	–	–
		3	noS_n	–	–	–
		4	**-**	–	–	–
		5	noS_n	–	–	–
		6	**-**	–	–	–
		7	noS_n	–	–	–

Analysis of generators from S2 for S_n(directed graph)						
n	Max diam	k	Diam	Std	Skew	Kurtosis
17	–	1	-	–	–	–
		2	-	–	–	–
		3	-	–	–	–
		4	-	–	–	–
		5	-	–	–	–
		6	-	–	–	–
		7	-	–	–	–
18	–	1	noS_n	–	–	–
		2	noS_n	–	–	–
		3	noS_n	–	–	–
		4	-	–	–	–
		5	noS_n	–	–	–
		6	-	–	–	–
		7	noS_n	–	–	–
		8	noS_n	–	–	–
19	–	1	noS_n	–	–	–
		2	noS_n	–	–	–
		3	noS_n	–	–	–
		4	noS_n	–	–	–
		5	noS_n	–	–	–
		6	noS_n	–	–	–
		7	noS_n	–	–	–
		8	noS_n	–	–	–
20	–	1	noS_n	–	–	–
		2	-	–	–	–
		3	noS_n	–	–	–
		4	noS_n	–	–	–
		5	noS_n	–	–	–
		6	-	–	–	–
		7	noS_n	–	–	–
		8	-	–	–	–
		9	noS_n	–	–	–
21	–	1	-	–	–	–
		2	noS_n	–	–	–
		3	-	–	–	–
		4	-	–	–	–
		5	noS_n	–	–	–
		6	noS_n	–	–	–
		7	-	–	–	–
		8	noS_n	–	–	–
		9	-	–	–	–

We can conclude for which n and k the set of permutations generates S_n. The check was performed up to $n = 44$.

- $n \equiv 3(mod4)$. This case is the simplest, since at no k do these pairs of permutations generate S_n. This is because in this case both permutations for any k turn out to be even.
- $n \equiv 1 \pmod 4$. For odd k, S_n is always generated, except in the first case. Moreover, if n is prime, then S_n is generated for all k.
- n-even. S_n is not generated for k odd numbers, and S_n is often (but not always) generated for k even numbers. It can also be noted that if n is also a multiple of 3, then for $k = 2, 8, 14, 20, ...$ (the difference between neighboring 6) S_n is not generated, but there are exceptions to this rule.
- $n \equiv 2, 3(mod4)$. For various reasons, but no k has ever given a maximum diameter.

- $n \equiv 0, 1(mod 4)$. Starting from $n = 8$, there was always some k that gave a maximum diameter (currently known to us).

E.2 ML PREDICTIONS

We are investigating the ability of a machine learning model to predict the diameter of the Cayley graph of a group formed by two permutations of n elements.
In the experiment, we fix one of the two generators of The dataset is formed from N pairs of the form $(G_{2_i}, diam_i), i = 1, ..., N$ where G_{2_i} is a random permutation of n elements and $diam_i$ is the diameter of the corresponding Cayley graph. Obviously, $N \leq n!$, where n! is the maximum number of samples in dataset.
As a model, we used MLP with architecture $256 \times 256 \times 256 \times 256 \times 256 \times 256$ with GELU activation between layers. The Adam optimizer with the 64 batch and the 5×10^{-4} learning rate was chosen for training. We were able to achieve ... More detailed results are shown in the table...

Analyzing the R^2 coefficient of the model depending on the proportion of the train set					
n	G_1	0.25	0.5	0.75	0.9
8	$[1, 0, 3, 2, 5, 4, 7, 6]$	0.75 ± 0.021	0.99 ± 0.004	0.99 ± 0.002	0.99 ± 0.000
9	$[1, 0, 3, 2, 5, 4, 7, 6, 8]$	0.95 ± 0.02	0.99 ± 0.000	0.99 ± 0.000	0.99 ± 0.000

F GENERALIZED SYMMETRIC GROUP

The generalized symmetric group is defined as the wreath product $S(m,n) := \mathbb{Z}_m \wr S_n = (\mathbb{Z}_m)^n \rtimes S_n$ of the cyclic group of order m and the symmetric group on n elements. Note that $S(1,n) = S_n$, and $S(2,n) = W(B_n) = W(C_n)$ is the signed symmetric group, also called the hyperoctahedral group, which is the Coxeter group of type $B_n = C_n$. For general m, elements of $S(m,n)$ can be represented as $n \times n$ matrices whose entries are either 0 or m-th roots of unity, with exactly one nonzero entry in each row and each column.

We can also describe this groups in terms of generators and relations. Indeed, let $w_i = ((0,\dots,0,1,0,\dots,0),(1))$ be the element of $S(m,n)$ such that the projection $(0,\dots,0,1,0,\dots,0)$ onto $\mathbb{Z}_m^n$ have 1 as the i-th component and the rest equal to 0, and let $r_i = ((0,\dots,0),(i\ i+1))$. One can check (see, e.g., Davies & Morris (1974)) that the generalized symmetric group $S(m,n)$ is generated by w_i and r_j for $1 \le i \le n$ and $1 \le j \le n-1$, and that these generators satisfy the following relations:

(i) $r_i^2 = (r_i r_{i+1})^3 = w_j^m = 1$,
(ii) $w_i w_j = w_j w_i$,
(iii) $r_i w_i = w_{i+1} r_i$,
(iv) $(r_i r_j)^2 = 1$ for $|i-j| \ge 2$,
(v) $r_i w_j = w_j r_i$ for $j \ne i, i+1$.

Let m be even. We define three group homomorphisms $\varphi_1, \varphi_2, \varphi_3 : S(m,n) \to \mathbb{Z}_m$. Namely, let φ_1 be given by the sum of the projections onto $(Z_m)^n$ modulo 2, let φ_2 be given by the sign of the projection onto S_n (i.e. 0 for even permutations, 1 for odd permutations), and let φ_3 be the sum of the other two.

Let $S \subset S_n$ be a subset of permutations that is closed under inverse. We construct two subsets $S^{\text{fr}}(m,n)$ and $S^{\text{all}}(m,n)$ of $S(m,n)$ as follows: $S^{\text{fr}}(m,n)$ is the closure under inverse of the set $\{((a_1,\dots,a_n),\sigma))|\sigma \in S, a_i = \delta_j \text{ where } \sigma(i) = i \text{ for } i < j, \sigma(j) \ne j\}$ and $S^{\text{all}}(m,n)$ is the closure under inverse of $\{((a_1,\dots,a_n),\sigma))|\sigma \in S, a_i = 1 \text{ if } \sigma(i) \ne i \text{ and } a_i = 0 \text{ if } \sigma(i) = i\}$.

The subsets $S^{\text{fr}}(m,n)$ and $S^{\text{all}}(m,n)$, respectively, generate subgroups $G^{\text{fr}}(m,n)$ and $G^{\text{all}}(m,n)$ of $S(m,n)$. We are interested in the corresponding Cayley graphs.

F.1 COXETER LIKE GENERATORS

Let us consider $G^{\text{fr}}(m,n)$ and $G^{\text{all}}(m,n)$ in the case when $S \subset S_n$ consists of the A_n type Coxeter generators (i.e. the transpositions $(i\ j)$). In terms of w_i, r_j, we see that $G^{\text{fr}}(m,n)$ is the subgroup generated by the elements $w_i r_i$ for $1 \le i \le n-1$ and $G^{\text{all}}(m,n)$ is the subgroup generated by the elements $w_i w_{i+1} r_i$ for $1 \le i \le n-1$. We can use these generators to give explicit descriptions of the two groups.

Proposition 1. *The following statements are true:*

(a) for $n > 2$ and odd m we have $G^{fr}(m,n) = G^{all}(m,n) = S(m,n)$,

(b) for $n > 2$ and even n we have $G^{fr}(m,n) = \mathrm{Ker}(\varphi_3) \subset S(m,n)$, which is a normal subgroup of index 2,

(c) for $n = 2$ we have $G^{first}(m,2) = \mathbb{Z}_{2m}$, while $G^{all}(m,2)$ is $\mathbb{Z}_m$ when m is even and $\mathbb{Z}_{2m}$ when m is odd,

(d) for $m = 2$ we have $G^{all}(2,n) = S_n$.

Proof. Using the relations between the elements w_i, r_j we get $w_i r_i = w_{i+1} r_i$ and $(w_i r_i)^2 = w_i w_{i+1}$. We also have $w_{i+1} r_{i+1} w_i r_i = w_{i+1} w_i r_{i+1} r_i$ and $w_i r_i w_{i+1} r_{i+1} = w_i r_i r_{i+1}$. Thus for $1 \le i \le n-2$ the subgroup $G^{\text{fr}}(m,n)$ contains w_i^2. Since it also contains $w_i w_{i+1}$ for $1 \le i \le n-1$, then w_{n-1}^2, w_n^2 belong to the group as well. If m is odd, this implies $w_i \in G^{\text{fr}}(m,n)$ for $1 \le i \le n$. Consequently, $G^{\text{fr}}(m,n) = S(m,n)$ in this case.

Similarly, $(w_i w_{i+1} r_i)^2 = w_i^2 w_{i+1}^2$ for $1 \leq i \leq n-1$, so for odd m we have $w_i w_{i+1} \in G^{\text{all}}(m,n)$. This means $r_i \in G^{\text{all}}(m,n)$. Additionally, $w_i w_{i+1} r_i w_{i+1} w_{i+2} r_{i+1} = w_i^2 w_{i+1} w_{i+2} r_i r_{i+1}$, so $w_i^2 \in G^{\text{all}}(m,n)$ for $1 \leq i \leq n-2$. Noting, once again, that m is odd, we get $w_i \in G^{\text{all}}(m,n)$ for $1 \leq i \leq n$, so $G^{\text{all}}(m,n) = S(m,n)$. This completes the proof of (a).

If m is even, an induction argument shows that $G^{\text{fr}}(m,n) \subset \text{Ker}(\varphi_3)$. Conversely, the $w_i r_i$ can be used to generate elements with every possible projection to S_n, so by composing these with w_i^2 and $w_i w_{i+1}$ we can obtain all elements of $\text{Ker}(\varphi_3)$. Clearly, $\text{Ker}(\varphi_3)$ is a normal subgroup of index 2. This proves (b).

For $n = 2$, the $G^{\text{first}}(m,2)$ and $G^{\text{all}}(m,2)$ are generated by $w_1 r_1$ and $w_1 w_2 r_1$, respectively. The first is an element of order $2m$, while the second has order m is m is even and $2m$ if it is odd. This proves (c).

It is easy to see that for $m = 2$, the elements $w_i w_{i+1} r_i$ satisfy the Coxeter relations for a group of type A_n, so (d) holds. □

For odd m we have even more than just the subgroups coinciding.

Corollary 1. *For $n > 2$ and odd m, the Cayley graphs of $G^{fr}(m,n)$ with respect to $S^{fr}(m,n)$ and $G^{all}(m,n)$ with respect to $S^{all}(m,n)$ are isomorphic.*

Proof. It suffices to show there exists an automorphism of $S(m,n)$ that bijectively maps $S^{\text{fr}}(m,n)$ to $S^{\text{all}}(m,n)$. On the generators w_i, r_j, define the mapping $w_i \mapsto w_i^2$ and $r_j \mapsto w_j^{-1} w_{j+1} r_j$. It is not hard to check this mapping preserves the relations (i)-(v), so it extends to an endomorphism of $S(m,n)$. Since m is odd, then w_i is contained in the image, for $1 \leq i \leq n$, and therefore r_j is as well, for $1 \leq j \leq n-1$. This makes the endomorphism surjective, and consequently, it is an automorphism. We also have $w_i r_i \mapsto w_i w_{i+1} r_i$, for $1 \leq i \leq n-1$, so this automorphism is a bijection on generating sets. □

Starting with the set of Coxeter generators of S_n, we can collect some useful data on the first few examples of the groups $G^{\text{fr}}(m,n)$ and $G^{\text{all}}(m,n)$. Namely, the diameters of the Cayley graphs and the values (?) of the growth function.

For $G^{\text{fr}}(3,n) = G^{\text{all}}(3,n)$, they are given in the table below.

n	Order	Diameter	Growth
1	1	0	1
2	6	3	1, 2, 2, 1
3	162	9	1, 4, 12, 26, 38, 36, 26, 14, 4, 1
4	1944	9	1, 6, 26, 91, 253, 508, 596, 355, 96, 12
5	29160	11	1, 8, 44, 196, 732, 2224, 5139, 8160, 7748, 3936, 916, 56
6	524880	15	1, 10, 66, 349, 1563, 5944, 18807, 47414, 89521, 120304, 113148, 75232, 35665, 12458, 3669, 729
7	11022480	21	1, 12, 92, 558, 2866, 12696, 48464, 156962, 418514, 886978, 1463483, 1884548, 1922083, 1584315, 1108675, 707398, 423861, 231846, 110079, 43740, 13122, 2187
8	264539520	28	1, 14, 122, 831, 4777, 23828, 104050, 396654, 1303998, 3622961, 8331402, 15688174, 24327620, 31464441, 34443624, 32819710, 28645158, 23943784, 19235009, 14602728, 10371507, 6850413, 4168422, 2311659, 1150362, 498636, 177147, 45927, 6561

Similarly, for $G^{\text{fr}}(4,n)$, they are:

n	Order	Diameter	Growth
1	1	0	1
2	8	4	1, 2, 2, 2, 1
3	192	6	1, 4, 12, 28, 48, 64, 35
4	3072	9	1, 6, 26, 94, 276, 630, 936, 786, 297, 20
5	61440	12	1, 8, 44, 200, 772, 2496, 6281, 11850, 15963, 14358, 7480, 1808, 179
6	1474560	16	1, 10, 66, 354, 1624, 6434, 21426, 58822, 130468, 229378, 312080, 318594, 233826, 117308, 37459, 6380, 330
7	41287680	21	1, 12, 92, 564, 2952, 13484, 53463, 182958, 535474, 1325314, 2740738, 4688248, 6574551, 7509344, 6948297, 5200024, 3141994, 1525076, 596772, 190624, 49506, 8192
8	1321205760	28	1, 14, 122, 838, 4892, 25006, 112592, 447338, 1565876, 4806076, 12837766, 29614040, 58643862, 99403154, 144205985, 179555186, 192940456, 180355000, 147906472, 107581100, 70749954, 43060784, 24556834, 12969064, 6160564, 2555904, 884736, 229376, 32768

For $G^{\text{fr}}(5,n) = G^{\text{all}}(5,n)$, we get:

n	Order	Diameter	Growth
1	1	0	1
2	10	5	1, 2, 2, 2, 2, 1
3	750	15	1, 4, 12, 28, 50, 74, 98, 108, 108, 96, 74, 50, 28, 14, 4, 1
4	15000	15	1, 6, 26, 94, 279, 653, 1244, 2036, 2762, 2983, 2404, 1404, 696, 304, 88, 20
5	375000	16	1, 8, 44, 200, 776, 2536, 6976, 16258, 32456, 55240, 77396, 83146, 62186, 29074, 7599, 1038, 66
6	11250000	20	1, 10, 66, 354, 1629, 6495, 22576, 68400, 180981, 419184, 846869, 1465336, 2095793, 2369053, 2009982, 1195810, 455924, 99908, 11173, 450, 6
7	393750000	25	1, 12, 92, 564, 2958, 13570, 55148, 199558, 644094, 1854896, 4765416, 10886496, 21895721, 38138992, 56462764, 69747326, 70572112, 57303337, 36381314, 17387479, 5918762, 1330141, 176414, 12628, 204, 1

G GENERATOR FAMILIES

G.1 COXETER GENERATORS

The Bubble-sort graph $BS_n = Cay(\mathrm{Sym}_n, \mathcal{B})$, $n \geqslant 2$, is a Cayley graph over the symmetric group with the generating set $\mathcal{B} = \{(i\, i+1) \in \mathrm{Sym}_n : 1 \leqslant i \leqslant n-1\}$ of all bubble-sort transpositions that swap neigbour elements of a permutation. It is a connected bipartite $(n-1)$–regular graph of order $n!$ and diameter $\binom{n}{2}$. The diameter is achieved on the permutation $[n\, n-1 \ldots 2\, 1]$ from the identity permutation $I_n = [1\, 2\, \ldots n-1\, n]$, where both permutations are written in one-line notation. Since this graph is bipartite it does not contain odd cycles but it contains all even l–cycles where $l = 4, 6, 8, \ldots, n!$. The generating set $\mathcal{B}$ plays an important role in computer science for generating all permutations, in the theory of polytopes where the graph BS_n is known as 1-skeleton of the Permutahedron, and in the theory of reflection and Coxeter groups. Transpositions from $\mathcal{B}$ are known as $(n-1)$ braids on n strands forming the braid group. Growth function (layer sizes) elements are given in the table.

n	Dia-meter	Growth (layer sizes)
1	0	1
2	1	1,1
3	3	1, 2, 2, 1
4	6	1, 3, 5, 6, 5, 3, 1
5	10	1, 4, 9, 15, 20, 22, 20, 15, 9, 4, 1
6	15	1, 5, 14, 29, 49, 71, 90, 101, 101, 90, 71, 49, 29, 14, 5, 1
7	21	1, 6, 20, 49, 98, 169, 259, 359, 455, 531, 573, 573, 531, 455, 359, 259, 169, 98, 49, 20, 6, 1
8	28	1, 7, 27, 76, 174, 343, 602, 961, 1415, 1940, 2493, 3017, 3450, 3736, 3836, 3736, 3450, 3017, 2493, 1940, 1415, 961, 602, 343, 174, 76, 27, 7, 1
9	36	1, 8, 35, 111, 285, 628, 1230, 2191, 3606, 5545, 8031, 11021, 14395, 17957, 21450, 24584, 27073, 28675, 29228, 28675, 27073, 24584, 21450, 17957, 14395, 11021, 8031, 5545, 3606, 2191, 1230, 628, 285, 111, 35, 8, 1
10	45	1, 9, 44, 155, 440, 1068, 2298, 4489, 8095, 13640, 21670, 32683, 47043, 64889, 86054, 110010, 135853, 162337, 187959, 211089, 230131, 243694, 250749, 250749, 243694, 230131, 211089, 187959, 162337, 135853, 110010, 86054, 64889, 47043, 32683, 21670, 13640, 8095, 4489, 2298, 1068, 440, 155, 44, 9, 1
11	55	1, 10, 54, 209, 649, 1717, 4015, 8504, 16599, 30239, 51909, 84591, 131625, 196470, 282369, 391939, 526724, 686763, 870233, 1073227, 1289718, 1511742, 1729808, 1933514, 2112319, 2256396, 2357475, 2409581, 2409581, 2357475,2256396, 2112319, 1933514, 1729808, 1511742, 1289718, 1073227, 870233, 686763, 526724, 391939, 282369, 196470, 131625, 84591, 51909, 30239, 16599, 8504, 4015, 1717, 649, 209, 54, 10, 1
12	66	1, 11, 65, 274, 923, 2640, 6655, 15159, 31758, 61997, 113906, 198497, 330121, 526581, 808896, 1200626, 1726701, 2411747, 3277965, 4342688, 5615807, 7097310, 8775209, 10624132, 12604826, 14664752, 16739858, 18757500, 20640357, 22311069, 23697232, 24736324, 25380120, 25598186, 25380120, 24736324, 23697232, 22311069, 20640357, 18757500, 16739858, 14664752, 12604826, 10624132, 8775209, 7097310, 5615807, 4342688, 3277965, 2411747, 1726701, 1200626, 808896, 526581, 330121, 198497, 113906, 61997, 31758, 15159, 6655, 2640, 923, 274, 65, 11, 1

G.2 Cyclic Coxeter Generators

We analyze the Cayley graph of the symmetric group S_n generated by the set of n cyclically adjacent transpositions:

$$S = \{(i,\, i+1 \bmod n) \mid i = 1, \ldots, n\}.$$

This set is also called the modified Bubble-sort generators and is standard in the literature Jerrum (1985). The generators produce the whole symmetric group S_n.

Our goal is to study the geometry of the resulting n-regular Cayley graphs, with a focus on the diameter D_n, the growth (BFS layer sizes), and the shape of the distance distribution from the identity. In line with the literature, our computations confirm the exact formula $D_n = \lfloor n^2/4 \rfloor$ for all tested sizes up to $n = 14$

Growth, Distance, and Diameter We perform a Breadth–First Search (BFS) from the identity to obtain the growth vector (number of elements at each distance). From this vector we compute the mean μ_n, standard deviation σ_n, mode (the distance attaining the maximum layer size), skewness, and excess kurtosis.

Table 13 consolidates summary and shape statistics for $n = 3$ through $n = 14$.

- **Diameter.** The computed diameters equal the theoretical value $\lfloor n^2/4 \rfloor$ for all $3 \le n \le 14$ (Fig. 16, left).
- **Mean and spread.** The mean distance grows roughly quadratically with n; the standard deviation grows approximately linearly (Fig. 15).
- **Shape (skewness & kurtosis).** Skewness is negative and small in magnitude; excess kurtosis is positive but small. Both move toward 0 with n. For $n = 14$, we have skewness -0.323 and excess kurtosis 0.078, indicating a slightly left-skewed, mildly leptokurtic shape relative to a Gaussian. These numbers quantify a small but persistent deviation from normality rather than a large one.

Table 13: Diameter and distance statistics for Cayley graphs generated by cyclically adjacent transpositions.

n	D_n	Mean μ_n	Std. σ_n	Mode	Skewness	Excess Kurtosis
3	2	1.17	0.69	1	-0.228	-0.893
4	4	2.17	0.90	2	-0.333	-0.136
5	6	3.50	1.13	4	-0.413	0.064
6	9	5.17	1.40	5	-0.427	0.154
7	12	7.17	1.68	8	-0.422	0.165
8	16	9.50	2.00	10	-0.408	0.156
9	20	12.17	2.33	13	-0.392	0.141
10	25	15.17	2.68	16	-0.376	0.125
11	30	18.50	3.05	20	-0.361	0.111
12	36	22.17	3.43	24	-0.347	0.098
13	42	26.17	3.83	28	-0.334	0.087
14	49	30.50	4.25	31	-0.323	0.078

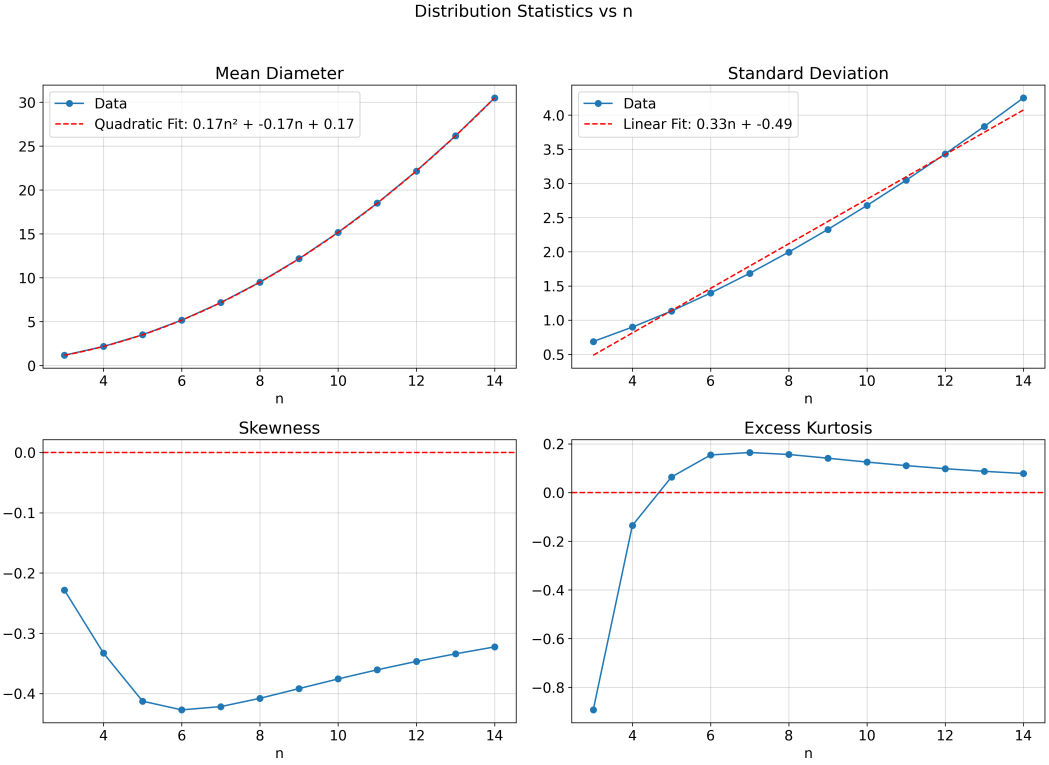


Figure 15: Summary statistics vs. n for $n = 3, \ldots, 14$: mean, standard deviation, skewness, and excess kurtosis. The fit for the mean is the quadratic $y \approx 0.17n^2 - 0.17n + 0.17$, and the fit for the standard deviation is the linear function $y \approx 0.33n - 0.49$.

Shape of the Distance Distribution The empirical distance distribution is close to Gaussian for larger n. Figure 16 (right) shows the case $n = 14$ with a Gaussian curve of $\mu = 30.50$ and $\sigma = 4.25$. The slight left tail and mild peakiness are consistent with the skewness and kurtosis reported above.

Growth Vectors (Layer Sizes) Figure 17 shows the growth functions (layer sizes) on a $\log_{10}$ scale. Table 14 lists the full growth vectors for $3 \leq n \leq 14$.

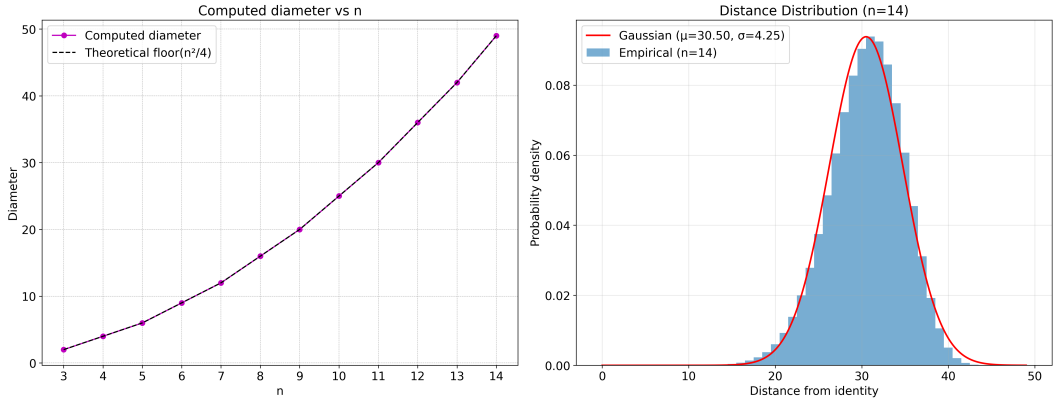


Figure 16: Left: Computed diameter D_n (markers) versus n with the theoretical curve $\lfloor n^2/4 \rfloor$ (dashed). Right: Distance distribution for $n = 14$ with fitted Gaussian ($\mu = 30.50$, $\sigma = 4.25$).

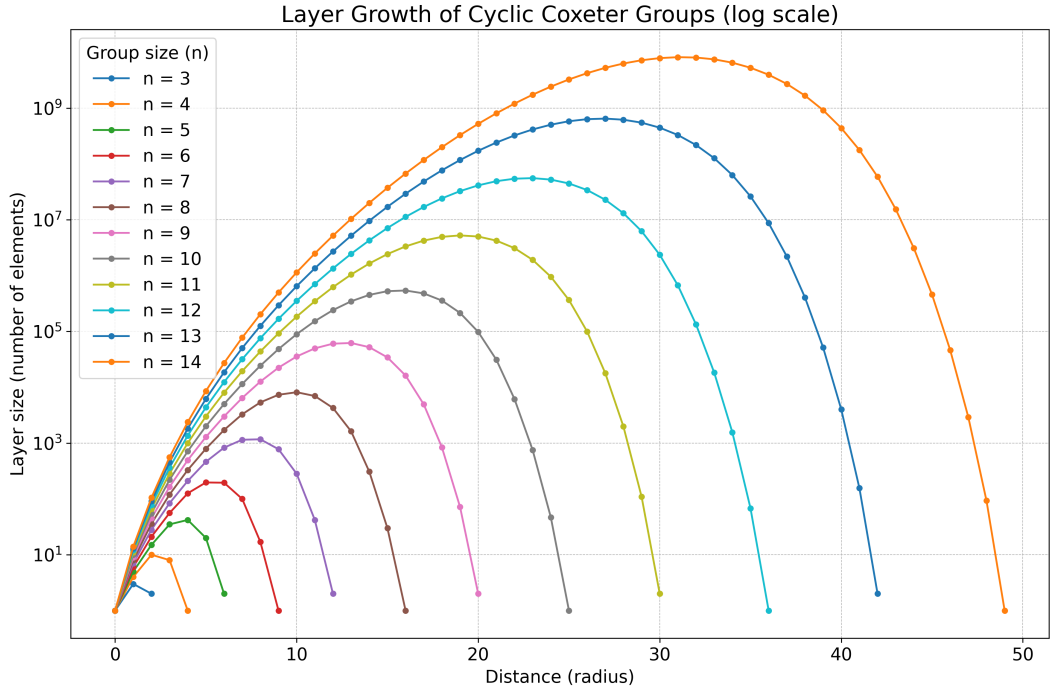


Figure 17: Growth functions on a $\log_{10}$ scale for $n = 3, \ldots, 14$: size of each layer at distance r from the identity.

Analysis of the Longest Elements The growth vectors (Table 14) show that for even n the last layer (at the diameter distance) contains exactly one element, while for odd n it contains two. Analysis of these longest elements reveals distinct structural patterns:

- **Even n:** The unique longest element is an involution decomposing into disjoint transpositions. For $n = 6$, the cycle structure is $((0, 5), (1, 4), (2, 3))$, which swaps symmetric indices.
- **Odd n:** The two longest elements are full n-cycles with different block-swap structures:
  - For $n = 5$: Cycle structures $((0, 4), (1, 3), (2))$ (both elements share this structure).

Table 14: Growth (BFS layer sizes) for cyclically adjacent transpositions ($3 \leq n \leq 14$).

n	D_n	Growth (layer sizes)
3	2	1, 3, 2
4	4	1, 4, 10, 8, 1
5	6	1, 5, 15, 35, 42, 20, 2
6	9	1, 6, 21, 56, 126, 197, 195, 100, 17, 1
7	12	1, 7, 28, 84, 210, 462, 828, 1148, 1169, 777, 282, 42, 2
8	16	1, 8, 36, 120, 330, 792, 1716, 3278, 5362, 7336, 8148, 6972, 4258, 1624, 308, 30, 1
9	20	1, 9, 45, 165, 495, 1287, 3003, 6435, 12638, 22452, 35592, 49740, 60360, 62064, 52250, 34272, 16212, 4944, 842, 72, 2
10	25	1, 10, 55, 220, 715, 2002, 5005, 11440, 24310, 48287, 89367, 153060, 240969, 346500, 451365, 526326, 540842, 479874, 357498, 214764, 98076, 31166, 6150, 750, 47, 1
11	30	1, 11, 66, 286, 1001, 3003, 8008, 19448, 43758, 92378, 184296, 348084, 621214, 1044098, 1646964, 2429284, 3335453, 4237673, 4944656, 5249838, 5012337, 4236771, 3103716, 1914242, 955286, 365244, 99660, 17930, 1982, 110, 2
12	36	1, 12, 78, 364, 1365, 4368, 12376, 31824, 75582, 167960, 352716, 704816, 1345245, 2454980, 4280474, 7119684, 11275682, 16967390, 24198306, 32607146, 41357978, 49151872, 54430794, 55780626, 52440520, 44725516, 34116522, 22851182, 13117467, 6246108, 2360644, 668514, 133487, 18370, 1562, 68, 1
13	42	1, 13, 91, 455, 1820, 6188, 18564, 50388, 125970, 293930, 646646, 1352078, 2703352, 5190562, 9593896, 17086602, 29320473, 48446229, 77001405, 117589745, 172292328, 241807150, 324427820, 415130716, 505183107, 582714561, 634535759, 649118041, 620101482, 549149614, 446756884, 330117788, 218374585, 126938097, 63301667, 26257959, 8713564, 2208492, 406978, 51636, 4006, 156, 2
14	49	1, 14, 105, 560, 2380, 8568, 27132, 77520, 203490, 497420, 1144066, 2496144, 5200300, 10399573, 20044817, 37346764, 67385500, 117857285, 199872075, 328616470, 523576508, 807898884, 1206399194, 1741769068, 2428791549, 3266926299, 4232447674, 5272211438, 6301765938, 7210522410, 7875671024, 8184285564, 8059876006, 7486458696, 6521589932, 5291298298, 3964966720, 2715665810, 1678335828, 920955932, 439630193, 177894717, 59073300, 15497794, 3095274, 457459, 46501, 2912, 93, 1

Table 15: Eigenvalues and multiplicities for small n. Values are rounded and summarized.

n	Eigenvalues (value$^{\text{multiplicity}}$)
3	$\pm 3.00^{1}$, 0.00^{4}
4	$\pm 4.00^{1}$, $\pm 2.00^{8}$, 0.00^{6}
5	$\pm 5.00^{1}$, $\pm 3.62^{8}$, $\pm 3.24^{10}$, $\pm 2.24^{6}$, $\pm 1.38^{8}$, $\pm 1.24^{10}$, $\pm 1.00^{5}$, 0.00^{24}
6	$\pm 6.00^{1}$, $\pm 5.00^{10}$, $\pm 4.61^{5}$, $\pm 4.56^{18}$, $\pm 4.00^{19}$, $\pm 3.24^{9}$, $\pm 3.20^{32}$, $\pm 3.00^{10}$, $\pm 2.61^{5}$, $\pm 2.57^{32}$, $\pm 2.00^{55}$, $\pm 1.24^{9}$, $\pm 1.00^{90}$, $\pm 0.44^{18}$, $\pm 0.36^{32}$, 0.00^{30}
7	$\pm 7.00^{1}$, $\pm 6.25^{12}$, $\pm 5.84^{28}$, $\pm 5.73^{28}$, $\pm 5.49^{15}$, $\pm 5.10^{28}$, $\pm 5.00^{14}$, $\pm 4.86^{70}$, $\pm 4.55^{12}$, $\pm 4.51^{42}$, $\pm 4.30^{21}$, $\pm 4.09^{70}$, $\pm 4.08^{28}$, $\pm 4.04^{70}$, $\pm 3.80^{60}$, $\pm 3.75^{21}$, $\pm 3.59^{42}$, $\pm 3.20^{12}$, $\pm 3.16^{28}$, $\pm 3.08^{70}$, $\pm 3.06^{28}$, $\pm 3.05^{40}$, $\pm 3.00^{70}$, $\pm 2.54^{42}$, $\pm 2.45^{60}$, $\pm 2.27^{42}$, $\pm 2.26^{28}$, $\pm 2.21^{28}$, $\pm 2.11^{15}$, $\pm 2.09^{140}$, $\pm 2.04^{70}$, $\pm 2.00^{28}$, $\pm 1.98^{70}$, $\pm 1.86^{28}$, $\pm 1.85^{42}$, $\pm 1.72^{70}$, $\pm 1.69^{40}$, $\pm 1.55^{21}$, $\pm 1.36^{40}$, $\pm 1.28^{28}$, $\pm 1.19^{70}$, $\pm 1.16^{70}$, $\pm 1.04^{70}$, $\pm 1.00^{119}$, $\pm 0.84^{70}$, $\pm 0.75^{60}$, $\pm 0.70^{70}$, $\pm 0.69^{42}$, $\pm 0.60^{15}$, $\pm 0.38^{42}$, $\pm 0.28^{42}$, $\pm 0.11^{28}$, $\pm 0.08^{42}$, $\pm 0.04^{28}$, 0.00^{300}

  - For $n = 7$: The elements are $[3, 4, 5, 6, 0, 1, 2]$ (shift by $\lfloor n/2 \rfloor$) and $[4, 5, 6, 0, 1, 2, 3]$ (shift by $\lceil n/2 \rceil$).

A clear parity-dependent pattern emerges:

- **Even n:** The permutation swaps two equal-sized blocks (size $n/2$).
- **Odd n:** The two elements correspond to near-even block divisions (sizes $\lfloor n/2 \rfloor$ and $\lceil n/2 \rceil$) with different offsets.

This nuanced behavior contrasts with simple reversal permutations and highlights the combinatorial complexity of the cyclic generators. The pattern holds consistently for $3 \leq n \leq 14$, with the last layer size always being 1 (even n) or 2 (odd n) as seen in the growth vectors.

Spectral View For small n we also computed eigenvalues of the adjacency matrix; eigenvalues are real since the graph is undirected. Table 15 lists the spectra for $n = 3, 4, 5, 6, 7$. To compare across sizes, we normalize by the degree n; the normalized distributions approach a semicircle-like shape (Fig. 18). Figure 19 shows the unscaled spectrum for $n = 6$.

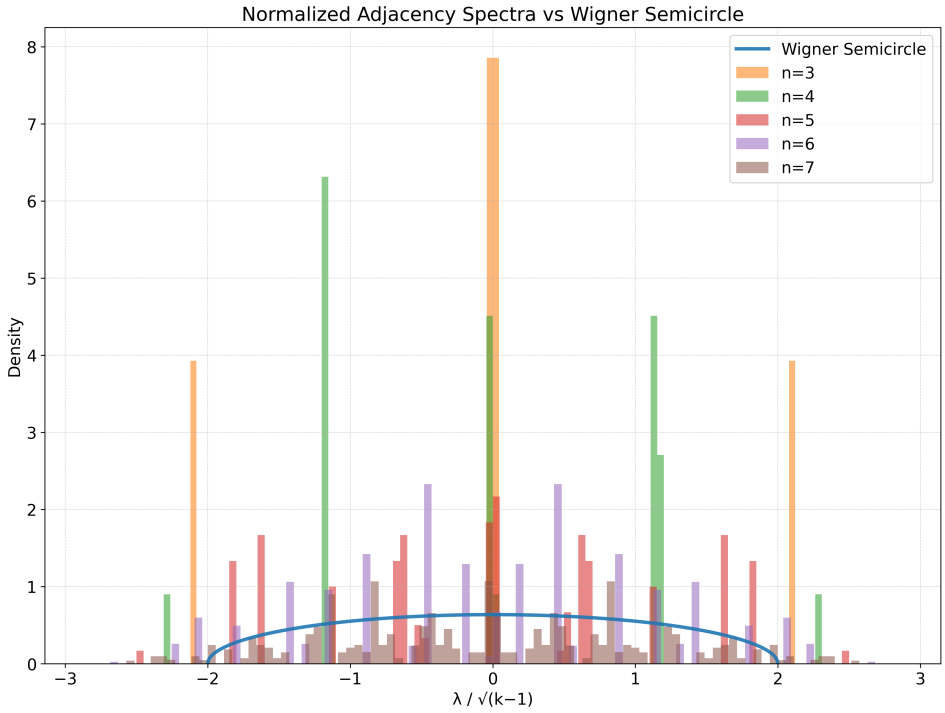


Figure 18: Normalized eigenvalue distributions for $n = 3, 4, 5, 6, 7$ vs. the Wigner semicircle law.

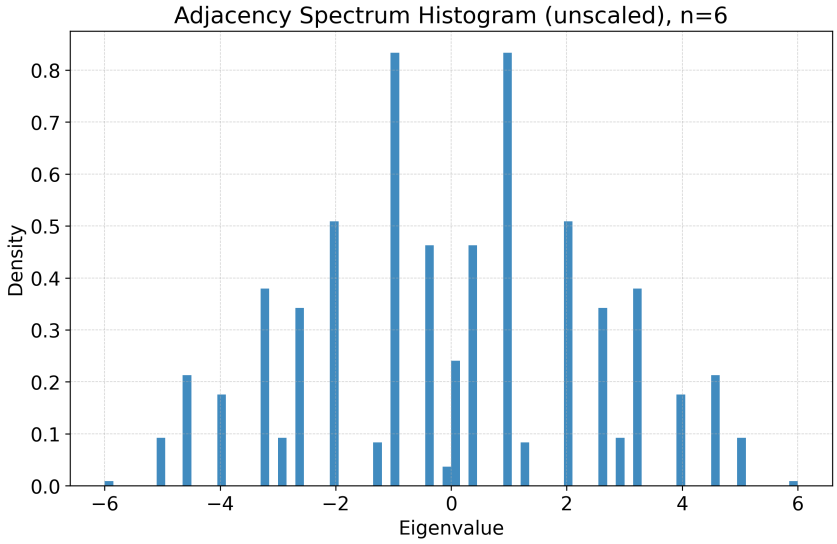


Figure 19: Adjacency spectrum histogram (unscaled) for $n = 6$.

G.3 ALL TRANSPOSITIONS (AND STRONG BRUHAT ORDER)

The transposition graph $T_n = Cay(\mathrm{Sym}_n, T), n \geqslant 2$, is the Cayley graph over the symmetric group generated by all transpositions from the set $T = \{(i\,j) \in \mathrm{Sym}_n,\ 1 \leqslant i < j \leqslant n\},\ |T| = \binom{n}{2}$. The distance in this graph is defined as the minimal number of transpositions that transform one permutation into another. The graph is bipartite since the endpoints of every edge consist of an even and odd permutation. The diameter is at most $(n-1)$ since this number of transpositions suffices to transform any permutation of n elements into another. On the other hand, transforming the identity permutation into an n-cycle requires $(n-1)$ transpositions. Thus, the diameter D is $n-1$. On Figure 20 the vertices [0123] and [1230], [3102] and [2310], [3210] and [0321] (written in one-line notations) are diametrical vertices at distance 3 from each other. The cardinalities of the metric spheres $|S_i|, 1 \leqslant i \leqslant n-1$, of radius i centered at the identity permutation are the same as the signless Stirling numbers of the first kind. These numbers are presented as Growth (layer sizes) in Table 16 and on Figure 21 as Growth of the transposition graph $T_n, 3 \leqslant n \leqslant 14$.

It is known that $T_n, n \geqslant 2$, is an integral graph such that for each $k, 1 \leqslant k \leqslant n$, the value $\frac{n(n-2k+1)}{2}$ is an eigenvalue of T_n with multiplicity at least $\frac{n!}{n(n-k)!(k-1)!}$. Since T_n is bipartite then its spectrum is symmetric with respect to zero. Its largest eigenvalues and their multiplicities are known as follows:

eigenvalue	$\frac{n(n-1)}{2}$	$\frac{n(n-3)}{2}$	$\frac{(n-1)(n-4)}{2}$	$\frac{n(n-5)}{2}$	$\frac{(n-3)(n-4)}{2}$
multiplicity	1	$(n-1)^2$	$\left(\frac{n(n-3)}{2}\right)^2$	$\left(\frac{(n-1)(n-2)}{2}\right)^2$	$\left(\frac{n(n-1)(n-5)}{2}\right)^2$

Eigenvalues and their multiplicities of $T_n,\ 3 \leqslant n \leqslant 8$, are presented in Table 17.

Eigenvalue distribution in the graphs $T_n,\ 3 \leqslant n \leqslant 7$, compared to Wigner's law is given on Figure 22.

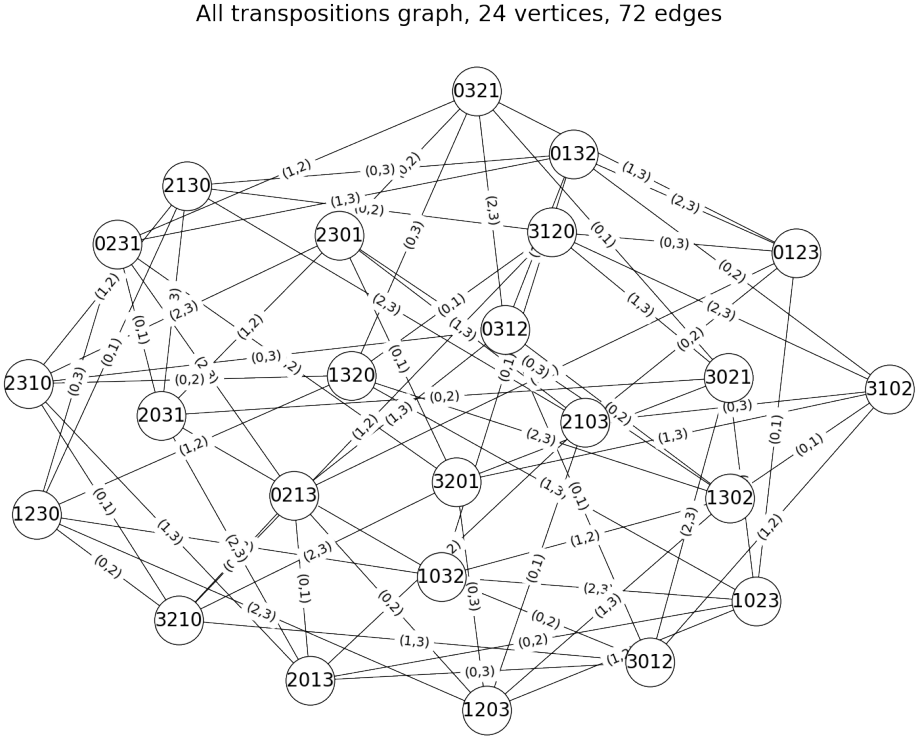


Figure 20: The diametrical vertices [0123] and [1230], [3102] and [2310], [3210] and [0321] are at distance 3 from each other in the graph T_4

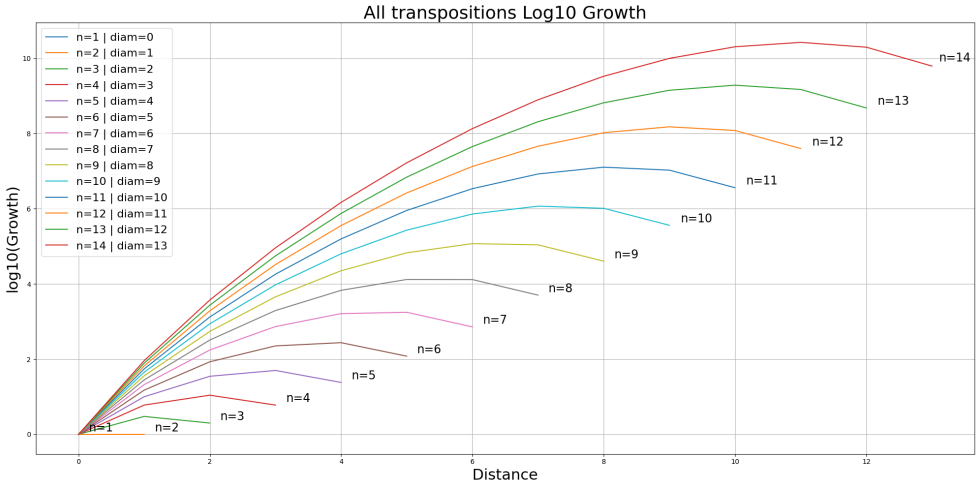


Figure 21: Growth of the transposition graph T_n, $3 \leqslant n \leqslant 14$

Table 16: All transpositions Growth

n	D	Growth (layer sizes)
1	0	1
2	1	1,1
3	2	1, 3, 2
4	3	1, 6, 11, 6
5	4	1, 10, 35, 50, 24
6	5	1, 15, 85, 225, 274, 120
7	6	1, 21, 175, 735, 1624, 1764, 720
8	7	1, 28, 322, 1960, 6769, 13132, 13068, 5040
9	8	1, 36, 546, 4536, 22449, 67284, 118124, 109584, 40320
10	9	1, 45, 870, 9450, 63273, 269325, 723680, 1172700, 1026576, 362880
11	10	1, 55, 1320, 18150, 157773, 902055, 3416930, 8409500, 12753576, 10628640, 3628800
12	11	1, 66, 1925, 32670, 357423, 2637558, 13339535, 45995730, 105258076, 150917976, 120543840, 39916800
13	12	1, 78, 2717, 55770, 749463, 6926634, 44990231, 206070150, 657206836, 1414014888, 1931559552, 1486442880, 479001600
14	13	1, 91, 3731, 91091, 1474473, 16669653, 135036473, 790943153, 3336118786, 9957703756, 20313753096, 26596717056, 19802759040, 6227020800

Table 17: All transpositions eigenvalues (format: value$^{\text{multiplicity}}$)

n	Eigenvalues (value $^{\text{multiplicity}}$)
3	-3.0^{1}, 0.0^{4}, 3.0^{1}
4	-6.0^{1}, -2.0^{9}, 0.0^{4}, 2.0^{9}, 6.0^{1}
5	-10.0^{1}, -5.0^{16}, -2.0^{25}, 0.0^{36}, 2.0^{25}, 5.0^{16}, 10.0^{1}
6	-15.0^{1}, -9.0^{25}, -5.0^{81}, -3.0^{125}, 0.0^{256}, 3.0^{125}, 5.0^{81}, 9.0^{25}, 15.0^{1}
7	-21.0^{1}, -14.0^{36}, -9.0^{196}, -7.0^{225}, -6.0^{196}, -3.0^{1225}, -1.0^{441}, 0.0^{400}, 1.0^{441}, 3.0^{1225}, 6.0^{196}, 7.0^{225}, 9.0^{196}, 14.0^{36}, 21.0^{1}
8	-28.0^{1}, -20.0^{49}, -14.0^{400}, -12.0^{441}, -10.0^{784}, -8.0^{196}, -7.0^{4096}, -4.0^{6125}, -2.0^{3136}, 0.0^{9864}, 2.0^{3136}, 4.0^{6125}, 7.0^{4096}, 8.0^{196}, 10.0^{784}, 12.0^{441}, 14.0^{400}, 20.0^{49}, 28.0^{1}

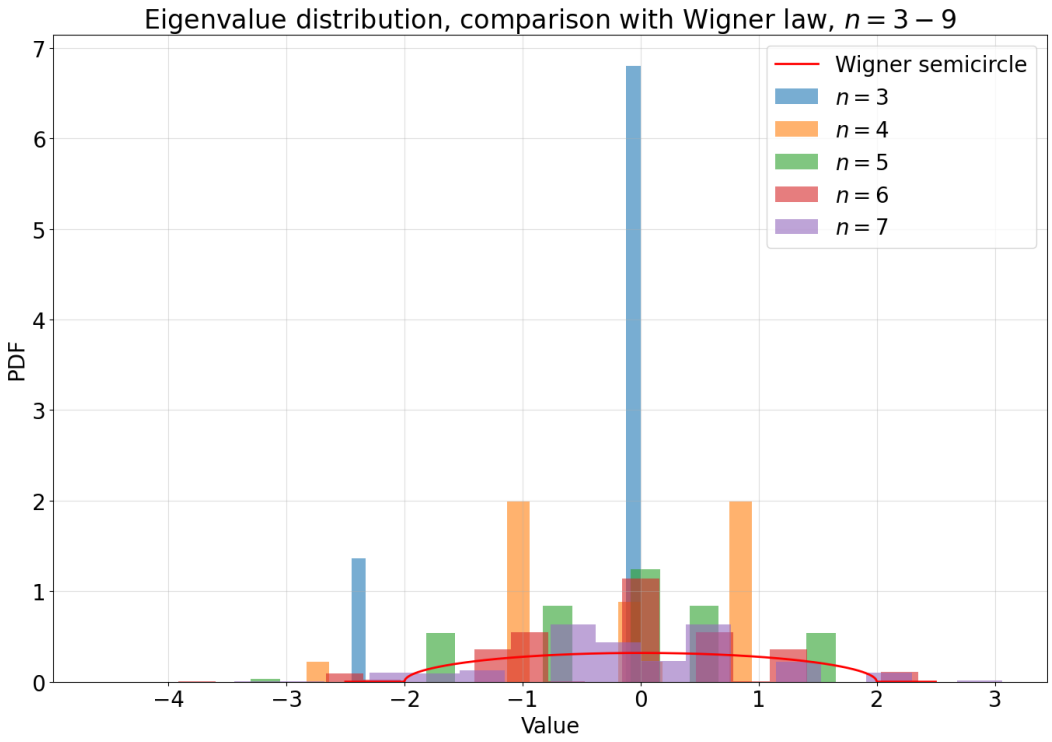


Figure 22: All transpositions eigenvalue distribution compared to Wigner's law

G.4 STAR TRANSPOSITIONS

The Star graph $\mathrm{Star}_n = Cay(\mathrm{Sym}_n, S), n \geqslant 2$, is the Cayley graph over the symmetric group generated by transpositions from the set $S = \{(1\,i) \in \mathrm{Sym}_n,\ 1 < i \leqslant n\},\ |S| = n-1$. This graph is a subgraph of the transposition graph T_n. It is a connected bipartite $(n-1)$–regular graph of order $n!$ with no odd cycles but with even cycles of lengths $2\,l$, where $3 \leqslant l \leqslant \lfloor \frac{n}{2} \rfloor$. This graph is one of the most investigated in the theory of interconnection networks since many parallel algorithms are efficiently mapped on this graph. It is shown that the diameter of Star_n is $\lfloor \frac{3(n-1)}{2} \rfloor$. Moreover,

$$Diam(\mathrm{Star}_n) = \begin{cases} \frac{3(n-1)}{2}, & \text{if } n \text{ odd,} \\ 1 + \frac{3(n-2)}{2}, & \text{if } n > 3 \text{ even.} \end{cases}$$

This is shown by considering the worst cases in a special sorting algorithm and then by giving permutations requiring at least $\lfloor \frac{3(n-1)}{2} \rfloor$ steps for this algorithm. If n is odd then the permutation $[13254 \ldots n\, n-1]$ is considered. It is clear that three steps are needed to sort each pair $(i\, i-1)$ in π. Since there are $\frac{n-1}{2}$ such pairs, hence the above diameter follows. Likewise, if n is even then for the permutation $[214365 \ldots n\, n-1]$ is shown that one can swap 2 with 1, but the remaining $\frac{n-2}{2}$ pairs again each require three steps. Thus, the indicated diameter again follows. Exact values of the diameter for Star_n, $1 \leqslant n \leqslant 19$, are given as follows:

Table 18: Star Graph Diameters for Star Transpositions generators

n	1	2	3	4	5	6	7	8	9	10	11	12	13	14	15	16	17	18	19
$Diam(\mathrm{Star}_n)$	0	1	3	4	6	7	9	10	12	13	15	16	18	19	21	22	24	25	27

Two diametrical vertices of the graph Star_5 are shown on Figure 23. They are marked by the red color while other vertices are marked by the green color. Growth (layer sizes) of the graph Star_n, $3 \leqslant n \leqslant 14$, is shown on Figure 24, and in Table 19.

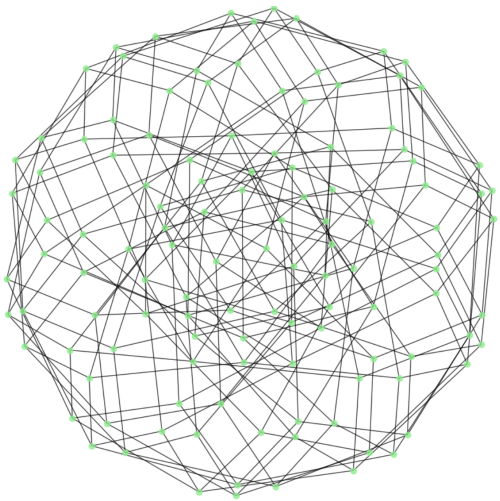


Figure 23: Two diametrical vertices and their diametrical path in the graph Star_5

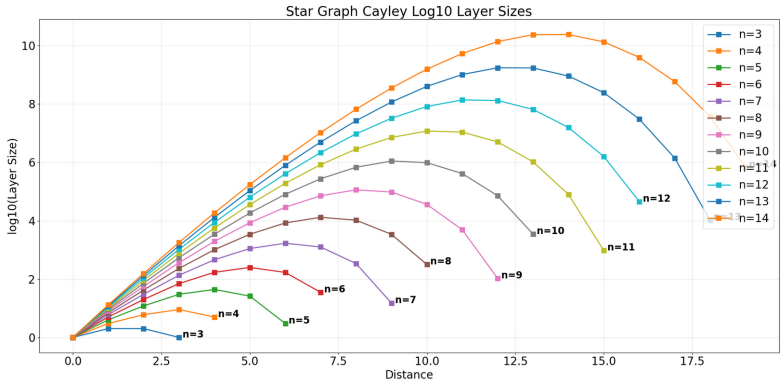


Figure 24: Growth of the Star graph Star_n, $3 \leqslant n \leqslant 14$

Table 19: Star transpositions Growth

n	Growth (layer sizes)
3	1, 2, 2, 1
4	1, 3, 6, 9, 5
5	1, 4, 12, 30, 44, 26, 3
6	1, 5, 20, 70, 170, 250, 169, 35
7	1, 6, 30, 135, 460, 1110, 1689, 1254, 340, 15
8	1, 7, 42, 231, 1015, 3430, 8379, 13083, 10408, 3409, 315
9	1, 8, 56, 364, 1960, 8540, 28994, 71512, 114064, 96116, 36260, 4900, 105
10	1, 9, 72, 540, 3444, 18396, 80262, 273546, 680448, 1106460, 978696, 411984, 71477, 3465
11	1, 10, 90, 765, 5640, 35700, 190638, 832860, 2849160, 7145310, 11821860, 10899180, 5012261, 1043630, 78750, 945
12	1, 11, 110, 1045, 8745, 64020, 404778, 2161698, 9459120, 32484210, 82091130, 137957160, 131848001, 65250691, 15643870, 1581965, 45045
13	1, 12, 132, 1386, 12980, 107910, 788733, 4984056, 26630736, 116749908, 402464700, 1024351020, 1746041351, 1722332292, 907063212, 243577026, 30498160, 1406790, 10395
14	1, 13, 156, 1794, 18590, 173030, 1435863, 10485189, 66251328, 354297372, 1556343360, 5384808000, 13796929211, 23823787403, 24169860636, 13429848354, 3961024210, 585068770, 37282245, 675675

Table 20: Star Transpositions Growth Statistics

n	D	mean	std	median	skewness	excess
3	3	1.5	0.96	1	0.0	-0.942
4	4	2.58	1.08	3	-0.516	-0.382
5	6	3.68	1.14	4	-0.54	0.253
6	7	4.78	1.18	5	-0.503	0.341
7	9	5.88	1.22	6	-0.458	0.34
8	10	6.97	1.25	7	-0.416	0.321
9	12	8.05	1.28	8	-0.377	0.301
10	13	9.13	1.3	9	-0.343	0.282
11	15	10.2	1.33	10	-0.313	0.266
12	16	11.27	1.35	11	-0.285	0.252
13	18	12.33	1.37	12	-0.261	0.241
14	19	13.39	1.39	14	-0.239	0.231

Spectral properties of the Star graph were studied in Krakovski & Mohar (2012); Chapuy & Féray (2012). It was proved in Krakovski & Mohar (2012) that for $n \geqslant 2$ and for each integer $1 \leqslant k \leqslant n-1$, the values $\pm(n-k)$ are eigenvalues of Star_n with multiplicity at least $\binom{n-2}{k-1}$. If $n \geqslant 4$, then 0 is an eigenvalue of Star_n with multiplicity at least $\binom{n-1}{2}$. Since the Star graph is bipartite, $\mathrm{mul}(n-k) = \mathrm{mul}(-n+k)$ for each integer $1 \leqslant k \leqslant n$. Moreover, $\pm(n-1)$ are simple eigenvalues of the graph. At the same time, it was shown in Chapuy & Féray (2012) that the spectrum of the Star graphs was already described in another context, since it is equivalent to studying the spectrum of Jucys-Murphy elements in the algebra of the symmetric group. This connection between two kinds of spectra implies that the Star graph is integral.

Thus, the spectrum of the graph Star_n contains all integers in the range from $-(n-1)$ to $n-1$, with the exception that when $n \leqslant 3$, zero is not an eigenvalue of Star_n. A lower bound on multiplicities of eigenvalues for this graph was improved in Chapuy & Féray (2012) as follows:

$$\mathrm{mul}(n-k) \geqslant \binom{n-2}{n-k-1}\binom{n-1}{n-k}.$$

In Avgustinovich et al. (2016), it was shown that for a fixed integer eigenvalue of Star_n, its multiplicity is at least $2^{\frac{1}{2}n\log n(1-o(1))}$. A combinatorial method for getting explicit formulas for multiplicities of eigenvalues in the Star graphs is described in Khomyakova & Konstantinova (2021) with showing all eigenvalues with their multiplicities for $n \leqslant 50$ in a catalogue.

Eigenvalue distribution in the graphs $\mathrm{Star}_n, 3 \leqslant n \leqslant 6$, compared to Wigner's law is given on Figure 25.

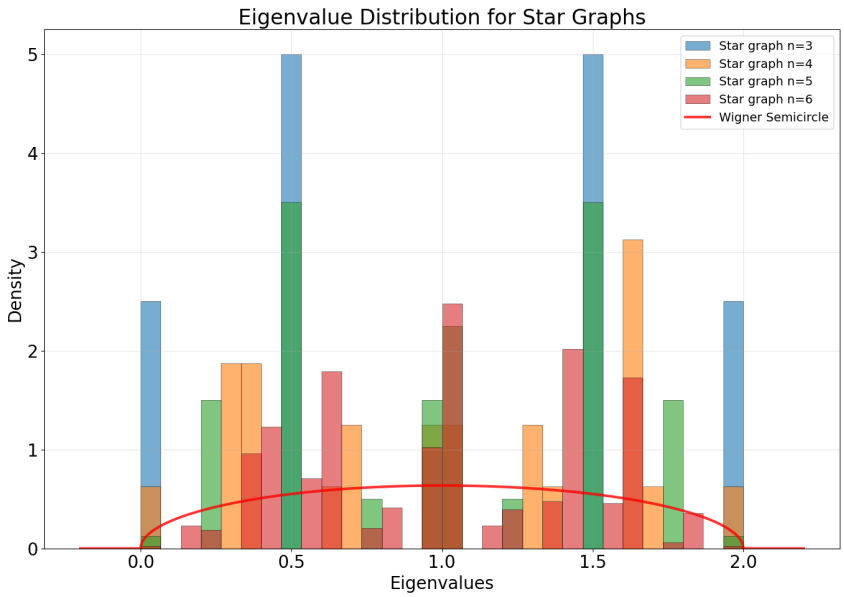


Figure 25: Star transpositions eigenvalue distribution compared to Wigner's law

G.5 Generalized star transpositions

For $1 \le k \le n-1$, define

$$S_{n,k} = \{(i\ j) : 1 \le i \le k < j \le n\}, \qquad \mathrm{GST}(n,k) = \mathrm{Cay}(S_n, S_{n,k}).$$

The transposition graph is the complete bipartite graph $K_{k,n-k}$. In particular, $k = 1$ gives the ordinary star-transposition graph. The diameter is

$$\operatorname{diam} \mathrm{GST}(n,k) = n - 1 + \max\left\{ \left\lfloor \frac{k}{2} \right\rfloor, \left\lfloor \frac{n-k}{2} \right\rfloor \right\}.$$

See Heydemann (1997); the exact complete-bipartite token-swapping distance formula in Yamanaka et al. (2014, Lemma 4) also gives this diameter by maximization. The tables below specialize to $k = 3$ and the displayed values of n.

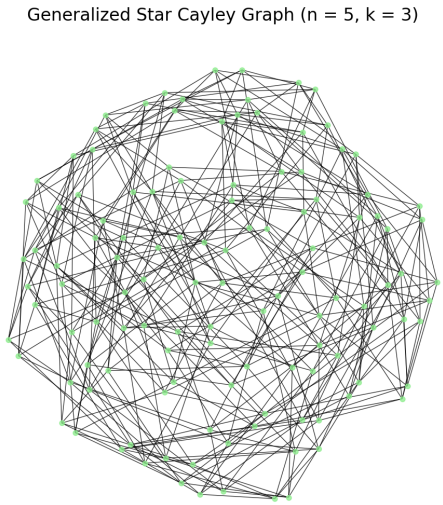


Figure 26: The generalized-star example $\mathrm{GST}(5,3)$.

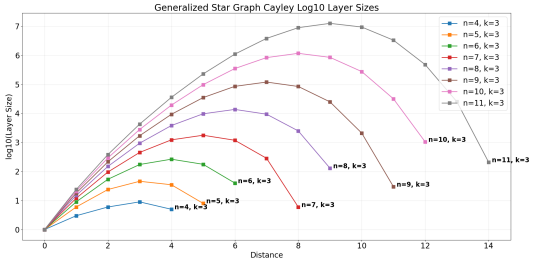


Figure 27: Growth data for generalized-star generators; parameters are indicated in the plot.

Table 21: Caylay Graph Diameters for Generalized Star generators with $k = 3$ and different values of n

n	4	5	6	7	8	9	10	11
$Diam(\mathrm{GST}(n,k))$	4	5	6	8	9	11	12	14

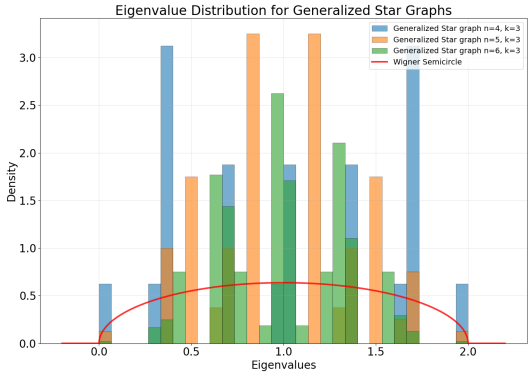


Figure 28: Spectral data for generalized-star generators; parameters are indicated in the plot.

Table 22: Caylay Graph Growth for Generalized Star generators with $k = 3$ and different values on n

n	Growth (layer sizes)
4	1, 3, 6, 9, 5
5	1, 6, 24, 46, 35, 8
6	1, 9, 54, 174, 265, 177, 40
7	1, 12, 96, 453, 1228, 1770, 1189, 285, 6
8	1, 15, 150, 943, 3817, 9680, 13699, 9392, 2493, 130
9	1, 18, 216, 1704, 9285, 34950, 85319, 119829, 84514, 24909, 2105, 30
10	1, 21, 294, 2796, 19245, 97293, 349769, 832986, 1168663, 849531, 275378, 31773, 1050
11	1, 24, 384, 4279, 35670, 227612, 1095374, 3814678, 8936500, 12569516, 9412448, 3317056, 477813, 25235, 210

Table 23: Generalized Star Generators Growth Statistics

n	D	mean	std	mode	skewness	excess
4	4	2.58	1.08	3	-0.516	-0.382
5	5	3.1	1.01	3	-0.298	-0.044
6	6	3.92	1.07	4	-0.257	-0.063
7	8	4.86	1.13	5	-0.281	-0.014
8	9	5.85	1.18	6	-0.292	0.06
9	11	6.86	1.22	7	-0.287	0.112
10	12	7.88	1.25	8	-0.274	0.142
11	14	8.92	1.28	9	-0.258	0.159

Table 24: Caylay Graph Eigenvalues with their multiplicities for Generalized Star generators with $k = 3$ and different values on n

n	Eigenvalues with multiplicities
4	$3.00^{1}, 2.00^{6}, 1.00^{3}, 0.00^{4}, -1.00^{3}, -2.00^{6}, -3.00^{1}$
5	$6.00^{1}, 4.00^{8}, 3.00^{14}, 2.00^{11}, 1.00^{26}, -1.00^{26}, -2.00^{11}, -3.00^{14}, -4.00^{8}, -6.00^{1}$
6	$9.00^{1}, 6.00^{20}, 5.00^{36}, 3.00^{154}, 2.00^{36}, 1.00^{9}, 0.00^{208}, -1.00^{9}, -2.00^{36}, -3.00^{154}, -5.00^{36}, -6.00^{20}, -9.00^{1}$

G.6 RX/LRX (TRANSPOSITION AND LONG CYCLE)

Let $L = (1\,2\,\cdots\,n)$, $R = L^{-1}$, and $X = (1\,2)$. The LRX family uses the inverse-closed generating set $\{L, R, X\}$ on S_n. Its diameter conjecture is $D_{\mathrm{LRX}}(n) = n(n-1)/2$ for $n \geq 4$. The directed RX (equivalently LX with the opposite cycle orientation) family uses one long-cycle orientation and the transposition; its parity-dependent conjecture is given below in Conjecture 2. The following statistics and growth vectors expand the corresponding catalogue entries.

G.6.1 RX - "V.M. GLUSHKOV PROBLEM"

Table 25: RX Growth Statistics

n	diameter	mean	std	median	skewness	excess
3	2	1.33	0.75	2	−0.626	−0.96
4	6	3.58	1.63	3	−0.35	−0.668
5	11	6.87	2.31	8	−0.641	−0.003
6	18	11.31	3.02	13	−0.673	0.362
7	25	16.67	3.69	18	−0.691	0.436
8	35	23.31	4.55	25	−0.661	0.381
9	45	30.96	5.37	33	−0.658	0.41
10	58	39.93	6.34	43	−0.648	0.364
11	71	49.94	7.22	53	−0.672	0.458
12	87	61.26	8.27	65	−0.652	0.427
13	103	73.67	9.22	78	−0.68	0.493
14	122	87.36	10.32	90	−0.66	0.481
15	141	102.19	11.35	107	−0.684	0.517

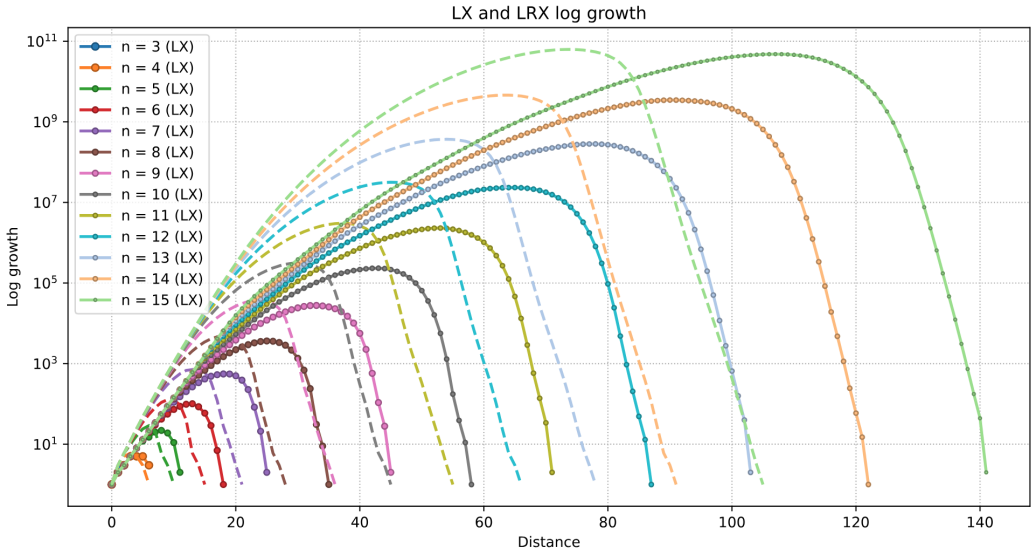


Figure 29: LX and LRX growth

Conjecture 2. *Based on numerical data for $n \leq 15$ we propose the following conjecture:*

$$d(S_n, RX) = \frac{3n^2 - 8n + 9 + 3 \cdot [n \equiv 0 \mod 2]}{4}$$

n	Full	Diameter	Growth
16	No	120^{2}	1, 3, 6, 12, 24, 48, 91, 172, 324, 596, 1092, 1992, 3589, 6432, 11484, 20355, 35881, 62975, 109909, 190552, 327513, 556338, 932643, 1543216, 2518151, 4047906, 6413758, 10029116, 15472319, 23541477, 35363771, 52510599, 77046169, 111701646, 160203409, 227455054, 319592852, 444506094, 612530084, 836536158, 1132149102, 1518848759
17	No	$136^{conjectural}$	3, 6, 12, 24, 48, 91, 172, 325, 598, 1097, 2004, 3619, 6500, 11636, 20695, 36622, 64566, 113305, 197928, 343997, 593523, 1014167, 1713828, 2862022, 4719086, 4719086, 12322523, 19525250, 30545435, 47171938, 71948269, 108484824, 161715604, 238341059, 347565044, 501807681, 717289814, 1015374627, 1424409540, 1980624511
18	No	No	3, 6, 12, 24, 48, 91, 172, 325 , 599, 1099, 2009, 3631, 6530, 11704, 20847, 36962, 65307, 114897, 201349, 351633, 611434, 1056943, 1813030, 3080558, 5179815, 8612622, 14146837, 22944379, 36763863, 58204766, 91018529, 140613990, 214832327, 324657341, 485209391, 717543731, 1050968217, 1524593337
19	No	No	3, 6, 12, 24, 48, 91, 172, 325, 600, 1101, 2014, 3643,6560, 11772, 20999, 37300, 66044, 116481, 204713, 358730, 626606, 1090461, 1889028, 3251855, 5553160, 9397426, 15744674, 26090871, 42737694, 69204377, 110786443, 175301582, 274190126, 424174740 649262217, 983257468, 1473766991, 2187812570
20	No	No	3, 6, 12, 24, 48, 91, 172, 325, 600, 1102, 2016, 3648, 6572, 11802, 21067, 37452, 66382, 117218, 206297, 362095, 633731, 1105961, 1924552, 3336573, 5754830, 9860484, 16764306, 28252288, 47148975, 77856800, 127186480, 205551832, 328568960, 519386825, 812291725, 1257401793, 1926394302

G.6.2 LRX COSETS WITH K-REPEATS

We computed growth and diameters for $3 \leq n \leq 12$ and repeats of elements whose numbers range from k to n-1. Then we plotted the dependence of the diameter on the number k.

Table 26: LRX coset diameters and growth vectors for the reported values of n and k.

n	k	Diameter	Growth
3	0	2	1 3 2
3	2	1	1 2
4	0	6	1 3 5 6 5 3 1
4	2	3	1 3 5 3
4	3	2	1 2 1
5	0	10	1, 3, 6, 10, 16, 24, 29, 21, 6, 3, 1
5	2	7	1, 3, 6, 9, 12, 14, 12, 3
5	3	5	1, 3, 6, 6, 3, 1
5	4	2	1, 2, 2
6	0	15	1, 3, 6, 11, 20, 35, 55, 81, 109, 128, 126, 95, 40, 6, 3, 1
6	2	12	1, 3, 6, 10, 17, 29, 41, 55, 65, 64, 50, 15, 4
6	3	9	1, 3, 6, 10, 15, 20, 22, 22, 16, 5
6	4	6	1, 3, 6, 7, 7, 5, 1
6	5	3	1, 2, 2, 1
7	0	21	1, 3, 6, 12, 22, 42, 73, 124, 203, 303, 425, 559, 678, 713, 746, 611, 355, 122, 28, 10, 3, 1
7	2	19	1, 3, 6, 11, 19, 36, 60, 96, 149, 210, 281, 345, 384, 361, 315, 171, 53, 13, 5, 1
7	3	15	1, 3, 6, 11, 18, 32, 47, 68, 94, 116, 130, 136, 108, 50, 18, 2
7	4	11	1, 3, 6, 11, 16, 24, 30, 34, 37, 30, 17, 1
7	5	7	1, 3, 6, 8, 8, 8, 6, 2
7	6	3	1, 2, 2, 2
8	0	28	1 3 6 12 23 44 80 142 247 411 662 1019 1481 2059 2745 3465 4126 4633 4913 4777 4163 3079 1612 488 94 25 6 3 1
8	2	25	1 3 6 11 20 38 67 116 196 314 488 726 1021 1365 1739 2107 2370 2496 2437 2100 1566 723 181 51 15 3
8	3	21	1 3 6 11 19 34 58 95 150 223 320 442 576 702 799 856 843 718 507 257 81 19
8	4	17	1 3 6 11 19 33 50 73 104 137 174 205 223 230 195 147 58 11
8	5	13	1 3 6 11 17 25 34 42 48 49 45 36 17 2
8	6	8	1 3 6 8 9 10 9 7 3
8	7	4	1 2 2 2 1

Continued on next page

n	k	Diameter	Growth
9	0	36	1 3 6 12 24 46 85 156 283 492 845 1415 2258 3476 5188 7448 10303 13816 17827 22311 26810 31091 34664 36935 37516 35651 31354 23197 13382 4680 1212 268 88 25 8 3 1
9	2	33	1 3 6 11 21 40 72 129 232 394 658 1068 1660 2504 3634 5062 6829 8926 11125 13480 15658 17458 18670 18949 18073 15631 11661 6294 2352 621 154 49 12 3
9	3	29	1 3 6 11 20 36 63 111 191 307 489 754 1115 1598 2198 2896 3677 4516 5263 5920 6325 6453 6165 5267 3944 2116 768 212 50 5
9	4	25	1 3 6 11 20 35 59 97 156 234 345 494 669 879 1107 1321 1496 1638 1669 1600 1416 1092 559 164 43 6
9	5	20	1 3 6 11 20 34 52 78 115 153 201 253 297 335 360 338 311 249 147 51 9
9	6	14	1 3 6 11 18 26 36 47 58 62 66 66 54 37 13
9	7	10	1 3 6 8 10 11 10 11 8 3 1
9	8	4	1 2 2 2 2
10	0	45	1 3 6 12 24 47 87 161 297 528 927 1611 2726 4492 7184 11109 16751 24624 35105 48718 66154 87373 111996 140388 171657 204213 236429 266276 291271 308831 316158 310824 290837 254374 199563 129134 61718 20467 5183 1116 302 92 21 6 3 1
10	2	42	1 3 6 11 21 41 74 134 245 431 745 1267 2092 3378 5298 8024 11857 17091 23863 32460 43240 55769 69928 86059 102549 118696 134384 147372 155938 159658 157396 146957 127970 99765 62609 27469 8689 2218 483 145 49 13 2
10	3	38	1 3 6 11 20 37 65 116 208 354 590 966 1531 2373 3584 5232 7431 10279 13812 18021 22927 28352 33978 39622 44929 49452 52633 53922 52985 49535 43010 33258 21146 9895 3272 906 259 66 13
10	4	33	1 3 6 11 20 36 61 106 184 297 471 732 1095 1602 2287 3152 4208 5478 6882 8393 9951 11385 12553 13536 13928 13689 12967 11209 8706 5398 2036 630 168 19
10	5	29	1 3 6 11 20 36 60 98 158 239 352 510 704 941 1236 1561 1885 2210 2519 2735 2854 2888 2757 2427 1925 1300 614 158 29 3
10	6	23	1 3 6 11 20 35 53 80 120 164 216 280 340 404 463 497 514 497 462 382 297 157 34 4
10	7	17	1 3 6 11 18 27 37 49 63 72 79 86 82 74 62 37 12 1
10	8	11	1 3 6 8 10 12 12 12 11 9 5 1
10	9	5	1 2 2 2 2 1
11	0	55	1 3 6 12 24 48 89 166 309 560 1001 1776 3097 5314 8937 14618 23293 36288 55172 81871 118838 169112 235115 319961 427229 559464 716979 903686 1116773 1352909 1609076 1880395 2148532 2408704 2650204 2844421 2980448 3049721 3017424 2878200 2626374 2235627 1702643 1044515 475424 155851 42082 10262 2835 937 328 100 32 10 3 1
11	2	52	1 3 6 11 21 42 76 139 256 461 815 1427 2450 4128 6811 10943 17158 26267 39248 57300 81868 114641 156749 209951 276166 355971 448153 555874 676029 804381 939797 1079114 1209443 1328381 1431391 1499996 1530281 1518778 1446939 1314243 1115200 839377 516503 234611 77831 21582 5414 1458 492 170 44 7 2
11	3	48	1 3 6 11 20 38 67 121 219 386 669 1141 1893 3082 4924 7665 11641 17283 25052 35463 49113 66694 88391 114769 146217 182178 221995 266584 312894 358824 404749 447118 479630 504056 517513 510788 487438 445261 375467 281631 167883 76005 26654 8033 2311 683 182 48 6
11	4	43	1 3 6 11 20 37 63 111 198 340 565 926 1472 2289 3495 5201 7564 10741 14869 20128 26590 34401 43462 53661 65043 76997 89076 101163 111971 120924 128027 131341 130391 124887 114206 97198 73594 43736 19286 6544 2019 552 87 4
11	5	38	1 3 6 11 20 37 62 107 184 299 474 738 1110 1632 2350 3296 4502 6012 7826 9896 12232 14758 17339 19944 22425 24448 25949 27012 26853 25826 23966 20678 16178 10122 4566 1416 315 45 2
11	6	32	1 3 6 11 20 37 61 100 161 247 365 531 743 1005 1339 1732 2165 2645 3137 3595 4023 4383 4616 4720 4645 4367 3905 3189 2252 1066 309 56 5
11	7	26	1 3 6 11 20 36 54 82 123 173 231 301 375 457 542 610 672 710 705 689 633 561 460 298 136 30 1
11	8	18	1 3 6 11 18 28 38 51 66 79 90 101 104 104 101 84 63 36 6
11	9	12	1 3 6 8 10 13 13 13 13 12 10 6 2
11	10	5	1 2 2 2 2 2

Continued on next page

n	k	Diameter	Growth
12	0	66	1 3 6 12 24 48 90 168 314 572 1033 1850 3263 5701 9863 16759 27866 45291 72099 112521 171929 257112 377904 545894 773038 1075171 1473589 1986076 2630262 3432644 4416186 5590709 6971232 8572605 10385539 12397678 14595522 16933499 19356689 21817886 24222746 26460935 28458315 30093680 31217047 31732310 31542112 30496145 28508698 25523039 21432297 16273946 10527747 5424324 2143159 658412 170062 42140 10995 3283 1066 361 100 23 6 3 1
12	2	63	1 3 6 11 21 42 77 141 261 472 845 1498 2619 4529 7713 12888 21117 33829 53041 81547 122807 181152 262865 374618 523044 718688 974057 1295104 1691940 2183495 2775888 3464584 4264467 5185282 6200857 7299609 8484537 9717668 10952893 12168126 13311929 14311521 15133824 15713671 15968920 15858593 15336955 14325310 12790604 10718516 8057343 5078921 2500177 942109 285693 76439 19990 5569 1690 497 138 37 10 2
12	3	59	1 3 6 11 20 38 68 123 224 397 702 1228 2099 3531 5851 9509 15138 23588 36038 53977 79179 113935 161246 224023 305403 409871 541422 701997 895879 1127304 1395382 1699837 2042209 2416409 2812961 3228184 3650821 4060278 4444856 4791982 5071286 5261016 5353707 5321305 5138405 4799520 4285184 3578714 2687158 1708915 866788 343841 114050 34191 9791 2823 875 245 51 5
12	4	54	1 3 6 11 20 37 64 113 203 355 615 1044 1724 2801 4473 6992 10713 16114 23761 34314 48609 67558 92200 123549 162576 210507 268029 334740 411322 498546 594093 695838 803519 913607 1019963 1120363 1211213 1284096 1335584 1361582 1354110 1309480 1224711 1093651 914513 682036 418016 195362 72511 23512 7092 2022 457 66 3
12	5	49	1 3 6 11 20 37 63 109 193 329 548 895 1419 2205 3363 5014 7341 10538 14801 20397 27583 36502 47367 60399 75614 92952 112260 133189 155431 178334 200845 222358 242034 258115 269759 276393 276198 268357 252664 227797 193175 148548 96317 47845 17330 5175 1453 331 55 7
12	6	42	1 3 6 11 20 37 63 108 185 299 476 741 1113 1641 2369 3332 4598 6222 8219 10620 13476 16700 20304 24229 28307 32432 36518 40162 43399 46014 47416 47934 47072 44422 40796 35377 28035 19330 9348 3089 737 114 5
12	7	36	1 3 6 11 20 37 62 101 163 250 373 544 763 1041 1397 1821 2308 2883 3514 4147 4806 5470 6037 6518 6918 7123 7130 6970 6574 5856 4936 3738 2268 967 240 40 4
12	8	28	1 3 6 11 20 36 55 83 125 176 240 316 398 492 595 686 782 869 917 954 953 924 853 779 656 504 337 96 13
12	9	20	1 3 6 11 18 28 39 52 68 82 97 112 119 126 130 121 109 94 64 31 9
12	10	13	1 3 6 8 10 13 14 15 14 13 14 11 7 3
12	11	6	1 2 2 2 2 2 1

G.6.3 GENERALIZED LRX(N,K)

LRX(n,k) is a family of LRX graphs in which the transposition $X = (0, 1)$ of the first two positions is replaced by the transposition $X = (0, k)$ of the first and k-th positions.

The "sym?" column indicates whether the last BFS element belongs to the dihedral symmetries.

n	k	Dia-meter	Size /n!	sym?	Growth
4	1	6	1	+	1, 3, 5, 6, 5, 3, 1
5	1	10	1	+	1, 3, 6, 10, 16, 24, 29, 21, 6, 3, 1
6	1	15	1	+	1, 3, 6, 11, 20, 35, 55, 81, 109, 128, 126, 95, 40, 6, 3, 1
7	1	21	1	+	1, 3, 6, 12, 22, 42, 73, 124, 203, 303, 425, 559, 678, 713, 746, 611, 355, 122, 28, 10, 3, 1
8	1	28	1	+	1, 3, 6, 12, 23, 44, 80, 142, 247, 411, 662, 1019, 1481, 2059, 2745, 3465, 4126, 4633, 4913, 4777, 4163, 3079, 1612, 488, 94, 25, 6, 3, 1
9	1	36	1	+	1, 3, 6, 12, 24, 46, 85, 156, 283, 492, 845, 1415, 2258, 3476, 5188, 7448, 10303, 13816, 17827, 22311, 26810, 31091, 34664, 36935, 37516, 35651, 31354, 23197, 13382, 4680, 1212, 268, 88, 25, 8, 3, 1
10	1	45	1	+	1, 3, 6, 12, 24, 47, 87, 161, 297, 528, 927, 1611, 2726, 4492, 7184, 11109, 16751, 24624, 35105, 48718, 66154, 87373, 111996, 140388, 171657, 204213, 236429, 266276, 291271, 308831, 316158, 310824, 290837, 254374, 199563, 129134, 61718, 20467, 5183, 1116, 302, 92, 21, 6, 3, 1
11	1	55	1	+	1, 3, 6, 12, 24, 48, 89, 166, 309, 560, 1001, 1776, 3097, 5314, 8937, 14618, 23293, 36288, 55172, 81871, 118838, 169112, 235115, 319961, 427229, 559464, 716979, 903686, 1116773, 1352909, 1609076, 1880395, 2148532, 2408704, 2650204, 2844421, 2980448, 3049721, 3017424, 2878200, 2626374, 2235627, 1702643, 1044515, 475424, 155851, 42082, 10262, 2835, 937, 328, 100, 32, 10, 3, 1
12	1	66	1		1, 3, 6, 12, 24, 48, 90, 168, 314, 572, 1033, 1850, 3263, 5701, 9863, 16759, 27866, 45291, 72099, 112521, 171929, 257112, 377904, 545894, 773038, 1075171, 1473589, 1986076, 2630262, 3432644, 4416186, 5590709, 6971232, 8572605, 10385539, 12397678, 14595522, 16933499, 19356689, 21817886, 24222746, 26460935, 28458315, 30093680, 31217047, 31732310, 31542112, 30496145, 28508698, 25523039, 21432297, 16273946, 10527747, 5424324, 2143159, 658412, 170062, 42140, 10995, 3283, 1066, 361, 100, 23, 6, 3, 1
13	1	78	1		1, 3, 6, 12, 24, 48, 91, 170, 319, 584, 1063, 1920, 3421, 6052, 10634, 18473, 31652, 53352, 88140, 142883, 227466, 355271, 544412, 820735, 1216936, 1773910, 2544596, 3598674, 5013032, 6880807, 9320848, 12458079, 16429644, 21396997, 27535909, 34994952, 43951613, 54575165, 66975698, 81275047, 97554526, 115780301, 135902073, 157819493, 181229759, 205792009, 231141361, 256581125, 281453793, 305079428, 326430281, 344503519, 358540900, 367339920, 369741101, 365143802, 352536210, 330855376, 299705540, 258322962, 205546603, 144249635, 84147086, 39002166, 14317977, 4377538, 1218565, 328146, 90104, 26947, 9121, 3190, 1094, 363, 107, 28, 8, 3, 1
14	1	91	?	+	1, 3, 6, 12, 24, 48, 91, 171, 321, 589, 1075, 1950, 3491, 6210, 10986, 19263, 33514, 57769, 98159, 163941, 269338, 435449, 691859, 1080005, 1659436, 2512942, 3746333, 5498978, 7963527, 11386406, 16058844, 22353988, 30759714, 41839872, 56238352, 74757850, 98340264, 127996579, 164875626, 210268514, 265518647, 332061277, 411414715, 504958674, 614075484, 740272276, 884534812, 1047413235, 1229737728, 1431700846, 1652211880, 1890258403, 2144499030, 2411711632, 2688028475, 2969737924, 3251282972, 3525714941, 3786625399, 4026316754, 4235611752, 4406074739, 4529134791, 4595116230, 4595217203, 4521988761, 4367186737, 4123660173, 3785800928, 3347488055, 2805032872, 2167875057, 1486173810, 866316389, 416461908, 164327289, 54789051, 16347103, 4650644, 1305284, 367812, 107719, 34044, 11050, 3538, 1133, 379, 110, 25, 6, 3, 1

n	k	Dia-meter	Size /n!	Growth
4	2	3	0.(3)	1, 3, 3, 1
5	2	10	1	1, 3, 6, 10, 16, 24, 29, 21, 6, 3, 1
6	2	8	0.1	1, 3, 6, 11, 16, 17, 12, 5, 1
7	2	21	1	1, 3, 6, 12, 20, 34, 58, 96, 158, 234, 334, 456, 562, 672, 731, 737, 583, 280, 45, 12, 5, 1
8	2	15	0.0286	1, 3, 6, 12, 21, 36, 61, 96, 146, 199, 231, 201, 100, 27, 10, 2
9	2	38	1	1, 3, 6, 12, 22, 38, 68, 120, 206, 349, 570, 914, 1412, 2123, 3133, 4504, 6327, 8625, 11505, 15021, 19099, 23613, 28154, 32397, 35872, 37701, 37249, 34491, 28822, 18996, 8738, 2270, 381, 85, 31, 12, 6, 3, 1
10	2	24	0.0079	1, 3, 6, 12, 22, 39, 70, 125, 216, 361, 590, 945, 1457, 2109, 2835, 3551, 4159, 4437, 3904, 2556, 1114, 258, 25, 4, 1
11	2	57	1	1, 3, 6, 12, 22, 40, 72, 130, 230, 397, 682, 1154, 1937, 3191, 5111, 8001, 12251, 18465, 27423, 39892, 57045, 80628, 112557, 154908, 210147, 281345, 371408, 483838, 621765, 785674, 976164, 1194403, 1436429, 1696458, 1970193, 2248594, 2519496, 2767436, 2969625, 3104916, 3151450, 3079981, 2867329, 2488212, 1936233, 1270751, 645163, 238422, 61536, 12173, 2461, 679, 244, 85, 22, 6, 3, 1
12	2	36	0.0022	1, 3, 6, 12, 22, 40, 73, 132, 235, 409, 704, 1198, 2019, 3359, 5490, 8754, 13455, 20040, 29013, 40559, 54910, 71309, 88725, 105254, 117594, 122887, 117879, 100035, 70970, 39564, 16233, 4532, 988, 297, 80, 16, 3
13	2	82	1	1, 3, 6, 12, 22, 40, 74, 134, 240, 421, 730, 1266, 2173, 3700, 6235, 10395, 17066, 27435, 43210, 66841, 101927, 153313, 227103, 331927, 480041, 687370, 973409, 1363835, 1892662, 2602661, 3547099, 4789101, 6405188, 8489779, 11156231, 14533053, 18754480, 23958597, 30304552, 37980778, 47167690, 58025966, 70716104, 85383149, 102116959, 120956373, 141908283, 164907428, 189709842, 215886929, 242919508, 270199807, 296975805, 322328991, 345119584, 364018096, 377739711, 385092514, 384801443, 375470221, 355696676, 323955463, 279173963, 221713589, 156066489, 92855837, 44427067, 16520829, 4791012, 1143528, 244323, 53209, 13909, 4662, 1746, 640, 217, 76, 30, 12, 6, 3, 1

n	k	Diameter	Size /n!	Growth
5	3	10	1	1, 3, 6, 10, 16, 24, 29, 21, 6, 3, 1
6	3	4	0.0(3)	1, 3, 6, 9, 5
7	3	23	1	1, 3, 6, 12, 20, 34, 55, 83, 124, 185, 274, 395, 558, 726, 808, 739, 540, 323, 104, 26, 14, 6, 3, 1
8	3	30	1	1, 3, 6, 12, 21, 36, 60, 95, 150, 237, 366, 545, 795, 1155, 1666, 2327, 3086, 3854, 4530, 4996, 5119, 4583, 3383, 1984, 882, 305, 88, 25, 6, 3, 1
9	3	12	0.0018	1, 3, 6, 12, 22, 38, 63, 95, 122, 129, 105, 49, 3
10	3	51	0.0079	1, 3, 6, 12, 22, 39, 67, 112, 188, 314, 517, 838, 1329, 2045, 3068, 4545, 6708, 9838, 14207, 20110, 27999, 38546, 52466, 70349, 92556, 119062, 149223, 182190, 217730, 254890, 290234, 318231, 334637, 336252, 317313, 273013, 206542, 133786, 75747, 39938, 19829, 8816, 3454, 1259, 475, 178, 67, 27, 12, 6, 3, 1
11	3	63	1	1, 3, 6, 12, 22, 40, 69, 117, 200, 340, 569, 945, 1546, 2472, 3851, 5866, 8767, 12985, 19172, 28062, 40379, 57215, 80280, 111736, 154288, 210919, 284697, 378893, 496405, 639448, 810437, 1012363, 1246697, 1511100, 1797997, 2101015, 2409595, 2708575, 2972426, 3172407, 3276488, 3252060, 3063097, 2680655, 2110960, 1453697, 871460, 467175, 235761, 117422, 57204, 27172, 12461, 5294, 2184, 1004, 448, 199, 85, 33, 14, 6, 3, 1
12	3	23	8.66e-05	1, 3, 6, 12, 22, 40, 70, 119, 205, 350, 583, 949, 1510, 2311, 3426, 4720, 5903, 6586, 6257, 4778, 2641, 864, 112, 4
13	3	92	1	1, 3, 6, 12, 22, 40, 71, 121, 210, 364, 621, 1049, 1762, 2928, 4817, 7848, 12553, 19622, 30058, 45380, 67899, 100730, 147792, 214222, 307279, 437826, 620357, 872504, 1216894, 1684195, 2315857, 3163482, 4287274, 5758596, 7661077, 10094145, 13179609, 17060694, 21895790, 27855846, 35135571, 43952016, 54538109, 67115475, 81877523, 98965494, 118474162, 140458743, 164889502, 191539031, 219968432, 249529785, 279423663, 308717795, 336343816, 360949515, 380867599, 394310610, 399501048, 394694487, 378039911, 347686777, 302978792, 245959041, 183359347, 125334721, 80100780, 49450637, 30201815, 18322790, 10941718, 6378296, 3617024, 1996753, 1081169, 582241, 315314, 171967, 91407, 45728, 22078, 10648, 5203, 2545, 1212, 555, 246, 98, 33, 12, 6, 3, 1
14	3	109	?	1, 3, 6, 12, 22, 40, 71, 122, 212, 369, 633, 1075, 1814, 3036, 5041, 8312, 13607, 21989, 34807, 53928, 82205, 123995, 185510, 274721, 401826, 581387, 835038, 1192816, 1693041, 2384645, 3333355, 4628066, 6387591, 8768269, 11969785, 16235440, 21849617, 29149608, 38560443, 50630164, 66027193, 85510675, 109946940, 140388166, 178108441, 224552945, 281278284, 349968777, 432470242, 530761076, 646910325, 783033788, 941158639, 1122931324, 1329263656, 1560086116, 1814503087, 2091191012, 2388419140, 2703339336, 3031164434, 3365083502, 3696863442, 4017241516, 4315221587, 4577453038, 4788861931, 4934035687, 4998126405, 4966307104, 4822417543, 4548622627, 4129967064, 3566881565, 2893336550, 2185716764, 1540881308, 1029215420, 665793822, 424233089, 267900994, 167718459, 104169416, 64321940, 39444443, 23932599, 14356906, 8511230, 4960840, 2832401, 1589099, 883548, 485912, 257156, 127600, 59967, 28128, 13577, 6369, 2725, 1030, 371, 149, 73, 41, 23, 12, 6, 3, 1

n	k	Diameter	Size /n!	Growth
6	4	8	0.1	1, 3, 6, 11, 16, 17, 12, 5, 1
7	4	23	1	1, 3, 6, 12, 20, 34, 55, 83, 124, 185, 274, 395, 558, 726, 808, 739, 540, 323, 104, 26, 14, 6, 3, 1
8	4	6	0.0016	1, 3, 6, 12, 19, 17, 6
9	4	39	1	1, 3, 6, 12, 22, 38, 65, 107, 172, 268, 408, 620, 931, 1366, 1978, 2860, 4101, 5793, 8068, 11018, 14787, 19688, 25815, 32767, 39607, 44606, 45330, 40343, 29532, 17722, 8791, 3664, 1417, 597, 252, 92, 23, 6, 3, 1
10	4	24	0.0079	1, 3, 6, 12, 22, 39, 67, 112, 184, 294, 464, 733, 1138, 1704, 2452, 3334, 4258, 4842, 4519, 3051, 1265, 273, 23, 3, 1
11	4	61	1	1, 3, 6, 12, 22, 40, 69, 117, 196, 320, 520, 842, 1354, 2139, 3286, 4933, 7310, 10781, 15867, 23180, 33416, 47461, 66519, 92372, 127568, 175124, 238080, 319959, 425365, 559227, 726454, 931740, 1177770, 1465544, 1793585, 2153821, 2529419, 2893000, 3208036, 3423860, 3508459, 3421308, 3131851, 2631465, 1978755, 1309347, 763280, 393177, 184843, 81767, 33388, 12566, 4495, 1720, 701, 234, 73, 29, 14, 6, 3, 1
12	4	17	1.08e-05	1, 3, 6, 12, 22, 40, 70, 119, 199, 320, 488, 678, 844, 908, 813, 502, 149, 10
13	4	89	1	1, 3, 6, 12, 22, 40, 71, 121, 206, 344, 572, 954, 1574, 2578, 4197, 6749, 10635, 16390, 24760, 36970, 54980, 81494, 119892, 174219, 249764, 354342, 499383, 700865, 979980, 1362835, 1880218, 2569012, 3475394, 4660381, 6208151, 8225431, 10828539, 14138596, 18296413, 23486970, 29952677, 37984475, 47897868, 59998973, 74550360, 91755339, 111745066, 134564029, 160149616, 188367639, 218910399, 251287740, 284670301, 317739035, 348884372, 376440273, 398743635, 413998149, 420085770, 414236962, 393386088, 355531766, 301781832, 237759748, 172705947, 116007949, 72870469, 43363193, 24742132, 13674143, 7352284, 3836528, 1925457, 923936, 425844, 187653, 77819, 30642, 12410, 5319, 2302, 969, 384, 143, 54, 25, 12, 6, 3, 1

n	k	Dia-meter	Size /n!	Growth
7	5	21	1	1, 3, 6, 12, 20, 34, 58, 96, 158, 234, 334, 456, 562, 672, 731, 737, 583, 280, 45, 12, 5, 1
8	5	30	1	1, 3, 6, 12, 21, 36, 60, 95, 150, 237, 366, 545, 795, 1155, 1666, 2327, 3086, 3854, 4530, 4996, 5119, 4583, 3383, 1984, 882, 305, 88, 25, 6, 3, 1
9	5	39	1	1, 3, 6, 12, 22, 38, 65, 107, 172, 268, 408, 620, 931, 1366, 1978, 2860, 4101, 5793, 8068, 11018, 14787, 19688, 25815, 32767, 39607, 44606, 45330, 40343, 29532, 17722, 8791, 3664, 1417, 597, 252, 92, 23, 6, 3, 1
10	5	8	4.4091e-05	1, 3, 6, 12, 22, 37, 46, 28, 5
11	5	59	1	1, 3, 6, 12, 22, 40, 69, 117, 196, 320, 515, 813, 1263, 1949, 2977, 4451, 6522, 9486, 13802, 20007, 28733, 40838, 57261, 78870, 107061, 144266, 193601, 259069, 346004, 460027, 605751, 787463, 1011603, 1287822, 1625786, 2029039, 2486582, 2974318, 3447404, 3835812, 4035702, 3941321, 3488449, 2724519, 1829973, 1058798, 541720, 254325, 107982, 40699, 14139, 5375, 2345, 1037, 390, 110, 25, 6, 3, 1
12	5	70	1	1, 3, 6, 12, 22, 40, 70, 119, 201, 332, 541, 869, 1379, 2184, 3444, 5338, 8073, 11968, 17546, 25620, 37389, 54463, 78766, 112421, 157847, 218413, 299481, 408443, 553914, 746444, 1000256, 1333612, 1768417, 2330500, 3049951, 3961613, 5108108, 6543496, 8327072, 10504397, 13093568, 16091345, 19485592, 23246974, 27294044, 31443674, 35382422, 38631941, 40598844, 40677650, 38410724, 33718019, 27123253, 19732023, 12841214, 7457800, 3899160, 1857003, 814782, 332784, 127508, 45517, 15256, 5193, 1798, 554, 144, 33, 6, 3, 1
13	5	86	1	1, 3, 6, 12, 22, 40, 71, 121, 206, 344, 567, 925, 1495, 2411, 3873, 6163, 9626, 14706, 22029, 32574, 47942, 70478, 103323, 150507, 217133, 309754, 436875, 609928, 845017, 1163814, 1592804, 2163383, 2914951, 3898639, 5180440, 6846261, 9005514, 11793471, 15377846, 19966714, 25808146, 33174934, 42341427, 53575349, 67161647, 83435448, 102789299, 125628427, 152263963, 182789174, 217007693, 254394698, 294103101, 334671841, 374116596, 409755080, 438298392, 455882110, 458378041, 442524726, 407210952, 353702049, 286520504, 213728578, 145442593, 89899196, 50567121, 26119653, 12625399, 5827355, 2611900, 1130390, 463034, 178946, 65600, 23662, 8801, 3202, 1112, 386, 150, 72, 35, 17, 8, 3, 1
14	5	101	?	1, 3, 6, 12, 22, 40, 71, 122, 208, 349, 579, 951, 1551, 2527, 4101, 6611, 10581, 16721, 25889, 39219, 58499, 86675, 128189, 189032, 276895, 401777, 577041, 820971, 1159417, 1628933, 2278750, 3170739, 4377895, 5986448, 8105543, 10882174, 14518469, 19283785, 25512528, 33595215, 43994803, 57309006, 74343562, 96149055, 124017979, 159451146, 204083803, 259599658, 327743177, 410504861, 510366789, 630376965, 773934922, 944395742, 1144711338, 1377277761, 1643988873, 1946279650, 2284696892, 2658002871, 3061905991, 3488042472, 3923523680, 4351095592, 4750131167, 5097508707, 5368954008, 5540589468, 5588536542, 5487479959, 5212855233, 4750688847, 4113989138, 3354118308, 2555758702, 1814150199, 1202392351, 749363585, 442713883, 249315448, 134392877, 69706468, 34956057, 17003448, 8055675, 3734904, 1692058, 739356, 310194, 126383, 50649, 20154, 7946, 2973, 989, 280, 72, 23, 12, 6, 3, 1

n	k	Dia-meter	Size /n!	Growth
8	6	15	0.0286	1, 3, 6, 12, 21, 36, 61, 96, 146, 199, 231, 201, 100, 27, 10, 2
9	6	12	0.0018	1, 3, 6, 12, 22, 38, 63, 95, 122, 129, 105, 49, 3
10	6	24	0.0079	1, 3, 6, 12, 22, 39, 67, 112, 184, 294, 464, 733, 1138, 1704, 2452, 3334, 4258, 4842, 4519, 3051, 1265, 273, 23, 3, 1
11	6	59	1	1, 3, 6, 12, 22, 40, 69, 117, 196, 320, 515, 813, 1263, 1949, 2977, 4451, 6522, 9486, 13802, 20007, 28733, 40838, 57261, 78870, 107061, 144266, 193601, 259069, 346004, 460027, 605751, 787463, 1011603, 1287822, 1625786, 2029039, 2486582, 2974318, 3447404, 3835812, 4035702, 3941321, 3488449, 2724519, 1829973, 1058798, 541720, 254325, 107982, 40699, 14139, 5375, 2345, 1037, 390, 110, 25, 6, 3, 1
12	6	10	8.02e-07	1, 3, 6, 12, 22, 40, 68, 96, 92, 41, 3
13	6	83	1	1, 3, 6, 12, 22, 40, 71, 121, 206, 344, 567, 925, 1489, 2371, 3734, 5841, 9060, 13806, 20578, 30188, 44078, 64410, 93921, 136102, 195785, 279255, 393431, 545860, 747048, 1012781, 1365174, 1835237, 2465632, 3308669, 4420900, 5860264, 7689939, 9990005, 12872262, 16490911, 21045622, 26779418, 33984492, 43023428, 54340675, 68437191, 85827409, 107018827, 132523670, 162864781, 198532390, 239777665, 286324496, 337039807, 389672673, 440630325, 484728386, 515453094, 524956696, 505759640, 453901386, 372827768, 275681050, 181542407, 106728110, 56833648, 28031099, 13037188, 5770715, 2417544, 965062, 382127, 159909, 70306, 30568, 12634, 4974, 1815, 572, 146, 28, 6, 3, 1

n	k	Diameter	Size /n!	Growth
9	7	38	1	1, 3, 6, 12, 22, 38, 68, 120, 206, 349, 570, 914, 1412, 2123, 3133, 4504, 6327, 8625, 11505, 15021, 19099, 23613, 28154, 32397, 35872, 37701, 37249, 34491, 28822, 18996, 8738, 2270, 381, 85, 31, 12, 6, 3, 1
10	7	51	1	1, 3, 6, 12, 22, 39, 67, 112, 188, 314, 517, 838, 1329, 2045, 3068, 4545, 6708, 9838, 14207, 20110, 27999, 38546, 52466, 70349, 92556, 119062, 149223, 182190, 217730, 254890, 290234, 318231, 334637, 336252, 317313, 273013, 206542, 133786, 75747, 39938, 19829, 8816, 3454, 1259, 475, 178, 67, 27, 12, 6, 3, 1
11	7	61	1	1, 3, 6, 12, 22, 40, 69, 117, 196, 320, 520, 842, 1354, 2139, 3286, 4933, 7310, 10781, 15867, 23180, 33416, 47461, 66519, 92372, 127568, 175124, 238080, 319959, 425365, 559227, 726454, 931740, 1177770, 1465544, 1793585, 2153821, 2529419, 2893000, 3208036, 3423860, 3508459, 3421308, 3131851, 2631465, 1978755, 1309347, 763280, 393177, 184843, 81767, 33388, 12566, 4495, 1720, 701, 234, 73, 29, 14, 6, 3, 1
12	7	70	1	1, 3, 6, 12, 22, 40, 70, 119, 201, 332, 541, 869, 1379, 2184, 3444, 5338, 8073, 11968, 17546, 25620, 37389, 54463, 78766, 112421, 157847, 218413, 299481, 408443, 553914, 746444, 1000256, 1333612, 1768417, 2330500, 3049951, 3961613, 5108108, 6543496, 8327072, 10504397, 13093568, 16091345, 19485592, 23246974, 27294044, 31443674, 35382422, 38631941, 40598844, 40677650, 38410724, 33718019, 27123253, 19732023, 12841214, 7457800, 3899160, 1857003, 814782, 332784, 127508, 45517, 15256, 5193, 1798, 554, 144, 33, 6, 3, 1
13	7	83	1	1, 3, 6, 12, 22, 40, 71, 121, 206, 344, 567, 925, 1489, 2371, 3734, 5841, 9060, 13806, 20578, 30188, 44078, 64410, 93921, 136102, 195785, 279255, 393431, 545860, 747048, 1012781, 1365174, 1835237, 2465632, 3308669, 4420900, 5860264, 7689939, 9990005, 12872262, 16490911, 21045622, 26779418, 33984492, 43023428, 54340675, 68437191, 85827409, 107018827, 132523670, 162864781, 198532390, 239777665, 286324496, 337039807, 389672673, 440630325, 484728386, 515453094, 524956696, 505759640, 453901386, 372827768, 275681050, 181542407, 106728110, 56833648, 28031099, 13037188, 5770715, 2417544, 965062, 382127, 159909, 70306, 30568, 12634, 4974, 1815, 572, 146, 28, 6, 3, 1

n	k	Diameter	Size /n!	Growth
10	8	24	0.0079	1, 3, 6, 12, 22, 39, 70, 125, 216, 361, 590, 945, 1457, 2109, 2835, 3551, 4159, 4437, 3904, 2556, 1114, 258, 25, 4, 1
11	8	63	1	1, 3, 6, 12, 22, 40, 69, 117, 200, 340, 569, 945, 1546, 2472, 3851, 5866, 8767, 12985, 19172, 28062, 40379, 57215, 80280, 111736, 154288, 210919, 284697, 378893, 496405, 639448, 810437, 1012363, 1246697, 1511100, 1797997, 2101015, 2409595, 2708575, 2972426, 3172407, 3276488, 3252060, 3063097, 2680655, 2110960, 1453697, 871460, 467175, 235761, 117422, 57204, 27172, 12461, 5294, 2184, 1004, 448, 199, 85, 33, 14, 6, 3, 1
12	8	17	1.08e-05	1, 3, 6, 12, 22, 40, 70, 119, 199, 320, 488, 678, 844, 908, 813, 502, 149, 10
13	8	86	1	1, 3, 6, 12, 22, 40, 71, 121, 206, 344, 567, 925, 1495, 2411, 3873, 6163, 9626, 14706, 22029, 32574, 47942, 70478, 103323, 150507, 217133, 309754, 436875, 609928, 845017, 1163814, 1592804, 2163383, 2914951, 3898639, 5180440, 6846261, 9005514, 11793471, 15377846, 19966714, 25808146, 33174934, 42341427, 53575349, 67161647, 83435448, 102789299, 125628427, 152263963, 182789174, 217007693, 254394698, 294103101, 334671841, 374116596, 409755080, 438298392, 455882110, 458378041, 442524726, 407210952, 353702049, 286520504, 213728578, 145442593, 89899196, 50567121, 26119653, 12625399, 5827355, 2611900, 1130390, 463034, 178946, 65600, 23662, 8801, 3202, 1112, 386, 150, 72, 35, 17, 8, 3, 1

n	k	Diameter	Size /$n!$	Growth
11	9	57	1	1, 3, 6, 12, 22, 40, 72, 130, 230, 397, 682, 1154, 1937, 3191, 5111, 8001, 12251, 18465, 27423, 39892, 57045, 80628, 112557, 154908, 210147, 281345, 371408, 483838, 621765, 785674, 976164, 1194403, 1436429, 1696458, 1970193, 2248594, 2519496, 2767436, 2969625, 3104916, 3151450, 3079981, 2867329, 2488212, 1936233, 1270751, 645163, 238422, 61536, 12173, 2461, 679, 244, 85, 22, 6, 3, 1
12	9	23	8.66e-05	1, 3, 6, 12, 22, 40, 70, 119, 205, 350, 583, 949, 1510, 2311, 3426, 4720, 5903, 6586, 6257, 4778, 2641, 864, 112, 4
13	9	89	1	1, 3, 6, 12, 22, 40, 71, 121, 206, 344, 572, 954, 1574, 2578, 4197, 6749, 10635, 16390, 24760, 36970, 54980, 81494, 119892, 174219, 249764, 354342, 499383, 700865, 979980, 1362835, 1880218, 2569012, 3475394, 4660381, 6208151, 8225431, 10828539, 14138596, 18296413, 23486970, 29952677, 37984475, 47897868, 59998973, 74550360, 91755339, 111745066, 134564029, 160149616, 188367639, 218910399, 251287740, 284670301, 317739035, 348884372, 376440273, 398743635, 413998149, 420085770, 414236962, 393386088, 355531766, 301781832, 237759748, 172705947, 116007949, 72870469, 43363193, 24742132, 13674143, 7352284, 3836528, 1925457, 923936, 425844, 187653, 77819, 30642, 12410, 5319, 2302, 969, 384, 143, 54, 25, 12, 6, 3, 1

n	k	Diameter	Size /$n!$	Growth
12	10	36	0.0022	1, 3, 6, 12, 22, 40, 73, 132, 235, 409, 704, 1198, 2019, 3359, 5490, 8754, 13455, 20040, 29013, 40559, 54910, 71309, 88725, 105254, 117594, 122887, 117879, 100035, 70970, 39564, 16233, 4532, 988, 297, 80, 16, 3
13	10	92	1	1, 3, 6, 12, 22, 40, 71, 121, 210, 364, 621, 1049, 1762, 2928, 4817, 7848, 12553, 19622, 30058, 45380, 67899, 100730, 147792, 214222, 307279, 437826, 620357, 872504, 1216894, 1684195, 2315857, 3163482, 4287274, 5758596, 7661077, 10094145, 13179609, 17060694, 21895790, 27855846, 35135571, 43952016, 54538109, 67115475, 81877523, 98965494, 118474162, 140458743, 164889502, 191539031, 219968432, 249529785, 279423663, 308717795, 336343816, 360949515, 380867599, 394310610, 399501048, 394694487, 378039911, 347686777, 302978792, 245959041, 183359347, 125334721, 80100780, 49450637, 30201815, 18322790, 10941718, 6378296, 3617024, 1996753, 1081169, 582241, 315314, 171967, 91407, 45728, 22078, 10648, 5203, 2545, 1212, 555, 246, 98, 33, 12, 6, 3, 1

n	k	Diameter	Size /$n!$	Growth
13	11	82	1	1, 3, 6, 12, 22, 40, 74, 134, 240, 421, 730, 1266, 2173, 3700, 6235, 10395, 17066, 27435, 43210, 66841, 101927, 153313, 227103, 331927, 480041, 687370, 973409, 1363835, 1892662, 2602661, 3547099, 4789101, 6405188, 8489779, 11156231, 14533053, 18754480, 23958597, 30304552, 37980778, 47167690, 58025966, 70716104, 85383149, 102116959, 120956373, 141908283, 164907428, 189709842, 215886929, 242919508, 270199807, 296975805, 322328991, 345119584, 364018096, 377739711, 385092514, 384801443, 375470221, 355696676, 323955463, 279173963, 221713589, 156066489, 92855837, 44427067, 16520829, 4791012, 1143528, 244323, 53209, 13909, 4662, 1746, 640, 217, 76, 30, 12, 6, 3, 1

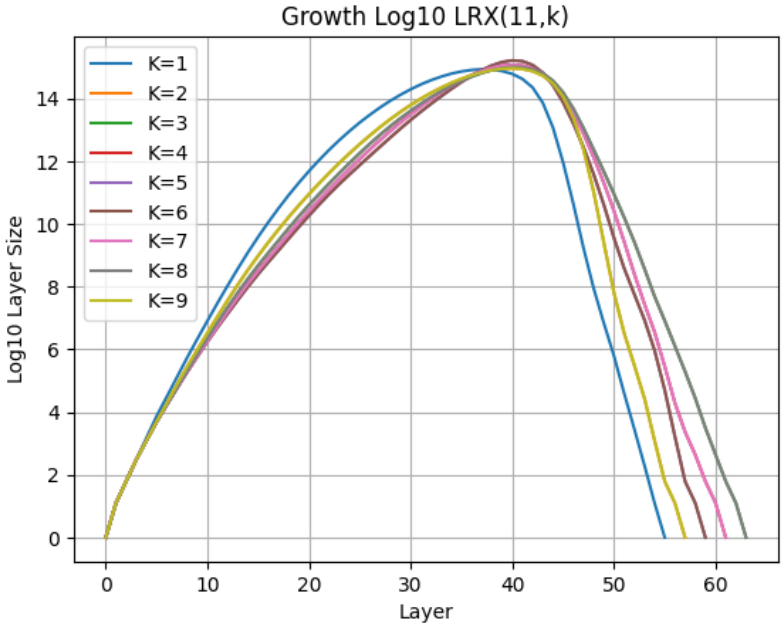


Figure 30: LRX(11,k)

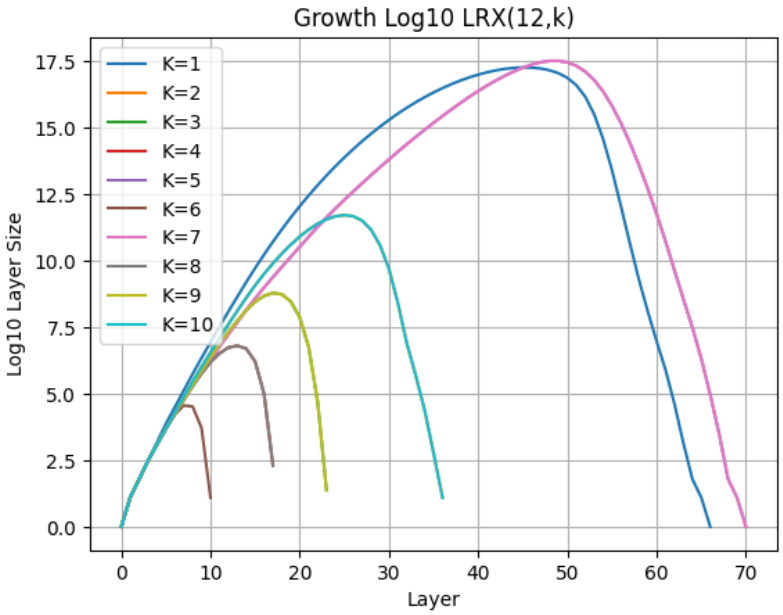


Figure 31: LRX(12,k)

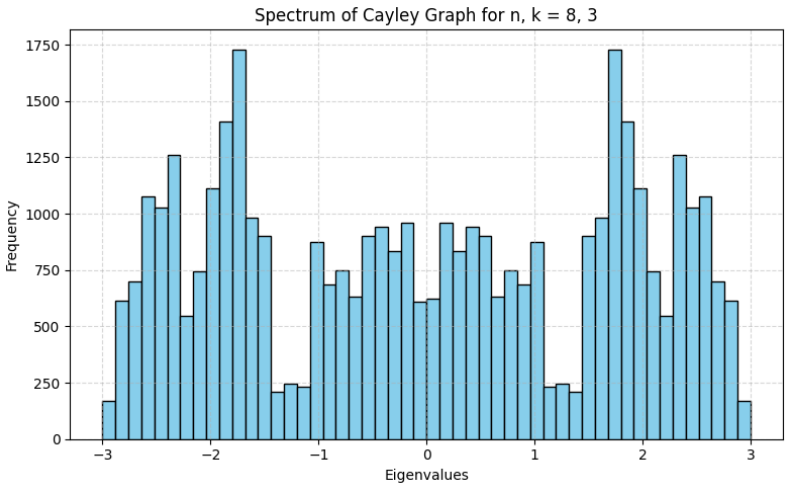


Figure 32: LRX(8,2) Spectrum

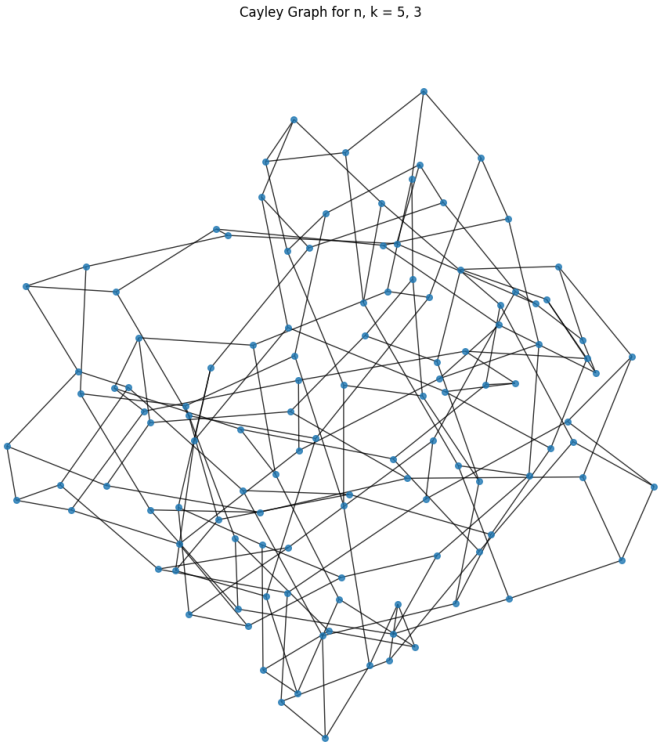


Figure 33: LRX(5,3) Graph

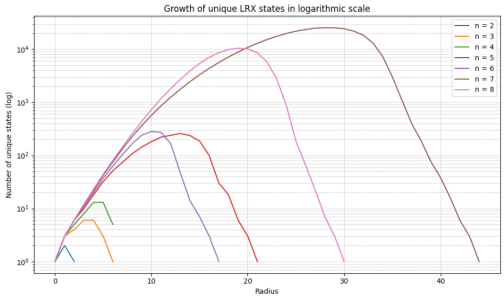


Figure 34: Two minuses LRX states grows

G.6.4 SIGNED LRX

The diameter of the LRX permutation group where X changes *both* signs can be *estimated* as follows. It is *at least* the diameter of the *un*signed group, which is at least $n(n-1)/2 - n/2 - 1$.

On the other hand, the diameter of the signed permutation group is also estimated from above as follows. Solve the *un*signed permutation. Then we end up with some combination of signs. After some combination of transpositions and rotations every element returns to its original place, this time with the right signs.

If n is even, then the number of transpositions of every element has the same parity as the number of rotations. Therefore, the number of sign changes of every element is the same, and once the unsigned permutation is solved, the signed one is such that all signs are the same. If they are negative, then we apply $(LX)^{n-1}$. Then all elements stay at the same place and change the signs.

Next we consider the case when n is odd. Recall that the algorithm for solving the unsigned permutation by using all cyclic transpositions required us to move every element to its rightful place. If we revise the algorithm by choosing the different path, then the sign of all elements, except for the moved one, changes. Therefore, if the solution to the unsigned problem made some elements negative, then we change the path of precisely these (or of precisely the positive ones). Therefore, the number of operations used in a cycle of m elements is at most $m + \sum_{cycle} 2[dist(i, \sigma(i))$ or $n - dist(i, \sigma(i)))]$. Therefore, the total amount of operations is at most

$$3n + \sum 2[dist(i, \sigma(i)) \text{ or } n - dist(i, \sigma(i)))].$$

Summing the numbers in two different cases, we obtain $6n + 2n^2$, and one of the numbers is at most $n^2 + 3n$.

n	Full	Dia-meter	Growth
2	Yes	2	1,2,1
3	Yes	6	1,3,4,6,6,3,1
4	Yes	6	1,3,5,8,13,13,5
5	Yes	21	1,3,6,10,18,32,51,74,107,143,181,220,238,257,236,186,99,30,18,6,3,1
6	Yes	17	1,3,6,11,20,37,63,103,165,239,281,272,167,47,14,7,3,1
7	Yes	44	1,3,6,12,22,42,75,132,225,363,567,856,1244,1752,2436,3298,4344,5612,7112,8817,10793,12889,15138,17404,19705,21751,23381,248
8	Yes	30	1,3,6,12,23,44,80,144,255,433,722,1167,1797,2682,3894,5368,7012,8603,9832,10395,10031,8510,5727,2749,867,185,65,22,7,3,1

This version contains two minuses in the X permutation. Here, below, we can see the growth of unique LRX states of this case on log scale:

n	Full	Dia-meter	Growth
2	Yes	3	1,2,3,2
3	Yes	5	1,3,5,9,5,1
4	Yes	10	1,3,6,13,27,55,91,105,65,16,2
5	Yes	12	1,3,7,15,34,73,141,250,409,486,359,119,23
6	Yes	19	1,3,7,16,36,81,169,340,671,1278,2319,3904,5983,8212,9221,7744,4360,1414,273,48
7	Yes	25	1,3,7,17,38,88,189,396,818,1630,3143,5851,10402,17051,25883,36449,46253,52508,51536,40153,21755,6772,1335,232,40,10
8	Yes	34	1,3,7,17,39,90,196,416,877,1801,3620,7156,13834,25996,47401,82662,137849,221602,341736,505969,715529,954964,1191570,13717

This version contains one minus in the X permutation. Here, below, we can see the growth of unique LRX states of this case on log scale:

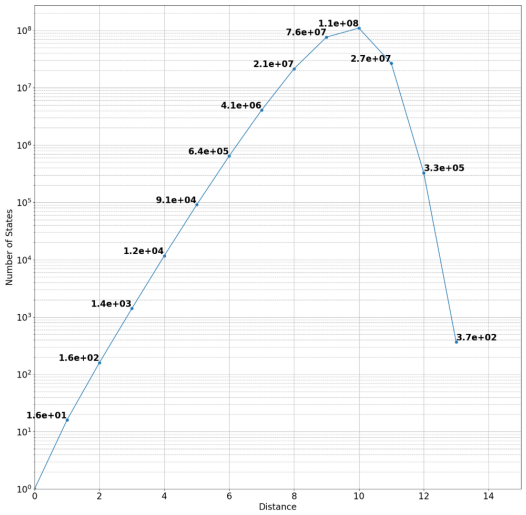


Figure 35: One minus LRX states grows

G.7 LSL - THE LONGEST CYCLE AND THE SUB-LONGEST CYCLE

The LSL graph, denoted as $G_{LSL}(n)$, is constructed from the symmetric group S_n, consisting of all possible permutations of n elements. The generating set of this graph is defined by two distinguished cycles: the longest cycle, given by the n-cycle $(1\,2\,\ldots\,n)$, and the sub-longest cycle, taken as $(1)(2\,3\,\ldots\,n)$, which fixes one element while permuting the remaining $n-1$ elements cyclically. The vertices of $G_{LSL}(n)$ correspond to the elements of S_n, and two vertices are adjacent if one can be obtained from the other by multiplying with either the longest cycle or the sub-longest cycle.

The resulting Cayley graph inherits several important structural properties. It is vertex-transitive by construction, as all Cayley graphs are, and it is regular of degree two since each vertex has exactly two neighbors (corresponding to the two generators). The graph is connected for $n \geq 3$, and questions of Hamiltonicity have been studied in relation to such two-generator Cayley graphs. The diameter of $G_{LSL}(n)$ is finite and grows with n, though precise asymptotic bounds remain an area of investigation.

A key feature of $G_{LSL}(n)$ is that the pair of generators $(1\,2\,\ldots\,n)$ and $(1)(2\,3\,\ldots\,n)$ already suffices to generate the entire symmetric group S_n. This makes the graph a compact yet rich model for studying group-theoretic and graph-theoretic phenomena simultaneously. The interplay between the longest and sub-longest cycles produces nontrivial cycle structures within the graph, providing insights into the connectivity and expansion properties of Cayley graphs defined by minimal generating sets.

Despite these structural insights, several open problems remain. In particular, the Hamiltonicity of $G_{LSL}(n)$ for all n has not been fully resolved, and precise values or bounds for parameters such as the diameter and girth are not yet established. Moreover, extremal invariants such as the clique number $\omega(G_{LSL}(n))$ and the chromatic number remain unknown in general. Only partial results and small-n cases have been studied, leaving the global extremal properties of $G_{LSL}(n)$ an open area of research.

Table 27: Generators L and S and their inverses for $n = 3, \ldots, 10$ in cycle notation.

n	L (longest cycle)	S (sub-longest cycle)	L^{-1}	S^{-1}
3	(1 2 3)	(1)(2 3)	(1 3 2)	(1)(2 3)
4	(1 2 3 4)	(1)(2 3 4)	(1 4 3 2)	(1)(2 4 3)
5	(1 2 3 4 5)	(1)(2 3 4 5)	(1 5 4 3 2)	(1)(2 5 4 3)
6	(1 2 3 4 5 6)	(1)(2 3 4 5 6)	(1 6 5 4 3 2)	(1)(2 6 5 4 3)
7	(1 2 3 4 5 6 7)	(1)(2 3 4 5 6 7)	(1 7 6 5 4 3 2)	(1)(2 7 6 5 4 3)
8	(1 2 3 4 5 6 7 8)	(1)(2 3 4 5 6 7 8)	(1 8 7 6 5 4 3 2)	(1)(2 8 7 6 5 4 3)
9	(1 2 3 4 5 6 7 8 9)	(1)(2 3 4 5 6 7 8 9)	(1 9 8 7 6 5 4 3 2)	(1)(2 9 8 7 6 5 4 3)
10	(1 2 3 4 5 6 7 8 9 10)	(1)(2 3 4 5 6 7 8 9 10)	(1 10 9 8 7 6 5 4 3 2)	(1)(2 10 9 8 7 6 5 4 3)

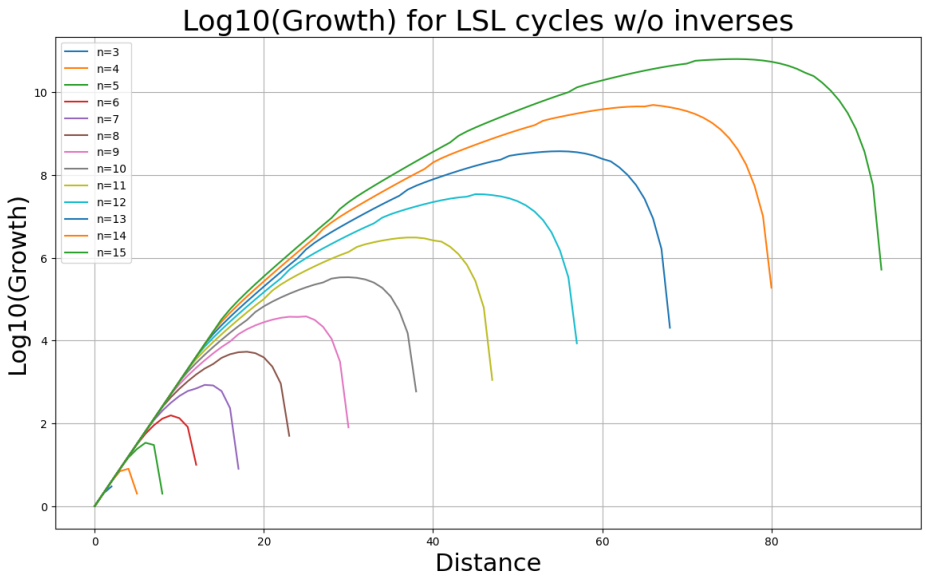


Figure 36: Growth of LSL cycles without inverses for $n = 3, \ldots, 15$.

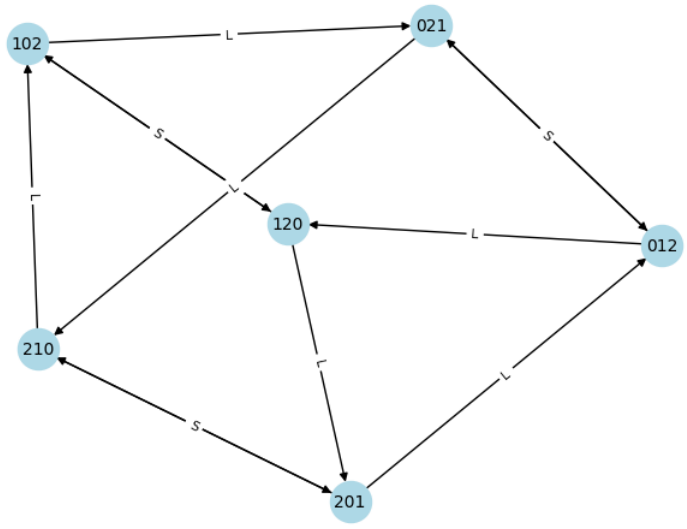


Figure 37: LSL graph without inverses for n = 3 size

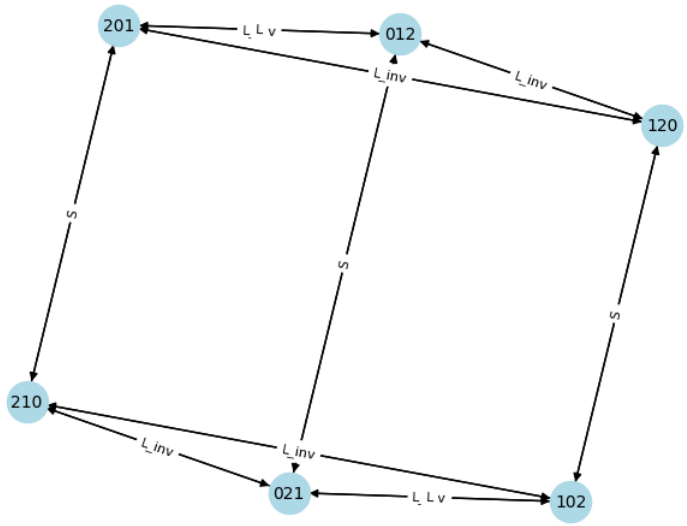


Figure 38: LSL graph with inverses for n = 3 size

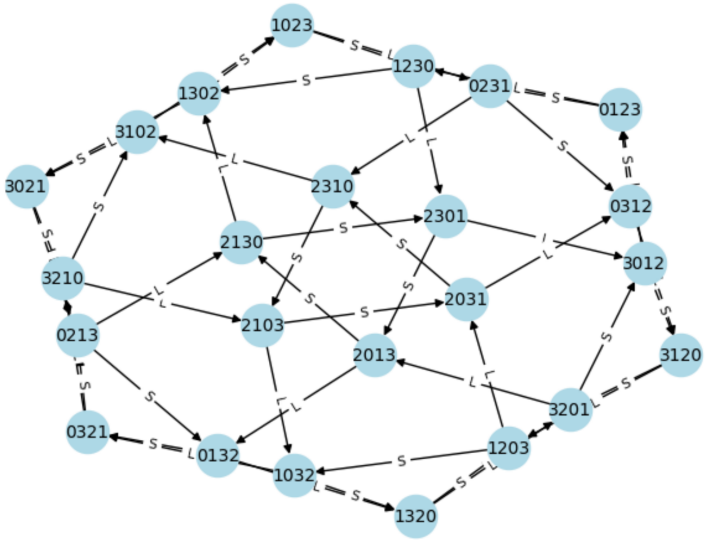


Figure 39: LSL graph without inverses for n = 4 size

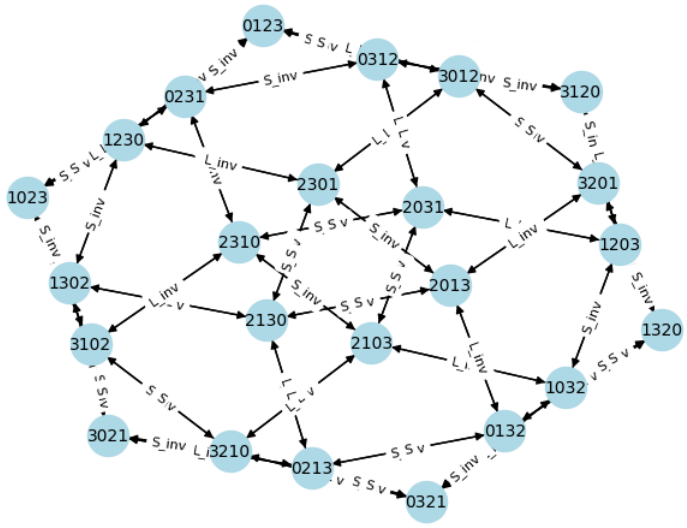


Figure 40: LSL graph with inverses for n = 4 size

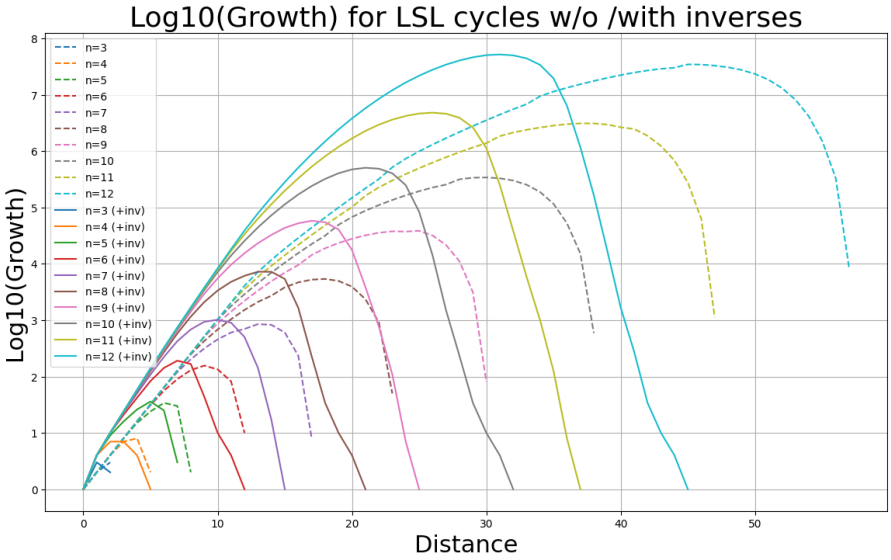


Figure 41: Growth of LSL cycles with and without inverses for $n = 3, \ldots, 12$

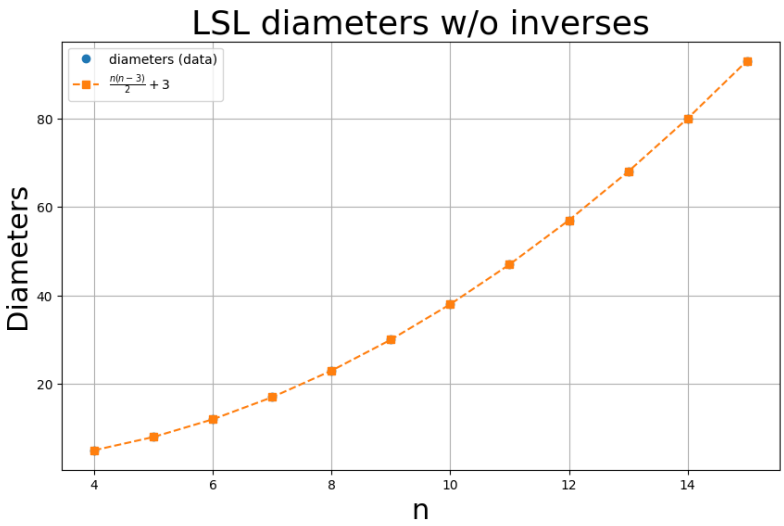


Figure 42: LSL diameters without inverses.

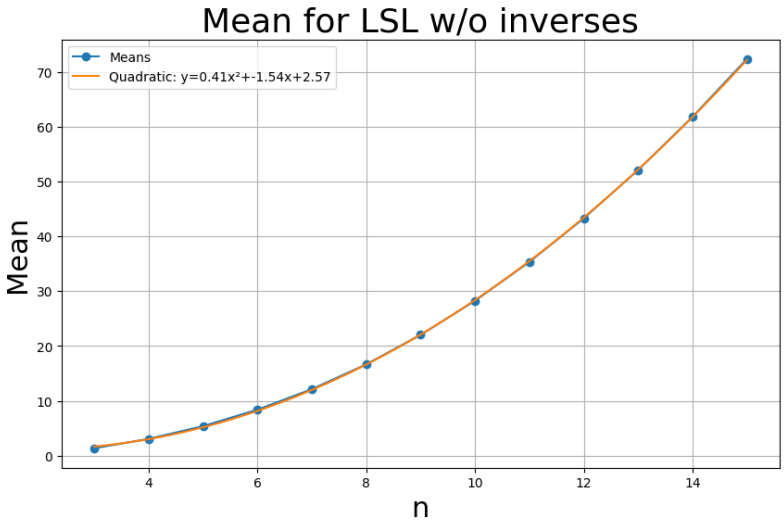


Figure 43: LSL mean without inverses.

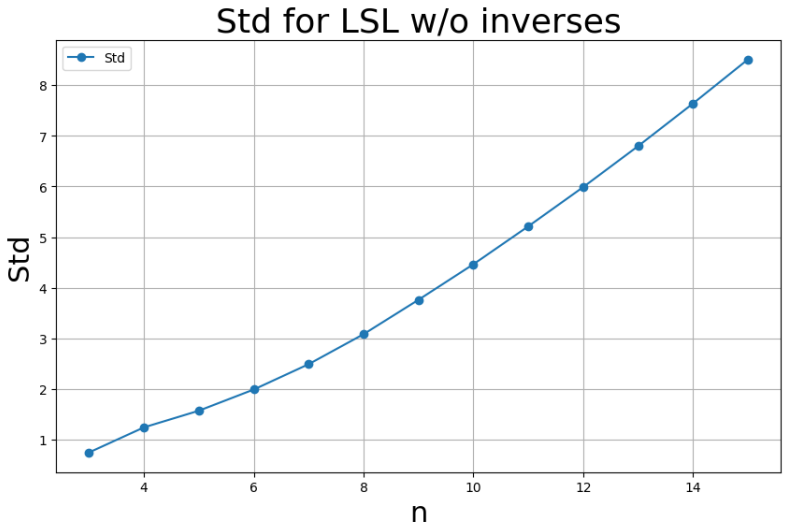


Figure 44: LSL standard deviation without inverses.

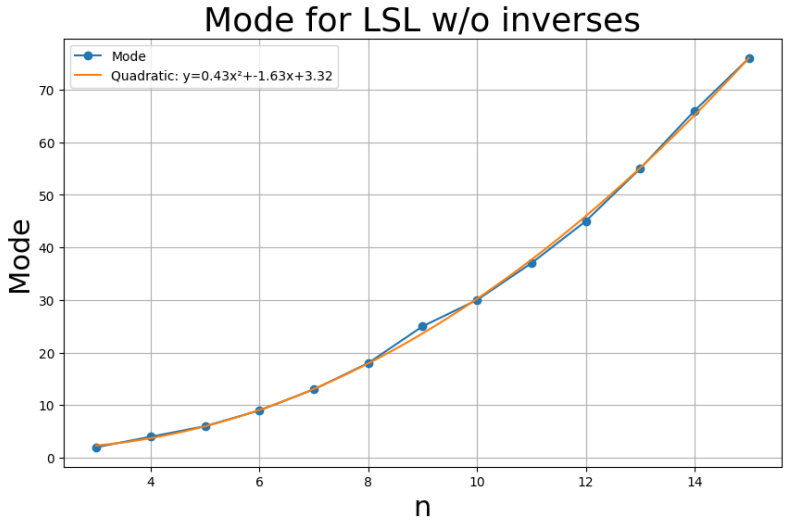


Figure 45: LSL mode without inverses.

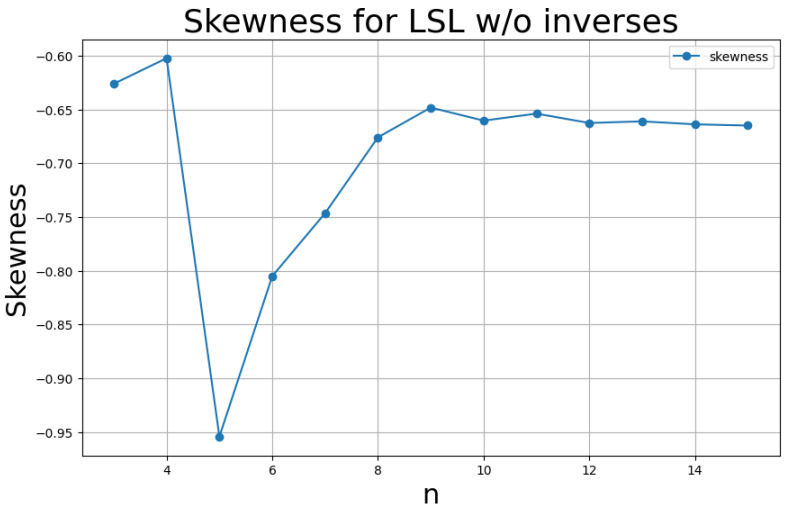


Figure 46: LSL skewness without inverses.

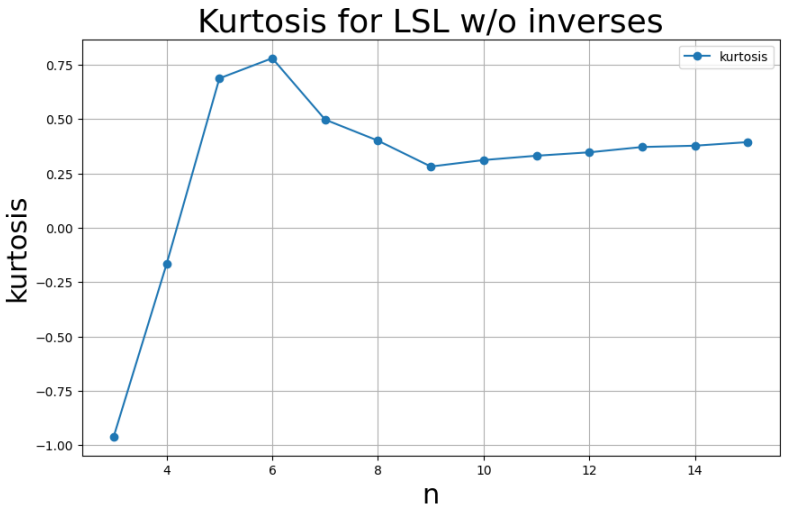


Figure 47: LSL kurtosis without inverses.

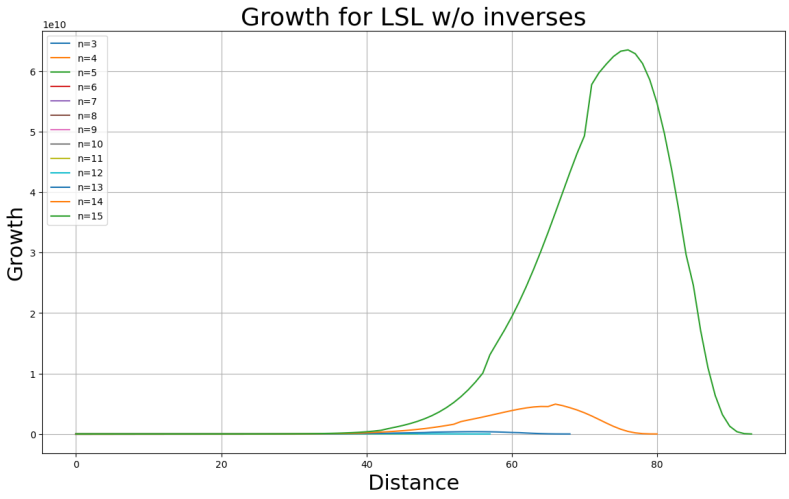


Figure 48: LSL growth without inverses.

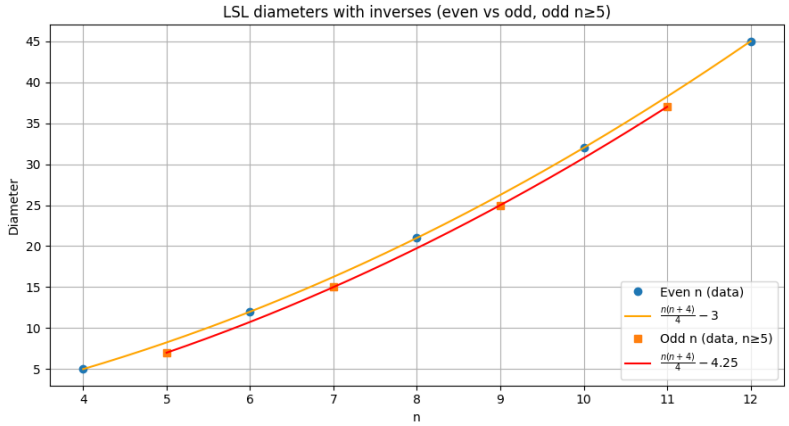


Figure 49: LSL diameters with inverses.

Table 28: Growth sequences of LSL without inverses for $n = 3, \ldots, 15$.

n	Growth sequence
3	1, 2, 3
4	1, 2, 4, 7, 8, 2
5	1, 2, 4, 8, 15, 24, 34, 30, 2
6	1, 2, 4, 8, 16, 31, 56, 90, 130, 156, 134, 82, 10
7	1, 2, 4, 8, 16, 32, 63, 120, 202, 314, 456, 604, 698, 850, 826, 602, 234, 8
8	1, 2, 4, 8, 16, 32, 64, 127, 248, 426, 682, 1040, 1520, 2108, 2714, 3830, 4680, 5232, 5382, 4960, 3926, 2354, 914, 50
9	1, 2, 4, 8, 16, 32, 64, 128, 255, 504, 874, 1418, 2208, 3336, 4904, 6980, 9506, 14310, 18842, 23358, 27818, 31996, 35474, 37656, 37286, 38440, 31692, 21484, 11092, 3112, 80
10	1, 2, 4, 8, 16, 32, 64, 128, 256, 511, 1016, 1770, 2890, 4544, 6968, 10480, 15480, 22396, 31522, 49214, 67380, 87392, 109922, 135354, 163618, 194082, 225460, 254162, 315364, 336460, 339658, 328312, 300044, 252466, 187792, 115860, 52416, 15166, 590
11	1, 2, 4, 8, 16, 32, 64, 128, 256, 512, 1023, 2040, 3562, 5834, 9216, 14232, 21632, 32464, 48136, 70404, 101162, 161486, 226302, 301018, 389682, 496262, 624290, 776570, 954716, 1158536, 1381418, 1835422, 2127806, 2378858, 2614010, 2826978, 2998410, 3097320, 3092454, 2949398, 2640744, 2460302, 1863214, 1230582, 679598, 277040, 62536, 1120
12	1, 2, 4, 8, 16, 32, 64, 128, 256, 512, 1024, 2047, 4088, 7146, 11722, 18560, 28760, 43936, 66432, 99600, 148120, 218268, 317898, 514694, 731992, 988852, 1302330, 1691146, 2175586, 2777526, 3519884, 4425424, 5514744, 6793766, 9367782, 11333004, 13260792, 15305396, 17503630, 19835300, 22241852, 24629482, 26867798, 28770498, 30052458, 34487060, 34193076, 32755588, 30558096, 27430264, 23313078, 18396140, 13134800, 8161546, 4140678, 1513038, 337094, 8582
13	1, 2, 4, 8, 16, 32, 64, 128, 256, 512, 1024, 2048, 4095, 8184, 14314, 23498, 37248, 57816, 88544, 134368, 202528, 303536, 452424, 670180, 985010, 1609654, 2311522, 3153966, 4199426, 5519814, 7198906, 9335382, 12045044, 15461812, 19736944, 25035600, 31507138, 44484042, 55280554, 66430666, 78774758, 92728230, 108498492, 126160770, 145686430, 166920472, 189570000, 213059528, 236187442, 291013966, 314157242, 332464386, 349335090, 363544420, 373258030, 376408296, 371328368, 356347828, 330681618, 293858760, 246491380, 214626792, 154466624, 100449232, 57336688, 26709264, 8995936, 1644032, 20416
14	1, 2, 4, 8, 16, 32, 64, 128, 256, 512, 1024, 2048, 4096, 8191, 16376, 28650, 47050, 74624, 115928, 177760, 270240, 408384, 614368, 920720, 1374680, 2043836, 3022706, 4970318, 7184252, 9867912, 13233674, 17532546, 23067786, 30211566, 39422244, 51261912, 66413160, 85693280, 110062936, 140573526, 201691118, 255269364, 312134776, 376566788, 451319414, 538449542, 639681234, 756535950, 890325832, 1042060440, 1212334668, 1400764972, 1603921006, 2048400854, 2305267858, 2547395432, 2801873574, 3068388520, 3340901234, 3611201476, 3870420458, 4107954030, 4311078364, 4464632116, 4548976476, 4535980344, 4938651698, 4682703246, 4346164812, 3959668692, 3502670572, 2976096338, 2400838250, 1813485652, 1258946048, 782368614, 418342366, 180429586, 55406426, 10176826, 189418
15	1, 2, 4, 8, 16, 32, 64, 128, 256, 512, 1024, 2048, 4096, 8192, 16383, 32760, 57322, 94154, 149376, 232152, 356192, 541984, 820096, 1236032, 1857312, 2783664, 4161416, 6203204, 9213626, 15214110, 22089158, 30477698, 41071570, 54701246, 72391258, 95427774, 125435948, 164469160, 215111048, 280589484, 364899312, 472926912, 610449810, 885862474, 1135838910, 1405622062, 1715821530, 2081527526, 2515708898, 3030977246, 3640378684, 4357646372, 5197141292, 6173525684, 7301315436, 8593022144, 10049461346, 13129758206, 15171866814, 17196677598, 19393682148, 21799895422, 24415385652, 27227241082, 30217575760, 33359274242, 36617117108, 39939575648, 43256038590, 46449001706, 49307255768, 57796972762, 59738594536, 61158505736, 62443922690, 63312948852, 63530381562, 62894823878, 61278697580, 58562777940, 54715194876, 49742673718, 43774985150, 36983759134, 29627713754, 24565186322, 17098895578, 10999886774, 6390959702, 3192687284, 1282999960, 367503152, 56556768, 518400

Table 29: Growth sequences of LSL with inverses for $n = 3, \ldots, 12$.

n	Growth sequence
3	1, 3, 2
4	1, 4, 7, 7, 4, 1
5	1, 4, 9, 16, 26, 36, 25, 3
6	1, 4, 10, 21, 42, 83, 142, 191, 167, 44, 10, 4, 1
7	1, 4, 10, 23, 50, 108, 223, 424, 684, 935, 1016, 900, 502, 142, 17, 1
8	1, 4, 10, 24, 55, 124, 271, 581, 1156, 2090, 3353, 4785, 6122, 7224, 7206, 5379, 1658, 228, 34, 10, 4, 1
9	1, 4, 10, 24, 57, 132, 295, 658, 1415, 2932, 5516, 9646, 15384, 23219, 32526, 43403, 52315, 57918, 54565, 40546, 17571, 3858, 768, 109, 7, 1
10	1, 4, 10, 24, 58, 137, 311, 706, 1561, 3401, 7137, 13995, 25555, 44212, 72557, 113338, 169552, 239510, 320258, 403237, 472291, 504473, 486514, 402386, 248327, 83454, 14016, 1494, 232, 34, 10, 4, 1
11	1, 4, 10, 24, 58, 139, 319, 730, 1637, 3636, 7896, 16871, 33546, 63450, 113812, 198403, 328150, 528008, 806787, 1189704, 1673854, 2273338, 2932617, 3603390, 4191992, 4629140, 4793942, 4593641, 3888143, 2619653, 1127060, 251559, 38345, 5808, 998, 126, 8, 1
12	1, 4, 10, 24, 58, 140, 324, 746, 1685, 3782, 8316, 18209, 38864, 78858, 151509, 281583, 507133, 883792, 1482630, 2415039, 3788433, 5742635, 8425924, 11988377, 16445107, 21731766, 27688786, 34132983, 40411271, 46071816, 50210615, 51675549, 49769923, 44078612, 33793841, 19474697, 6353433, 1161757, 164243, 17124, 1675, 277, 34, 10, 4, 1

Table 30: Eigenvalues for different n of LSL without inverses (format: value$^{\text{multiplicity}}$)

n	Eigenvalues
3	$1.8^1, -1.25^1, -0.45^1, 0.45^1, 1.25^1, 1.8^1$
4	$-2.14^2, -2.06^1, -1.73^1, -1.41^1, -1.0^3, -0.66^1, -0.4^1, 0.0^4, 0.43^1, 0.66^1, 0.69^1, 1.0^1, 1.41^1,$ $1.44^1, 1.73^1, 1.76^1, 2.14^1, 2.27^1$
5	$-2.12^1, -2.05^2, -1.93^2, -1.9^1, -1.85^4, -1.73^3, -1.62^1, -1.41^12, -1.21^2, -1.18^1,$ $-1.16^1, -1.0^1, -0.77^4, -0.62^1, -0.57^2, -0.52^2, -0.41^1, 0.0^{38}, 0.41^1, 0.52^2, 0.57^2, 0.62^1,$ $0.77^4, 1.0^1, 1.16^1, 1.18^1, 1.21^2, 1.41^12, 1.62^1, 1.73^3, 1.85^4, 1.9^1, 1.93^2, 2.05^2, 2.12^1$
6	$-2.39^2, -2.24^2, -2.12^1, -2.11^2, -2.1^2, -2.05^2, -2.0^2, -1.96^2, -1.95^2, -1.93^1,$ $-1.85^4, -1.77^2, -1.73^8, -1.63^2, -1.62^{10}, -1.41^{108}, -1.34^2, -1.22^2, -1.21^2, -1.16^1,$ $-1.09^2, -1.0^{12}, -0.98^2, -0.94^2, -0.77^4, -0.62^{10}, -0.57^2, -0.52^1, -0.49^2, -0.47^2,$ $-0.41^1, -0.35^2, -0.23^2, 0.0^{314}, 0.23^2, 0.35^2, 0.41^1, 0.47^2, 0.49^2, 0.52^1, 0.57^2, 0.62^{10},$ $0.77^4, 0.94^2, 0.98^2, 1.0^{12}, 1.09^2, 1.16^1, 1.21^2, 1.22^2, 1.34^2, 1.41^{108}, 1.62^{10},$ $1.63^2, 1.73^8, 1.77^2, 1.85^4, 1.93^1, 1.95^2, 1.96^2,$ $2.0^2, 2.05^2, 2.1^2, 2.11^2, 2.12^1, 2.24^2, 2.39^2$
7	$-2.31^2, -2.27^3, -2.26^1, -2.21^4, -2.2^2, -2.18^2, -2.16^{10}, -2.15^4,$ $-2.12^5, -2.1^6, -2.07^4, -2.05^{40}, -2.04^6, -2.0^{10}, -1.99^1, -1.93^{16}, -1.9^5, -1.85^{81}, -1.82^1,$ $-1.8^1, -1.78^2, -1.76^2, -1.73^{38}, -1.71^2, -1.68^2, -1.66^1, -1.65^4, -1.64^4, -1.62^{95},$ $-1.55^1, -1.53^{10}, -1.52^6, -1.49^1, -1.41^{577}, -1.34^2, -1.27^2, -1.26^6, -1.22^2, -1.21^{40}, -1.2^1,$ $-1.19^4, -1.18^8, -1.16^1, -1.14^2, -1.13^2, -1.0^{56},$ $-0.91^5, -0.85^{10}, -0.83^4, -0.81^1, -0.77^{81}, -0.72^6, -0.64^2, -0.62^{95}, -0.59^2, -0.57^{40},$ $-0.56^1, -0.54^2, -0.52^{16}, -0.5^{10}, -0.47^4, -0.42^3, -0.41^1, -0.37^2, -0.31^1,$ $0.0^{2318}, 0.31^1, 0.37^2, 0.41^1, 0.42^3, 0.47^4, 0.5^{10}, 0.52^{16},$ $0.54^2, 0.56^1, 0.57^{40}, 0.59^2, 0.62^{95}, 0.64^2, 0.72^6, 0.77^{81},$ $0.81^1, 0.83^4, 0.85^{10}, 0.91^5, 1.0^{56}, 1.13^2, 1.14^2, 1.16^1, 1.18^8, 1.19^4,$ $1.2^1, 1.21^{40}, 1.22^2, 1.26^6, 1.27^2, 1.34^2, 1.41^{577}, 1.49^1, 1.52^6, 1.53^{10},$ $1.55^1, 1.62^{95}, 1.64^4, 1.65^4, 1.66^1, 1.68^2, 1.71^2, 1.73^{38}, 1.76^2, 1.78^2, 1.8^1,$ $1.82^1, 1.85^{81}, 1.9^5, 1.93^{16}, 1.99^1, 2.0^{10}, 2.04^6, 2.05^{40}, 2.07^4,$ $2.1^6, 2.12^5, 2.15^4, 2.16^{10}, 2.18^2, 2.2^2, 2.21^4, 2.26^1, 2.27^3, 2.31^2$

Table 31: Eigenvalues for different n of LSL with inverses (format: value$^{\text{multiplicity}}$)

n	Eigenvalues
3	$-2.0^{2}, -0.0^{2}, 1.0^{1}, 3.0^{1}$
4	$-3.0^{2}, -2.56^{3}, -1.0^{6}, 0.0^{4}, 1.0^{2}, 1.56^{3}, 3.0^{3}, 4.0^{1}$
5	$-3.56^{4}, -3.35^{5}, -3.0^{4}, -2.62^{5}, -2.1^{6}, -1.62^{6}, -1.3^{10}, -1.0^{4},$ $-0.38^{5}, 0.0^{20}, 0.56^{4}, 0.62^{6}, 1.0^{4}, 1.1^{5}, 1.66^{6}, 2.0^{4}, 2.3^{10}, 3.25^{5}, 3.44^{6}, 4.0^{1}$
6	$-3.58^{5}, -3.5^{9}, -3.37^{5}, -3.26^{10}, -3.24^{10}, -3.17^{10}, -3.0^{14}, -2.95^{16}, -2.72^{16},$ $-2.56^{5}, -2.51^{10}, -2.48^{9}, -2.26^{9}, -2.17^{16}, -2.0^{16}, -1.73^{18}, -1.43^{9}, -1.38^{10},$ $-1.34^{10}, -1.25^{16}, -1.21^{5}, -1.06^{16}, -1.0^{10}, -0.65^{10}, -0.57^{10}, -0.42^{9}, -0.41^{5},$ $0.0^{135}, 0.23^{16}, 0.33^{16}, 1.0^{14}, 1.14^{10}, 1.15^{9}, 1.19^{9}, 1.2^{16}, 1.4^{16},$ $1.56^{5}, 1.6^{10}, 1.73^{18}, 1.87^{10}, 2.09^{10}, 2.19^{16}, 2.2^{9}, 2.37^{5}, 2.4^{10},$ $2.41^{5}, 2.55^{16}, 2.78^{5}, 2.96^{16}, 3.0^{10}, 3.29^{16}, 3.36^{10}, 3.56^{9}, 3.65^{10}, 4.0^{1}$
7	$-3.75^{6}, -3.66^{14}, -3.62^{30}, -3.57^{14}, -3.55^{20}, -3.45^{35}, -3.41^{35}, -3.39^{35}, -3.35^{21},$ $-3.29^{14}, -3.27^{14}, -3.25^{20}, -3.22^{35}, -3.09^{35}, -3.06^{35}, -3.03^{21}, -3.02^{35}, -3.0^{20},$ $-2.95^{14}, -2.88^{42}, -2.85^{35}, -2.81^{21}, -2.78^{21}, -2.68^{35}, -2.67^{14}, -2.61^{14}, -2.6^{15},$ $-2.59^{20}, -2.57^{15}, -2.54^{21}, -2.51^{35}, -2.45^{35}, -2.4^{56}, -2.35^{15}, -2.32^{26}, -2.25^{15},$ $-2.07^{56}, -2.05^{35}, -2.01^{20}, -1.97^{35}, -1.92^{21}, -1.91^{35}, -1.85^{21}, -1.8^{20}, -1.78^{35},$ $-1.71^{14}, -1.7^{35}, -1.66^{21}, -1.64^{14}, -1.63^{35}, -1.5^{14}, -1.48^{21}, -1.45^{6}, -1.41^{21},$ $-1.4^{15}, -1.38^{35}, -1.37^{35}, -1.36^{14}, -1.27^{56}, -1.25^{35}, -1.22^{21},$ $-1.16^{85}, -1.12^{21}, -1.1^{71}, -1.05^{15}, -1.03^{20}, -1.0^{14}, -0.89^{35}, -0.8^{35}, -0.49^{21},$ $-0.46^{35}, -0.43^{20}, -0.41^{14}, -0.31^{35}, -0.28^{14}, -0.2^{35}, -0.13^{14}, 0.0^{952}, 0.12^{15},$ $0.16^{20}, 0.23^{14}, 0.27^{15}, 0.32^{35}, 0.43^{21},$ $0.47^{56}, 0.54^{14}, 0.56^{15}, 0.64^{6}, 0.68^{20}, 1.0^{20},$ $1.04^{56}, 1.05^{35}, 1.06^{14}, 1.09^{35}, 1.14^{35}, 1.16^{21}, 1.17^{55}, 1.18^{21}, 1.19^{14}, 1.21^{21}, 1.25^{15},$ $1.32^{35}, 1.34^{20}, 1.35^{35}, 1.42^{21}, 1.45^{56}, 1.55^{21}, 1.59^{35}, 1.62^{15}, 1.63^{35},$ $1.68^{14}, 1.71^{35}, 1.75^{21}, 1.78^{35}, 1.95^{36}, 2.01^{14}, 2.02^{35},$ $2.05^{21}, 2.07^{15}, 2.15^{35}, 2.2^{6}, 2.23^{15}, 2.31^{34}, 2.32^{35},$ $2.37^{35}, 2.38^{50}, 2.42^{35}, 2.48^{35}, 2.57^{20}, 2.59^{15}, 2.6^{56},$ $2.68^{6}, 2.72^{56}, 2.77^{35}, 2.85^{35}, 2.92^{21}, 2.93^{35}, 2.94^{14}, 3.02^{35},$ $3.04^{56}, 3.13^{21}, 3.14^{14}, 3.2^{35},$ $3.34^{15}, 3.36^{20}, 3.37^{21}, 3.38^{20},$ $3.4^{14}, 3.47^{35}, 3.48^{35}, 3.54^{35}, 3.57^{15}, 3.71^{14}, 3.77^{15}, 4.0^{1}$

G.8 RMK - THE LONGEST CYCLE AND K-CYCLE $(M, M+1, ..., M+K-1)$

Table 32: RMK diameters

n	m	k	Diameter
n	m	k	Diameter
7	0	2	35
7	1	2	35
7	2	2	35
7	3	2	35
7	4	2	35
7	5	2	35
7	0	3	25
7	1	3	25
7	2	3	25
7	3	3	25
7	4	3	25
7	0	4	22
7	1	4	22
7	2	4	22
7	3	4	22
7	0	5	21
7	1	5	21
7	2	5	21
8	0	2	45
8	1	2	45
8	2	2	45
8	3	2	45
8	4	2	45
8	5	2	45
8	6	2	45
8	0	3	28
8	1	3	28
8	2	3	28
8	3	3	28
8	4	3	28
8	5	3	28
8	0	4	25
8	1	4	25
8	2	4	25
8	3	4	25
8	4	4	25
8	0	5	24
8	1	5	24
8	2	5	24
8	3	5	24
8	0	6	25
8	1	6	25
8	2	6	25
9	0	2	58
9	1	2	58
9	2	2	58
9	3	2	58
9	4	2	58
9	5	2	58
Continued on next page			

Table 32 – continued from previous page

n	m	k	Diameter)
9	6	2	58
9	7	2	58
9	0	3	35
9	1	3	35
9	2	3	35
9	3	3	35
9	4	3	35
9	5	3	35
9	6	3	35
9	0	4	29
9	1	4	29
9	2	4	29
9	3	4	29
9	4	4	29
9	5	4	29
9	0	5	28
9	1	5	28
9	2	5	28
9	3	5	28
9	4	5	28
9	0	6	29
9	1	6	29
9	2	6	29
9	3	6	29
9	0	7	30
9	1	7	30
9	2	7	30
10	0	2	71
10	1	2	71
10	2	2	71
10	3	2	71
10	4	2	71
10	5	2	71
10	6	2	71
10	7	2	71
10	8	2	71
10	0	3	40
10	1	3	40
10	2	3	40
10	3	3	40
10	4	3	40
10	5	3	40
10	6	3	40
10	7	3	40
10	0	4	33
10	1	4	33
10	2	4	33
10	3	4	33
10	4	4	33
10	5	4	33
10	6	4	33
10	0	5	31
10	1	5	31
10	2	5	31

Continued on next page

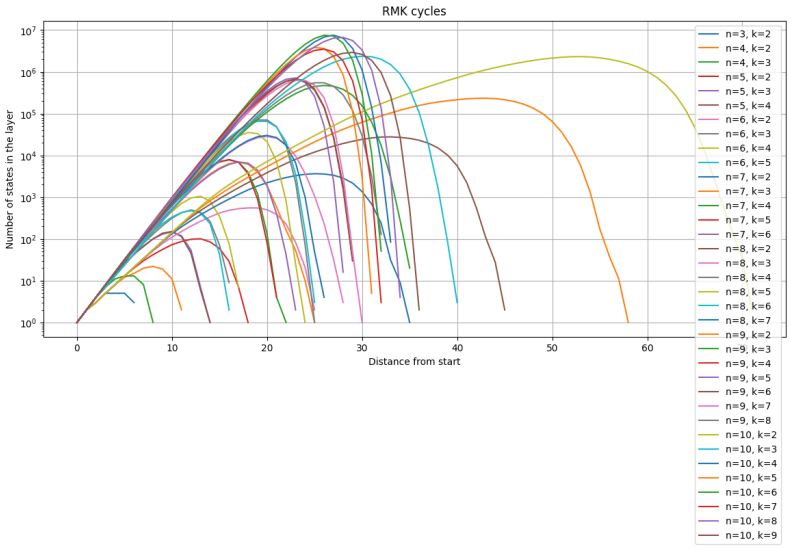


Figure 50: RMK states growth

Table 32 – continued from previous page

n	m	k	Diameter)
10	3	5	31
10	4	5	31
10	5	5	31
10	0	6	32
10	1	6	32
10	2	6	32
10	3	6	32
10	4	6	32
10	0	7	32
10	1	7	32
10	2	7	32
10	3	7	32
10	0	8	34
10	1	8	34
10	2	8	34

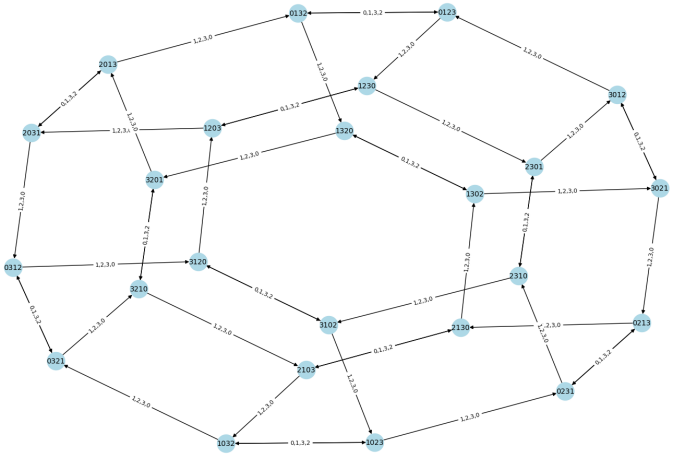


Figure 51: RMK graph for n = 4 size

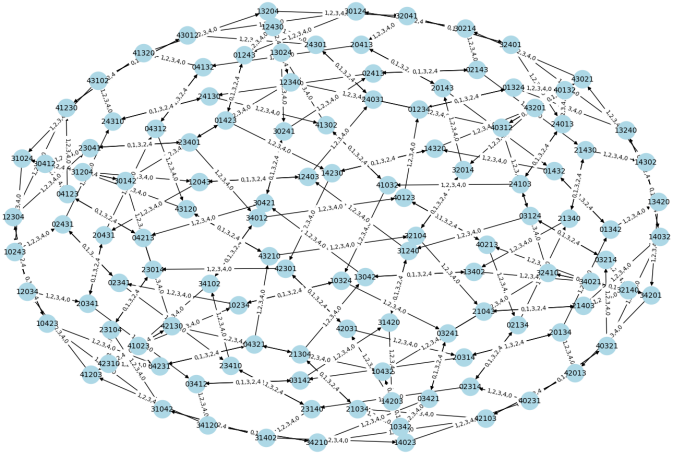


Figure 52: RMK graph for n = 5 size

G.9 LARX - TRANSPOSITION AND SUB-LONG CYCLE

n	Diameter	Growth
2	1	1, 1
3	3	1, 2, 2, 1
4	7	1, 2, 3, 4, 5, 5, 3, 1
5	10	1, 2, 3, 5, 7, 10, 15, 20, 25, 23, 9
6	17	1, 2, 3, 5, 8, 12, 18, 28, 43, 63, 88, 113, 125, 108, 70, 24, 8, 1
7	22	1, 2, 3, 5, 8, 13, 20, 31, 49, 77, 120, 180, 259, 357, 464, 566, 634, 663, 660, 535, 288, 91, 14
8	31	1, 2, 3, 5, 8, 13, 21, 33, 52, 83, 132, 209, 325, 488, 708, 996, 1356, 1794, 2301, 2856, 3509, 4249, 4782, 4781, 4309, 3461, 2277, 1108, 359, 84, 14, 1
9	38	1, 2, 3, 5, 8, 13, 21, 34, 54, 86, 138, 221, 353, 557, 858, 1281, 1860, 2640, 3668, 5008, 6720, 8881, 11637, 15164, 19442, 23650, 27327, 30609, 33092, 34213, 33489, 31016, 27782, 22015, 13360, 5811, 1609, 234, 18
10	49	1, 2, 3, 5, 8, 13, 21, 34, 55, 88, 141, 227, 365, 586, 933, 1458, 2220, 3290, 4769, 6795, 9539, 13230, 18143, 24650, 33362, 45025, 60152, 78614, 98894, 120372, 144041, 169496, 195848, 222186, 248258, 275588, 305255, 322702, 307418, 275708, 232663, 179189, 120964, 67228, 27874, 8497, 2479, 376, 34, 1
11	58	1, 2, 3, 5, 8, 13, 21, 34, 55, 89, 143, 230, 371, 598, 963, 1542, 2434, 3757, 5655, 8321, 12031, 17167, 24232, 33906, 47068, 64915, 89282, 122811, 168181, 226785, 298638, 381350, 476174, 587681, 717886, 868232, 1039753, 1235113, 1463436, 1738282, 2062170, 2356060, 2563507, 2723102, 2844017, 2901766, 2870699, 2727357, 2462375, 2110149, 1760495, 1362648, 864905, 435838, 175359, 49805, 8498, 842, 40
12	71	1, 2, 3, 5, 8, 13, 21, 34, 55, 89, 144, 232, 374, 604, 975, 1573, 2528, 4019, 6270, 9555, 14234, 20812, 30010, 42831, 60635, 85281, 119258, 165973, 230435, 320091, 444462, 611949, 826730, 1091058, 1405437, 1780624, 2236972, 2790851, 3459712, 4262287, 5222286, 6383241, 7820863, 9602316, 11709144, 13862038, 15820044, 17831083, 19949104, 22099204, 24192272, 26106328, 27712811, 28978342, 30117093, 31441927, 31883272, 29635063, 26238452, 22375776, 18046536, 13490074, 9120955, 5381519, 2631638, 983174, 264173, 65579, 10343, 770, 32, 1
13	82	1, 2, 3, 5, 8, 13, 21, 34, 55, 89, 144, 233, 376, 607, 981, 1585, 2560, 4124, 6590, 10368, 15968, 24045, 35502, 51627, 74251, 105931, 150189, 211885, 297655, 416642, 581967, 813044, 1136993, 1584874, 2181762, 2942189, 3882688, 5025684, 6425321, 8162324, 10317905, 12986211, 16275873, 20319063, 25307426, 31556237, 39487006, 49353895, 61014380, 73373151, 85988227, 99798220, 115262200, 132359249, 151007460, 171021343, 192129290, 214248383, 238211503, 266000035, 298869852, 327661137, 343622121, 352294453, 358029073, 358796502, 352570663, 338093190, 314634361, 282015651, 241310913, 196684025, 156317859, 118463447, 77206270, 41645694, 19165198, 7140323, 1958987, 343338, 30730, 1548, 68

n	Diameter	Growth
14	97	1 , 2 , 3 , 5 , 8 , 13 , 21 , 34 , 55 , 89 , 144 , 233 , 377 , 609 , 984 , 1591 , 2572 , 4157 , 6707 , 10757 , 17037 , 26479 , 40269 , 60001 , 87930 , 127281 , 182624 , 260360 , 369388 , 522076 , 735515 , 1033399 , 1449315 , 2032289 , 2853081 , 4003393 , 5578934 , 7654790 , 10287594 , 13561749 , 17605428 , 22640839 , 28974396 , 36946036 , 46966341 , 59529030 , 75238057 , 94894580 , 119698611 , 151429151 , 192044419 , 242380073 , 301634435 , 366561261 , 436199411 , 515344881 , 606650805 , 711346086 , 830638478 , 965474359 , 1116571596 , 1285007630 , 1474558229 , 1695226539 , 1960349495 , 2272410441 , 2582505827 , 2831560762 , 3066948252 , 3311982930 , 3557255537 , 3791049828 , 4002706091 , 4180745572 , 4311894674 , 4382740421 , 4391974394 , 4372259317 , 4378787624 , 4311861407 , 3948347816 , 3454278402 , 2946450622 , 2421064505 , 1889039197 , 1380943490 , 930210456 , 564393565 , 299190383 , 132598789 , 45811487 , 11503968 , 2485464 , 433401 , 33411 , 1112 , 22 , 1

These results support the working hypothesis: Without inverses

$$d_n = \begin{cases} 1, & n = 2, \\ 3, & n = 3 \\ \dfrac{i^2}{2} - 1, & n = 2m \text{ (even)}, \\ \dfrac{i^2}{2} - 2.5, & n = 2m \text{ (odd)},\ m \geq 4. \end{cases}$$

With inverses

$$d_n = \begin{cases} 3, & n = 3, \\ 6, & n = 4, \\ \dfrac{i^2 + 6i - 12}{4}, & n = 2m \text{ (even)}, \\ \dfrac{i^2 + 6i - 19}{2}, & n = 2m \text{ (odd)},\ m \geq 5. \end{cases}$$

Table 33: LARX eigenvalues for different n (format: value$^{\text{multiplicity}}$)

n	Eigenvalues (value$^{\text{multiplicity}}$)
3	$-2.0^1, -1.0^2, 1.0^2, 2.0^1$
4	$-1.88^2, -1.62^2, -1.53^2, -1.0^2, -0.62^2, -0.35^2,$ $0.35^2, 0.62^2, 1.0^2, 1.53^2, 1.62^2, 1.88^2$
5	$-2.1^1, -2.04^1, -2.03^1, -2.0^1, -1.99^1, -1.93^1,$ $-1.83^1, -1.8^7, -1.75^1, -1.62^5, -1.54^1, -1.49^1,$ $-1.47^1, -1.37^1, -1.32^1, -1.25^7, -1.23^1, -1.1^1,$ $-1.0^4, -0.92^1, -0.81^1, -0.68^1, -0.62^5, -0.54^1,$ $-0.52^1, -0.45^7, -0.42^1, -0.37^1, -0.33^1, -0.32^1,$ $-0.24^1, 0.24^1, 0.32^1, 0.33^1, 0.37^1, 0.42^1,$ $0.45^7, 0.52^1, 0.54^1, 0.62^5, 0.68^1, 0.81^1,$ $0.92^1, 1.0^4, 1.1^1, 1.23^1, 1.25^7, 1.32^1,$ $1.37^1, 1.47^1, 1.49^1, 1.54^1, 1.62^5, 1.75^1,$ $1.8^7, 1.83^1, 1.93^1, 1.99^1, 2.0^1, 2.03^1,$ $2.04^1, 2.1^1$
6	$-2.21^1, -2.17^1, -2.16^1, -2.14^1, -2.13^1, -2.1^1,$

Continued on next page

Table 33 – continued from previous page

n	Eigenvalues (value$^{\text{multiplicity}}$)
	$-2.08^{1}, -2.07^{2}, -2.04^{1}, -2.03^{1}, -2.02^{1}, -2.01^{1},$
	$-1.99^{13}, -1.95^{1}, -1.93^{4}, -1.92^{2}, -1.91^{1}, -1.88^{4},$
	$-1.87^{1}, -1.84^{1}, -1.83^{1}, -1.81^{1}, -1.8^{22}, -1.75^{2},$
	$-1.68^{3}, -1.67^{1}, -1.62^{40}, -1.58^{1}, -1.57^{1}, -1.53^{4},$
	$-1.49^{12}, -1.46^{1}, -1.44^{2}, -1.36^{1}, -1.35^{3}, -1.34^{3},$
	$-1.32^{1}, -1.31^{2}, -1.3^{1}, -1.27^{1}, -1.26^{1}, -1.25^{22},$
	$-1.17^{2}, -1.14^{1}, -1.09^{1}, -1.06^{1}, -1.0^{63}, -0.92^{1},$
	$-0.9^{1}, -0.89^{1}, -0.88^{1}, -0.83^{2}, -0.81^{12}, -0.74^{1},$
	$-0.67^{1}, -0.66^{2}, -0.65^{1}, -0.62^{40}, -0.56^{2}, -0.52^{5},$
	$-0.5^{1}, -0.48^{1}, -0.45^{22}, -0.44^{1}, -0.43^{1}, -0.42^{12},$
	$-0.37^{1}, -0.36^{2}, -0.35^{4}, -0.34^{1}, -0.33^{1}, -0.28^{3},$
	$-0.27^{3}, -0.26^{1}, -0.25^{1}, -0.24^{1}, 0.24^{1}, 0.25^{1},$
	$0.26^{1}, 0.27^{3}, 0.28^{3}, 0.33^{1}, 0.34^{1}, 0.35^{4},$
	$0.36^{2}, 0.37^{1}, 0.42^{12}, 0.43^{1}, 0.44^{1}, 0.45^{22},$
	$0.48^{1}, 0.5^{1}, 0.52^{5}, 0.56^{2}, 0.62^{40}, 0.65^{1},$
	$0.66^{2}, 0.67^{1}, 0.74^{1}, 0.81^{12}, 0.83^{2}, 0.88^{1},$
	$0.89^{1}, 0.9^{1}, 0.92^{1}, 1.0^{63}, 1.06^{1}, 1.09^{1},$
	$1.14^{1}, 1.17^{2}, 1.25^{22}, 1.26^{1}, 1.27^{1}, 1.3^{1},$
	$1.31^{2}, 1.32^{1}, 1.34^{3}, 1.35^{3}, 1.36^{1}, 1.44^{2},$
	$1.46^{1}, 1.49^{12}, 1.53^{4}, 1.57^{1}, 1.58^{1}, 1.62^{40},$
	$1.67^{1}, 1.68^{3}, 1.75^{2}, 1.8^{22}, 1.81^{1}, 1.83^{1},$
	$1.84^{1}, 1.87^{1}, 1.88^{4}, 1.91^{1}, 1.92^{2}, 1.93^{4},$
	$1.95^{1}, 1.99^{13}, 2.01^{1}, 2.02^{1}, 2.03^{1}, 2.04^{1},$
	$2.07^{2}, 2.08^{1}, 2.1^{1}, 2.13^{1}, 2.14^{1}, 2.16^{1},$
	$2.17^{1}, 2.21^{1}$
7	$-2.24^{1}, -2.23^{1}, -2.22^{2}, -2.21^{2}, -2.2^{1}, -2.19^{2},$
	$-2.18^{3}, -2.17^{8}, -2.16^{1}, -2.15^{6}, -2.14^{3}, -2.13^{7},$
	$-2.12^{7}, -2.11^{2}, -2.1^{6}, -2.09^{1}, -2.08^{7}, -2.07^{7},$
	$-2.06^{17}, -2.04^{3}, -2.03^{19}, -2.02^{1}, -2.01^{2}, -2.0^{3},$
	$-1.99^{79}, -1.98^{1}, -1.96^{1}, -1.95^{3}, -1.94^{1}, -1.93^{37},$
	$-1.92^{11}, -1.91^{5}, -1.9^{1}, -1.88^{18}, -1.87^{1}, -1.86^{2},$
	$-1.84^{4}, -1.83^{7}, -1.82^{3}, -1.81^{1}, -1.8^{117}, -1.79^{1},$
	$-1.78^{1}, -1.77^{1}, -1.76^{9}, -1.75^{5}, -1.74^{6}, -1.73^{1},$
	$-1.72^{2}, -1.71^{4}, -1.69^{2}, -1.68^{14}, -1.66^{1}, -1.65^{1},$
	$-1.64^{1}, -1.62^{294}, -1.6^{2}, -1.57^{1}, -1.56^{8}, -1.53^{18},$
	$-1.52^{2}, -1.5^{6}, -1.49^{79}, -1.48^{2}, -1.47^{1}, -1.46^{5},$
	$-1.45^{7}, -1.44^{11}, -1.38^{1}, -1.37^{3}, -1.36^{6}, -1.35^{2},$
	$-1.34^{9}, -1.32^{19}, -1.31^{11}, -1.3^{2}, -1.29^{3}, -1.28^{2},$
	$-1.27^{11}, -1.25^{118}, -1.22^{5}, -1.21^{1}, -1.19^{5}, -1.18^{3},$
	$-1.17^{5}, -1.16^{7}, -1.15^{2}, -1.14^{3}, -1.13^{3}, -1.1^{2},$
	$-1.09^{1}, -1.08^{1}, -1.06^{1}, -1.0^{545}, -0.93^{1}, -0.92^{1},$
	$-0.9^{7}, -0.88^{2}, -0.85^{6}, -0.83^{12}, -0.82^{2}, -0.81^{80},$
	$-0.79^{4}, -0.78^{8}, -0.77^{1}, -0.74^{4}, -0.73^{2}, -0.71^{6},$
	$-0.7^{5}, -0.69^{8}, -0.68^{2}, -0.67^{1}, -0.66^{5}, -0.63^{1},$
	$-0.62^{294}, -0.6^{3}, -0.59^{1}, -0.56^{12}, -0.52^{42}, -0.5^{1},$
	$-0.49^{2}, -0.48^{5}, -0.47^{2}, -0.46^{4}, -0.45^{117}, -0.44^{1},$
	$-0.43^{4}, -0.42^{81}, -0.41^{7}, -0.4^{9}, -0.38^{2}, -0.37^{19},$
	$-0.36^{13}, -0.35^{21}, -0.34^{4}, -0.33^{1}, -0.31^{16}, -0.3^{1},$
	$-0.29^{2}, -0.28^{14}, -0.27^{12}, -0.26^{4}, -0.25^{6}, -0.24^{2},$
	$0.24^{2}, 0.25^{6}, 0.26^{4}, 0.27^{12}, 0.28^{14}, 0.29^{2},$
	$0.3^{1}, 0.31^{16}, 0.33^{1}, 0.34^{4}, 0.35^{21}, 0.36^{13},$
	$0.37^{19}, 0.38^{2}, 0.4^{9}, 0.41^{7}, 0.42^{81}, 0.43^{4},$
	$0.44^{1}, 0.45^{117}, 0.46^{4}, 0.47^{2}, 0.48^{5}, 0.49^{2},$
	$0.5^{1}, 0.52^{42}, 0.56^{12}, 0.59^{1}, 0.6^{3}, 0.62^{294},$

Continued on next page

Table 33 – continued from previous page

n	Eigenvalues (value$^{\text{multiplicity}}$)
	$0.63^{1}, 0.66^{5}, 0.67^{1}, 0.68^{2}, 0.69^{8}, 0.7^{5},$
	$0.71^{6}, 0.73^{2}, 0.74^{4}, 0.77^{1}, 0.78^{8}, 0.79^{4},$
	$0.81^{80}, 0.82^{2}, 0.83^{12}, 0.85^{6}, 0.88^{2}, 0.9^{7},$
	$0.92^{1}, 0.93^{1}, 1.0^{545}, 1.06^{1}, 1.08^{1}, 1.09^{1},$
	$1.1^{2}, 1.13^{3}, 1.14^{3}, 1.15^{2}, 1.16^{7}, 1.17^{5},$
	$1.18^{3}, 1.19^{5}, 1.21^{1}, 1.22^{5}, 1.25^{118}, 1.27^{11},$
	$1.28^{2}, 1.29^{3}, 1.3^{2}, 1.31^{11}, 1.32^{19}, 1.34^{9},$
	$1.35^{2}, 1.36^{6}, 1.37^{3}, 1.38^{1}, 1.44^{11}, 1.45^{7},$
	$1.46^{5}, 1.47^{1}, 1.48^{2}, 1.49^{79}, 1.5^{6}, 1.52^{2},$
	$1.53^{18}, 1.56^{8}, 1.57^{1}, 1.6^{2}, 1.62^{294}, 1.64^{1},$
	$1.65^{1}, 1.66^{1}, 1.68^{14}, 1.69^{2}, 1.71^{4}, 1.72^{2},$
	$1.73^{1}, 1.74^{6}, 1.75^{5}, 1.76^{9}, 1.77^{1}, 1.78^{1},$
	$1.79^{1}, 1.8^{117}, 1.81^{1}, 1.82^{3}, 1.83^{7}, 1.84^{4},$
	$1.86^{2}, 1.87^{1}, 1.88^{18}, 1.9^{1}, 1.91^{5}, 1.92^{11},$
	$1.93^{37}, 1.94^{1}, 1.95^{3}, 1.96^{1}, 1.98^{1}, 1.99^{79},$
	$2.0^{3}, 2.01^{2}, 2.02^{1}, 2.03^{19}, 2.04^{3}, 2.06^{17},$
	$2.07^{7}, 2.08^{7}, 2.09^{1}, 2.1^{6}, 2.11^{2}, 2.12^{7},$
	$2.13^{7}, 2.14^{3}, 2.15^{6}, 2.16^{1}, 2.17^{8}, 2.18^{3},$
	$2.19^{2}, 2.2^{1}, 2.21^{2}, 2.22^{2}, 2.23^{1}, 2.24^{1}$

G.9.1 WITH THE INVERSES

n	Diameter	Mean	Variance	Std. dev.	Mode	Skewness	Excess kurtosis
3	3	1.5	0.917	0.957	1	0.0	-0.942
4	6	3.083	2.16	1.47	3	-0.144	-0.593
5	9	5.633	3.532	1.879	7	-0.735	0.009
6	15	8.322	4.346	2.085	9	-0.705	1.164
7	18	11.813	5.646	2.376	13	-0.813	1.012
8	25	15.368	6.562	2.562	17	-0.818	1.007
9	29	19.731	8.666	2.944	21	-0.727	0.702
10	37	24.179	10.35	3.217	26	-0.728	0.602
11	42	29.437	13.525	3.678	31	-0.667	0.422
12	51	34.813	16.289	4.036	37	-0.674	0.377
13	57	40.993	20.733	4.553	43	-0.644	0.299

G.9.2 WITHOUT THE INVERSES

n	Diameter	Mean	Variance	Std. dev.	Mode	Skewness	Excess kurtosis
3	3	1.5	0.917	0.957	1	0.0	-0.942
4	7	3.75	3.104	1.762	4	-0.257	-0.655
5	10	6.9	4.923	2.219	8	-0.858	0.275
6	17	10.892	7.127	2.67	12	-0.869	1.019
7	22	15.654	9.878	3.143	17	-0.825	0.925
8	31	21.201	13.447	3.667	22	-0.771	0.807
9	38	27.64	18.675	4.322	29	-0.703	0.576
10	49	34.904	24.731	4.973	37	-0.708	0.538
11	58	43.051	32.493	5.7	45	-0.681	0.503
12	71	52.043	41.383	6.433	56	-0.689	0.483
13	82	61.921	52.197	7.225	65	-0.676	0.479

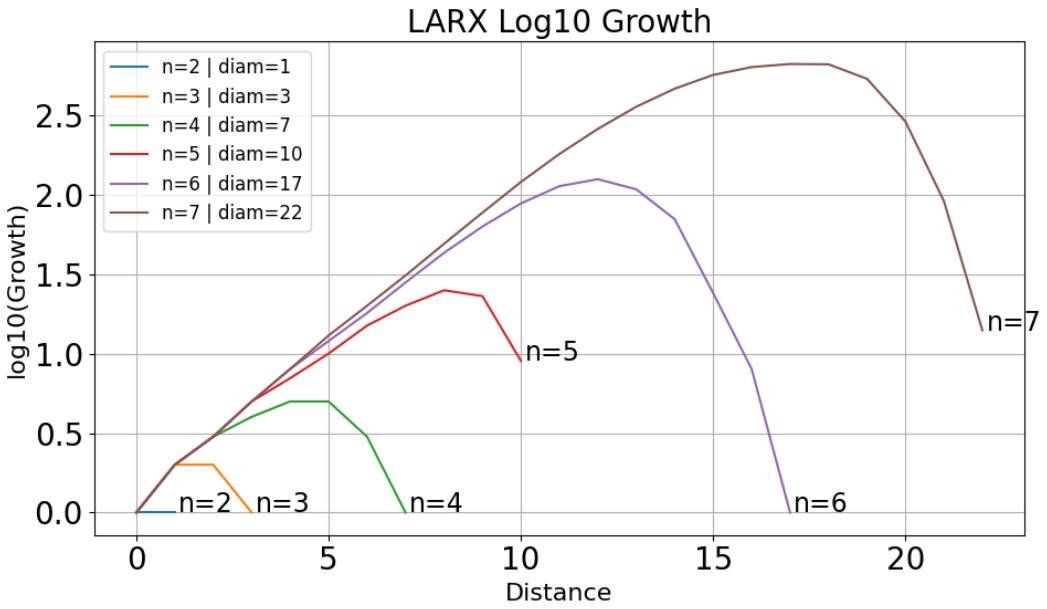


Figure 53: LARX Growth

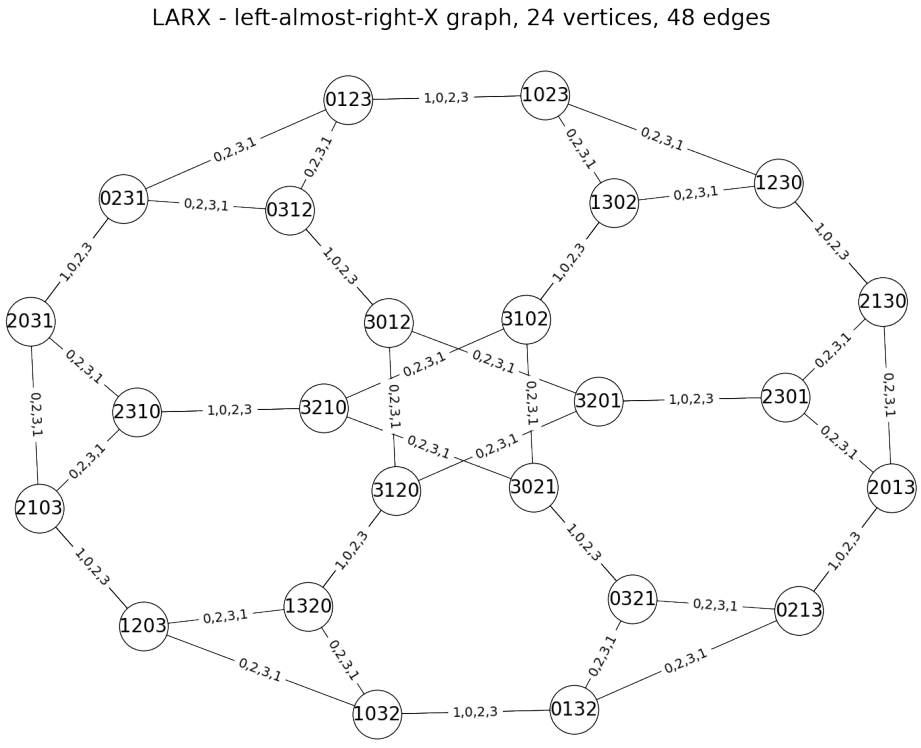


Figure 54: LARX $n = 4$ Graph

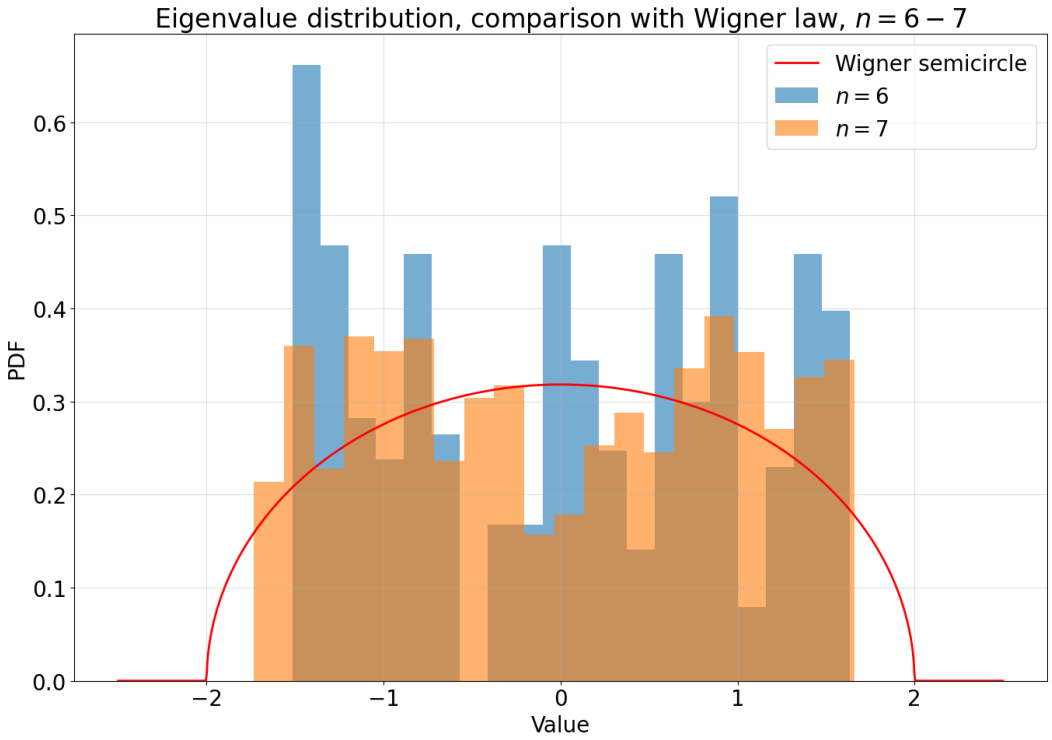


Figure 55: LARX eigenvalue distribution compared to Wigner's law

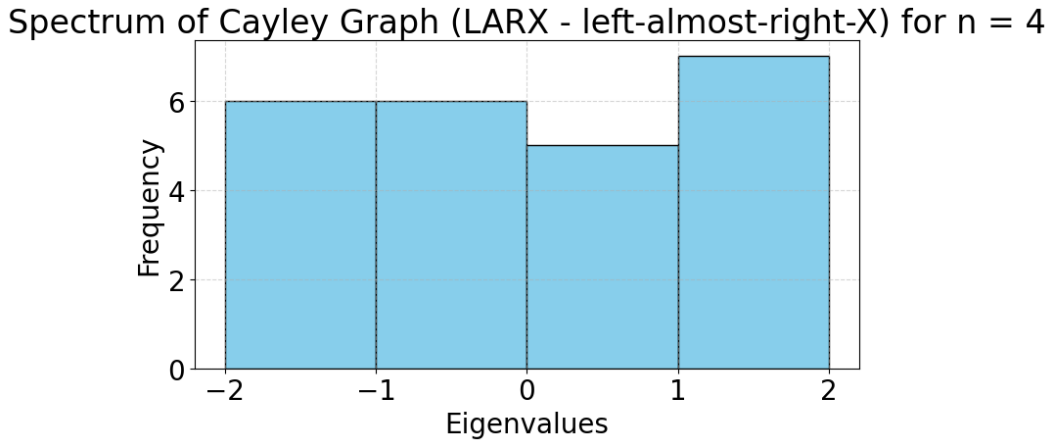


Figure 56: Eigenvalue spectrum histogram for LARX at $n = 4$. The histogram shows multiplicities of eigenvalues

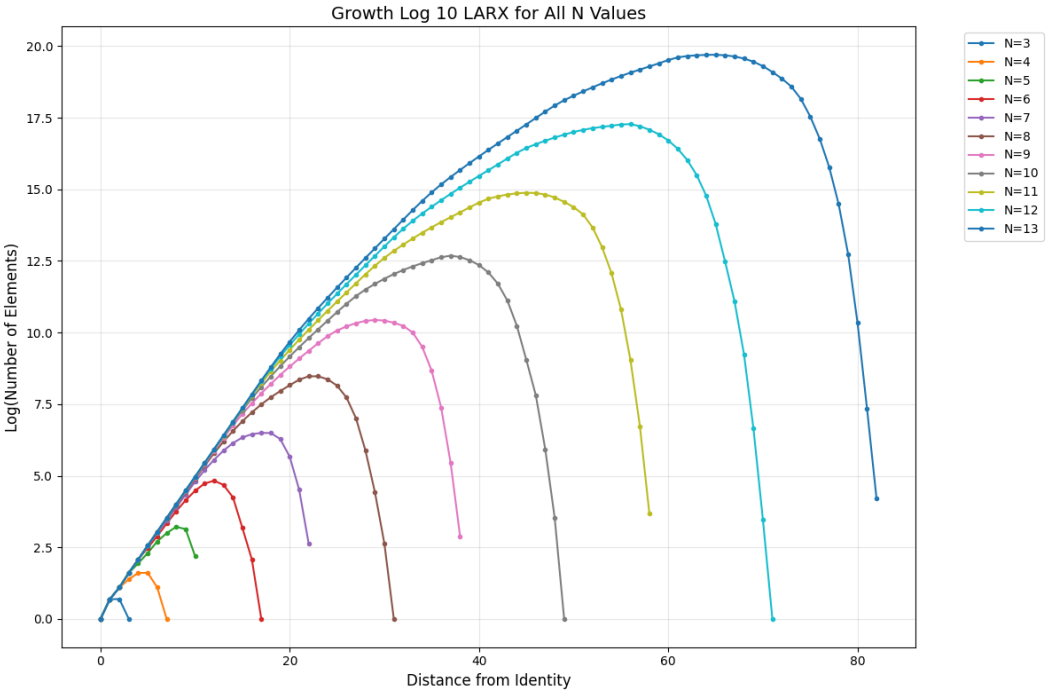


Figure 57: LARX Growth

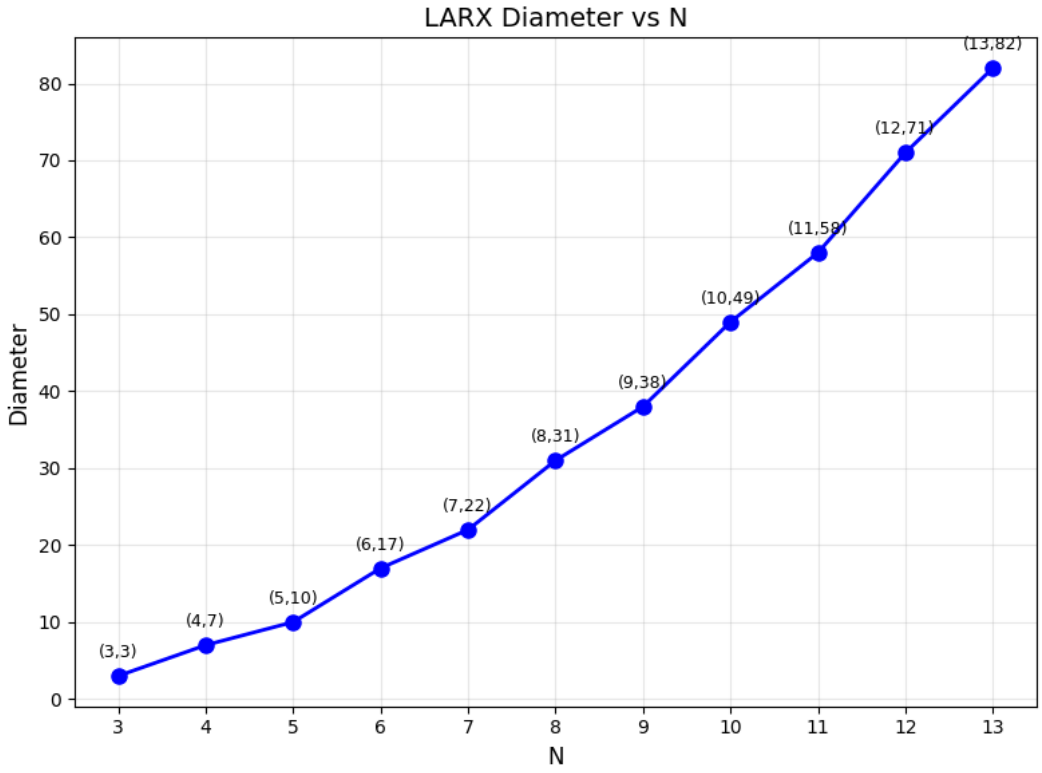


Figure 58: LARX diameter as a function of n.

G.10 ALL 3-CYCLES

For $n \geq 3$, let T_n contain both orientations of every 3-cycle on $\{0, \ldots, n-1\}$. This inverse-closed set generates A_n and has $2\binom{n}{3}$ elements. It provides a useful reference family: its distance is explicitly computable, so growth can be studied without approximating shortest paths. If $o(g)$ is the number of odd-length cycles of g, including fixed points, then

$$d_{T_n}(e, g) = \frac{n - o(g)}{2}, \qquad D_{T_n} = \left\lfloor \frac{n}{2} \right\rfloor. \tag{4}$$

The metric formula is given in Mühle & Nadeau (2019), following Herzog & Reid (1976). For odd n, an n-cycle attains the diameter. For even $n \geq 4$, a product of two disjoint even-length cycles covering all n letters has $o(g) = 0$ and attains it; for example, $(0\,1)(2\,3\,\cdots\,n-1)$.

Write $\gamma_n(r)$ for the number of states at distance r from the identity. The exact growth vectors include

n	$(\gamma_n(0), \ldots, \gamma_n(D_n))$
4	$(1, 8, 3)$
5	$(1, 20, 39)$
6	$(1, 40, 229, 90)$
8	$(1, 112, 2674, 12648, 4725)$.

For $n = 6$, the sum is $360 = |A_6|$, the diameter is three, and the largest layer is at distance two. The mean is $(40 + 2 \cdot 229 + 3 \cdot 90)/360 = 32/15$. Thus the diameter, mean, and mode in the catalogue describe different properties of the same growth vector. The exact distance formula also supplies labels with which to check a search implementation on every tractable instance.

The metric identifies the asymptotic scale of the mean more precisely. Let m be the largest odd integer not exceeding n. Counting cycles in a uniformly chosen even permutation gives

$$\mathbb{E}[o(g)] = \sum_{\substack{1 \leq j \leq n \\ j \text{ odd}}} \frac{1}{j} + \frac{1}{m}, \qquad \mu_n = \frac{n}{2} - \frac{1}{4}\log n + O(1).$$

For an odd cycle length at most $n-2$, the expected number of such cycles is $1/j$; the last possible odd length has expectation $2/m$ because its remaining permutation has at most one letter. Thus the mean lies a logarithmically growing distance below $n/2$.

The undirected adjacency spectrum is integral. One way to see this is to regard the sum of all 3-cycles as a central element of the group algebra of S_n: its eigenvalues are rational character ratios and also algebraic integers, hence integers. The Cayley graph on S_n has two components isomorphic to the graph on A_n, so this conclusion applies to the graph considered here.

G.11 3-CYCLES THROUGH ONE DISTINGUISHED LETTER

The catalogue entry $(0ij)$ uses

$$X_n = \{(0\,i\,j), (0\,j\,i) : 1 \leq i < j < n\}, \qquad n \geq 3.$$

It is an inverse-closed generating set of A_n with $(n-1)(n-2)$ moves. Its distance has a direct relationship to the star transpositions in Appendix G.4. Let $d_\star$ denote distance using $\{(0\,i) : 1 \leq i < n\}$. For every $g \in A_n$,

$$d_{X_n}(e, g) = \tfrac{1}{2} d_\star(e, g), \qquad D_{X_n} = \left\lfloor \frac{3(n-1)}{4} \right\rfloor. \tag{5}$$

Indeed, a move in X_n is a product of two star transpositions, giving one inequality. Conversely, a shortest star word for an even permutation has even length. Pair its successive letters. Equal letters cancel, while two distinct letters form an allowed 3-cycle, giving the reverse inequality. The largest even star distance is the largest even integer not exceeding the star diameter $\lfloor 3(n-1)/2 \rfloor$, which gives the displayed diameter.

The first growth vectors show how imposing the distinguished letter changes the distribution relative to all 3-cycles:

n	$(\gamma_n(0), \ldots, \gamma_n(D_n))$
4	$(1, 6, 5)$
5	$(1, 12, 44, 3)$
6	$(1, 20, 170, 169)$
7	$(1, 30, 460, 1689, 340)$.

At $n = 5$, restricting the generators raises the diameter from two to three and leaves three states in the final layer. At $n = 6$, the diameter remains three, but the last layer increases from 90 to 169 states. This distinction is relevant when choosing targets for search: matching diameters does not imply matching distributions of difficult states. Equation 5 gives exact distances for this family, independently of the quality of a learned heuristic.

G.12 3-CYCLES THROUGH TWO DISTINGUISHED LETTERS

Let $\sigma_i = (0\,1\,i)$ for $2 \le i < n$, with $n \ge 3$. The forward set $X_n^{\rightarrow} = \{\sigma_i\}$ and its inverse closure $X_n^{\pm} = \{\sigma_i, \sigma_i^{-1}\}$ both generate A_n. Their distances differ even though they have the same states. The catalogue uses $(01i)$ for the directed family and $(01i)I$ for the inverse-closed family.

Directed diameter conjecture. The exact computations for $3 \le n \le 12$ give diameters $2, 4, 5, 6, 8, 10, 11, 12, 14, 16$. We conjecture that, for every $n \ge 3$,

$$D_n^{\rightarrow} = \frac{3n-5}{2} + \frac{1}{2}\cos\frac{\pi n}{2} = \begin{cases} (3n-4)/2, & n \equiv 0 \pmod 4, \\ (3n-5)/2, & n \text{ odd}, \\ (3n-6)/2, & n \equiv 2 \pmod 4. \end{cases} \tag{6}$$

The cosine is the real form of the catalogue's periodic term $(\mathrm{i}^n + (-\mathrm{i})^n)/4$, where $\mathrm{i}^2 = -1$. Grouping the data by $n \bmod 4$ reveals the same slope $3/2$ and different intercepts, giving a concrete example of how a periodic diameter formula emerges from a sequence of exact computations.

Constructive decompositions can complement this numerical pattern without solving the shortest-word problem for every state. For example, with products composed from right to left,

$$(0\,2\,1\,3\,4\,5\,6) = \sigma_6\sigma_2\sigma_5\sigma_4\sigma_4\sigma_3.$$

This six-move representation improves on the seven-move representation $\sigma_2\sigma_2\sigma_5\sigma_6\sigma_4\sigma_5\sigma_3$ produced by the cycle-decomposition construction. Shorter valid words are therefore informative even when the construction already has a useful worst-case bound. This supplies an explicit target for evaluating whether search improves a constructive decomposition.

Inverse-closed metric. For $g \in A_n$, let $m(g)$ count its non-fixed letters other than 0 and 1, and let $c_*(g)$ count its nontrivial disjoint cycles containing neither 0 nor 1. Then

$$d_{X_n^{\pm}}(e, g) = m(g) + c_*(g), \qquad D_n^{\pm} = \left\lfloor \frac{3n-6}{2} \right\rfloor. \tag{7}$$

For the lower bound, every moved letter outside $\{0, 1\}$ must be used by a generator. A disjoint cycle avoiding both distinguished letters requires at least one of its letters to be used again: if each were used only once, the last such use would leave a letter at a distinguished position rather than at its prescribed successor. These extra uses are required separately for disjoint cycles. For the matching construction, put $t = (0\,1)$ and $s_i = (0\,i) = \sigma_i t$ for $i \ge 2$; then $t\sigma_i t = \sigma_i^{-1}$. Factor the disjoint cycles of g into star transpositions about 0. A cycle avoiding $0, 1$ uses $\ell + 1$ non-t letters, a cycle containing 0 uses one per outside letter, and a cycle containing 1 but avoiding 0 can use 1 as its repeated pivot, contributing two t letters and one letter per other entry. The total number of non-t letters is $m(g) + c_*(g)$. Substitute $s_i = \sigma_i t$ and move all t letters to the right by conjugation. Since g and every σ_i are even, the final power of t is even and cancels. The remaining word has exactly $m(g) + c_*(g)$ allowed generators.

The formula explains why disjoint transpositions are useful extremal patterns: they maximize the number of additional cycles per moved letter. When n is even, pair all $n - 2$ outside letters into

transpositions and, if necessary, include $(0\,1)$ to make the permutation even. This gives distance $3(n-2)/2$. For odd $n \geq 5$, use one 3-cycle on outside letters and pair the rest, again correcting parity with $(0\,1)$; this gives $(3n-7)/2$. The case $n = 3$ is direct.

The exact metric also permits growth calculations by counting cycle types rather than enumerating all permutations. The resulting statistics show that a convincing small-size mode pattern can fail: the mode equals $n-2$ for $3 \leq n \leq 12$, but the larger calculations give mode 49 at $n = 50$, 100 at $n = 100$, and 1002 at $n = 1000$. The corresponding reported means are 49.08, 99.73, and 1002.0. Over the computed range through $n = 1000$, the fitted mean

$$\mu_n \approx n + 1.245 \log n - 1.455 \log\log n - 3.786$$

describes the slow correction to linear growth. It is an empirical fit, whereas Equation 7 is a distance formula.

G.13 Consecutive cycles on a line

For $2 \leq k < n$, define

$$C_{n,k} = \{(j\; j+1 \cdots j+k-1) : 0 \leq j \leq n-k\}.$$

The generated group is S_n when k is even and A_n when k is odd. The directed graph uses $C_{n,k}$, and the undirected graph uses $C_{n,k} \cup C_{n,k}^{-1}$. The endpoint restriction is part of the definition: these moves do not wrap around the line.

For $k = 3$, the computed diameters support the formulas

$$D^{\rightarrow}_{n,3} = \left\lfloor \frac{n^2+1}{4} \right\rfloor, \qquad D^{\pm}_{n,3} = \left\lfloor \frac{n(n-1)}{4} \right\rfloor, \qquad n \geq 3. \tag{8}$$

The formulas are stated here as diameter conjectures. Selected exact values and growth statistics are

	Directed		Inverse-closed	
n	D_n	μ_n	D_n	μ_n
6	9	4.93	7	3.85
8	16	8.67	14	7.07
10	25	13.39	22	11.29
12	36	19.11	33	16.53
14	49	25.83	45	22.77.

The means are rounded to two decimal places. The inverse-closed variance increases from 1.55 at $n = 6$ to 20.64 at $n = 14$; at the latter size the skewness is 0.018 and excess kurtosis is -0.178. Such measurements motivate the catalogue's proposed Gaussian growth shape and illustrate why distributional conjectures require more than a formula for the last nonempty layer.

The local structure gives a useful independent bound. Each move, in either orientation, changes the inversion number by at most $k-1$. Consequently the inverse-closed diameter is at least

$$\left\lceil \frac{n(n-1)}{2(k-1)} \right\rceil \quad (k \text{ even}), \qquad \left\lceil \frac{2\lfloor n(n-1)/4 \rfloor}{k-1} \right\rceil \quad (k \text{ odd}).$$

These bounds use the maximum inversion number in S_n or A_n and explain the natural quadratic scale for fixed k. For inverse-closed 4-cycles, the exact diameters at $n = 6, 8, 10, 12$ are $6, 10, 16, 23$. For inverse-closed 5-cycles at $n = 6, 8, 10, 12$, they are $9, 8, 11, 17$. The small-size nonmonotonicity in the latter sequence is a reason to state a fitting range explicitly. At $n = k$, there is only one cyclic generator and the group is cyclic; that boundary case is not an S_n or A_n member of the family above.

G.14 Wrapped consecutive cycles

Indices are now read modulo n, and every starting position is allowed:

$$W_{n,k} = \{(j\; j+1 \cdots j+k-1) : j \in \mathbb{Z}/n\mathbb{Z}\}, \qquad 2 \leq k < n.$$

As before, use $W_{n,k}$ for the directed graph and its inverse closure for the undirected graph. The catalogue suffix C denotes wrapping, and CI denotes wrapping with inverses. This change in geometry has a substantial effect even at fixed group and cycle length.

For inverse-closed wrapped 3-cycles, we conjecture

$$D_{n,3}^{\mathrm{wrap},\pm} = \left\lfloor \frac{n^2}{8} \right\rfloor, \qquad n \geq 4. \tag{9}$$

The same formula gives the cyclic boundary value one at $n = 3$. The computed values for $n = 4, \ldots, 14$ are $2, 3, 4, 6, 8, 10, 12, 15, 18, 21, 24$. At $n = 8$, for example, the full growth vector is

$$(1, 16, 160, 1136, 4758, 8582, 5020, 472, 15).$$

Its entries sum to $20\,160 = |A_8|$ and its support ends at eight, compared with diameter fourteen for non-wrapped inverse-closed 3-cycles. The mean also decreases, from 7.07 to 4.92. Thus wrapping changes both the extremal distance and typical distance, rather than merely increasing the number of available moves.

The directed wrapped 3-cycle diameters at $n = 6, 8, 10, 12$ are $5, 9, 14, 20$, while the inverse-closed values are $4, 8, 12, 18$. For wrapped 4-cycles, the corresponding directed values are $7, 9, 12, 16$ and inverse-closed values are $5, 7, 10, 13$. These comparisons fix the orientation before comparing formulas. The quadratic wrapped-3-cycle conjecture can be tested beyond enumeration by searching for shorter words for proposed antipodes and by developing matching lower bounds; the latter are essential to certify that a difficult state actually attains the proposed distance.

G.15 Prefix cycles

On S_n, let $P_n = \{(1\,2\,\cdots\,j) : 2 \leq j \leq n\}$. The forward generating set has $n - 1$ moves, while its inverse closure has $2n - 3$ moves because the transposition is its own inverse. The directed diameter is $n - 1$; see Glukhov & Zubov (1999) for the classical result and its attribution. The computations for the inverse-closed family also give $n - 1$ for $3 \leq n \leq 12$, motivating the corresponding catalogue conjecture.

The two orientations have different growth despite sharing those diameters. At $n = 5$ their growth vectors are

$$\gamma_5^{\rightarrow} = (1, 4, 15, 40, 60),$$
$$\gamma_5^{\pm} = (1, 7, 33, 60, 19).$$

Half of the directed graph lies in the final layer, whereas only $19/120$ of the undirected graph does. At $n = 10$, the directed mean and mode are 8.28 and 9, compared with 7.36 and 8 after adding inverses; both diameters are nine. At $n = 12$, the directed last layer contains $239\,500\,800$ states, again half of S_{12}, whereas the inverse-closed last layer contains $36\,348\,834$ states.

This family is a particularly simple example of how to use the catalogue. Reading the diameter cell alone suggests the same linear growth law for both move sets. Reading the mean, mode, or growth vector poses a different question: how much of the group lies near that diameter? A search benchmark should specify both the orientation and the target distribution, since adding inverses changes the latter even when the diameter stays fixed.

G.16 Downcycles

The downcycle generating set consists of all consecutive intervals,

$$Q_n = \{(i\,i+1\,\cdots\,j) : 1 \leq i < j \leq n\} \subset S_n.$$

Its directed version uses one orientation of every interval; its inverse closure permits both. These sets contain $\binom{n}{2}$ and $(n-1)^2$ distinct moves, respectively. Each includes the adjacent transpositions and therefore generates S_n.

Exact enumeration for $3 \leq n \leq 12$ gives diameter $n - 1$ in both orientations, leading to the two diameter conjectures in the catalogue. For $n = 6$, the growth vectors are

$$\gamma_6^{\rightarrow} = (1, 15, 85, 225, 274, 120),$$
$$\gamma_6^{\pm} = (1, 25, 181, 381, 131, 1).$$

They both sum to 720, but there are 120 antipodes in the directed graph and only one in the undirected graph. At $n = 12$, the same contrast is $39\,916\,800$ versus one, with means 8.90 and 7.15. The latter

family therefore offers a sharply specified search target: the unique last-layer state in each computed instance can be inspected to propose an extremal permutation pattern for larger n.

The directed vectors agree, throughout the enumerated range, with the unsigned Stirling numbers of the first kind in reverse order:

$$\gamma_n^{\rightarrow}(r) = \begin{bmatrix} n \\ n-r \end{bmatrix}.$$

This observation explains the catalogue's "Stirling" entry. If the identity holds for all n, the normalized distance distribution has mean $n - H_n$ and variance $H_n - H_n^{(2)}$, where $H_n = \sum_{j=1}^{n} 1/j$ and $H_n^{(2)} = \sum_{j=1}^{n} 1/j^2$. It gives a concrete route from a growth table to several connected conjectures: one coefficient formula predicts the diameter, number of antipodes, mean, and variance simultaneously. These exact-enumeration examples complement the RL/search workflow of Appendix B; their finite growth tables do not rely on a learned distance estimate.

G.17 Additional generator families and finite growth profiles

The following families complement the local sorting generators with simultaneous swaps, mechanical puzzle moves, dense generating sets, and matrix multiplication. For a generating set X, write $a_k = |\{g : d_X(e, g) = k\}|$. A displayed growth sequence starts with $a_0 = 1$ and ends at the last nonempty sphere. Thus its sum is the order of the reachable group and its final index is the diameter. For directed generators, distance counts positive words; for symmetric generators, inverse moves have unit cost. These conventions matter even when the underlying group is unchanged. The finite data below describe exact enumeration, rather than a separate learned-search experiment for each family.

G.17.1 Rapaport generators: changing the cost of simultaneous swaps

Let $t_i = (i\ i+1)$ for $1 \le i < n$. Define the partial odd and even packets

$$a_j = \prod_{r=1}^{j} t_{2r-1}, \qquad b_j = \prod_{r=1}^{j} t_{2r},$$

where the allowed ranges are $1 \le j \le \lfloor n/2 \rfloor$ and $1 \le j \le \lfloor (n-1)/2 \rfloor$, respectively. All factors within a packet are disjoint transpositions. The Rapaport M1 generating set consists of every such a_j and b_j, giving $n - 1$ involutions. It generates S_n: with $a_0 = b_0 = e$, consecutive packet products recover $t_{2j-1} = a_j a_{j-1}$ and $t_{2j} = b_j b_{j-1}$. One packet costs one move, regardless of its number of transpositions.

For $n = 5$, the complete growth sequence is

$$(1, 4, 10, 19, 34, 42, 10),$$

with sum 120 and diameter 6. For $n = 6$, it is

$$(1, 5, 16, 41, 95, 176, 240, 143, 3),$$

with sum 720 and diameter 8. The catalogue diameter sequence for $n = 3, \ldots, 14$ is

$$3, 4, 6, 8, 9, 11, 13, 15, 16, 18, 19, 21.$$

Its final six values support the specific conjecture

$$D_{\mathrm{M1}}(n) = \left\lfloor \frac{3n}{2} \right\rfloor \qquad (n \ge 9).$$

This is a conjecture for the displayed packet generators. The floor is essential: the observed value at $n = 9$ is 13, not 14. Neither this finite agreement nor the approximately linear trend supplies an upper-bound algorithm for arbitrary n.

The three-generator variant. The M2 variant retains just three involutions,

$$X_{\mathrm{M2}} = \{t_1, a_{\lfloor n/2 \rfloor}, b_{\lfloor (n-1)/2 \rfloor}\}.$$

For $n \geq 4$ these are distinct; the first two commute. The generator set is a subset of M1, so its distances cannot be smaller. At $n = 5$, its growth sequence is

$$(1, 3, 5, 8, 13, 20, 26, 33, 11),$$

and the diameter increases from 6 to 8. At $n = 6$, M2 has diameter 16, twice the M1 diameter. The catalogue reports M2 diameters

$$8, 16, 22, 30, 40, 49, 62, 74, 87, 101, 117 \qquad (n = 5, \ldots, 15).$$

These values motivate studying a quadratic scale, but do not identify an exact quadratic or quasi-polynomial law. In particular, $(n^2 + n)/2$ should be treated as a rough comparison, not an equality. M1 and M2 therefore provide a useful controlled algebraic contrast: the same adjacent transpositions underlie both constructions, while the permitted packet sizes change the metric substantially.

G.17.2 A CONCRETE ALTERNATING-GROUP TRIPLE

Commuting pairs among three involutions also arise in the alternating-group constructions studied by Nuzhin (1992). A fully specified small example acts on $\{0, 1, 2, 3, 4\}$:

$$t = (0\ 1)(2\ 3), \qquad u = (0\ 3)(1\ 2), \qquad v = (1\ 2)(3\ 4).$$

All three are even involutions, and $tu = ut$. Enumeration gives 60 reachable permutations, so the generated group is A_5. Its growth sequence is

$$(1, 3, 5, 7, 9, 11, 12, 12),$$

and its diameter is 7. This example preserves the degree-three comparison with M2 while changing the ambient group and local relations. It also illustrates why the degree of a permutation action must accompany a generator formula: the symbol 4 makes this a five-point action. We use this explicit triple without extrapolating a general residue-dependent construction from the small example.

G.17.3 TOPSPIN: THE FLIP LENGTH CHANGES THE REACHABLE GROUP

For $2 \leq k \leq n$, let

$$L = (0\ 1\ \cdots\ n-1), \qquad X_k = \prod_{j=0}^{\lfloor k/2 \rfloor - 1} (j\ k-1-j).$$

The TopSpin group is $OT_{n,k} = \langle L, X_k \rangle$, and the metric used here has generators $\{L, L^{-1}, X_k\}$. A move is a one-position rotation or a reversal of a fixed window of k positions. The general reachable-group classification is discussed by Nash & Randall (2018); for enumeration, the relevant state space is the generated subgroup, rather than an assumed copy of S_n.

Two six-position examples make this distinction concrete. For $(n, k) = (6, 3)$, the growth sequence is

$$(1, 3, 6, 11, 16, 17, 12, 5, 1),$$

which sums to 72 and has diameter 8. For $(n, k) = (6, 4)$, it is

$$(1, 3, 6, 11, 20, 37, 63, 103, 165, 152, 106, 46, 7),$$

which sums to 720 and has diameter 12. The first case therefore explores only a proper subgroup, while the second reaches all of S_6. Comparing their diameters without their state counts would obscure this change. Further catalogue values at fixed $k = 4$ are $17, 22, 23, 28$ for $n = 7, 8, 9, 10$, respectively. These finite values are useful test cases, but are not themselves an eventual diameter formula. When $k = 2$, the construction reduces to rotation, inverse rotation, and an adjacent swap, connecting this family directly to LRX.

G.17.4 A PRECISELY DEFINED NARROW-GLOBE FAMILY

Consider positions (i, c) with $0 \le i \le A$ and $c \in \{0, 1\}$. The two-column globe has $A + 1$ row moves

$$r_i = ((i, 0)\ (i, 1))$$

and two column flips

$$f_c = \prod_{0 \le i < A - i} ((i, c)\ (A - i, c)), \qquad c \in \{0, 1\}.$$

Every generator is an involution. This defines the $B = 1$ slice of the globe family without appealing to a geometric picture or to a convention for wider globes. The column flips simultaneously exchange mirror rows, whereas each row move affects just one pair of positions.

For $A = 1$, the four generators are the edge transpositions of a four-cycle; the growth sequence is $(1, 4, 10, 8, 1)$, with 24 states and diameter 4. For $A = 2$, the sequence is $(1, 5, 14, 18, 9, 1)$, with 48 states and diameter 5. For $A = 3$, it is

$$(1, 6, 23, 72, 179, 202, 85, 8),$$

with 576 states and diameter 7. These examples show how simultaneous reflection moves can couple otherwise separate row operations.

The catalogue reports diameters

$$7, 8, 10, 11, 12, 13, 15, 16, 17, 18, 20, 21 \qquad (A = 3, \ldots, 14),$$

which agree with the candidate formula

$$D_{\text{globe}}(A, 1) = \left\lceil \frac{5A + 12}{4} \right\rceil \qquad (A \ge 3).$$

The threshold is necessary: the same expression gives incorrect values at $A = 1, 2$. This conjecture fixes the width parameter and the displayed involutory moves; it does not make a uniform claim when both dimensions vary. The period-four expression provides a compact mathematical target for a constructive sorting proof and matching lower bound.

G.17.5 HUNGARIAN RINGS: INTERSECTION PLACEMENT AFFECTS DISTANCE

Take two cycles

$$L = (l_0\ l_1\ \cdots\ l_{M-1}), \qquad R = (r_0\ r_1\ \cdots\ r_{N-1})$$

that share exactly two positions, $l_0 = r_0$ and $l_m = r_q$, with all other positions distinct. The parameters are (M, m, N, q), the total number of positions is $M + N - 2$, and the move set is $\{L, L^{-1}, R, R^{-1}\}$. This fixes both the geometry and the unit-cost convention: rotating several positions is several moves.

For $(3, 1, 3, 1)$, one may take $L = (0\ 1\ 2)$ and $R = (0\ 1\ 3)$. The growth sequence $(1, 4, 6, 1)$ sums to 12 and has diameter 3. More revealingly, two five-position examples generate the same number of states but have different metrics. With $L = (0\ 1\ 2)$ and $R = (0\ 1\ 3\ 4)$, corresponding to $(3, 1, 4, 1)$, the growth sequence is

$$(1, 4, 9, 20, 38, 41, 6, 1),$$

and the diameter is 7. Moving the second intersection to the opposite position on the four-cycle gives $R = (0\ 3\ 1\ 4)$ and parameters $(3, 1, 4, 2)$. Its sequence is

$$(1, 4, 9, 14, 16, 24, 24, 12, 8, 6, 2),$$

with diameter 10. Both sums are 120, so both actions reach S_5. Intersection spacing is therefore a structural parameter that cannot be discarded when fitting a diameter law. Equal ring sizes and antipodal intersections can impose further restrictions on reachability; a formula indexed only by the total number of positions would merge distinct families.

G.17.6 Dense generators: all cycles and all derangements

Let C_n consist of permutations with exactly one nontrivial cycle, of any length from 2 to n. Its cardinality is

$$c_n = \sum_{j=2}^{n} \binom{n}{j} (j-1)!.$$

The corresponding Cayley graph is the graph of the Birkhoff polytope. Every permutation is a product of at most two members of C_n: connect its nontrivial disjoint cycles successively by transpositions between chosen representatives. Multiplying by this chain merges them into one cycle, while the chain itself is a cycle on the representatives. For $n \geq 4$, a product of two disjoint transpositions is not a generator, so the diameter is exactly 2. The complete growth sequence is consequently

$$(1, c_n, n! - 1 - c_n).$$

For $n = 4, 5, 6$, this gives $(1, 20, 3)$, $(1, 84, 35)$, and $(1, 409, 310)$. For $n = 2, 3$, every nonidentity permutation is already a generator, and the diameter is 1.

Derangements. Now let $\Delta_n = \{\pi \in S_n : \pi(i) \neq i \text{ for every } i\}$ be the set of all derangements. For $n \geq 4$, this also gives diameter 2, with growth

$$(1, !n, n! - 1 - !n), \qquad !n = n! \sum_{j=0}^{n} \frac{(-1)^j}{j!}.$$

A short argument explains the two-step bound. Given σ, choose a permutation τ satisfying both $\tau(i) \neq i$ and $\tau(i) \neq \sigma(i)$. In the associated bipartite assignment problem, each row and column has at most two forbidden entries. Hall's condition holds for $n \geq 4$: a set of at most $n-2$ rows has at least $n-2$ available columns, and a set of at least $n-1$ rows reaches every column. Thus τ and $\tau^{-1}\sigma$ are derangements. Since a transposition has fixed points, the diameter is not 1. At $n = 4, 5, 6$ the sequences are $(1, 9, 14)$, $(1, 44, 75)$, and $(1, 265, 454)$. At $n = 3$, derangements generate only A_3, whose growth is $(1, 2)$.

Involutive derangements. Requiring the derangements also to be involutions gives a more selective family. Its generators are perfect matchings, numbering $n!/(2^{n/2}(n/2)!)$ for even n. The catalogue sequences are

n	growth
4	$(1, 3)$
6	$(1, 15, 85, 225, 274, 120)$
8	$(1, 105, 2590, 11640, 5824)$
10	$(1, 945, 168231, 1611855, 1646168, 201600)$.

Their sums are 4, 720, 20160, and 3628800, respectively. In particular, the $n = 8$ case reaches A_8, consistent with every matching being even. The observed diameters $5, 4, 5$ at $n = 6, 8, 10$ motivate the conjecture $D(n) = 4 + ((n/2) \bmod 2)$ for even $n \geq 6$, always interpreting diameter in the generated subgroup. This is a three-size observation, not a proved continuation. These dense families separate two sources of apparent search difficulty: a large state space can have a tiny diameter when each move is allowed to modify many positions.

G.17.7 Matrix groups: distinguish the dimension, modulus, and move set

The finite Heisenberg group consists of matrices

$$H_3(m) = \left\{ \begin{pmatrix} 1 & a & c \\ 0 & 1 & b \\ 0 & 0 & 1 \end{pmatrix} : a, b, c \in \mathbb{Z}/m\mathbb{Z} \right\},$$

with m^3 states. Take $x = I + E_{12}$, $y = I + E_{23}$ and symmetric moves $\{x, x^{-1}, y, y^{-1}\}$. The commutator $xyx^{-1}y^{-1} = I + E_{13}$ generates the central coordinate. In coordinates (a, b, c), right multiplication by x increments a, while right multiplication by y increments b and adds a to c. Thus exact transitions require only modular arithmetic. At $m = 2$, inverse moves coincide and the growth sequence is $(1, 2, 2, 2, 1)$, giving eight states and diameter 4.

For a related but different metric, let $U_4(m)$ be all upper unitriangular 4×4 matrices over $\mathbb{Z}/m\mathbb{Z}$, and use all six positive transvections

$$X_4^+ = \{I + E_{ij} : 1 \le i < j \le 4\}.$$

There are m^6 states. These are all upper-triangular elementary moves, not just the three adjacent transvections. At $m = 2$, the directed growth sequence is $(1, 6, 19, 31, 7)$, giving 64 states and diameter 4. The catalogue diameter plot gives 7 at $m = 3$. The corresponding diameters at $m = 4, 5$ are $10, 13$. These values support the catalogue's proposed linear continuation

$$D(U_4(m), X_4^+) = 3m - 2 \qquad (m \ge 2),$$

which remains a conjecture. The abelianization already gives the lower bound $3(m - 1)$: each of the three first-superdiagonal entries may require $m - 1$ positive increments. The proposed equality lies just one move above this elementary obstruction, but a proof must also control all higher entries.

Adding inverses changes the question. For $X_4^\pm = X_4^+ \cup (X_4^+)^{-1}$, the diameters at $m = 2, 3, 4, 5$ are $4, 5, 7, 8$. At $m = 3$, for example, the growth is $(1, 12, 76, 264, 360, 16)$. The catalogue suggests the separate candidate $D(U_4(m), X_4^\pm) = 3m/2$ for sufficiently large even m; its finite fit should not be extended to odd moduli or to the adjacent-generator metric. Both matrix conjectures fix dimension four and vary the modulus. They therefore pose specific problems about the effect of nilpotent coordinates on word length, without implying a universal formula for arbitrary matrix families.

The Heisenberg example also offers an algebraically explicit spectral diagnostic. For $m \ge 3$, the adjacency operator is $x + x^{-1} + y + y^{-1}$ in the regular representation. Since the central element $z = I + E_{13}$ has order m, its action decomposes the state space into invariant subspaces indexed by m-th roots of unity. Each eigenspace has dimension m^2: the central action partitions the m^3 group elements into m^2 cycles of length m. The adjacency operator preserves each such subspace because it commutes with the central action. This provides an exact reduction before any numerical diagonalization.

A second, smaller construction illustrates the origin of the structured spectra. On a vector space with basis e_j, indexed modulo m, put $Pe_j = e_{j+1}$ and $De_j = Q^j e_j$, where $Q^m = 1$. Then $DP = QPD$, and assigning $x = D$, $y = P$, $z = QI$ satisfies the Heisenberg relations. The associated adjacency block is

$$H_Q = P + P^{-1} + D + D^{-1}.$$

Its diagonal entries are $2\cos(2\pi rj/m)$ when $Q = \exp(2\pi ir/m)$, and the shift terms couple neighboring cyclic indices. These blocks supply part of the full spectrum; they need not form a complete list of irreducible representations for a composite modulus. The distinction prevents the omission of spectral components from being mistaken for a feature of the graph. This example links three independently checkable descriptions of the same finite object: multiplication of modular matrices, shortest-word enumeration, and representation-theoretic blocks. It supplies a concrete route to validating spectral computations without turning a visually suggestive histogram into a limiting-distribution theorem.

H PREFIX REVERSALS AND REARRANGEMENT FAMILIES

The following families expand the pancake, cubic-pancake, reversal, and transposon entries of the catalogue. They share a representation by ordered lists, but differ in which intervals can move and whether signs change. Specifying those choices is essential: a diameter formula belongs to a particular generating set. Write $a_n(t) = |\{g : d(e, g) = t\}|$ for the number of states in the tth layer. A complete growth vector determines the diameter, the number of antipodes, and the entire distribution of the distance of a uniformly sampled state. All numerical examples below are drawn from the computations reported in this paper.

H.1 PANCAKE AND BURNT-PANCAKE GENERATORS

For a permutation $\pi = [\pi_1, \ldots, \pi_n]$, the prefix reversal r_k, $2 \le k \le n$, acts by

$$\pi r_k = [\pi_k, \pi_{k-1}, \ldots, \pi_1, \pi_{k+1}, \ldots, \pi_n].$$

The pancake graph is $\mathrm{Cay}(S_n, \{r_2, \ldots, r_n\})$. Each generator is an involution, so the graph is undirected, has $n!$ vertices, and has degree $n - 1$. A path to the identity gives a sequence of flips that sorts the permutation. The distinction between a worst-case and a typical sorting problem can be read directly from the growth vector: its last nonzero index is the diameter, whereas its largest entry identifies the most frequent distance.

For example, at $n = 6$ the complete growth vector is

$$(a_6(0), \ldots, a_6(7)) = (1, 5, 20, 79, 199, 281, 133, 2).$$

The entries sum to $720 = 6!$. Thus the diameter is 7, exactly two permutations are at distance 7, and the modal distance is 5. The corresponding mean is $3295/720 \approx 4.576$. This example illustrates why a catalogue should retain distributional statistics as well as a diameter: the two antipodes occupy only a small fraction of the graph, even though they determine its worst-case sorting cost.

n	4	5	6	7	8	9
Pancake diameter	4	5	7	8	9	10
Number of antipodes	3	20	2	35	455	5804

Table 34: Diameter and final-layer size from complete pancake growth vectors.

The first layers have simple formulas: $a_n(0) = 1$, $a_n(1) = n - 1$, and $a_n(2) = (n - 1)(n - 2)$ for $n \ge 3$. They give immediate checks on an implementation before deeper layers are compared. The recorded full growth vectors extend through $n = 14$; the larger recorded cases contain initial layers only. Such partial vectors still describe local growth, but their last recorded layer is not a diameter estimate.

For burnt pancakes the state is a signed permutation in B_n, and the allowed operation is

$$\pi \bar{r}_k = [-\pi_k, -\pi_{k-1}, \ldots, -\pi_1, \pi_{k+1}, \ldots, \pi_n], \qquad 1 \le k \le n.$$

The state space therefore has $2^n n!$ elements and degree n. The move $\bar{r}_1$ changes the first sign, so it must be retained. This convention distinguishes burnt pancakes from unsigned prefix reversals and from signed reversals of arbitrary intervals. For example, the recorded first layers at $n = 10$ are $(1, 10, 90, 810, 6885)$, corresponding to distances 0 through 4. These layers provide a reproducible small-depth comparison without implying that the full graph has been enumerated at this size.

H.2 THE SEVEN CUBIC-PANCAKE FAMILIES

Restricting prefix reversal to three allowed lengths gives a graph of fixed degree while preserving a rapidly growing state space. Table 35 spells out the seven catalogue conventions. The parameter restrictions select the families on S_n; using a disallowed parity can produce a proper subgroup, whose diameter answers a different question. The classical restricted-prefix construction is discussed in Bass & Sudborough (2003).

Catalogue family	Allowed prefix reversals	Parameters
S_1	$\{r_n, r_{n-1}, r_2\}$	$n \geq 4$
S_2	$\{r_n, r_{n-1}, r_3\}$	odd $n \geq 5$
S_3	$\{r_n, r_{n-1}, r_{n-2}\}$	$n \geq 4$
S_4	$\{r_n, r_{n-1}, r_{n-3}\}$	odd $n \geq 5$
S_5	$\{r_n, r_{n-2}, r_2\}$	odd $n \geq 5$
S_6	$\{r_n, r_{n-2}, r_3\}$	even $n \geq 6$
S_7	$\{r_n, r_{n-2}, r_{n-3}\}$	$n \geq 5$

Table 35: Generator definitions for the seven cubic-pancake catalogue rows.

These families make the growth question concrete. Ordinary pancakes allow all $n-1$ prefix lengths. The cubic families allow only three, and the observed diameter scale is quadratic in several cases. For S_1, the recorded diameters at $n = 4, \ldots, 14$ are

$$4, 7, 12, 18, 24, 30, 39, 47, 57, 67, 78.$$

The full growth vector at $n = 6$ is

$$(1, 3, 6, 12, 22, 40, 70, 114, 150, 177, 94, 30, 1).$$

It has the same 720 states as the ordinary pancake example, but diameter 12 and a unique antipode. Changing only the move set nearly doubles the worst-case distance at this size.

Conjecture 3 (Even cubic-pancake diameters)**.** *For even $n \geq 6$, both S_1 and S_6 have diameter*

$$D_{S_1}(n) = D_{S_6}(n) = \frac{3n^2 + 6n - 48}{8}.$$

The recorded exact values at $n = 6, 8, 10, 12, 14$ are $12, 24, 39, 57, 78$ for both families. With the parameter advanced by two, their first differences are $12, 15, 18, 21$ and their second differences are constantly 3. These computations lead to the quadratic expression in Conjecture 3. The conjecture is a statement about all even sizes in its range; the listed values specify the finite evidence supporting it.

At larger sizes, the same three generators define the transitions used by learned search. A promising state suggested by a long random walk or by previous extremal examples can be solved with the learned heuristic, and the returned word can be replayed under precisely these reversals. This produces a concrete candidate sorting sequence to compare with the predicted scale. The RL/search workflow in Appendix B explains how candidate states and improved solutions guide this process. The complete vectors above are enumeration results; they are not themselves outcomes of an RL ablation.

H.3 Binary cubic-pancake orbits

Prefix reversals also act on binary strings. For each S_j use the reference state

$$s_0 = 1^{\lceil n/2 \rceil} 0^{\lfloor n/2 \rfloor}.$$

States with repeated symbols identify permutations that differ only by relabeling equal symbols. When the action reaches every string of this composition, the resulting orbit has $\binom{n}{\lfloor n/2 \rfloor}$ states. This reduction makes larger parameters accessible while retaining a nontrivial dependence on the allowed reversals.

Let $e_j(n) = \max_x d(s_0, x)$ denote the eccentricity of this specified reference state. Complete enumeration from s_0 gives $e_j(n)$ and the associated growth vector. Unlike a Cayley graph, such an orbit graph need not be vertex-transitive, so the reference state is part of the statement. For the "big-three" family S_3, at $n = 8$ the recorded vector is

$$(1, 3, 4, 4, 5, 7, 8, 8, 9, 9, 6, 4, 2).$$

Its entries sum to $70 = \binom{8}{4}$ and $e_3(8) = 12$.

Conjecture 4 (Even binary big-three growth radius)**.** *For the reference state and generators above,*

$$e_3(n) = \begin{cases} n^2/8 + 7n/4 - 13, & n \equiv 0 \pmod 8,\ n \geq 16, \\ n^2/8 + 7n/4 - 12, & n \equiv 4 \pmod 8,\ n \geq 12, \\ n^2/8 + 7n/4 - 14, & n \equiv 2 \pmod 4,\ n \geq 18. \end{cases}$$

The three formulas respectively match the recorded parameters $16, 24, 32, 40$; $12, 20, 28, 36$; and $18, 22, 26, 30, 34, 38$. Separating the residues reveals a shared quadratic term and small periodic corrections. The cutoff in each branch is explicit so that smaller exceptional cases are not silently included. These binary orbits provide a second setting in which the catalogue's growth conjectures can be formulated and tested.

H.4 Unsigned and signed interval reversals

An unsigned interval reversal $r_{i,j}$ reverses positions i through j, with $1 \leq i < j \leq n$, leaving the remaining positions unchanged. The corresponding Cayley graph on S_n has $\binom{n}{2}$ generators. In the permutation model of a chromosome, this operation reverses a contiguous block. Its established diameter is $n - 1$ Bafna & Pevzner (1996); Kececioglu & Sankoff (1995). The recorded growth vector at $n = 5$ is

$$(1, 10, 52, 55, 2).$$

Thus its diameter is 4, its mode is 3, and its two antipodes lie in the final layer. The first-layer size 10 agrees with the number of allowed intervals. More generally, the recorded complete vectors through $n = 14$ all have two states in the last layer.

For signed interval reversals, a move on $[i, j]$ both reverses the order and flips all signs in that interval. Here $i = j$ is allowed, so there are $\binom{n+1}{2}$ generators on B_n. For $n \geq 4$ the established diameter is $n + 1$; the small cases $n = 1, 2, 3$ have diameters $1, 3, 3$, respectively Knuth (1998). At $n = 4$ the complete vector is

$$(1, 10, 50, 170, 145, 8),$$

which sums to $384 = 2^4 4!$ and ends at distance 5. Allowing arbitrary intervals and allowing sign changes are separate modifications of the action set. Their effect is therefore reflected both in the degree of the graph and in the scale and shape of its growth distribution.

H.5 Block transpositions

The catalogue's "Transposons" row uses block transpositions, a different operation from swapping two individual entries. Choose $0 \leq i < j < k \leq n$ and write a permutation as a concatenation $ABCD$, where $B = \pi_{i+1} \cdots \pi_j$ and $C = \pi_{j+1} \cdots \pi_k$. The move replaces $ABCD$ by $ACBD$, retaining the internal order of both blocks. The set of all such moves is inverse-closed and has $\binom{n+1}{3}$ elements. It models moving one contiguous segment past its neighbor.

For $n = 6$ the recorded complete vector is

$$(1, 35, 259, 380, 45).$$

It gives diameter 4, modal distance 3, and 45 antipodes. The first layer has $35 = \binom{7}{3}$ states, which checks the three-cut convention. Over $n = 3, \ldots, 12$, the recorded diameters are $2, 3, 3, 4, 4, 5, 5, 6, 6, 7$, agreeing with $\lceil (n + 1)/2 \rceil$ on that finite range. A continuation to arbitrary n requires a separate conjecture and must account for exceptional sizes; the finite agreement alone does not specify one. The value of these data for learned search is that exact distances at small sizes provide a calibration set for the same move semantics at larger sizes.

H.6 A common binary growth pattern

For both arbitrary interval reversals and block transpositions, the recorded binary experiments use $s_0 = 0^m 1^{n-m}$ with $m = \lfloor n/2 \rfloor$. Their recorded central-state growth vectors agree, leading to the following growth conjecture:

$$a_n(t) = \binom{m}{t}\binom{n-m}{t}, \qquad 0 \leq t \leq m.$$

This is the same expression for even and odd n: at $n = 2m$ it becomes $\binom{m}{t}^2$, and at $n = 2m + 1$ it becomes $\binom{m}{t}\binom{m+1}{t}$. It matches the recorded vectors through $n = 28$. For example, $n = 8$ gives $(1, 16, 36, 16, 1)$, while $n = 9$ gives $(1, 20, 60, 40, 5)$. In each case the entries sum to the size of the binary orbit, $\binom{n}{m}$.

This comparison illustrates another use of the catalogue: different action sets can have identical growth from a chosen state even when their permutation Cayley graphs have different diameters. It suggests investigating an explanation of the shared binary distance statistic. Exact layer counts expose the pattern; a symbolic expression makes the proposed relationship precise; additional parameters and changed initial states test how broadly it extends. The same sequence of steps underlies the RL-assisted investigations of families too large for complete enumeration.

I TABULAR JUSTIFICATION FOR PATH-LENGTH CLIPPING

The following elementary observation explains why valid path lengths are safe upper clips for exact Bellman updates.

Lemma. Let a finite directed graph have unit edge costs, and let every state reach the target e. Write $d(s) = d(s, e)$ and $D = \max_s d(s)$. Let $k(e) = 0$ and $k(s) \geq d(s)$ be finite upper bounds, such as lengths of known paths to e. Define $(T_k f)(e) = 0$ and, for $s \neq e$,

$$(T_k f)(s) = \min\{k(s),\, 1 + \min_{t \in \mathcal{N}(s)} f(t)\}.$$

Then d is the unique nonnegative fixed point of T_k. Starting from $f_0 = k$, the synchronous iterates $f_{j+1} = T_k f_j$ decrease pointwise to d, reaching it within D sweeps. No consistency condition between neighboring values of k is required.

Proof. The operator is monotone, $T_k d = d$, and $T_k k \leq k$. Hence $d \leq f_{j+1} \leq f_j$. Along a shortest path to e, induction gives $f_j(s) \leq d(s)$ whenever $j \geq d(s)$, so $f_D = d$. For uniqueness, let $u \geq 0$ be a fixed point. The inequality $u(s) \leq 1 + u(t)$ on every outgoing edge, together with $u(e) = 0$, gives $u(s) \leq d(s)$ along a shortest path. Conversely, direct induction gives $(T_k^j 0)(s) = \min\{j, d(s)\}$. Monotonicity and $0 \leq u$ therefore yield $d = T_k^D 0 \leq T_k^D u = u$. □

This is an exact, synchronous tabular statement. Regression onto a neural function class, sampled updates, and inexact successor evaluation do not inherit its monotonicity or finite-sweep guarantee. Detaching a target during regression does not make that regression an exact Bellman update. In particular, diffusion pretraining does not ensure that the network itself is an upper bound on distance.

J FIXED CONJUGACY TYPES: SCOPE AND A PROVED EXAMPLE

Use the notation $X_\Lambda(n)$ and $H_\Lambda(n)$ from the main text. Full S_n-conjugacy classes are intended, including both halves if a class splits in A_n. The subgroup $H_\Lambda(n)$ is nontrivial and normal in S_n. For $n \geq 5$, the normal-subgroup classification gives $H_\Lambda(n) = A_n$ when all generators are even, and S_n otherwise.

For completeness, the linear order of the diameter follows elementarily. Let $r = \max_{\lambda \in \Lambda} |\lambda|$ and fix $M \geq \max(5, r)$. The subgroup $H_\Lambda(M)$ contains a 3-cycle, so some word of a fixed length L in $X_\Lambda(M)$ represents that 3-cycle. Embed this word in S_n for $n \geq M$ and conjugate it: every 3-cycle is consequently represented by at most L generators from $X_\Lambda(n)$. Every even permutation is a product of at most $n - 1$ 3-cycles. If odd permutations occur, multiplying by one fixed odd generator reduces to the even case. Thus the diameter is $O_\Lambda(n)$. Conversely, a product of t generators moves at most rt points, while $H_\Lambda(n)$ contains permutations moving every point for all sufficiently large n. Hence the diameter is at least n/r, proving $\Theta_\Lambda(n)$.

Let $C_5(n)$ be the set of all 5-cycles in S_n. Theorem A and Remark 1.5 of Kishnani et al. (2024) give the threshold

$$N(k, 5) = 3k + 1 - \mathbf{1}_{k \equiv 1 \pmod 4}, \qquad k \geq 2,$$

for $C_5(n)^k = A_n$, with the property holding for every $7 \leq n \leq N(k, 5)$. Since $c = (c^3)^2$ for a 5-cycle c and $e \in C_5(n)^2$, the ball of radius $k \geq 2$ equals $C_5(n)^k$. Consequently, inverting the threshold yields

$$\operatorname{diam} \operatorname{Cay}(A_n, C_5(n)) = \left\lceil \frac{n-1}{3} \right\rceil + \mathbf{1}_{n \equiv 4 \pmod{12}}, \qquad n \geq 7.$$

This period-12 formula is derived from the cited theorem; its use here is as an established benchmark for conjecture discovery.

K RECOVERED CUBE EXPERIMENT CONFIGURATION

The comparison in Table 2 uses the diffusion-trained model and test data identified by the following selectors: group `p002`, target `t000`, model `444`, epoch 8192, checkpoint `weights/p002-t000_`

444_e08192.pth, and dataset datasets/p002-t000-rnd.pt. The run uses rows 0–19. The checkpoint configuration is MLP2RB, with hidden widths 1010 and 592, four residual blocks, ReLU, batch normalization, and zero dropout. Its recorded training configuration uses Adam at learning rate 0.001, batch size 10,000, and random-walk depths 1–45 for 8,192 epochs. The public trainer uses non-backtracking random-walk depth supervision with MSE; no Bellman stage is part of this checkpoint. The original checkpoint's training time and random seed are not available. The training horizon 45 must not be mistaken for the evaluation scramble length. The repository describes this random dataset as 100 states generated by 10,000(+1)-step random walks; uniform sampling is not established by this description. The search seed is 20260802, and the RNG is reset after model construction for each heuristic so that hash construction and tie-breaking use the same seed.

The state contains 96 colored facelets. The 24 unit-cost generators are quarter turns of each of four individual layers along three axes, and their inverses. This explicitly specifies the source's UQTM convention. Goal testing is equality with the supplied facelet target, without an additional free whole-cube rotation. The training-free sticker-distance score sums shortest distances on the 96-position move graph to any target position of the same color; these distances are precomputed by multi-source BFS. The other baseline counts facelet-color mismatches.

The recorded environment is one H100 PCIe 80GB, PyTorch 2.12.0+cu130, and CUDA 13.0. The learned network and search ranking scores use FP16. All arms use a beam of 262,144, one attempt, and a 1,000-expansion ceiling. The 60-second cap is checked before each expansion, so the final expansion can overrun it. Recorded search time includes GPU synchronization but excludes loading, heuristic construction, sticker-distance preprocessing, path replay, and model training. This is a shared inference protocol, not an end-to-end training-cost comparison.

The search also retains the hashes of its last four beams. From the fifth expansion onward, it stops when every hash in the newest two beams belongs to the union of the preceding two. With one attempt this ends the search. This implementation-level repetition test is not proof that no solution exists. All 40 training-free failures triggered it before the time/depth ceilings. Candidate counts sum the numbers scored after hash deduplication at each expansion; repeated states can contribute at different depths. The exact recorded median counts are 324,745,448 for learned ranking, 2,133,641,462.5 for sticker distance, and 1,356,623,740 for misplaced stickers.

The first two dataset rows were used in a pilot that informed the final settings and were also included in the reported 20. Thus the experiment uses one fixed benchmark prefix and seed with calibration overlap. The saved execution report and runbook provide the aggregate results and state that all 18 solutions passed replay validation; source edits preserve the harness and configuration. The historical console record additionally preserves the 20 outcomes, times rounded to two decimal places, and exact candidate counts, summarized in Table 36. The two learned failures are rows 10 and 18, both reaching the time limit. The original result JSON and complete move sequences are no longer available in the recovered artifact set; their absence prevents a fresh replay of the historical solutions. The accompanying CSV is a transcription of the console record, not a reconstruction of the missing raw JSON.

The base repository revision recorded before upload was f02604fa7b665b82e5fbe5692b336a4fe4a01bdc; the ablation harness was a local uncommitted patch on that revision. The dataset and checkpoint are identified by the following SHA-256 fingerprints, which the recovery workflow matched to the current public downloads:

> Dataset:
> fa4094b0ef68c699304d3f064f771fc38470f8686e470ffffe44271008c85fdc.
> Checkpoint:
> e12b1c56581af2a9aa980977ffced5e97f050d8d14b43316c34e1c31af6d817b.

These identify the inputs; they do not replace the missing historical output certificates or supply a published commit for the harness modifications.

LRX experiment record. The LRX distance correlations, training-schedule comparison, GAP comparison, and beam-width results were also reported in a related manuscript. This paper incorporates those measurements into its integrated empirical and mathematical study.

Table 36: Per-instance cube outcomes recovered from the historical console record. A dash denotes no returned solution. All sticker-distance and misplaced-sticker runs failed under the shared stagnation rule; the two learned failures reached the time limit. Times were printed to two decimal places, so medians computed from these rounded rows may differ slightly from the full-precision summaries in Table 2. Rows 0 and 1 also participated in the configuration pilot. The accompanying `cube_recovered_results.csv` includes exact candidate counts.

Instance	Learned length	Learned (s)	Sticker distance (s)	Misplaced (s)
0	57	32.81	24.07	11.26
1	60	36.08	36.87	17.47
2	52	31.29	27.93	14.28
3	61	37.64	20.88	17.23
4	59	36.26	27.96	12.99
5	78	48.62	29.02	9.89
6	63	38.68	19.33	17.19
7	54	33.21	18.99	15.59
8	60	36.85	21.66	18.60
9	66	41.03	22.13	13.85
10	—	60.38	25.32	23.52
11	65	40.21	18.32	11.97
12	60	36.92	36.37	9.72
13	55	33.63	21.13	26.22
14	65	40.04	17.37	13.81
15	56	34.51	22.86	20.90
16	69	43.00	31.63	7.37
17	53	33.15	36.79	12.66
18	—	60.20	18.88	17.88
19	56	34.57	25.01	13.41

L Learned cube baselines and benchmark protocol

Table 3 consolidates previously reported cube experiments, rather than a new rerun for this revision. All rows use the 1,000 test states and QTM distances of Agostinelli et al. (2019); a quarter turn costs one move and a half turn costs two. DeepCubeA's published result is 21.50 mean moves and 60.3% optimal. EfficientCube (Takano, 2023) originally reports 21.26 and 69.6%; the reproduced configuration used in the table gives 21.255 and 69.8%. The dash in DeepCubeA's beam column indicates its different search procedure, not an unbounded beam.

The CayleyPy configurations use a single ten-layer ResMLP with approximately 4 million parameters and 8 billion random-walk training examples. The reproduced EfficientCube configuration uses approximately 14.7 million parameters and 52 billion examples. Equal beam width therefore controls frontier capacity, not model size, training effort, or total search cost. Both CayleyPy rows use diffusion supervision without Bellman refinement. The wider-search row increases the beam by a factor of 64; it is a search-capacity comparison. The table reports single-model results and does not incorporate a multi-model ensemble.

M PICTURE CUBE BASELINE AND COMBINED PIPELINE

Table 37 summarizes the recorded progression on the same 1,003 IHES Picture Cube inputs. Scores are total move counts under the benchmark's move convention; they are not compared numerically with the ordinary $3 \times 3 \times 3$ QTM scores. The initial baseline runs Kociemba two-phase solving with multi-prefix search and a center lookup. Subsequent configurations retain this fallback, keeping the shortest available valid solution for each instance.

Table 37: Picture Cube configurations on 1,003 common inputs. Reductions are relative to the adapted Kociemba baseline. These are combined-pipeline records, without equal training or inference budgets.

Configuration	Total moves ↓	Reduction
Adapted Kociemba baseline	42,718	—
Diffusion-guided pipeline (E5)	24,618	42.4%
Bellman refinement + NISS (E6)	24,068	43.7%
Final combined pipeline	23,224	45.6%

The final configuration combines wider-beam searches, inverse-state and multi-seed ensembling, value-to-action-value distillation, and local path post-processing, with per-instance selection of the shortest available solution. Its recorded validity check accepts all 1,003 outputs. The change from E5 to E6 introduces Bellman refinement and inverse-state ensembling together; the 550-move improvement cannot isolate either component. The larger reduction from the initial baseline to the final pipeline measures the complete solver configuration.